AN ASSESSMENT OF THE EXTENT OF THE CONTAMINATION OF MEASUREMENTS TAKEN ON PORTO SANTO DURING ASTEX

by: Cara-Lyn Lappen and Stephen K. Cox
Department of Atmospheric Science
Colorado State University
Fort Collins, CO 80523

Funding Agencies:

National Oceanic and Atmospheric Administration
Grant No. NAG-1-1146
Office of Naval Research
Contract No. N00014-91-J-1422, P00004
Department of Energy
Grant No. DE-FG02-90ER60970

Colorado State University

DEPARTMENT OF ATMOSPHERIC SCIENCE

PAPER NO. **549**

AN ASSESSMENT OF THE EXTENT OF THE CONTAMINATION OF MEASUREMENTS TAKEN ON PORTO SANTO DURING ASTEX

Cara-Lyn Lappen and Stephen K. Cox

Department of Atmospheric Science
Colorado State University
Fort Collins, CO 80523

Research Supported By

National Oceanic and Atmospheric Administration (Grant NAG 1-1146)
Office of Naval Research (Contract No. N00014-91-J-1422, P00004)
Department of Energy (DE-FG02-90ER60970)

February, 1994

Atmospheric Science Paper No. 549

ABSTRACT

AN ASSESSMENT OF THE EXTENT OF THE CONTAMINATION OF MEASUREMENTS TAKEN ON PORTO SANTO DURING ASTEX

The object of the Atlantic Stratocumulus Experiments(ASTEX) was to measure and examine properties of the marine atmosphere. Since instruments were placed on the island of Porto Santo, however, some degree of contamination of pure marine conditions was experienced due to the local effects of island topography. In order to assess the expected differences between a pure marine environment and measurements taken on the island of Porto Santo, a numerical model- the Regional Atmospheric Modelling System(RAMS) was used in direct comparison with observational data for the case of June 10, 1992. Specifically, this study focuses on the mean wind fields simulated by RAMS and compares them to the winds measured by the United Kingdom's C130 Meteorological Research Flight, a 400Mhz wind profiler, and rawinsondes. The model's inability to resolve a 100m cliff on the windward side of the island was found to cause a phase shift between the model-produced and the actual wind fields. This was determined to be a 1-2km upward phase shift and a 300m to 500m windward phase shift for the RAMS data. After applying this correction, and comparing these four sources of data, the extent of the island's effects in the horizontal as well as the vertical was determined. In the horizontal, the effects decrease with distance from the island until approximately 2km upwind or downwind where the effect was minimal. In the vertical, the effect of the island was detectable up to 3.5km, but not felt continuously. The maximum effect was found at the ground and at approximately 1.2km. Wind data taken at Porto Santo must be filtered at the ground, and near the 1.2km and 3.5km levels. In between these levels, wind measurements taken on the island would appear to provide an accurate representation of the pure marine environment.

ACKNOWLEDGEMENTS

Cara-Lyn Lappen:

I would like to thank the members of my graduate committee for their part in helping me complete this work and taking the time to address my concerns when asked.

The other people in the department who helped me through the ups and downs of this degree are my office mates- John Withrow, Gordon Beck, and Ran Song. Help with technical problems as well as emotional support was never in short supply in room 314. Anxiety attacks came progressively more often as all our theses neared completion and laughter in the office could always be found.

My roommate Karen Christoffersen, is a major reason why I was able to finish this program. She helped me through the most difficult time in my life and gave me the encouragement and support without which I may never have completed this degree.

Finally, I would like to thank my parents who I have gained a whole new respect for over the last two years. Everyone should have parents as wonderful and caring as mine.

Stephen K. Cox and Cara-Lyn Lappen:

This research was funded by the Department of Energy under Grant No. DE-FG02-90ER60970, the National Aeronautics and Space Administration under Grant No. NAG-1-1146 and the Office of Naval Research under Contract No. N00014-91-J-1422, P00004.

TABLE OF CONTENTS

LIST OF FIGURES

1. INTRODUCTION

1.1. BACKGROUND

In June, 1992, a major field campaign- the Atlantic Stratocumulus Experiments(ASTEX) was conducted in the vicinity of and on the islands of Santa Maria, Azores and Porto Santo, Madeira. The aim of these experiments was to measure and examine properties of the marine atmosphere. Included in the measurements taken on the islands are aircraft data, wind profiler data, and rawinsonde data. This study focuses on these measurements on the island of Porto Santo. Since instruments were placed on the island of Porto Santo, some degree of contamination of pure marine conditions was experienced due to effects of island topography. It is the aim of this study to determine the discrepancy between the desired measurements of a pure marine environment and the actual measurements taken. This is achieved by analyzing and comparing observations and model results.

The island of Porto Santo is located in the Atlantic Ocean at 33.06 north latitude and 16.33 west longitude. The topography of the island is fairly irregular (Figure 1.1). The eastern portion of the island has a hilly topography with the highest peak(500m) being about 2km east of the measurement site. The actual location of the measurement site was just to the west of the hills on the north side of the island. It was set back approximately 500m from a 100m cliff facing close to north and the predominant wind direction is from the north. Thus the cliff immediately represents a contamination to measurements as it is a barrier to wind flow. The center of the island is an elevated plateau of about the elevation of the cliff- 100m. In the western part of the island there are some smaller, more gently sloping hills.

This study is organized into five major components. A mesoscale model (RAMS) is applied to study the perturbations in the wind field induced by the island. Aircraft data collected on two occasions upwind of the island, over the island, and downwind of the island are analyzed to provide direct observational evidence of these three regimes. Then, a detailed comparison is

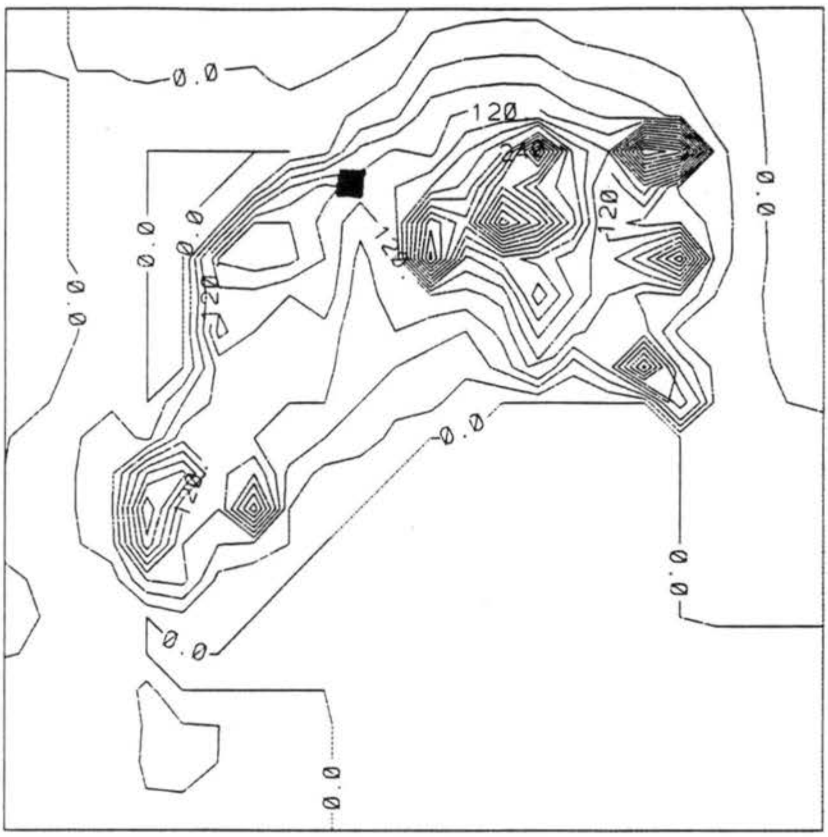

Figure 1.1: Topography of Porto Santo; contour interval is 30m; black square represents measurement site.

performed between the C130 aircraft wind data and the wind fields produced by the model. The fourth component of this study examines the problem of topography resolution in the model and assesses any necessary adjustments which should be made to the RAMS output so that an accurate picture of the wind fields is given. And, finally, ground based measurements taken from a 400Mhz wind profiler and rawinsonde data are analyzed to give additional comparisons as well as some additional information concerning the vertical structure of the over-island winds.

The model used to examine the effects the Island of Porto Santo has on the local wind fields is the Regional Atmospheric Modelling System(RAMS). The model uses the full set of primitive dynamical equations that govern atmospheric motions and supplements these with optional parametrizations for turbulence, microphysics, radiation, surface heat exchanges, kinematic effects of terrain, and cumulus convection. RAMS uses a two way interactive grid nesting system in which the setting of the finest grid's resolution has no lower limit. The nested gridding system allows for microscale features as small as boundary layer thermals to be resolved on the smallest grid while simultaneously allowing for the effects of synoptic features on the larger grids.

The objective in using RAMS is to simulate flow over and around the island of Porto Santo and compare the results of these simulations to observed measurements taken during ASTEX. By showing similarities between observed fields and RAMS, the ability of RAMS to simulate such conditions is validated. Also, simulating the marine environment with RAMS allows for the large scale marine atmosphere to be represented on larger grids while the finest grid can simulate the local effects of the island's topography.

The main day chosen for the simulations is June 10, 1992. This day was chosen due to the lack of clouds present during the daytime. Clouds may have produced wind fields of their own and it would have been difficult to isolate the effect of the island. In addition, aircraft data from the United Kingdom's Meteorological C130 Research flight are available for intercomparison on this day. June 22, 1992 was also simulated to help interpret the June 10 simulations.

Three grids are used for this simulation- the grids are all 26x26 with the largest grid being 10kmx10km on a side(260kmx260km total area) and the finest grid being 0.5kmx0.5km on a side(13kmx13km total area). This coarseness presents some problems with the horizontal resolution of some topographic features on the island such as the steep, north-facing cliff.

Thus, four other simulations were done in addition to clarify some of the problems in properly resolving the 100m cliff horizontally. These used the same initial sounding as the June 10th runs, but have varied grid resolution and simpler topography. The topography includes just a 100m cliff which is infinite in the south, east, and west directions. The cliff faces north and is horizontally resolved in four runs to 1000m, 500m, 250m, and 100m. The winds are initialized from the north in order to be perpendicular to the cliff. Since these four runs are identical except for the grid size domains, the difference between the winds for these results then depicts only the difference due to horizontal resolution of the topography. This difference is then applied to the more complicated terrain of the island which was resolved only to 500m in the simulations.

This paper is divided into six sections- an analysis of the model-produced fields, and analysis of the aircraft data, a comparison between the two, an assessment of the problems associated with inadequately resolving a cliff on the north side of Porto Santo, additional comparisons from the wind profiler and rawinsondes, and conclusions. All the analyses focus on determining the vertical and horizontal extent of surface measurement contamination so that an accurate picture of the properties of the marine atmosphere can be deduced.

1.2. PREVIOUS STUDIES

Some of the basic features of flow characteristics around and over various obstructions have been at least qualitatively understood for some time (for a historical view, see Hosker,1984). Quantitatively, however, the focus of research has been wind tunnel studies examining mean flow and turbulence structures near the surface of the obstacles and not extending too far upstream or downstream of these obstacles. In the 1980's, a lot of work was done studying flow and dispersion around isolated hills both in two and three dimensions (Bradley,1980;Jenkins et al.,1981;Strimaitis et al.,1983;Ryan et al.,1984). But, once again, these studies were restricted to low levels on the hills and did not extend into the far wake region of the disturbance or the far upstream region.

A large number of wind tunnel studies have been conducted on wakes behind fences and buildings(Hosker,1984). Fewer studies have been made of three dimensional obstacles. Hansen and Cermak(1975) studied the wake of a three dimensional hill and found evidence of its effect over 30 hill lengths downstream. Castro and Snyder(1982) have reported on results of flow around three dimensional hills having different aspect ratios. They have also reported on the flow fields only in the near wake region in the lee of the hills. Pearse(1982) made measurements of the mean flow over smooth conical hills of varying slopes but his investigation once again did not extend beyond the near wake region and was confined to an area near the ground.

Arya and Gadiyaram(1985) were the first to extend their investigation horizontally to the far wake region of the flow. They used a wind tunnel containing hills of two different slopes- 26.5 degrees and 17.5 degrees and measured the mean flow and the turbulence structure. These results were compared to observations without a hill to determine the actual hill-induced effect. They found that behind the steeper hill, there existed a well defined recirculating zone- the presence of weak trailing vortices in the lower region(Z=0.3H, H-hill height). This was not found behind the weaker sloping hill.

It has also been found that, for two dimensional hills with no flow separation, there exists a strong linear dependence of the speed up factor (average wind speed observed divided by the average wind speed at the same height level for the no hill case) with hill slope and shape (Jackson and

Hunt,1975; Hunt,1978; Mason and Sykes,1979; Taylor,1984). For three dimensional hills, the dependence is nonlinear and weaker (Taylor,1984). With flow separation, the speed up of flow becomes limited as the hill slope increases beyond a certain value (Arya and Gadiyaram,1985; Pearse,1982).

Arya and Gadiyaram (1985) also showed that the vertical extent of the flow is larger for steeper hills. This is something the present study will show as well.

Bowen and Lindley (1977) conducted another study involving use of a wind tunnel to investigate the flow over two dimensional forward facing escarpments of varying slopes. While they only looked at the flow near the ground, this study has much relevance to the last section of the present study where the variation in the horizontal resolution of topography can be thought of as analogous to varying the steepness of an escarpment. Bowen and Lindley (1977) calculated amplification factors (mean wind speed at a height Z above local ground level divided by the mean wind speed of the undisturbed flow at the same height above local flat ground, upstream of the hill) for the flow over the escarpment at various positions upstream and downstream. Sacre (1973) observed that the major effect on the amplification factor came from slopes less than 30 degrees with unseparated flows. Steeper slopes had a decreasing influence on the amplification factor which tended to a maximum value of between 1.4 and 1.5. The results from Bowen and Lindley (1977) show that about one-third the way up the slope, the amplification factor reached unity and rapidly increased in value toward the crest. An overall maximum value was approximately 1.7 for all slopes ranging from 14 degrees to 90 degrees found at the lowest level above the ground. De Bray (1973), Freeston (1974), and Sacre (1973) showed similar trends in the mean flow, but the peak values were slightly lower at 1.4 or 1.5.

The major region of influence from the escarpment defined by the amplification factor being greater than 1.1 was confined to a region below 3H above the local ground. The peaks in the amplification factor profiles can be seen to rise from ground level at the crest to approximately Z=H between 5 and 10H downstream. The peak values tended to be greater for the more gradual slopes where the wake was not so strong and the possibility of separation less likely.

The results mentioned above will be referred to in the last section of this paper where the problem of the horizontal resolution of a cliff on the north side of the island is discussed. Differences in the wind fields arising from the horizontal resolution of topography can make a topographic barrier more or less steep and thus is analogous to the ideas discussed above .

In addition, O'connor and Bromwich (1988) quantified flow separation regimes using Froude numbers. They found that the critical Froude number is 2.3. For higher values the flow is over the ridgeline while for lower values the flow is blocked up to some height on the ridge. These results will be discussed in chapter four and be applied to the problems associated with the horizontal resolution of the cliff in the model runs.

2. MODEL ANALYSIS

2.1. THE MODEL PARAMETERS FOR JUNE 10

RAMS uses the standard Arakawa-C grid (Arakawa and Lamb, 1981) which is staggered in both vertical and horizontal directions with a polar-stereographic horizontal grid. This model run used 3 grids- the largest being a 26x26 grid covering an area 260kmx260km. Grid two was a 27x27 grid covering 54kmx54km. Grid three was a 26x26 grid covering an area a little larger than the aerial extent of the island- 13kmx13km. Each grid was nested within the larger one so as to exactly be centered in the larger grid.

In the vertical, there were 30 levels beginning at the surface with 50m spacing and being vertically stretched by 1.1 for subsequent levels until the spacing reached 800m; Thereafter, layer thickness was held constant at 800m. This technique is used to ensure vertical stability. The vertical levels for all 3 grids are identical.

There are also 6 soil layers. A surface layer/ soil model was used. (Tremback et al., 1985).

Cloud microphysical properties are parameterized (Flatau et al., 1989) although little cloud activity took place for this simulation. The model is initialized horizontally homogeneous with a sounding taken from rawinsondes launched over the island. All three grids were initialized with the same sounding. The launch time was 805UTC(905 local time) and the model run begins at 800UTC. The run is done nonhydrostatically and runs for 6 hours. The model time step is 12 seconds on the coarsest grid, 4 seconds on grid two, and 1 second on the finest grid. Analysis files, however, are only printed every hour.

The radiation scheme employed in this study is described in Chen and Cotton (1983b). Radiative effects are allowed including cloud radiative effects as well as daytime heating and nighttime cooling of the topography.

These fields are updated every 10 minutes. The model takes into account the sun's deviation angle as well as the latitude and longitude of the area.

A number of boundary conditions are imposed. The top boundary condition is the "wall on top" condition where the vertical velocity is set to zero. This condition is completely reflective. Thus, it is used with a Rayleigh friction layer where model variables are nudged back to a reference state (Clark, 1977). The lateral boundary condition is Klemp/Wilhelmson in which the normal velocity component specified at the lateral boundary is effectively advected from the interior assuming a propagation speed set to 20m/sec.

This study used the deformation K turbulence scheme described in Tripoli and Cotton (1982) and in Tremback (1990). Several parameters must be set in the RAMS formulation of this scheme. The vertical length scale was set to the vertical grid spacing. Three dimensional deformation was used to calculate the vertical eddy exchange coefficients. The horizontal length scale was set to $\sqrt{\Delta x \Delta y}$. The horizontal exchange coefficients were calculated from only the horizontal deformation. The ratio of the eddy heat exchange coefficient to the eddy momentum exchange coefficient was set to three for both the horizontal and the vertical.

Sea surface temperature is set to 290 degrees Kelvin and the surface roughness is set to a value of 0.0006m over the ocean and to 0.05m over the island.

2.2. SUMMARY OF EXPERIMENTAL DESIGN

The model was run for two different days. It was initialized horizontally homogeneous with a sounding from June 10, 1992 at 850UTC and one from June22, 1992 at 727UTC. The finest grid which encompassed the topography of the island covered an area of 13kmx13km with 676 grid points.

On the 10th, the temperature at the ground was 290K, and decreased to 281K by approximately 1050m where an inversion began. This layer was stably stratified. In the inversion layer, between 1050m and 1700m, the temperature increased to 282.5K. The winds were north to north-easterly at approximately

8m/sec below the inversion and 5m/sec through the inversion. The air was relatively dry with relative humidities less than 70%. Very little cloudiness was observed over Porto Santo. The sounding from June 22nd was very similar with a few exceptions. The inversion began slightly higher: at approximately 1300m and continued through 2000m. The winds speeds were on the order of 5-6m/sec throughout the sounding for June 22nd.

The model was run for three hours on each of these days before being analyzed. It was shown to reach steady state by this time over the whole domain including that disturbed by the topography of the island.

On the north side of the island a steep, north-facing cliff provided a direct barrier to flow. Four other runs of RAMS focused on the model's ability to resolve cliffs of varying steepness. These runs used the sounding from June 10 with the wind direction changed to northerly. The topography input to the model was a simple sloped escarpment facing north and was horizontally resolved in the four runs to 100m, 250m, 500m, and 1000m. Results were analyzed in these four runs after one hour of simulation. Steady state had been reached by this time.

Froude numbers were calculated for each of these runs. For the 100m and 250m cases, Froude numbers were characteristic of flow separation regimes. In the 500m and 1000m cases, the Froude numbers were indicative of flow ascension over the barrier. RAMS accurately depicted this.

2.3. GENERAL FEATURES OF THE MODEL-PRODUCED WIND FIELDS

Results from the model simulation on June 10, 1992 over Porto Santo show some interesting features relating to the effects of the island. First, cross-sections of vertical velocity fields through the field site indicate upward motion ranging from 0.5m/sec to 1.5m/sec along the whole north side of the island where the wind strikes the barrier, and downward motion of 0.4m/sec a little downwind of the site (Fig 2.1- 2.2). Further downwind, a small amount of upward motion, 0.1m/sec, can again be detected indicating a damped wavelike flow pattern typical after wind hits a barrier such as this. Clearly, this

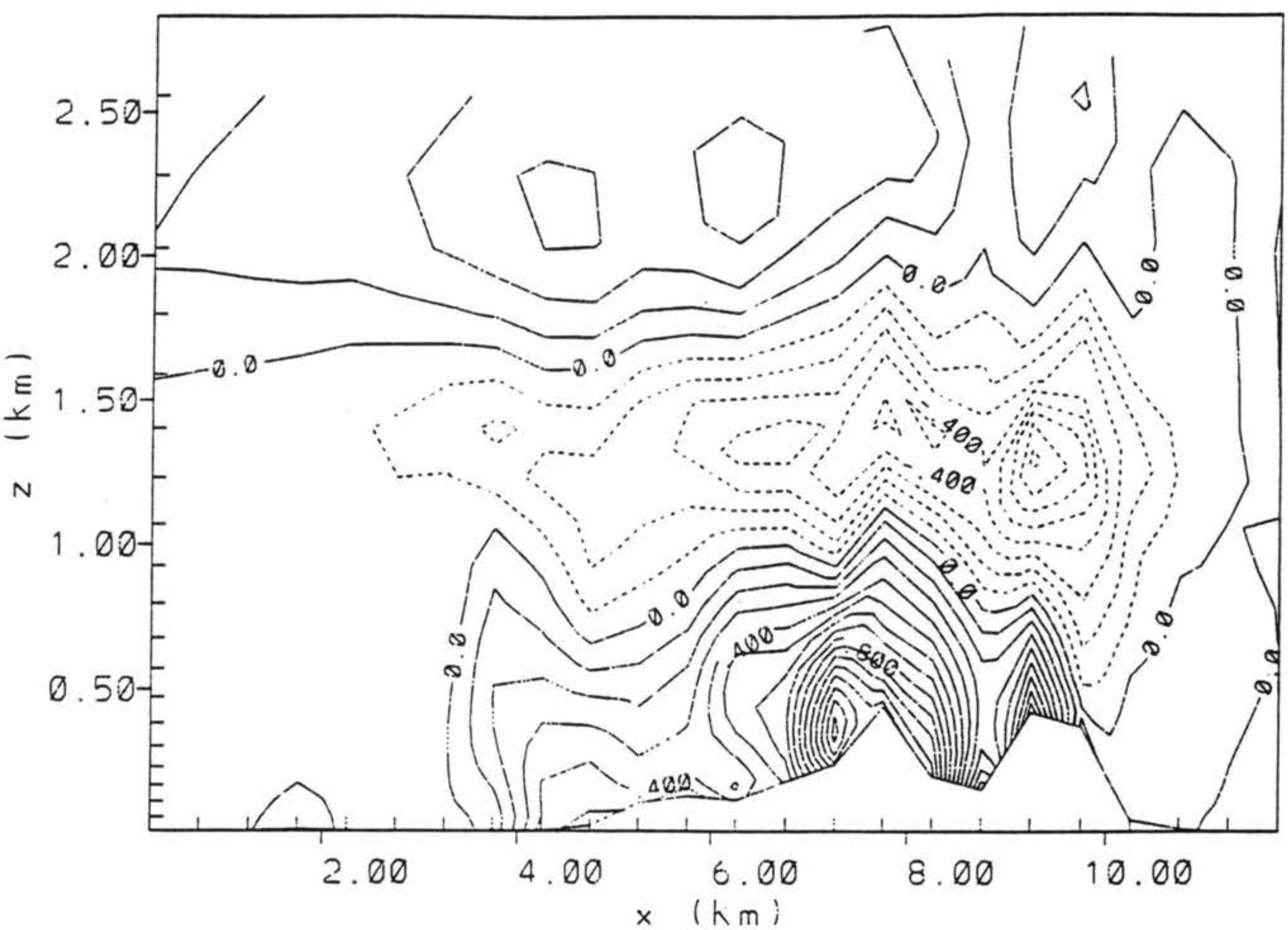

Figure 2.1: Xz cross section through the highest peaks on Porto Santo of vertical velocity in m/sec; solid lines are upward motion; dashed lines are downward motion. The contour interval is 0.1m/s. The topography is outlined at the bottom. The wind is out of the page.

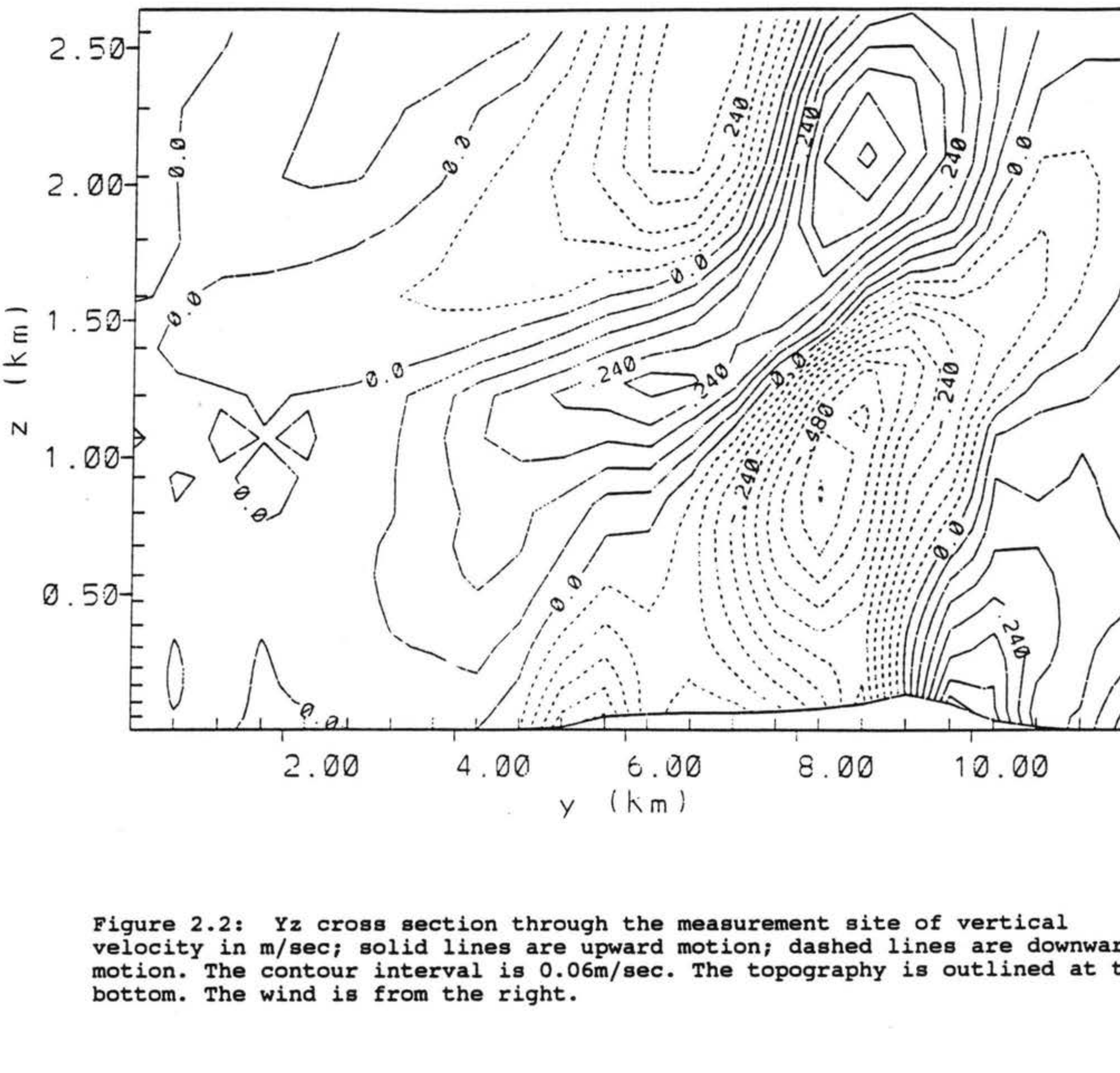

Figure 2.2: Yz cross section through the measurement site of vertical velocity in m/sec; solid lines are upward motion; dashed lines are downward motion. The contour interval is 0.06m/sec. The topography is outlined at the bottom. The wind is from the right.

pattern is produced as a result of the island. At various heights, the horizontal wind speeds along a north-south transect through the measurement site were calculated using an average of three grid points- the grid point of interest, and the grid points just to the east and west of it (Figs 2.3a-c). At low levels, these plots show a slight decrease just upwind of the experiment site, an increase over and downwind of the site, a fairly steady slight decrease over the rest of the island and a fairly steady slight increase downwind of the island. This pattern can be seen at levels from the ground up to approximately 1000m. From 1000m to approximately 1900m the pattern changes. There is an increase in wind speed upwind and over the site, followed by a steep decrease of about 2 m/sec over a kilometer. This is proceeded by a steady slight increase over the rest of the island and downwind of the island. Above this, the pattern seems to shift to one similar to the lower level pattern.

In addition, below the 2000m level, the wind speed maximum shifts upwind with height. This can be shown to be a direct result of pressure-induced fields. The pressure fields are initialized horizontally homogeneous. Thus, any perturbation pressure fields at a later time are indicative of relative pressure. Figure 2.4 shows the minimum perturbation pressure corresponds exactly to this wind speed maximum. For a stable environment such as this, the wind will speed up at the areas of lowest pressure.

The interesting thing to note here is that transects of wind direction show a very similar grouping (Figures 2.5a-c). From the surface up to about 1000m, the wind direction pattern along this north-south transect is very similar in nature. It stays between 0 and 10 degrees and there is a northerly shift directly after striking the island's cliff. Within the next grouping from 1000m to approximately 1900m, the transects all have a very similar shape but differ greatly from the lower level pattern. The wind direction no longer has the northerly dip but is fairly homogeneous until 1km upwind of the island where it turns eastward. The largest easterly component occurs about 2km downwind of the cliff. In addition, the entire pattern shifts eastward with height. And, similar to the wind speed, there appears to be a third

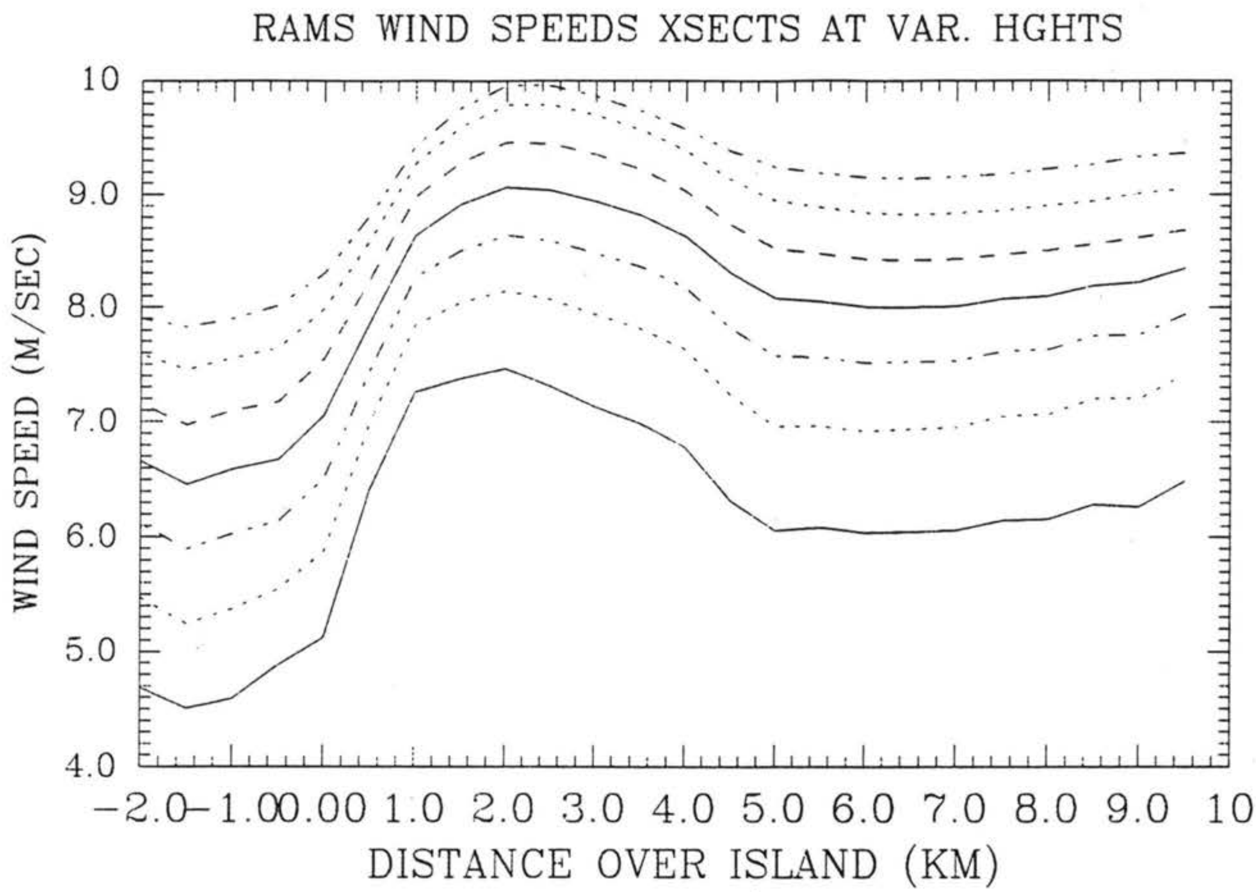

Figure 2.3a: Cross sections through the measurement site of wind speed at various heights. Negative distances refer to upwind of the island. The island begins at 0.0km and extends to 5.5km; The lines are from top to bottom- 24m, 76m, 134m, 198m, 267m, 344m, 429m.

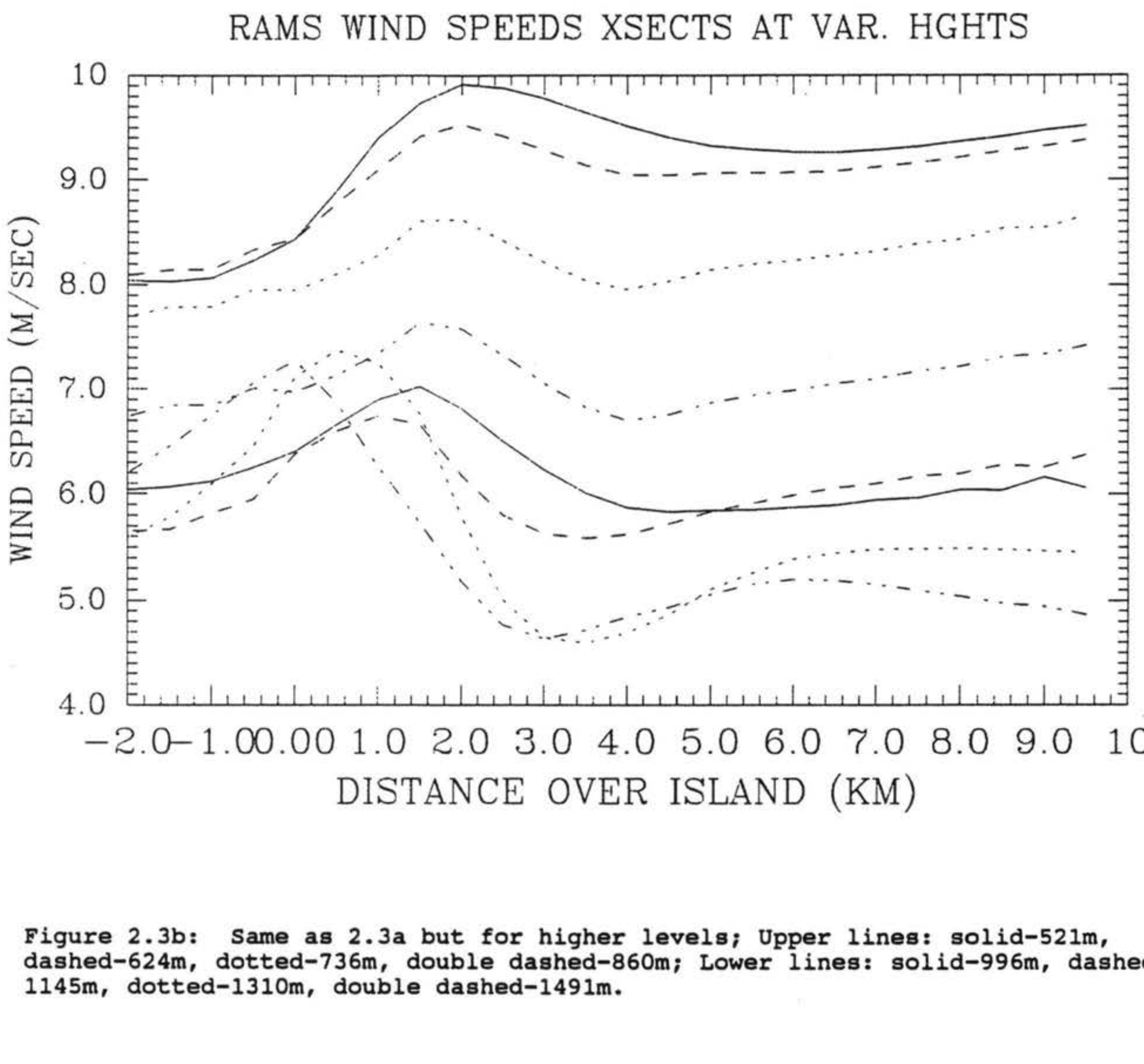

Figure 2.3b: Same as 2.3a but for higher levels; Upper lines: solid-521m, dashed-624m, dotted-736m, double dashed-860m; Lower lines: solid-996m, dashed-1145m, dotted-1310m, double dashed-1491m.

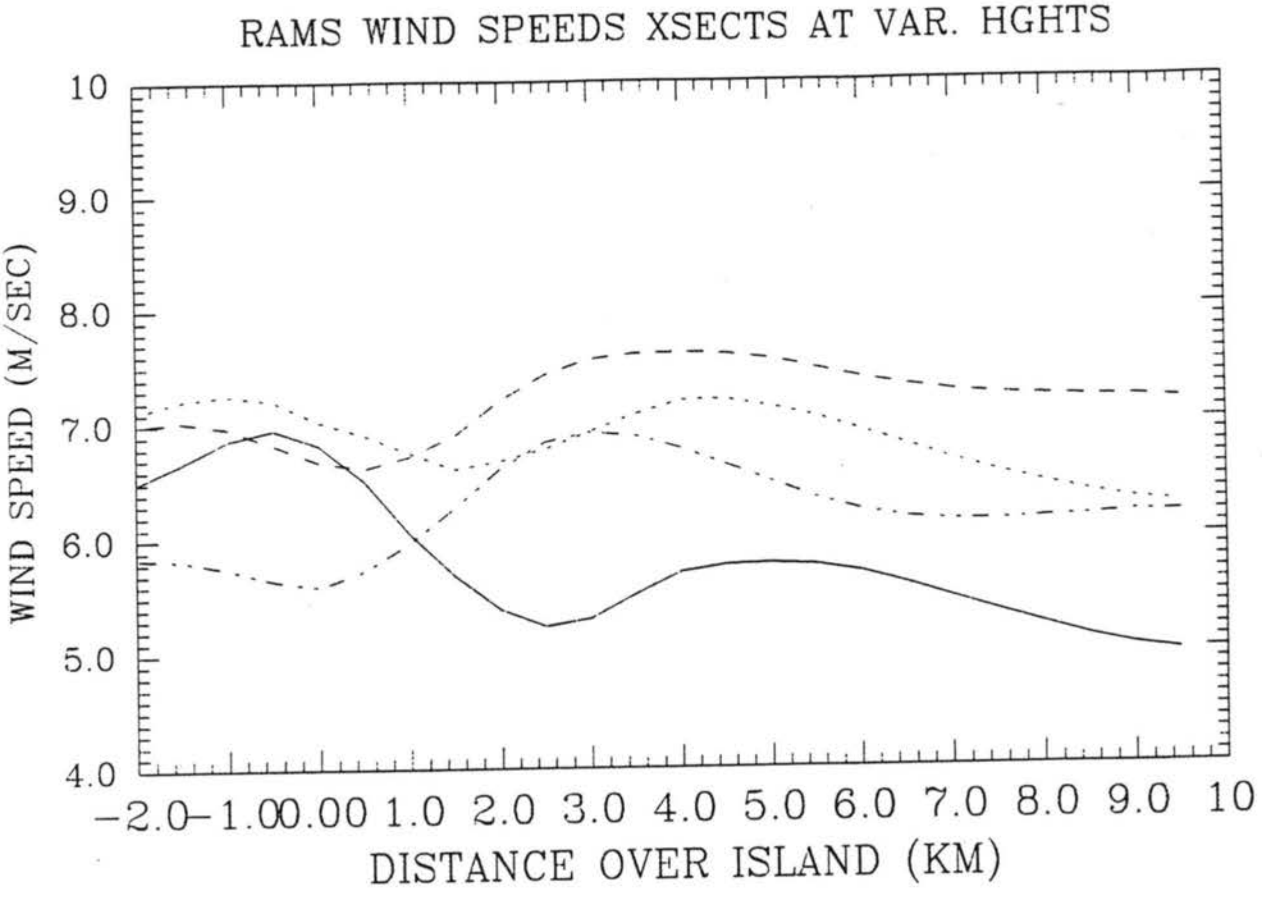

Figure 2.3c: Same as for 2.3b but for even higher levels; Solid line-1690m, dashed line-1909m, dotted line-2150m, double dashed line-2415m.

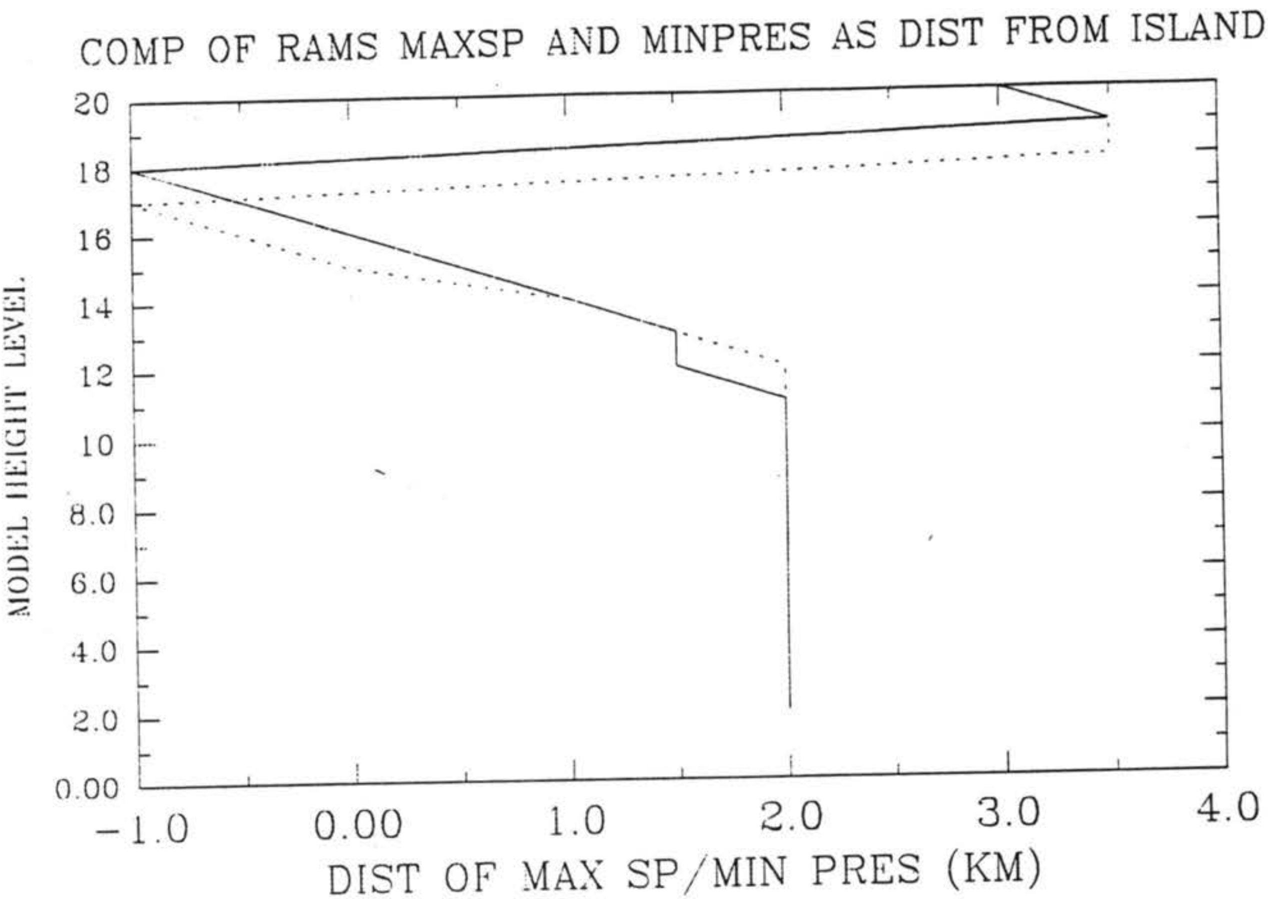

Figure 2.4: Comparison of the location of the wind speed maximum with the location of the minimum pressure with height. Negative distance refers to upwind of the island.

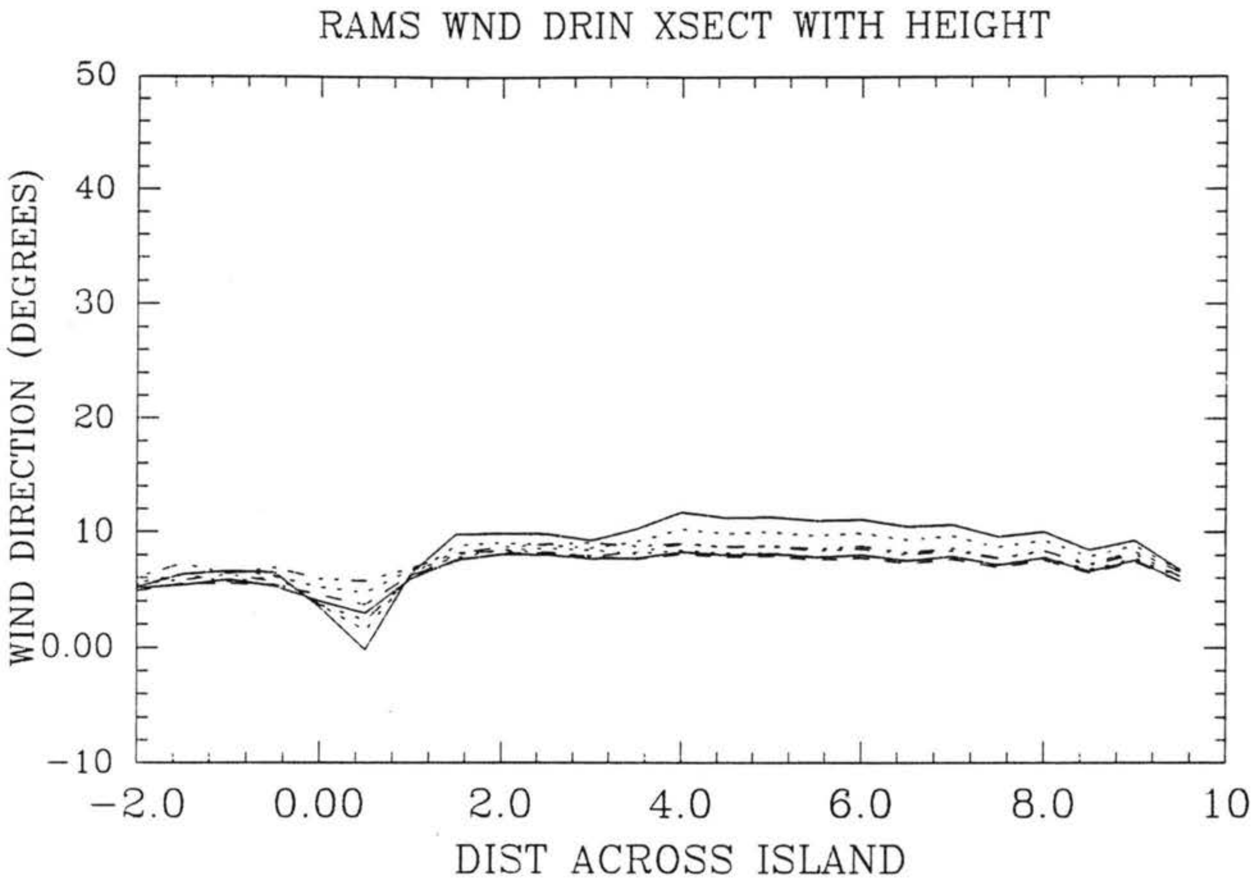

Figure 2.5a: Same as 2.3a but for wind direction; Shown are heights through 500m. Negative directions are subtracted from 360.

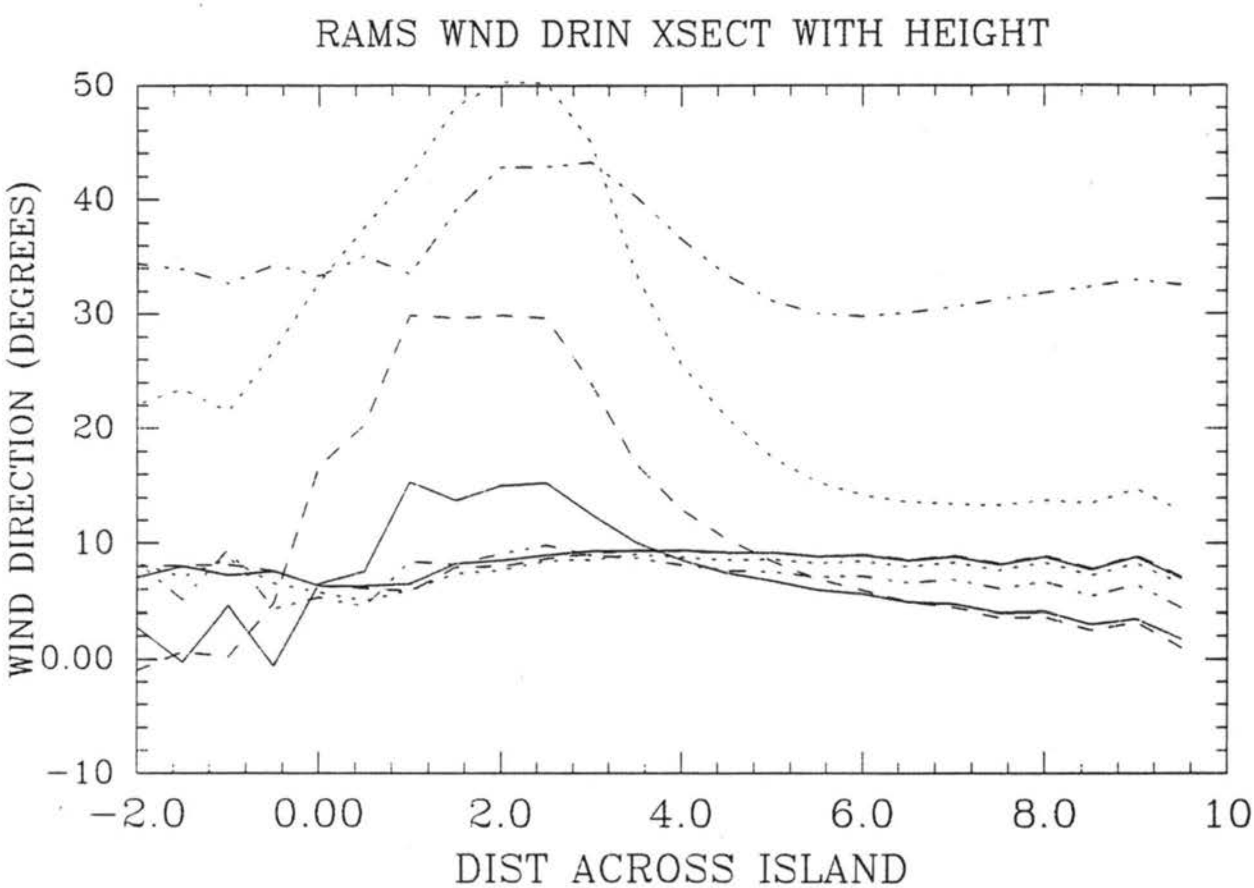

Figure 2.5b: Same as 2.3b but for wind direction; Lower lines: solid-624m, dashed-736m, dotted-866m; Upper lines: solid-1145m, dashed-1310m, dotted-1491m, double dashed-1690m.

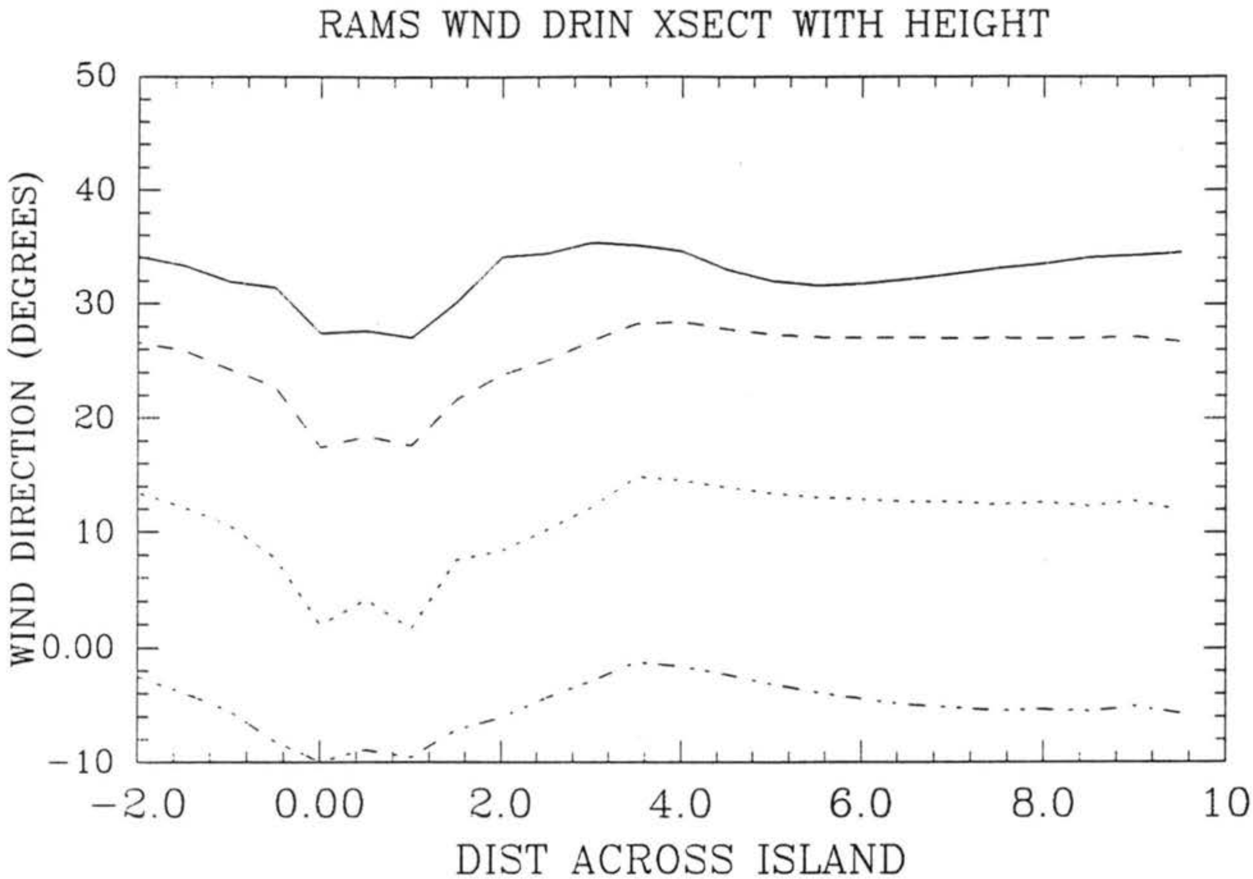

Figure 2.5c: Same as 2.3c but for wind direction; solid line-1909m, dashed line-2150m, dotted line-2415m, double dashed line-2707m.

grouping above 1900m. This grouping, like the wind speed, returns back to the original pattern where the transects are relatively unchanging except for a slight northerly dip directly downwind of the cliff. The transects above 1900m migrate northerly with height. The 1000m to 1900m group migrate easterly with height.

There are at least two viable explanations which could account for this pattern. First, these results could be an artifact of the model. Secondly, the pattern could somehow be an island-induced effect. This in itself brings up five contendable choices:

1. This could be an Ekman effect caused by the change in the surface friction as air goes from over the ocean to over the island.
2. This could be a result of a change in the surface stresses due to diabatic effects such as surface heating.
3. There are competing effects between the cliff and the other nearby topographic features that vary with height. At low levels, the effects of the cliff overpower the effects of the large prominances east of the measurement site. In the middle layers, the large prominances are the predominant effect.
4. This could be a result of an increase in the horizontal temperature gradient between 1000m and 1900m which produced a thermally-driven wind component at these levels.
5. This could be a standing wave phenomena induced by the air rising over the cliff.

All of these ideas were examined.

These results are somewhat confirmed by the wind profiler, rawinsonde measurements, and the United Kingdom's C130 aircraft data. The results showing this will be discussed in the next chapter for the C130 and in chapter five for the wind profiler and rawinsonde. Based on the observations, it can be said that this is probably not a model artifact. This leaves the possibility of this being an island-induced effect. Let us next examine the four contenders here.

The Ekman and the surface diabatic heating ideas are the least probable. Most likely, if the Ekman effect is important, it would be seen near the ground up to a certain level- the area closest to the surface where the frictional change is greatest. But, here the effect seems to be felt at mid-levels and not near the ground. Thus, this shall be ruled out for now.

For the diabatic surface heating to have a significant effect, the lowest layers should be either unstable or neutral. The temperature profile during this time period indicates a stable layer. Thus, this is most likely not was is occurring here.

For number three, the scenario could be as follows: At levels close to the ground, the effect of the cliff is the predominant influence. There is a small saddle in the topography just east of the site before the big peaks which are further east. This saddle could shield the lower levels from some of the influences of the large prominances to the east of the site. As you get into the second level pattern- from 1000m to 1900m, the cliff's effect is overpowered by the other nearby higher topographic features- the peaks to the east. Then, still higher, above the 1900m level, the effects of the peaks- of which the highest is 500m- is no longer felt and a return to some level pattern occurs with some slight residual effects still present. To further explore this possibility, streamlines were plotted and the area magnified in the vicinity of the site and the peaks to the east (Figure 2.6).

Upon examination of these plots, it is clear that this scenario probably does not account for what is taking place. First, at levels close to the ground, an overlay of the streamlines over the map topography shows clearly that the wind at low levels is affected by the peaks (Figure 2.7a). The streamlines bend around the peaks at these lower levels. Thus there may be a cliff effect here but the predominant effect is that of the major envelope of island topography. Further, at middle levels, the streamlines over the site and the neighboring peaks at the 1000m to 1900m levels show a decoupling from the topography. These streamlines bend eastward and show no deflection in the vicinity of the peaks (Figure 2.7b). Above 1900m, the streamlines are just out of the north. They do not bend or deflect. Thus, if anything is

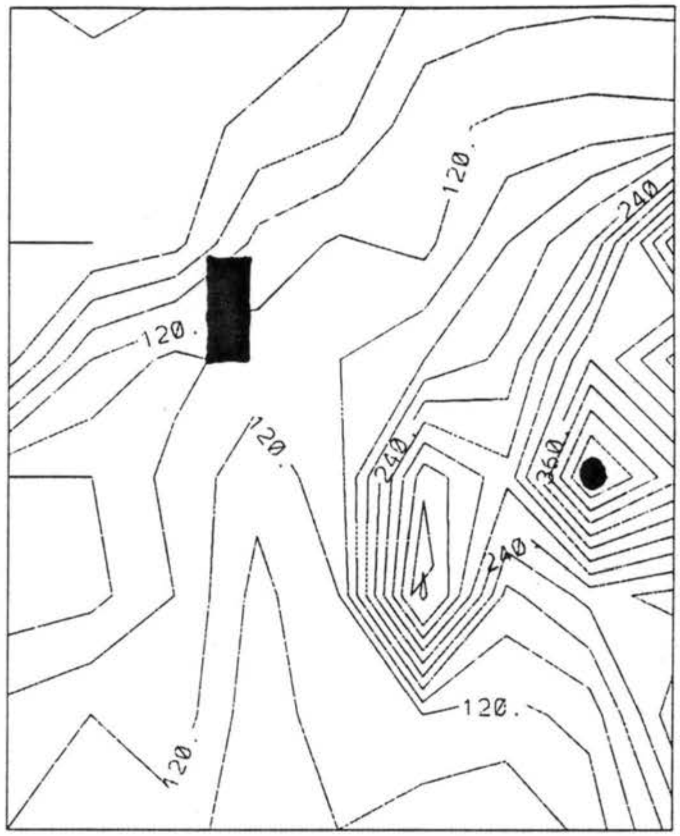

Figure 2.6: Blow up of topography around the measurement site. Contour interval is 30m; black square is the measurement site; black circle is the highest peak on the island.

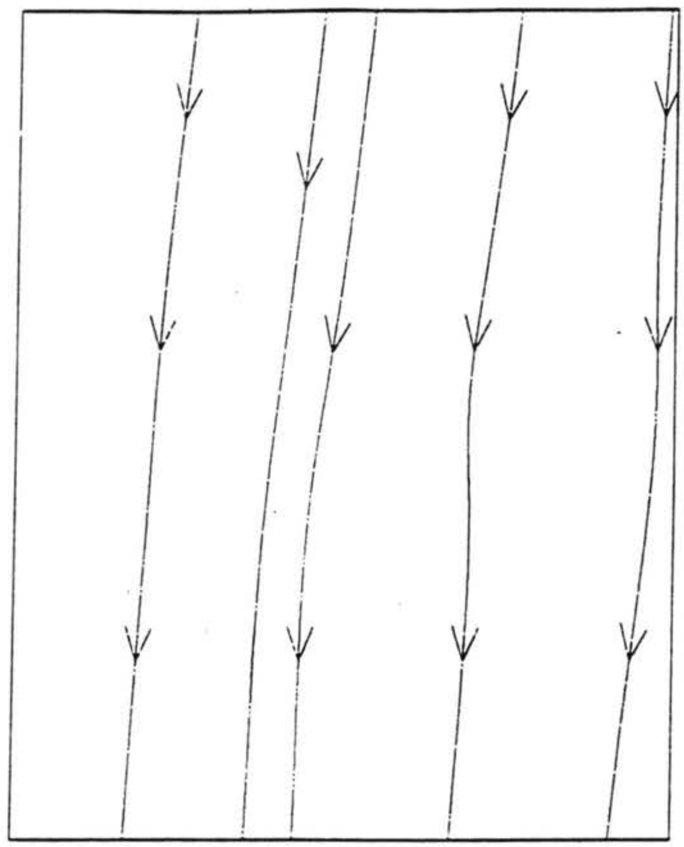

Figure 2.7a: Blow up showing streamlines at 344m; this can be overlayed on topography in figure 2.6.

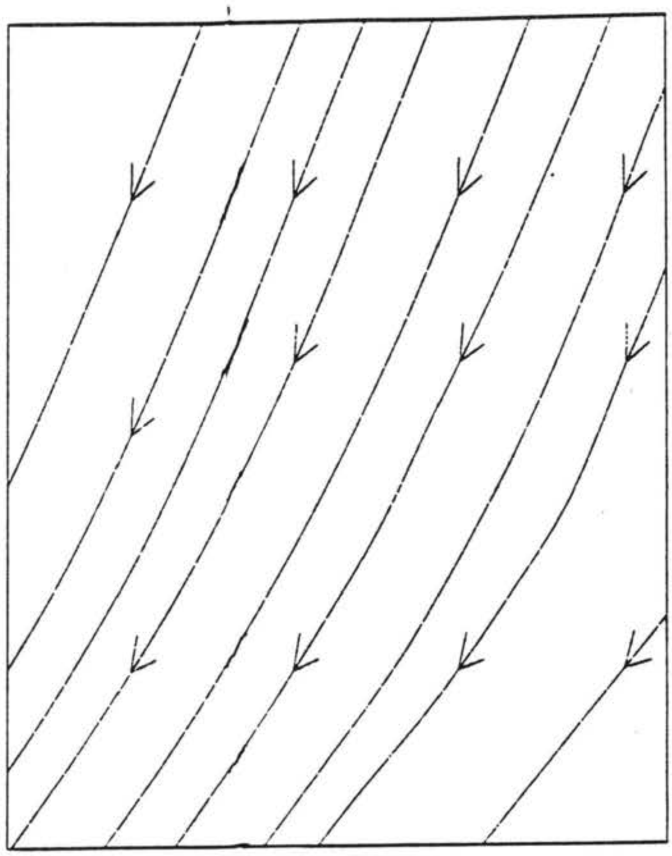

Figure 2.7b: Same as 2.7a but for 1491m.

happening here, there is a topographic effect at low levels, some other effect at middle levels, and no effect at all at higher levels.

This leaves the possibility of a wave phenomena or a thermally-driven wind. One or both of these is most likely responsible for the model results. Evidence showing both is fairly compelling. Each will be assessed individually and then together. First, the thermally-driven wind will be examined.

Although the model is initialized horizontally homogeneous, the pronounced temperature inversion may be displaced vertically in the vicinity of the island. This deformation would then produce horizontal temperature gradients and subsequent pressure gradients. Lavoie (1974) found a similar deformation in an inversion over the island of Oahu, Hawaii.

The streamlines at 1490m show most clearly what is taking place at these mid levels (Figure 2.8). They begin by being fairly straight and consistently northeasterly north of the island. When the air encounters the island, the streamlines begin to bend anticyclonically and by mid island they reverse and bend slightly cyclonically. South of the island, the streamlines return to the same northeasterly flow that was observed north of the island. Now, if this effect is thermally-driven, we would expect to see little change in horizontal temperature upwind of the island, an area of temperature increase which extends over the northern part of the island, and a decrease in temperature over the rest of the island. The warmest temperatures would produce a relative high pressure while the colder temperature a relative low pressure. This would create the bends in the streamline curves described above.

Horizontal crosssections of temperature at this level support this hypothesis (Figure 2.9). There is little or no temperature gradient outside the domain of the island. Over the northern part of the island, there is an increase in the temperature from 282.1K to 285.3K. This should produce a pressure gradient which will lead to an anticyclonic bend in the streamlines. Downwind of this, the temperature drops from 285.3K to 281.1K which should

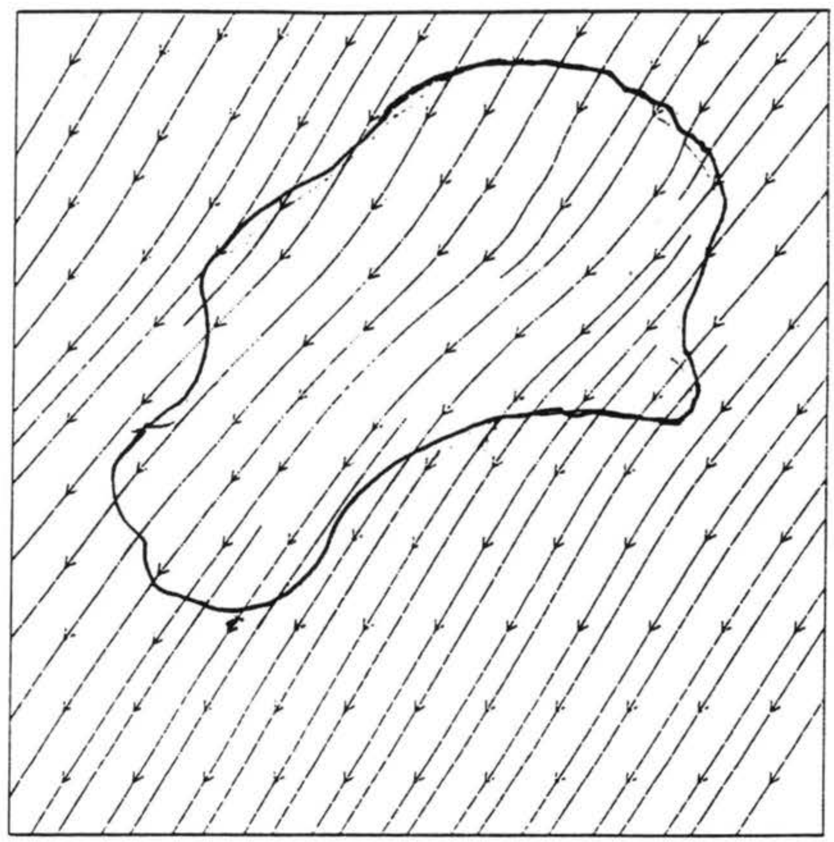

Figure 2.8: Streamlines at 1491m over Porto Santo. The black outline is the island.

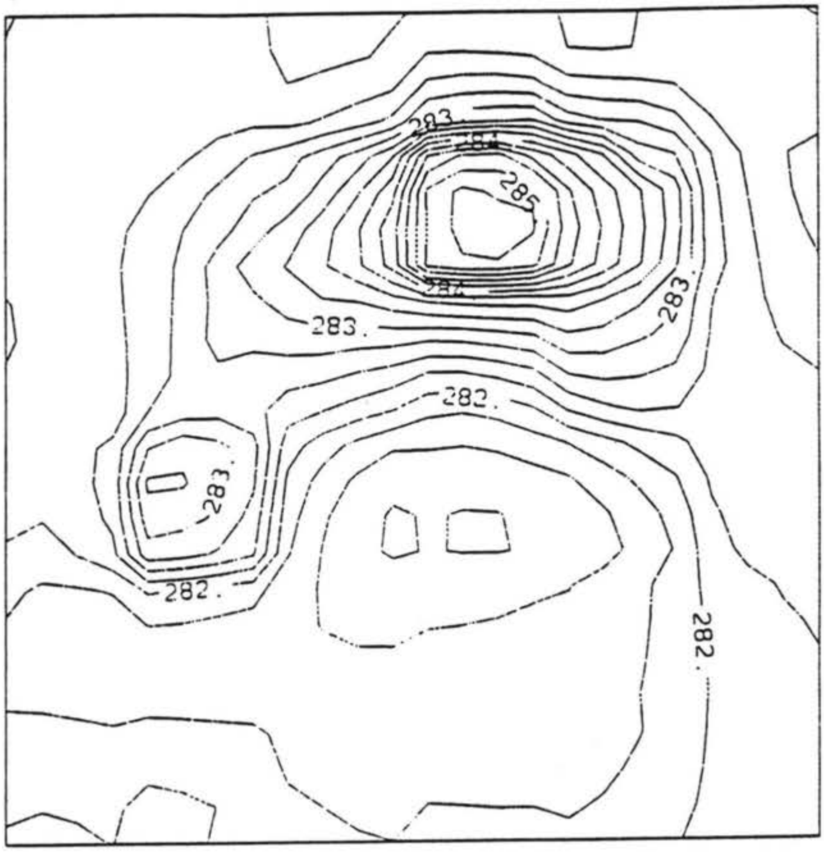

Figure 2.9: Contours of temperature over Porto Santo at 1491m. This can be overlayed on figure 2.8. Contour interval is 0.3 deg K.

induce a cyclonic bend in the streamlines. This is exactly what is seen in the streamline plots.

To further substantiate that a thermally-driven wind may be responsible, it must be shown that this temperature pattern exists for all the levels between 1000m and 1900m and that it does not exist above and below these levels. To help demonstrate this, transects through the site from north to south were plotted clearly depicting temperature changes over the island for different heights (Figures 2.10a-b); These again support the hypothesis. Below 900m, there is very little variation in temperature over the island. Between 900m and 1900m, the horizontal temperature shows a significant increase on the north side of the island and a significant decrease just south of this. Above this, there is little or no variation in temperature along this transect.

Thus, due to the evidence suggesting a thermally-driven wind being responsible for the deviations in wind speed and direction between 1000m and 1900m over the island, one can confidently conclude that the deformation of the horizontal temperature field by the island plays a role in determining the model-produced structure of the wind field. This does not rule out, however, that a wave phenomenon is also taking place.

While evidence for a thermally-driven wind being responsible for this effect is strong, there is also substantial evidence to indicate that a gravity wave is present. If a gravity wave is responsible, the wind and temperature fields should tilt with height and the phase speed of these tilting surfaces must be the opposite direction to the prevailing winds. Thus, in order for a northerly wind striking the topographic barrier to produce a gravity wave, the following must be true (Holton, 1992):

1. The atmosphere must be statically stable
2. The features of the wave must shift upstream with height.
3. The vertical wind and temperature fields must slope into the wind with height.

Below the level of the inversion, the lapse rate is slightly higher than the dry adiabatic lapse rate and is thus statically stable. Through the

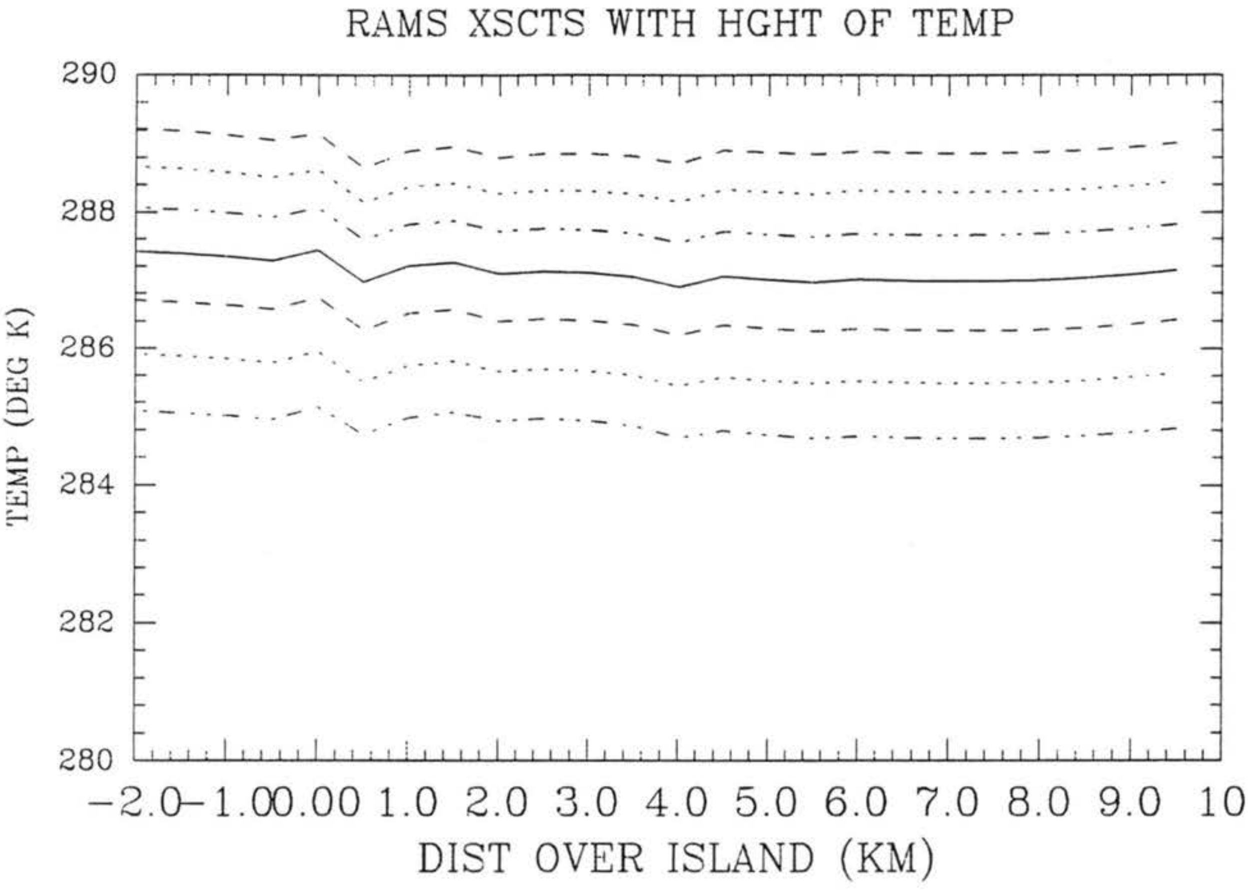

Figure 2.10a: Cross sections through the measurement site of temperature at various heights. Negative distances refer to upwind of the island. The island begins at 0.0km and extends to 5.5km; The lines are from top to bottom- 76m, 134m, 198m, 267m, 344m, 429m, 521m.

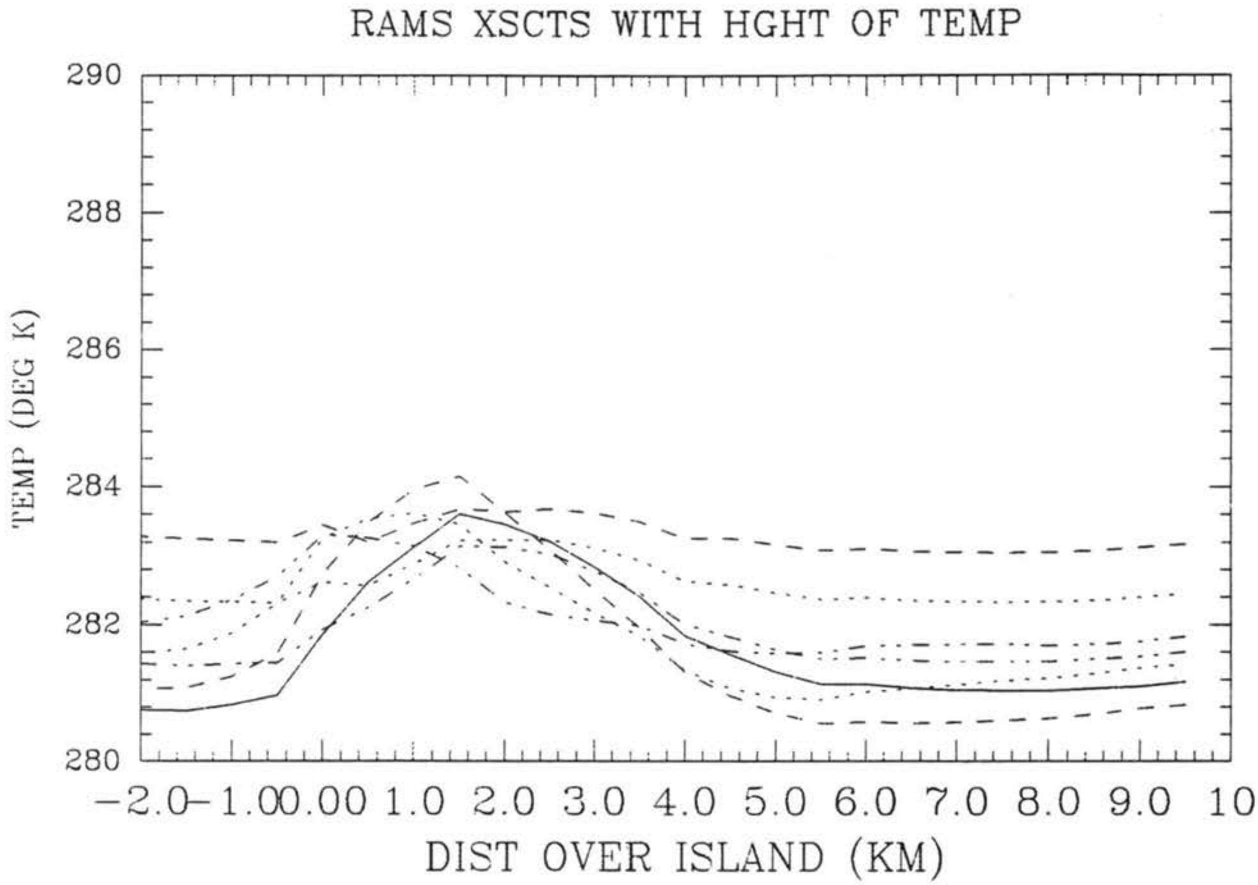

Figure 2.10b: Same as 2.10a but for higher levels; Upper dashed-736m, upper dotted-860m, lower double dashed-996m, lower solid-1145m, lower dashed-1310m, lower dotted-1491m, upper double dashed-1690m.

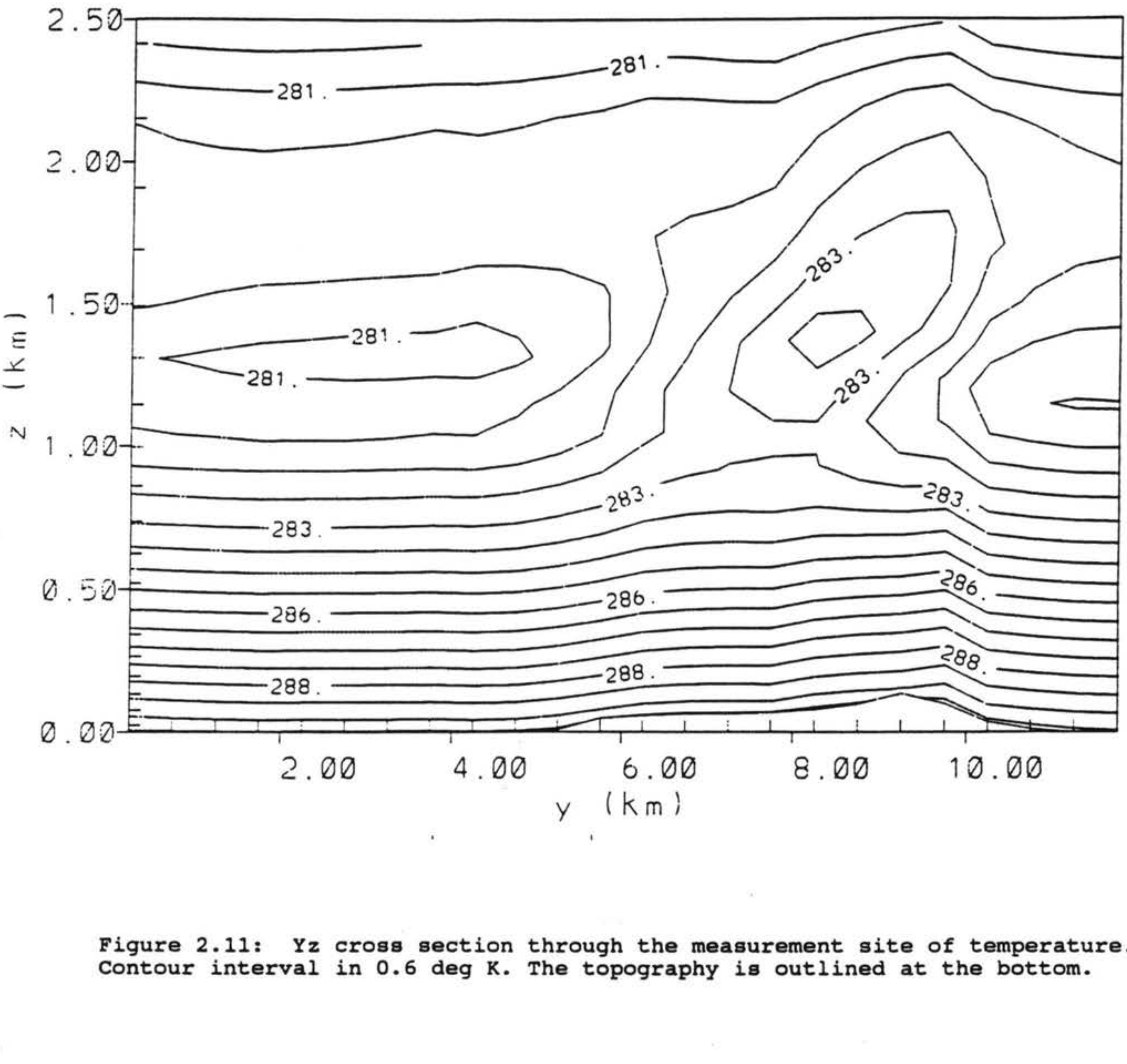

Figure 2.11: Yz cross section through the measurement site of temperature. Contour interval in 0.6 deg K. The topography is outlined at the bottom.

inversion, the atmosphere is always statically stable. Thus, criteria number one is established at least through the 2km level.

Upon examination of the wind speed transects through the measurement site (Figure 2.3b), it is clear that between 600m and 2000m, the maximum wind speed location shifts upwind with height. Thus, at upper levels, criteria number two is also satisfied. Below this, mesoscale wind flow induced by the island's topography may interfere with the location of the wind speed maximum and mask the existence of the gravity wave.

Criteria three is also satisfied. Figure 2.2 shows that the vertical velocity fields have a slope which tilts toward the wind with height. In addition, Figure 2.11 shows that the temperature fields also have this sloping structure close to the cliff.

While the thermally-driven wind argument is stronger in that the effect is seen at exactly the levels between 1000m and 1900m,- the levels where the wind patterns change in nature- there is most assuredly a gravity wave phenomena also taking place. Most likely, it is a combination of the two effects which sum up to account for the change in the nature of the wind fields through this discrete level- between 1000m and 1900m.

2.4. EXTENT OF ISLAND'S INFLUENCE ON WIND

At this point, it is of interest to note that all streamline plots over the smallest grid's domain show the wind direction vectors upwind and downwind of the island to be parallel. This will be discussed more later on, but gives us a preview into the extent of island-induced measurement contamination in the horizontal.

We are now ready to address the following major questions:

1. To what vertical and horizontal extents are the island's effects on the wind fields felt?
2. How do the vertical profiles of wind speed and direction differ over the open ocean, just upwind of the island, over the island, over the highest peak on the island, and downwind of the island?

And, how much have each of these changed compared with their homogeneous initialization?

2.4.1. VERTICAL AND HORIZONTAL EXTENT OF ISLAND'S INFLUENCE

To examine the vertical and horizontal effects of the island's influence, five locations were chosen. The first was over the open ocean 100km upstream of the island. This location was used as a reference point. Certainly, that far away from the island, the island has no influence. Thus profiles from this location represent accurately the changes that would have occurred and been measured of a pure marine environment without island contamination. The second location will be referred to as "upwind of the island". It is 2.0km upwind of the island. The third location referred to as "downwind of the island" is 3.0km downwind. The measurement site is the fourth location; It is situated in the center of the island east-west but is 0.5km south of the northern edge of the island. Finally, the "highest peak point" is the fifth location. It represents a 500m peak located in the center of the island approximately 2.5km east and 0.5km south of the measurement site (Figure 1.1).

It is important to note here the way the model treats a variable if the model level in question is lower than the height of the terrain. In these cases the model takes the value of the lowest point above the terrain and extrapolates downward. The elevation of the site is approximately 100m and the elevation of the peak is 500m. Thus, the values of data points below these levels do not hold much meaning.

Now, to address the aforementioned questions, horizontal cross-sections of the standard deviation of wind speed and wind direction were calculated and plotted. The method used to obtain a standard deviation value for each of the five desired grid locations was as follows: Five values were used for each calculation- the grid point value itself and grid point values immediately north, east, south, and west of the point desired. An average and a standard deviation were calculated for these 5 grid points and this value was assigned to the center point. In this manner, the variability of wind speed and direction over a small horizontal area of the island could be seen as well as the sections of the island that were most disturbed at a given height. Plots of standard deviation with height for a given x-y point such as the field site depict the vertical extent of the island's influence on the variability of wind fields in the horizontal.

On initial inspection, horizontal cross-sections of wind speed standard deviation show the greatest differences around the peaks on the island (Figure 2.12). This result is consistent for all heights. As one would expect, the values themselves decrease with height over the whole island as the island's influence diminishes. Wind direction plots exhibit a similar feature. The greatest deviation in horizontal wind direction is in the vicinity of the peaks for all heights and the values overall also decrease with height.

Line plots of standard deviation with height for wind speed and direction were also plotted for the five points- over the open ocean, upwind of the island, over the experiment site, over the tallest peak on the island, and downwind of the island (Figures 2.13a-e; 2.14a-e). Over the open ocean, there is negligible variation of both wind speed and direction (Figures 2.13a; 2.14a). Thus, one suspects that for the other four grid points near the island that observed variability is due to the island's influence.

Just upwind of the island, the variability in wind speed near the surface is small- approximately 0.1 m/sec, decreasing to near zero at one kilometer, then increasing to just over 0.1 m/sec and decreasing back to near zero again for higher levels (Figure 2.13b). This variability, although small, is significant compared to the open ocean, and is most likely due to the presence of the island. It is of interest here to note the increase in variability here at the 1.3km level. At points closer to the island, where the island's influence is stronger, this feature is retained and becomes stronger. This will be commented on later. Likewise, wind direction variability shows a pattern just upwind of the island which is small in magnitude (Figure 2.14b); approximately one degree at low levels, decreasing to 0.2 degrees at 0.8km and increasing again a little above the 1km level to 0.7 degrees before decreasing back to zero. Once again this is not very

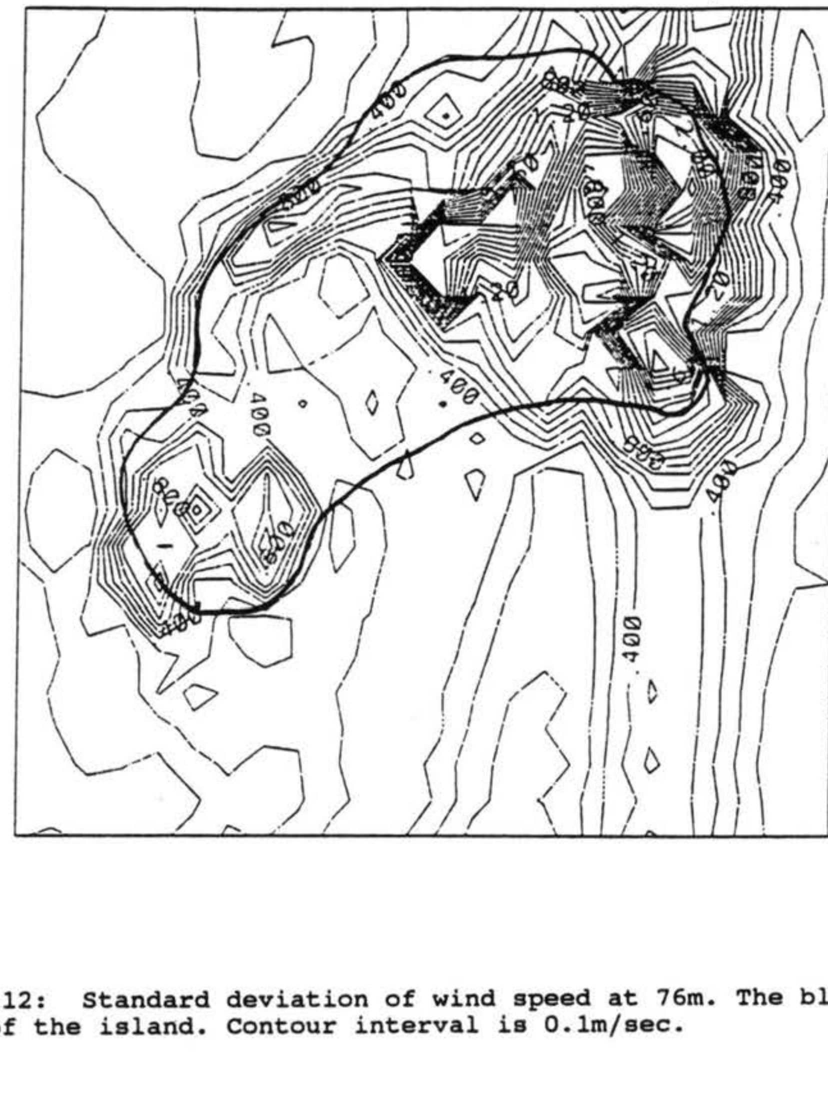

Figure 2.12: Standard deviation of wind speed at 76m. The black line is the outline of the island. Contour interval is 0.1m/sec.

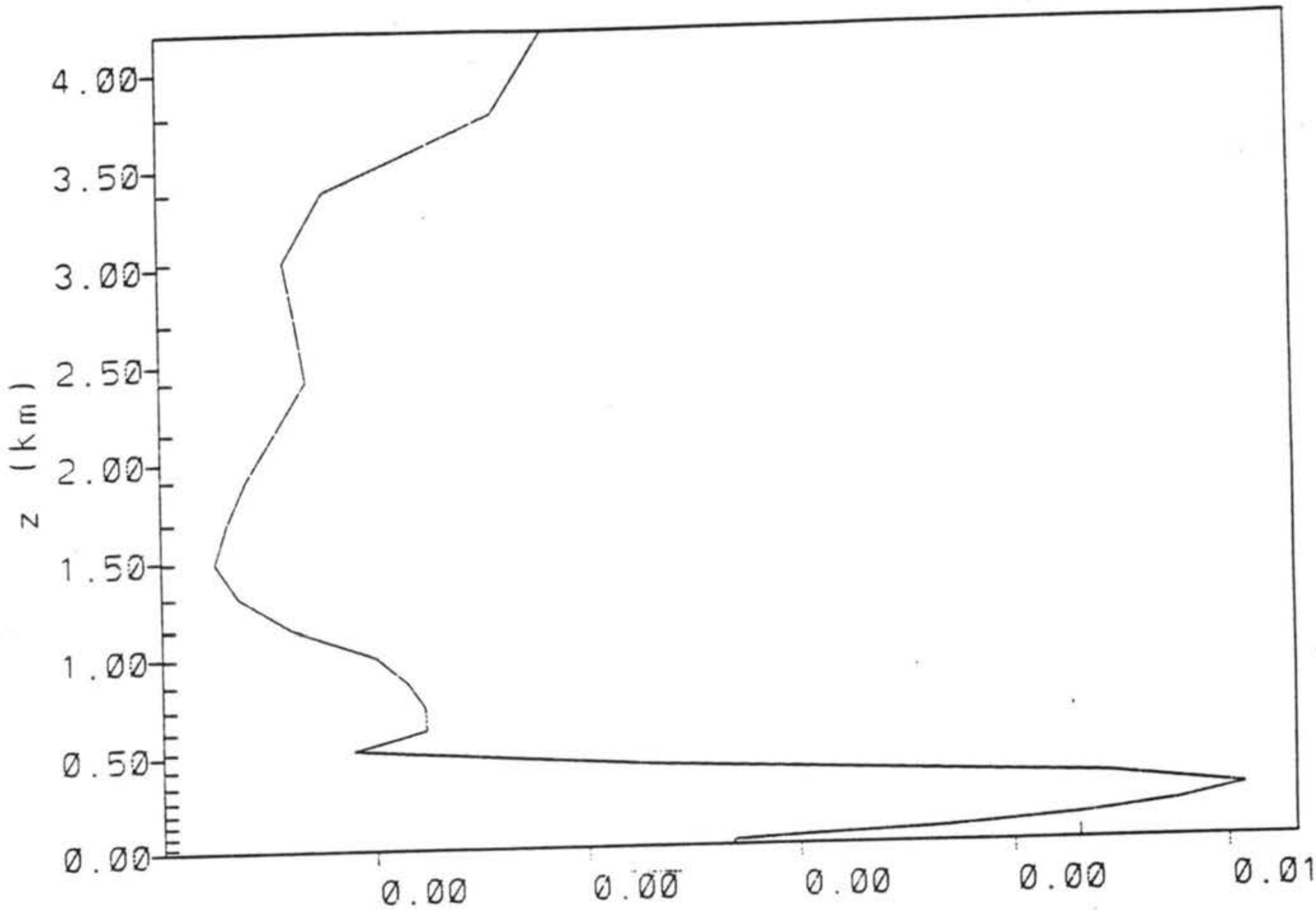

Figure 2.13a: Profile of wind speed standard deviation with height over the open ocean in m/sec.

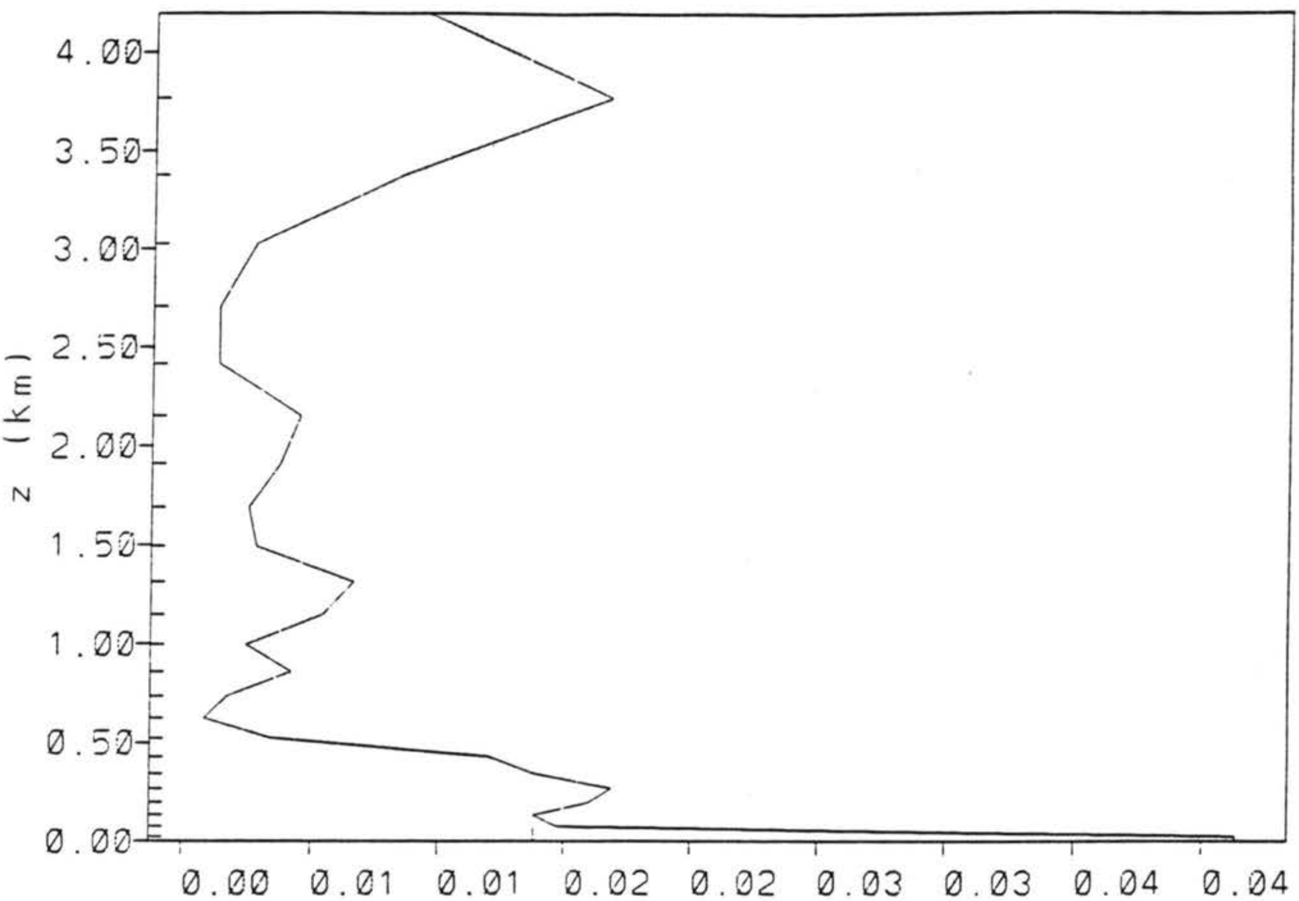

Figure 2.14a: Profile of wind direction standard deviation with height over the open ocean in degrees.

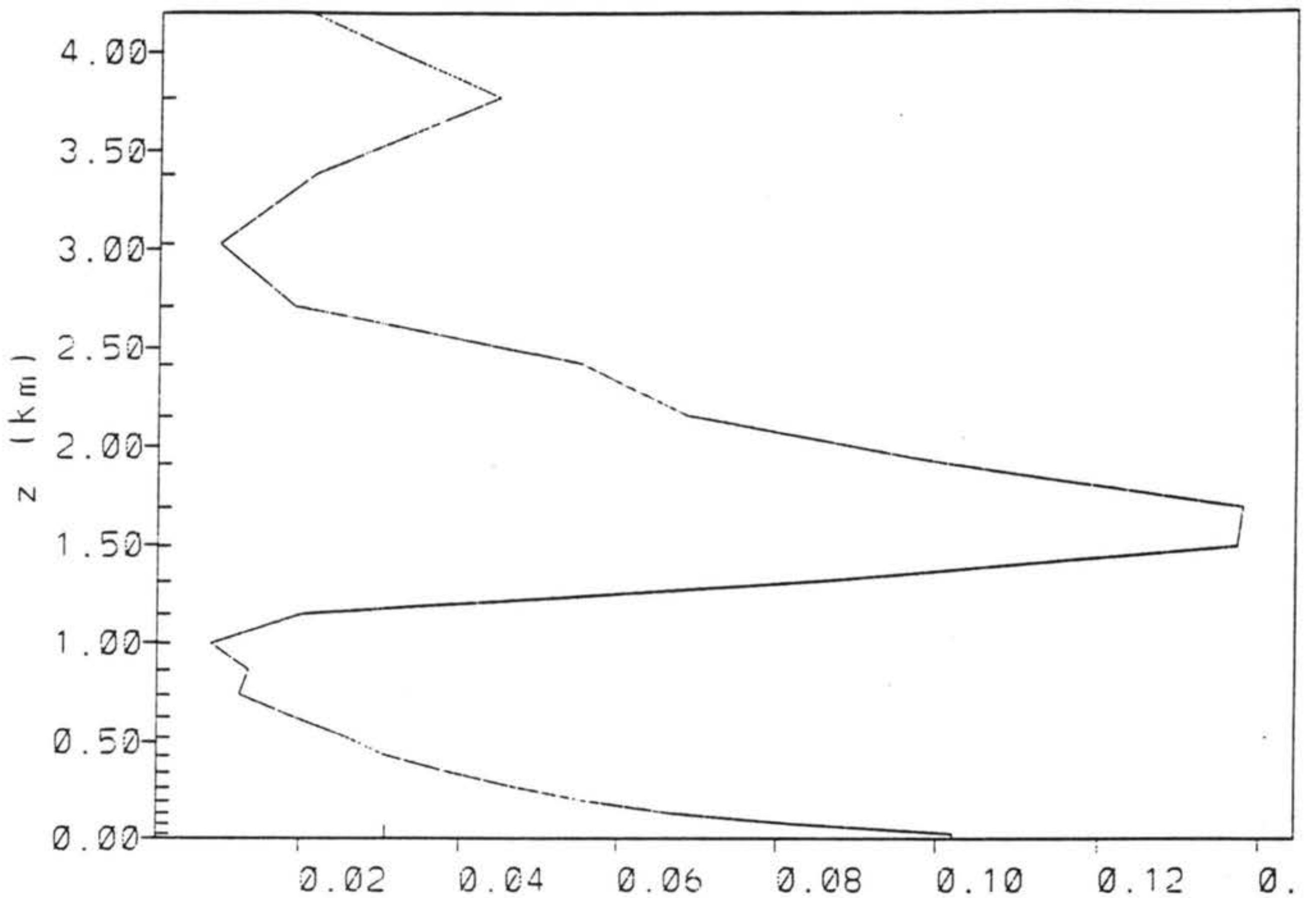

Figure 2.13b: Same as 2.13a but for a point 2km upwind of the island.

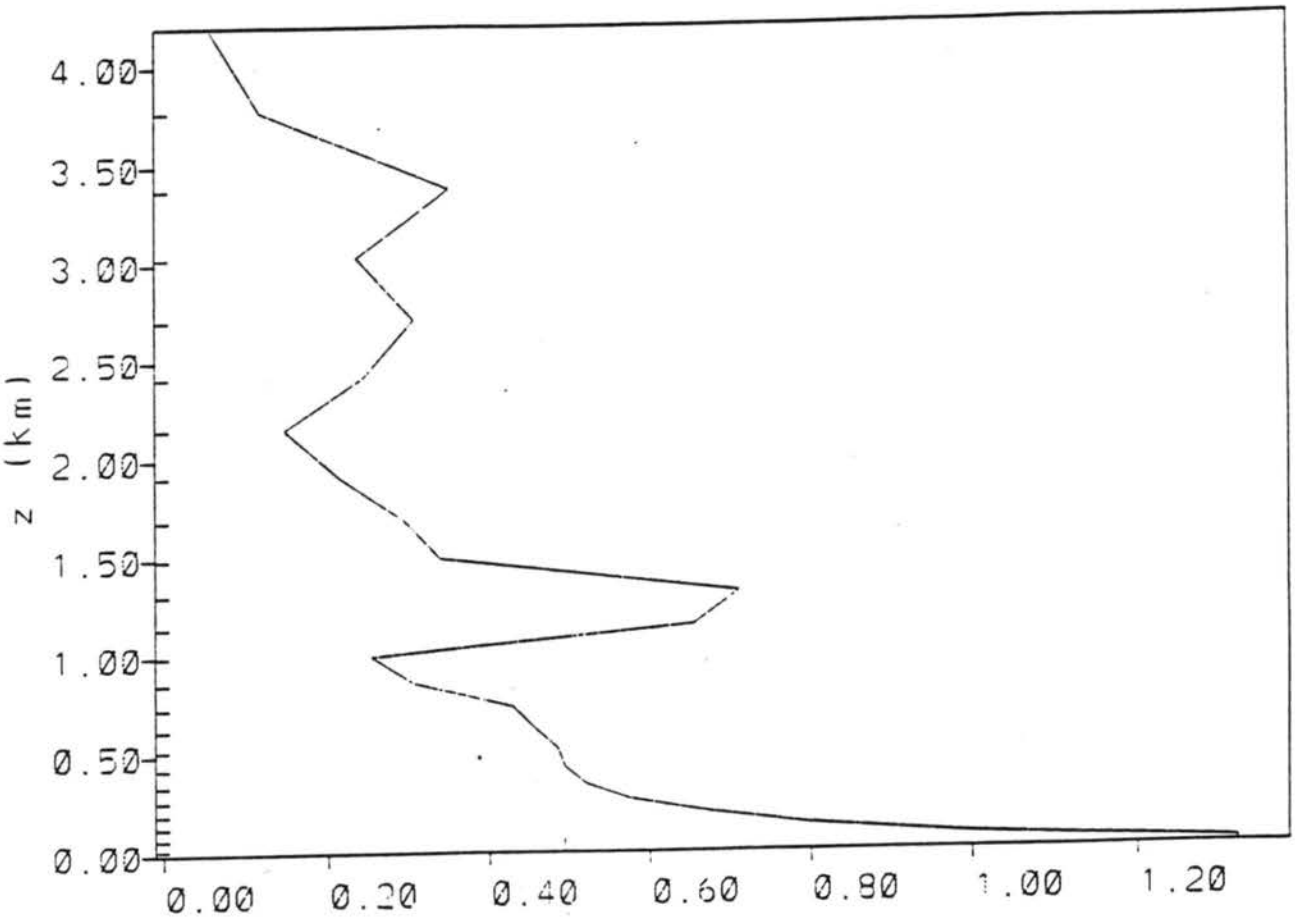

Figure 2.14b: Same as 2.14a but for a point 2km upwind of the island.

significant variability by itself but is greater than the open ocean cases and must be due to the island's influence nearby.

Over the experiment site, the plots become more interesting (Figures 2.13c; 2.14c). This is the focal point of this comparison study in order to assess the ability of measurements taken here to accurately represent the pure marine environment. In other words, the variability here can be said to be due to the island and the extent of variability can be equated to the extent of measurement contamination. The plots of wind speed deviation indicate deviations of 0.8 m/sec near the ground, decreasing to near zero at just under 1km, and once again show a relative maximum at 1.3km before decreasing back to zero. The wind direction deviations near the ground are about 1 degree and at 1.3km the wind direction deviation increases to more than 3.5 degrees. Clearly something is occurring in this layer to give such consistent increases in variability. For both of these plots, there appears also to be another minor region of standard deviation increase. This occurs at approximately 3.6km off the ground and its magnitude is less than half that of the 1.3km maximum.

To no surprise, over the highest peak on the island, the greatest degree of variability is found at all heights (Figures 2.13d; 2.14d). At levels near zero, deviations of six degrees are found in wind direction and deviations of over 2m/sec in wind speed. As explained, however, these levels are below the ground and are calculated by extrapolation downward. Thus, no weight should be given to any value below 500m- the elevation of the peak. The maxima at 1.3km are also present here with values of 5 degrees and 1m/sec. In addition, the secondary peak at 3.5km observed over the site is also observed here. Similar to the situation over the site its magnitude is less than the 1.3km maximum- approximately 4 degrees and 0.04m/sec. There appears to be a definite trend of variability with height within the range of the island's influence regardless of the location. The magnitudes of this variance, however varies.

Finally, downwind of the island, the deviations are much smaller in magnitude and a slightly different pattern appears. The wind direction

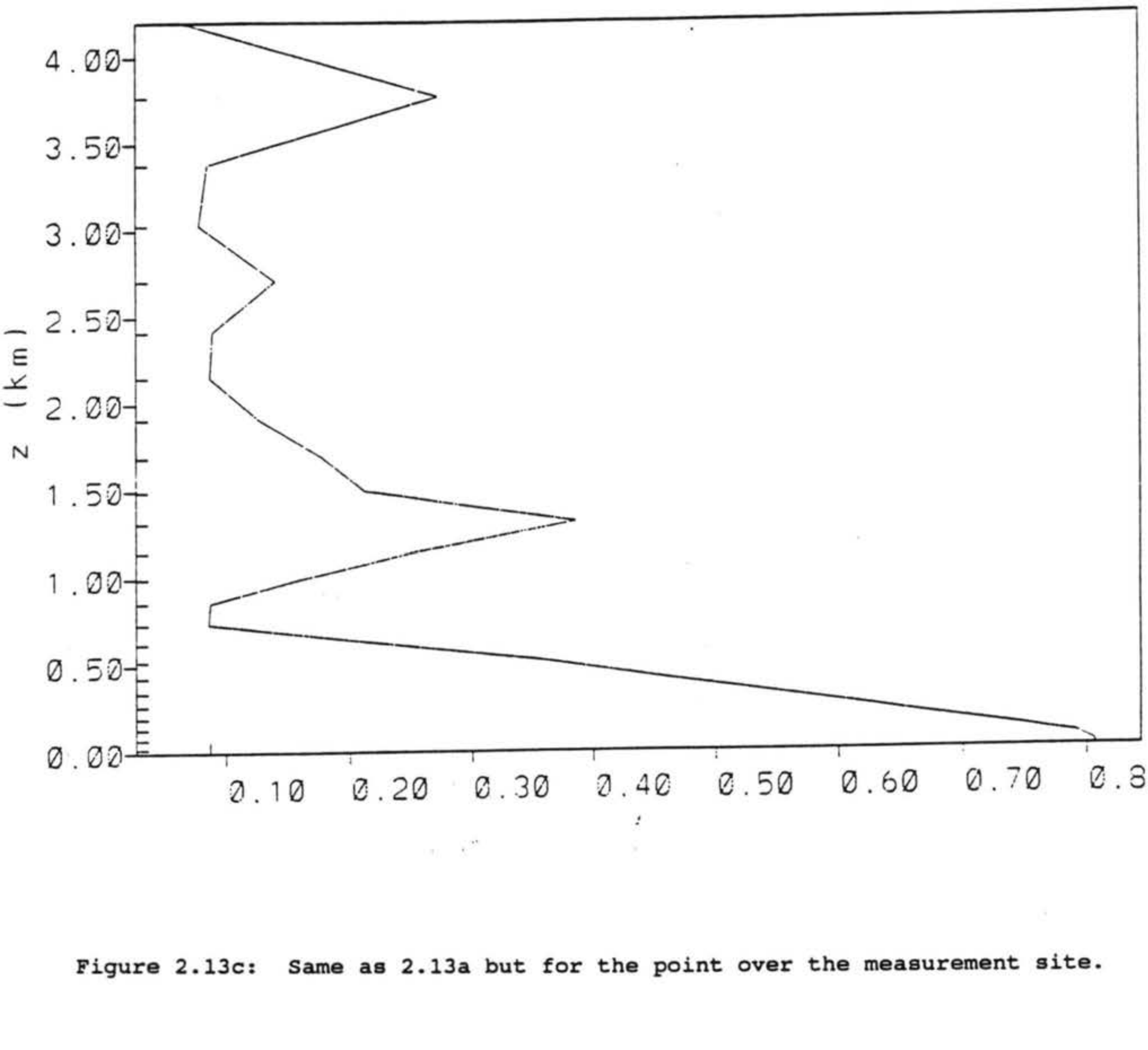

Figure 2.13c: Same as 2.13a but for the point over the measurement site.

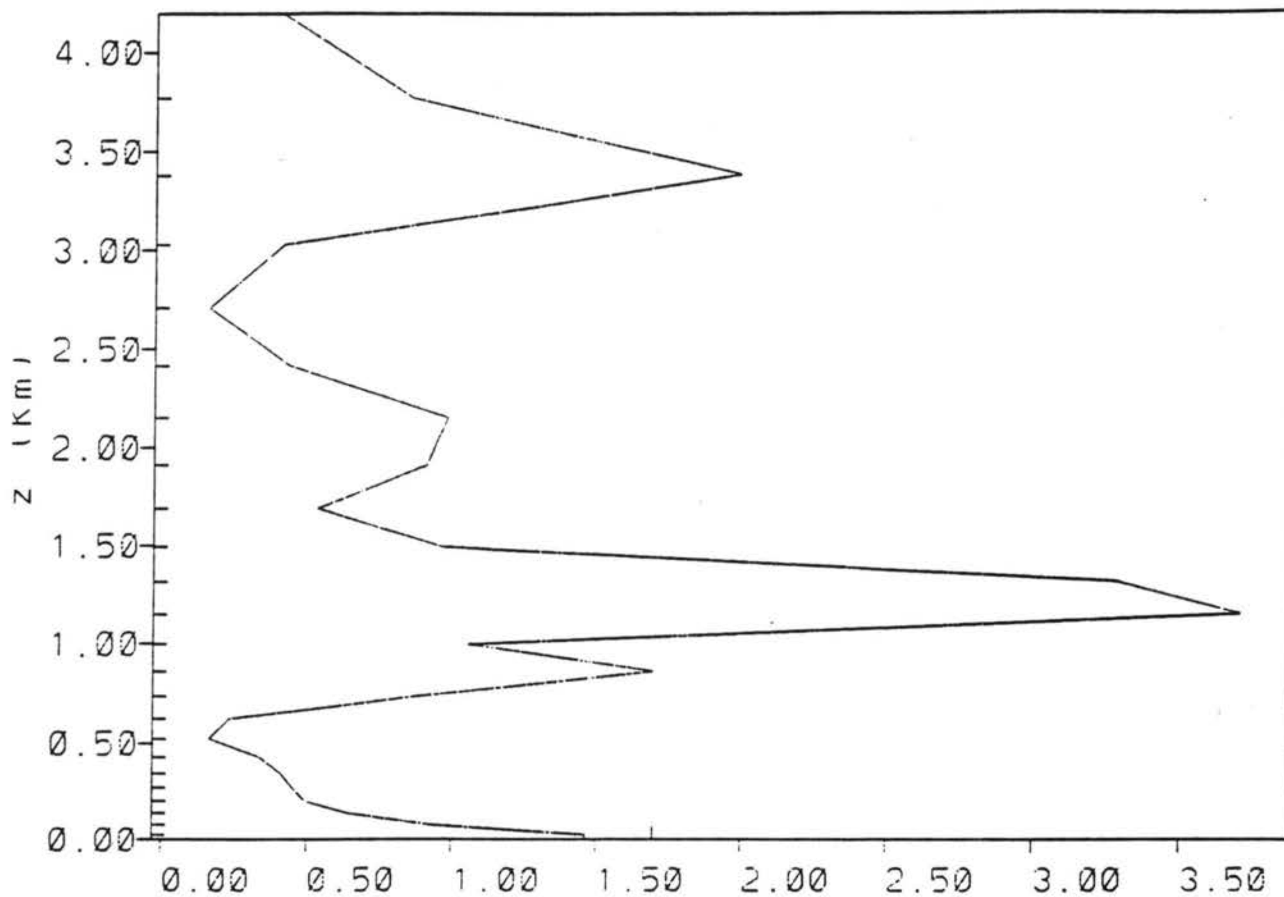

Figure 2.14c: Same as 2.14a but for the point over the measurement site.

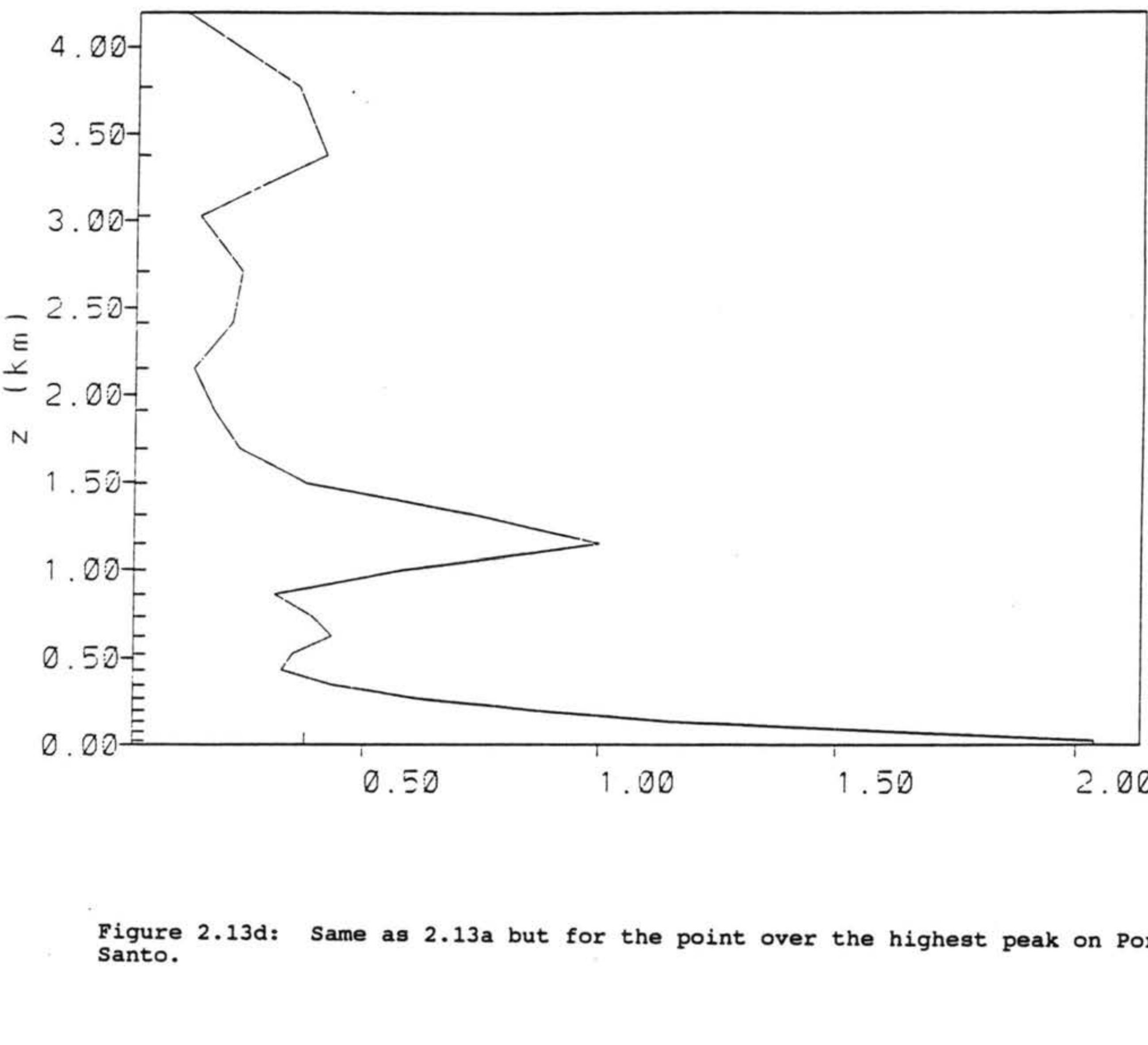

Figure 2.13d: Same as 2.13a but for the point over the highest peak on Porto Santo.

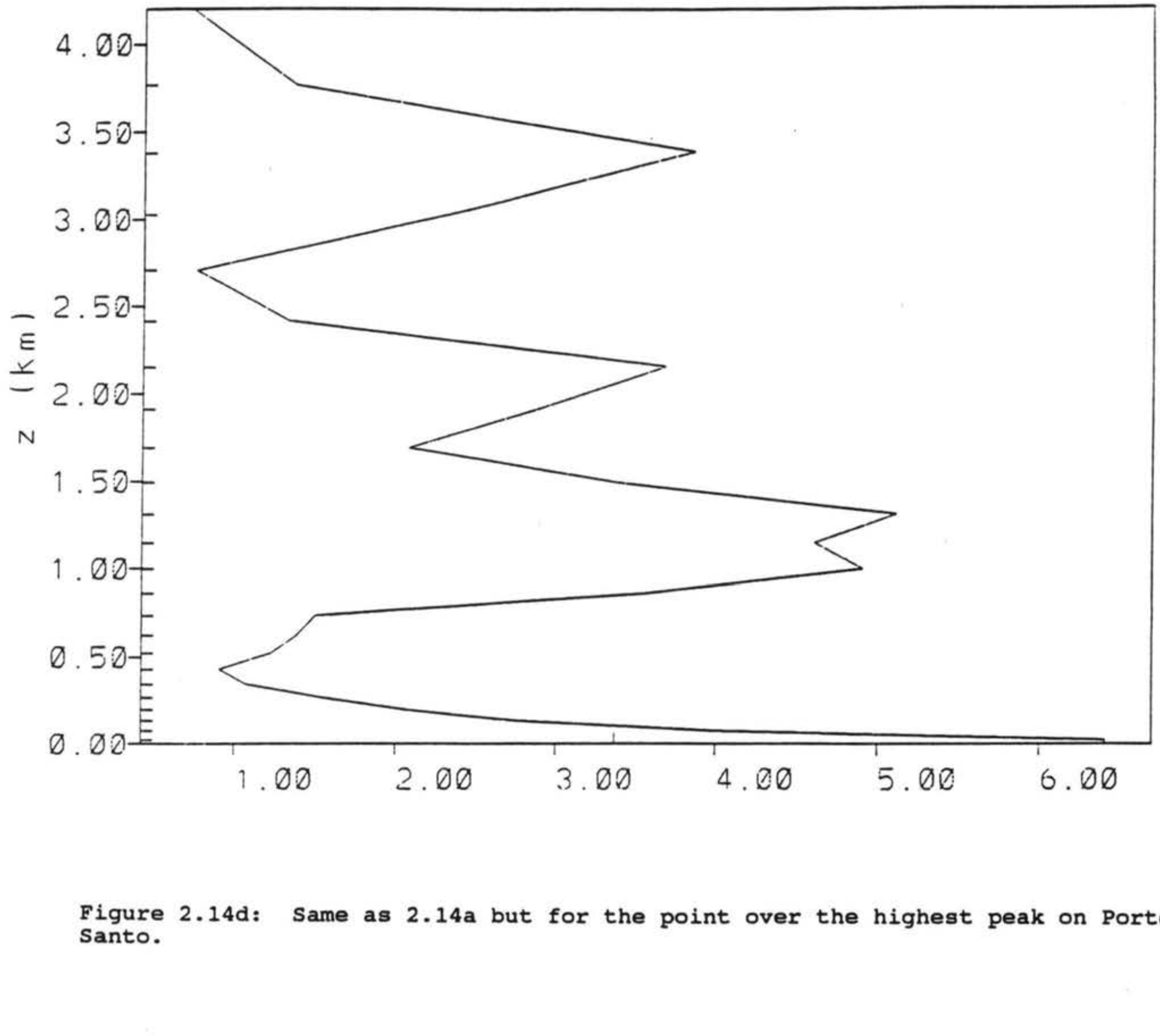

Figure 2.14d: Same as 2.14a but for the point over the highest peak on Porto Santo.

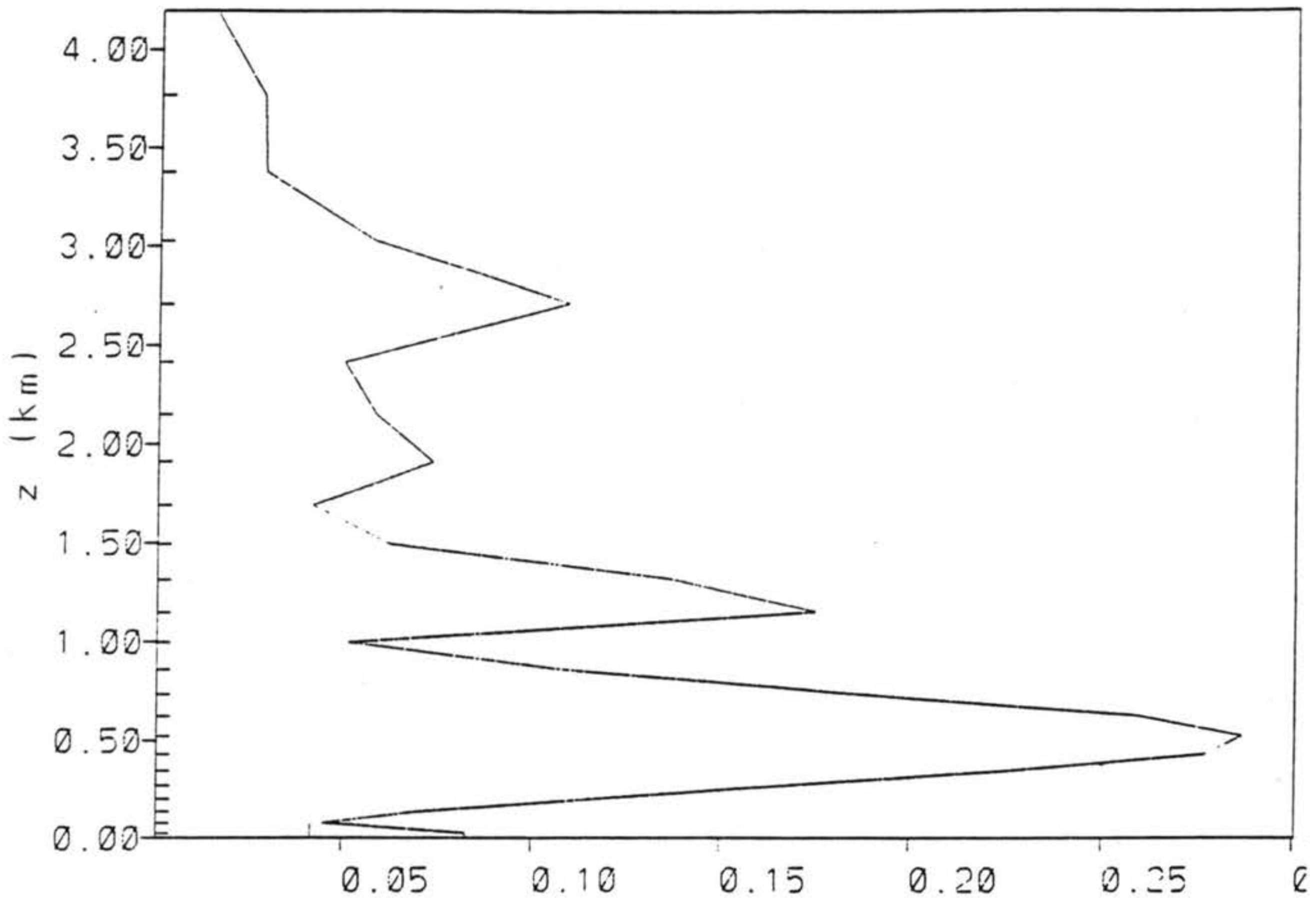

Figure 2.13e: Same as 2.13a but for a point 3km downwind of the island.

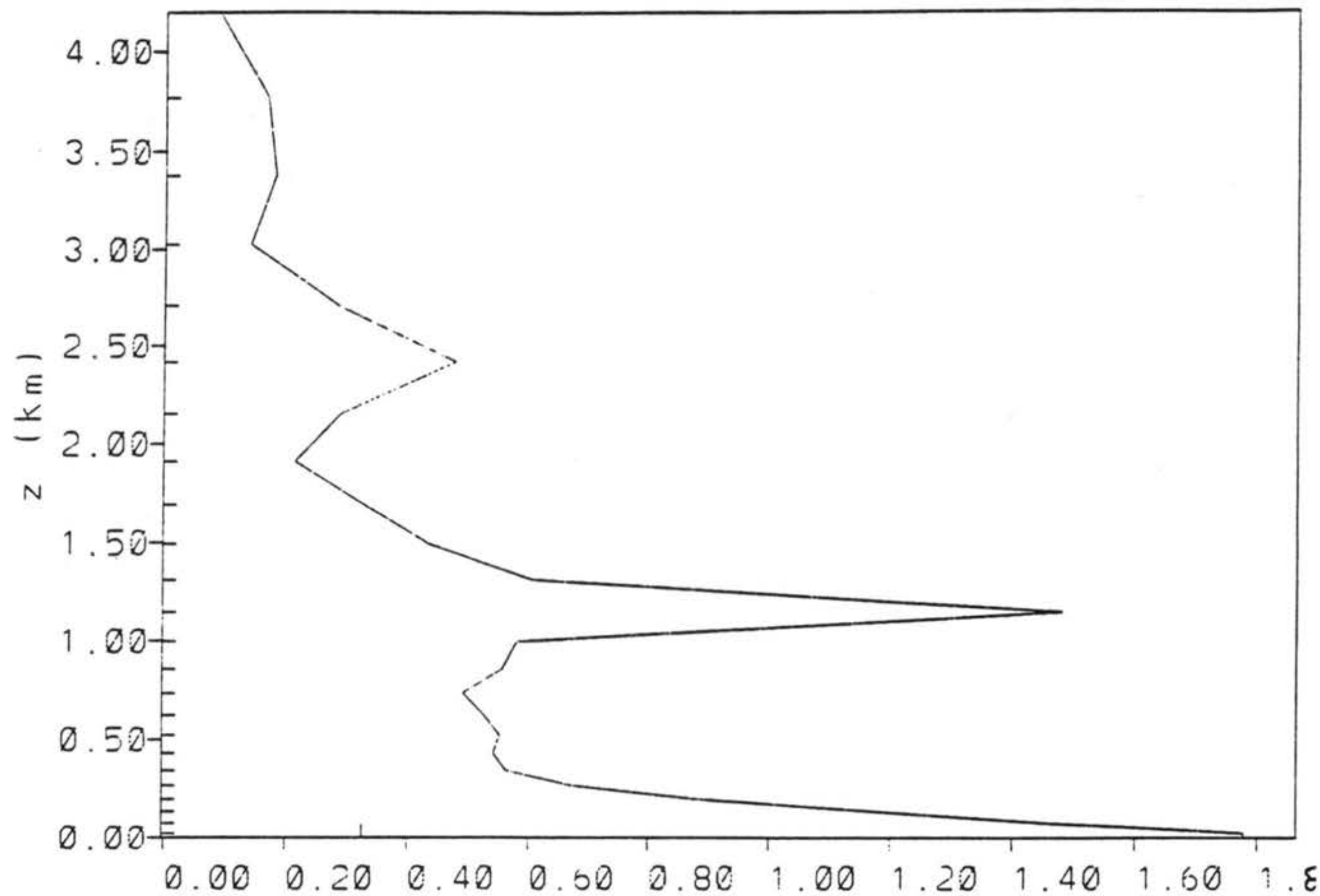

Figure 2.14e: Same as 2.14a but for a point 3km downwind of the island.

standard deviation is high near the ground- about 1.8 degrees, exhibits a maximum of 1.5 degrees at the 1.3km level and no secondary peak is found at 3.5km (Figure 2.14e). For wind speed, however, the deviation is very small near the ground- about .05m/sec and increases to a maximum at .5km of .28m/sec (Figure 2,13e). The relative maximum at 1.3km is present here and no secondary 3.5km maximum is observed. It appears that downwind of the island, the effect of the island is not felt above the 1.2km level.

Near the ground, there is a fairly consistent maxima in the standard deviations of the values covering a given horizontal area. This is obviously due to the influence of the surface on the winds. Over the island these magnitudes were greatest due to the greatest surface roughness and terrain changes. The relative maximum at 1.3km is not as easy to explain, however, and the secondary maximum at 3.5km over the island is even more difficult to explain.

One possible explanation for the 1.3km maximum could relate to the temperature inversion over the area on this day. The level of this inversion, as indicated by rawinsonde, was approximately 1300m. The model was initialized horizontally homogeneous, but the resulting island-induced wind fields could have forced a slope relative to the horizontal of this inversion (Lavoie, 1974). Thus, it would be expected that deviations taken over an area whose surface is horizontal and through this sloping inversion would exhibit higher variability. Another explanation could be a thermally-driven wind/gravity wave combination effect near this level which has already been discussed in section 2.2. The only thing which can be said at this time of the secondary peak at 3.5km is that its values are small and it is probably a residual effect of the island. This conclusion is reached because this peak does not appear upwind of the island, over the open ocean, or downwind of the island but appears only over the island.

In summary, to answer question number one, the variability of horizontal winds near the island can be felt at levels up to 3.5km but not felt continuously. There are definite areas where the island influence is at a minimum such as between 1.4km and 3km as well as definite areas where the influence is a maxima such as near the ground and at 1.3km. The contamination of measurements at the field site is most significant at the ground for wind speed and slight at 1.3km and 3.5km. And, the contamination for wind direction is greatest at 1.3km and slight near the ground and at 3.5km. By 3km downwind or 2km upwind, the island's effects can be felt through the 1.3km level, but are not noticeable above this.

2.4.2. THE MAGNITUDES OF WIND CHANGE FROM ITS INITIALIZATION

To address the issue of the magnitude of change of winds from their initialization, an examination of vertical profiles of wind speed and direction with height were examined over the open ocean, over the site, over the highest peak, and downwind of the island. These were compared with the original profile used in the horizontally homogeneous initialization of the model grids (Figures 2.15a-b)(Tables 2.1-2.2). The latter four locations were compared to the open ocean results after 3 hours of simulation so a statement could be made concerning the actual island contamination. This assumes that the open ocean represents pure marine influenced conditions. For consistency here, the results will always be discussed in terms of the original initialized value minus the value of the location of interest.

The purpose of this examination was to show how each of these five points changed over the three hour period and to intercompare them in an effort to corroborate the previous results indicating the extent of the island's influence. Also, from this part of the study, a statement can be made about the horizontal extent of the island's influence as well as the difference between the island's influence over different terrain heights.

The wind direction profiles for the open ocean case and the upwind of the island case show a structure almost identical to the original initialization. Over the site, however, the structure has changed significantly over the three hours. The wind shifted from 8 degrees at the ground to 348 degrees. It crossed back to northeasterly from 500m to 900m which is closer to the original sounding but then remained northwesterly above

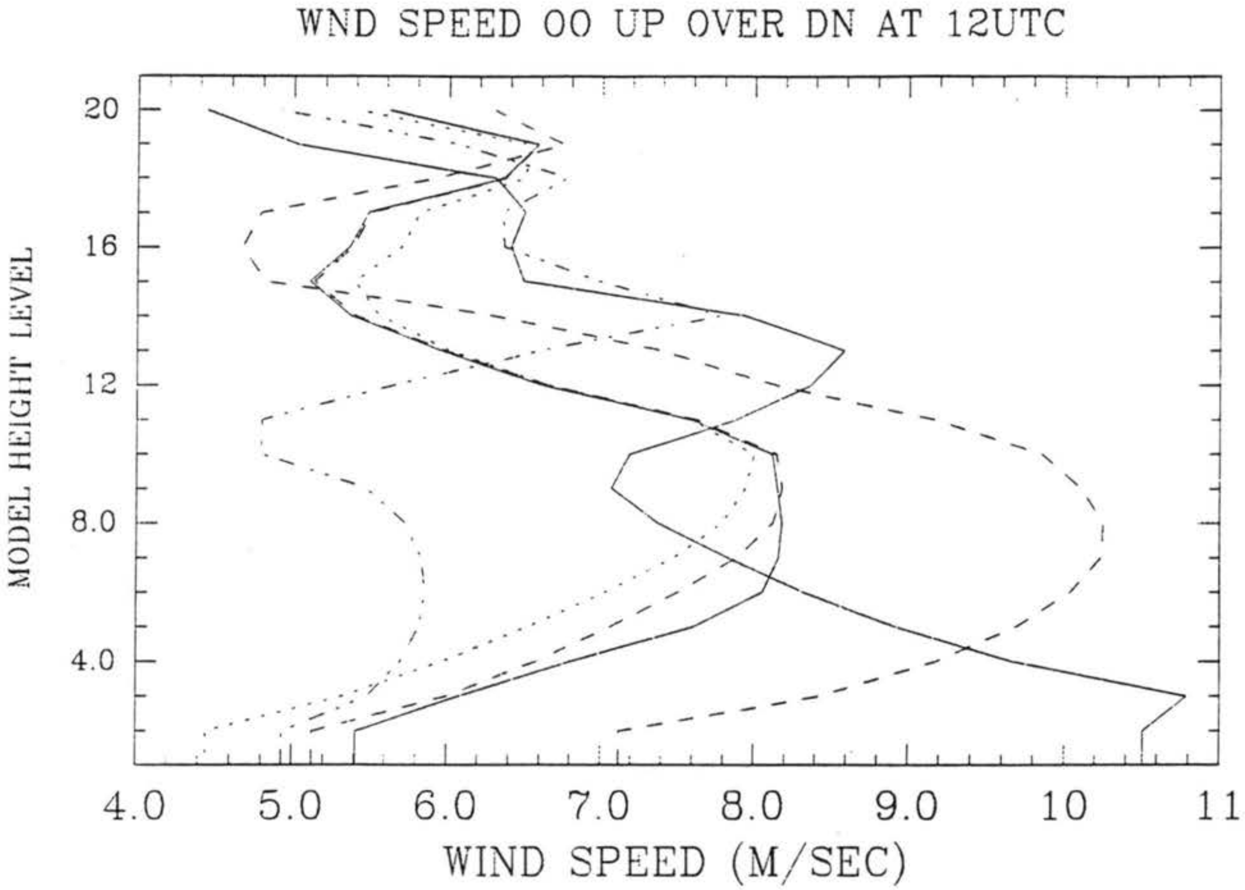

Figure 2.15a: Comparison of wind speed profiles between the original sounding (left solid line); over the open ocean (left dashed line); 2km upwind of the island (dotted line); over the measurement site (double dashed line); over the highest peak on the island (right solid line); and 3km downwind of the island (right dashed line).

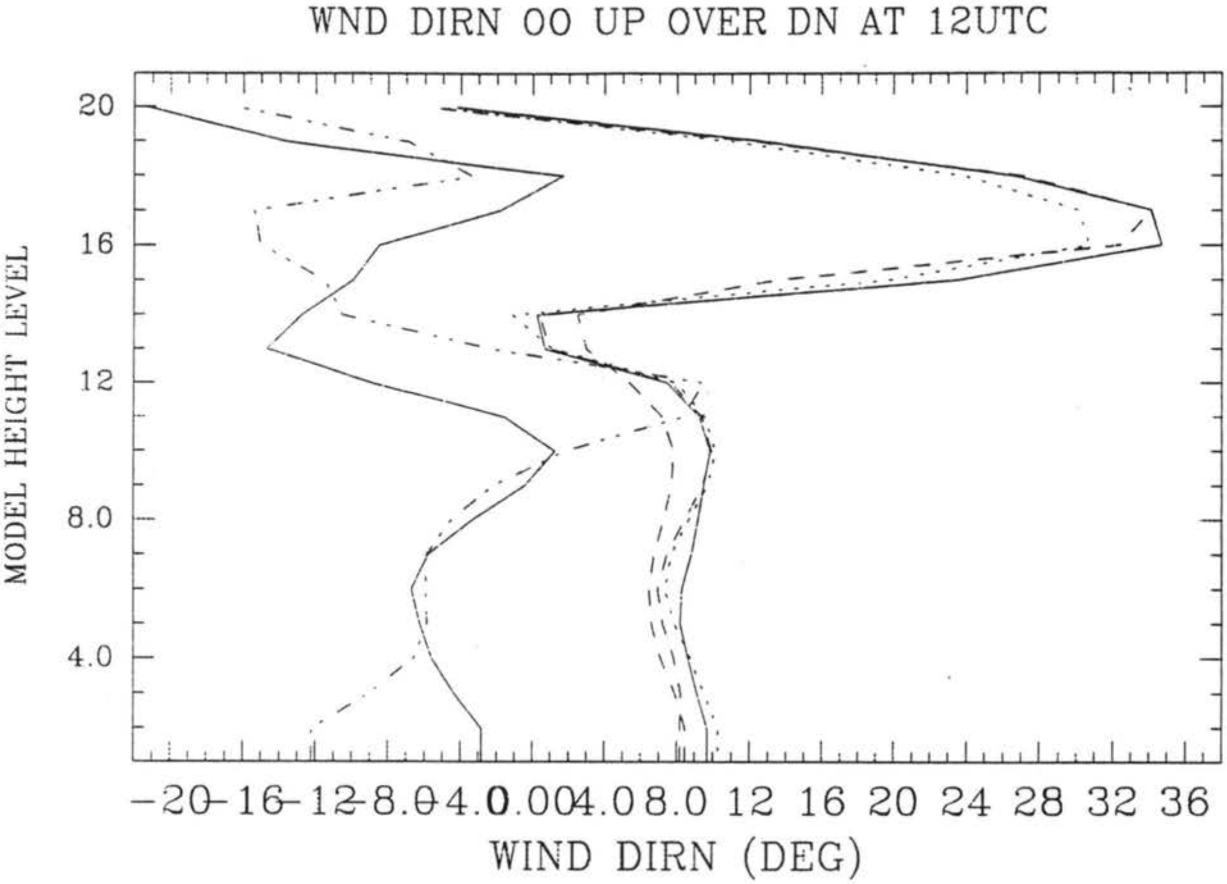

Figure 2.15b: Comparison of wind direction profiles between the original sounding and over the open ocean (right solid line); 2km upwind of the island (dotted line); over the measurement site (double dashed line); over the highest peak on the island (left solid line); and 3km downwind of the island (dashed line).

LEVEL	O-OO	O-UP	O-ST	O-PK	O-DN
1	0.28	0.96	0.47	-5.10	-1.71
2	0.28	0.96	0.47	-5.10	-1.71
3	0.08	0.76	0.59	-4.71	-2.36
4	0.23	0.83	1.10	-2.87	-2.37
5	0.54	1.08	1.79	-1.31	-2.09
6	0.55	1.02	2.19	-0.27	-1.98
7	0.27	0.68	2.33	0.33	-2.07
8	0.06	0.39	2.45	0.81	-2.07
9	-0.03	0.21	2.68	1.08	-1.96
10	-0.03	0.12	3.32	0.93	-1.74
11	-0.03	0.01	2.80	-0.27	-1.58
12	-0.03	-0.04	0.96	-1.75	-1.53
13	-0.02	-0.05	-0.66	-2.64	-1.44
14	-0.03	-0.19	-2.41	-2.57	-0.93
15	-0.03	-0.29	-1.88	-1.38	0.28
16	-0.02	-0.34	-1.00	-1.04	0.69
17	-0.02	-0.33	-0.87	-1.01	0.69
18	-0.01	-0.14	-0.42	0.05	0.45
19	-0.01	0.06	0.51	1.56	-0.17
20	0.00	0.20	0.70	1.17	-0.68

LEVEL	OO-UP	OO-ST	OO-PK	OO-DN
1	0.68	0.19	-5.38	-1.99
2	0.68	0.19	-5.38	-1.99
3	0.68	0.51	-4.79	-2.43
4	0.60	0.87	-3.09	-2.60
5	0.54	1.25	-1.85	-2.63
6	0.47	1.64	-0.82	-2.53
7	0.41	2.05	0.05	-2.35
8	0.33	2.40	0.75	-2.13
9	0.24	2.71	1.11	-1.93
10	0.15	3.35	0.96	-1.71
11	0.04	2.83	-0.24	-1.54
12	-0.01	0.99	-1.72	-1.49
13	-0.03	-0.63	-2.62	-1.41
14	-0.16	-2.38	-2.54	-0.90
15	-0.26	-1.85	-1.36	0.31
16	-0.32	-0.98	-1.02	0.71
17	-0.32	-0.85	-1.00	0.71
18	-0.13	-0.41	0.06	0.46
19	0.06	0.52	1.57	-0.16
20	0.21	0.70	1.18	-0.68

Table 2.1: Top: Wind speed deviation from initialization value after 3 hours of simulation time; O- original initialization value; OO- value over open ocean; UP- 2km upwind of the island; ST- over the measurement site; PK- over the highest peak on the island; DN- 3km downwind of the island. Level corresponds to model height level. Bottom: same as top but deviation from open ocean value.

LEVEL	O-OO	O-UP	O-ST	O-PK	O-DN
1	1.49	-0.61	21.89	12.53	1.23
2	1.49	-0.61	21.89	12.53	1.23
3	0.89	-0.40	18.11	13.47	1.23
4	0.78	-0.13	15.21	14.20	1.52
5	0.97	0.32	14.02	14.43	1.59
6	1.34	0.93	14.20	14.99	1.81
7	1.35	1.11	14.67	14.58	2.06
8	0.74	0.52	13.67	12.49	1.91
9	0.07	-0.21	11.66	9.93	1.79
10	-0.07	-0.31	8.07	8.61	2.03
11	-0.14	-0.29	0.99	10.81	2.07
12	-0.21	-0.53	-2.02	16.39	2.08
13	-0.26	-0.42	2.89	15.39	-2.31
14	-0.15	1.35	10.77	12.98	-2.26
15	0.05	3.88	35.01	33.44	9.97
16	0.01	3.99	49.75	43.18	2.29
17	-0.04	3.94	49.48	35.92	-0.02
18	-0.06	2.66	29.90	24.92	-0.43
19	-0.09	1.74	19.60	26.45	0.40
20	-0.13	1.04	12.14	17.07	1.34

LEVEL	OO-UP	OO-ST	OO-PK	OO-DN
1	-2.10	20.40	11.04	-0.27
2	-2.10	20.40	11.04	-0.27
3	-1.30	17.22	12.58	0.34
4	-0.92	14.42	13.42	0.73
5	-0.65	13.06	13.46	0.63
6	-0.41	12.86	13.65	0.47
7	-0.24	13.32	13.23	0.71
8	-0.22	12.93	11.75	1.17
9	-0.28	11.59	9.86	1.72
10	-0.23	8.15	8.68	2.10
11	-0.15	1.13	10.95	2.21
12	-0.32	-1.81	16.60	2.29
13	-0.16	3.15	15.65	-2.05
14	1.50	10.91	13.12	-2.11
15	3.83	34.96	33.39	9.93
16	3.98	49.74	43.17	2.29
17	3.98	49.52	35.96	0.02
18	2.73	29.97	24.98	-0.36
19	1.83	19.69	26.54	0.49
20	1.17	12.27	17.20	1.47

Table 2.2: Same as table 2.1 but for wind direction.

900m where the original sounding turned more easterly. The greatest disparity was at approximately 1500m where the original direction was 32 degrees and after three hours was 346 degrees. From 700m to 1000m, there is an area of good agreement.

Over the highest peak on the island, the wind direction profile does something interesting. Although in magnitude the values are quite different than the original, its shape is almost identical. The difference between the wind direction with height remain fairly constant. Another interesting thing to note is the downwind profile. It is almost identical to the original sounding indicating either that the island has no influence downwind or the island has an immediate impact downwind which goes away at some point to a steady state resembling the original. In other words, downwind of the island, there may be a tendency of negative response to disturbances. The streamline plots from the previous section support this as well showing a change back to the original wind direction downwind of the island.

For wind speed, there is more variability among the five points studied and they vary more when compared with the original sounding. Over the open ocean, again there is very little change. At levels below 425m there are some slight differences, but above this the lines are not distinguishable. Upwind of the island, there are once again differences below the 425m level. These differences are larger than for the open ocean case, about 1m/sec, but still are not too significant. There appears to be a weak island effect at lower levels 2km upwind of the island. This was also found in the last section.

It is of more interest to examine the two island points- over the measurement site and over the peak. Above both of these locations, there is a large change in the wind speed at almost all heights. Over the site, the shape of the wind speed trend with height is very similar to the original initialization below 625m although the magnitudes differ by as much as 3.32m/sec at 625m. Near the ground, the differences are the smallest- only 0.47m/sec. Another interesting thing to note is that the wind speeds are consistently lower than the original sounding over the site until the 1km level and then they become consistently higher. Thus, there is a tendency for wind speeds to decrease over the site at low levels and become amplified above the 1km level- the approximate level of the inversion. There is a slow increase in the wind speed differences from the surface to this level. Right above the 1km level, a sharp change occurs and there is a jump from a 2.8m/sec difference to -0.66 over a 250m height interval. Then at the 1200m level, another sharp change of 1.75m/sec takes place over a 150m height interval. The transitions that take place here could be due to the presence of the inversion near this level or once again a thermally-driven wind/ gravity wave combination phenomenon. Similar to wind direction, there is a range from 700m to 1000m where there is excellent agreement. This suggests that the magnitude of the effect of the island is not continuous in height.

A very radical difference can be seen over the peak. At the surface, the large differences that occur are probably a result of the model itself. The peak is 500m tall and, as explained previously, if a model grid level is below the surface, it extrapolates from the lowest level above the surface downward. Thus, the differences have meaning only above the 500m level. Beginning from this level, there appears to be a negative correlation between the original initialization and the trend over the peak after the three hours of simulation time. In other words, where the original had a minimum in wind speed, this profile has a maximum and visa-versa. The largest difference occurred at around 1100m and was -2.64m/sec. This is the same level as the highest difference over the site- once again in the vicinity of the inversion or the largest horizontal temperature gradients.

Downwind of the site, something very different is occurring. The shape of the profile is very close to the shape of the original profile. In fact, below 1200m the wind speed differences between this and the original profile are nearly a constant. They are all approximately -2m/sec. Then a slight transition occurs- near the level of the inversion. It jumps to a positive difference from 1200m to 2100m and then it becomes negative again. Above 1200m, however the differences are quite small; less than 1m/sec. It appears that 3km downwind of the island, the wind speed increases slightly at low levels only, but the direction remains unchanged indicating a minimal low level effect only. This confirms the results of the previous section that downwind of the island there is either little island influence or a tendency for a negative reaction to disturbances.

Now, in answer to the original questions about the extent in the horizontal as well as the vertical of the island's influence, some definite things can be said. Model results indicate that for wind direction, the only major effect the island had was over the site and over the peak. This would likely extend to any point over the surface of the island. Both 2km upwind and 3km downwind the effect on wind direction was negligible and can be thought of as small variations due to friction or just natural variability. For wind direction measurements taken at the experiment site, there appears to be contamination from the island up to a height of 2km. Within that range, between 700m and 1000m, an area of small measurement contamination can be found (negative bias). On top of the peak, the island does not appear to affect wind direction trends. However, the wind speed is significantly altered.

The island contamination of the wind speed is more widespread horizontally as well as vertically. Over the open ocean and upwind this contamination is, not surprisingly, minimal. Over the experiment site, below 625m, wind speed values approximately represent the shape of the original sounding. The magnitudes are quite different, and, above the 625m level the shape and magnitudes are different. Thus, wind speed measurements taken over the site may indicate a correct trend in the wind speed pattern below 625m, but other than that, the measurements are significantly affected by the island at least up to 2km. There appears, however, to be an area below the 2km level, between 700m and 1100m, where wind speeds and directions are less influenced.

The profile of wind speed over the peak is contaminated for the entire range of heights studied. It had an encouraging shape for wind direction, but here the island effect is highly variable. Finally, downwind the differences are smaller and more systematic. While the island still slightly influences the wind speed downwind of the island at low levels, wind direction appears unaffected. Thus the shape and the values of the wind profiles are still good indicators of the response of a pure marine environment to the forcing initialized by the sounding input to the model.

3. C130 AND RAMS COMPARISON

3.1. BACKGROUND OF C130 STUDY

The United Kingdom's Meteorological Research Flight C130 aircraft flew sixteen scientific sorties over a 26 day period from May 30, 1992 to June 24, 1992 during the Atlantic Stratocumulus Transition Experiment(ASTEX). Measurements of standard meteorological parameters, radiation, air chemistry, cloud physics, and aerosol constituents were made on June 10th and again on June 22nd over the island of Porto Santo. On both days, a comparison was done between RAMS results and the aircraft data.

On June 10th, RAMS was initialized with the 0800UTC(0900 local) sounding. A few cumulus clouds were observed over the island. Over the field site, however, it was clear. The aircraft flew north-south traverses over the field site between 1130UTC(1230 local) and 1215UTC(115 local) through clear skies at each of three levels- 424m, 1151m, and 1636m. The synoptic weather over the area included a high pressure system centered northwest of Porto Santo causing light, north to north-easterly winds over the island.

On the 22nd of June, two north-south traverses were done at 250m and 1490m. RAMS was also run with a sounding initialized on this day at 0800UTC. The intercomparison between RAMS and the aircraft on this day will be used to clarify and help confirm the results of the 10th. This day was also a clear day with light north-easterly synoptic winds.

The measurements taken from the aircraft during these traverses will be used for comparison with the RAMS output from corresponding levels. The aim of this comparison is threefold.

1. Achieve a greater understanding of the wind and temperature structure over the island.
2. Examine the credibility of the model by comparing its results with the observational data of the aircraft.
3. Apply aircraft data as an independent source of information in trying to assess the extent of the island's influence on the local

meteorological parameters.

3.2. C130 DATA PREPARATION

In order make a direct comparison between RAMS and the C130 aircraft data, some data manipulation and filtering was performed and several assumptions were made. Below is a detailed account of what was done as well as an assessment of the possible sources of error introduced in the process.

The C130 aircraft took measurements every second. For some parameters such as temperature, dew point, latitude, longitude, and altitude, more than one instrument made measurements. In the case of the first four of these variables, an average of all the measurements taken was performed giving a value for use in the comparison with RAMS. The aircraft's altitude was measured in three ways- pressure height, GPS altitude, and radar height. Pressure height was used to determine the plane's level for the comparison as this represents the closest correspondence with RAMS height levels. In addition to height, time scales and horizontal distance scales for the aircraft must also correspond to those scales in RAMS in order to make a direct comparison between the two.

To determine an appropriate time scale, the plane's latitude and longitude were plotted to determine the times the aircraft was in the vicinity of the island. This was determined for the level one traverse to be between 1139UTC to 1146UTC- with the plane being over the test site at approximately 1143UTC. For the level two traverse, it was estimated to be from 1153UTC to 1159UTC with the plane being over the site around 1156UTC. And for the level three traverse, it was in the vicinity from 1207UTC to 1213UTC and over the site approximately 1210UTC. The RAMS analysis fields are calculated every hour and thus the 1200UTC fields were chosen for the comparison for all three levels. This may introduce small errors due to time differences which are as large here as 15 minutes.

For a comparable distance scale, the problem was a little more difficult. On the smallest grid, RAMS encompasses 13km by 13km, representing

26 grid points in each direction- each grid box being 0.5km on a side. From north to south, across the island site, and excluding the boundary points, there were four grid boxes north or upwind of the island, eleven over the island, and nine downwind or south of the island. In Figures 3.2- 3.7, the upwind points will be referred to as negative distances and thus range from -2.0km to 0km. The points over the island will range from 0km to 5.5km, and the points downwind will range from 5.5km to 9.5km.

For the aircraft, both radar height and surface temperature measurements were examined in the vicinity of the island to determine at what time the aircraft was actually over land and when it was over water. A sudden decrease in the radar height without a corresponding decrease in the aircraft altitude was determined to be the point the aircraft entered the area directly above the island-ocean interface. Although measurements were made every second, the exact second this occurred was not always obvious. And, if the plane was flying on the order of 100m/sec, a five second error in determining this point would correspond to a 0.5km distance error. Thus, to help confirm the exact location of this point, radiometrically determined surface temperature data were also used. A point was sought in the vicinity of the determined radar height point where the surface temperature increased; the land being warmer than the ocean. Using both of these variables, a fairly accurate estimation of the relative position of the data could be determined. This process was repeated for all three levels.

After the point the aircraft entered the island's domain was determined for all three levels, aircraft ground speed was examined around this point. The ground speed was then averaged around this point and multiplied by the time between measurements, one second, to obtain a distance scale for the aircraft data. In order to make this scale comparable to RAMS, negative values will also represent upwind of the island and the values will go from -2.0km to 9.5km. The average ground speeds used were 99.5m/sec at level one, 101.0m/sec at level two, and 104m/sec at level three. Once again, some error is introduced in this process of determining an average plane speed since the plane's speed was not constant.

Finally, the plane's heading was examined to verify that the plane was on a true north-south course. With the island topography changing so dramatically east of the site, a small change in compass heading could introduce a large error.

3.3. WIND AND TEMPERATURE COMPARISON

3.3.1. DIRECT COMPARISONS

Wind speed, wind direction, and temperature fields were plotted for both RAMS and the C130 aircraft and compared. A degree of uncertainty is introduced here as the RAMS height levels were chosen to be the closest to the elevation of the aircraft traverse, but are not exact. The aircraft levels were 420m, 1180m, and 1640m. The closest corresponding RAMS levels were 429m, 1146m, and 1690m.

Initial inspection of the wind variables for the three levels on June 10th show somewhat encouraging results for level two, but poor agreement with levels one and three (Figures 3.1a-c; 3.2a-c). One major difference between the two occurs above the island-ocean interface consistently at all three levels. At all levels, the C130 shows very little change in the wind direction or speed above the transition zone from ocean to island. One would expect the wind fields, especially at low levels to be affected by the cliff on the north side of the island with the northerly winds observed on this day. The RAMS results show this disturbance. It appears as an increase in wind speed at levels one and two and as a decrease in wind speed at level three. This discrepancy will be examined more later.

In assessing these comparisons, it should be noted that while the actual values of a variable may differ between the C130 and RAMS in magnitude, the relative increase or decrease of these values across the topographic features of the island are of greater significance. It is the goal here to determine the effect the island's topography has on the local wind and temperature structure above it. Thus, the concern is that RAMS has the ability to accurately show these topographic-induced changes so that an island effect may be determined. Perhaps, the only exception to this is wind direction. Wind direction, unlike temperature and wind speed, was observed to remain constant-northerly, throughout the day and was also initialized northerly in the model. Thus, a change in wind direction from northerly should be an island effect both in RAMS and in the observations. The actual magnitude of the wind direction is then an actual indication of the wind direction trend and indicates to what degree the island's topography steered the flow. All three variables were examined individually and then compared.

For wind speed, at level one, there appears if anything to be a weak negative correlation between the C130 and RAMS (Figure 3.1a). At level two, an encouraging positive correlation is seen (Figure 3.1b). And, at level three, there appears to be a large negative correlation (Figure 3.1c).

In the case of wind direction, the pattern appears similar to the wind speed pattern. At level one, there is either no correlation or it is weakly negative (Figure 3.2a). Level two exhibits a good positive correlation both in magnitude and in trend (Figure 3.2b). And, at level three, the correlation seems negative (Figure 3.2c). One positive thing that can be said for wind direction is that the actual values are close indicating the model predicts well, on the average, how the wind direction changes due to topographic influences. Thus, the negative correlations seen are not that significant and represent merely small changes in the wind direction around an average which is close for both the aircraft and RAMS.

Temperature data were also plotted and compared to determine if the discrepancies observed with the wind fields carried over consistently with other variables (Figures 3.3a-c). Here RAMS showed a definite change in the temperature at all three levels at the ocean-island transition point. The C130 data did not exhibit this at all. The values of temperature are close between the two but the trends are not comparable. There is virtually no correlation at the lower levels and a negative correlation at level three. One thing to note here is that the temperature changes across the island are usually less than one degree in either direction. Thus, the terms "increasing

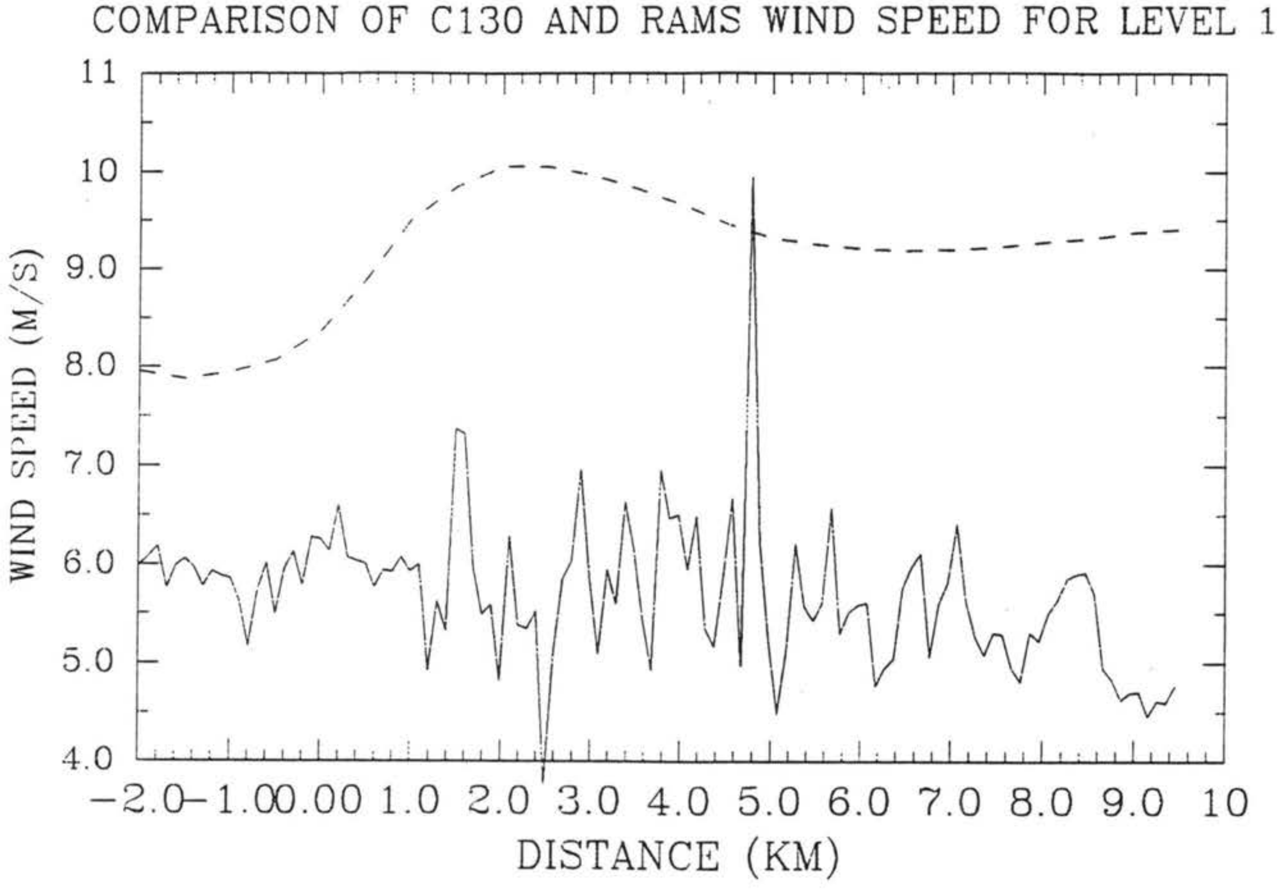

Figure 3.1a: Comparison of wind speed transects through the measurement site between RAMS (dashed line) and the C130 aircraft data (solid line) at 420m for June 10th. Negative distances are upwind of the island. The area from 0.0 to 5.5km encompasses the island from north to south. From 5.5km to 10km is the area downwind of the island.

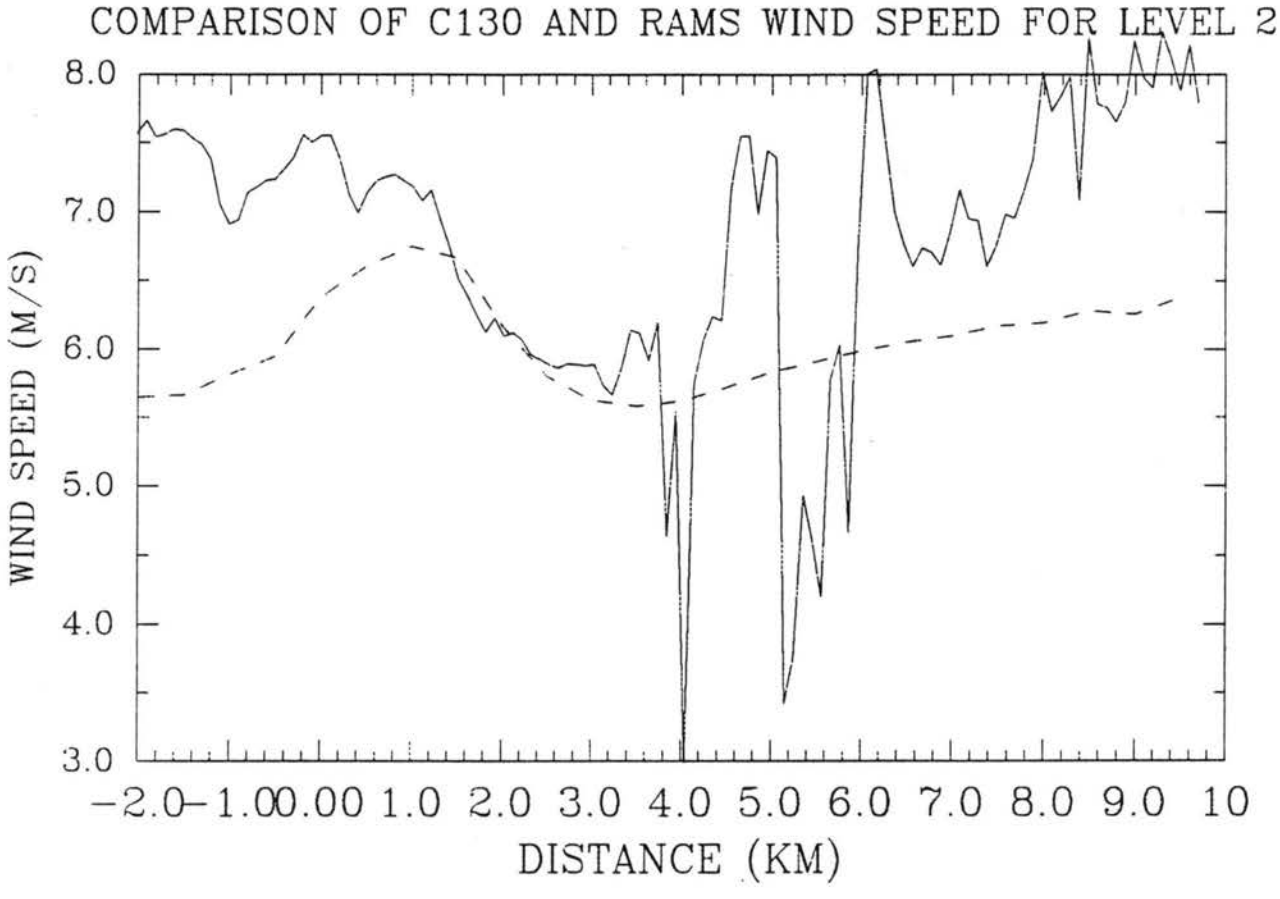

Figure 3.1b: Same as 3.1a but for 1180m.

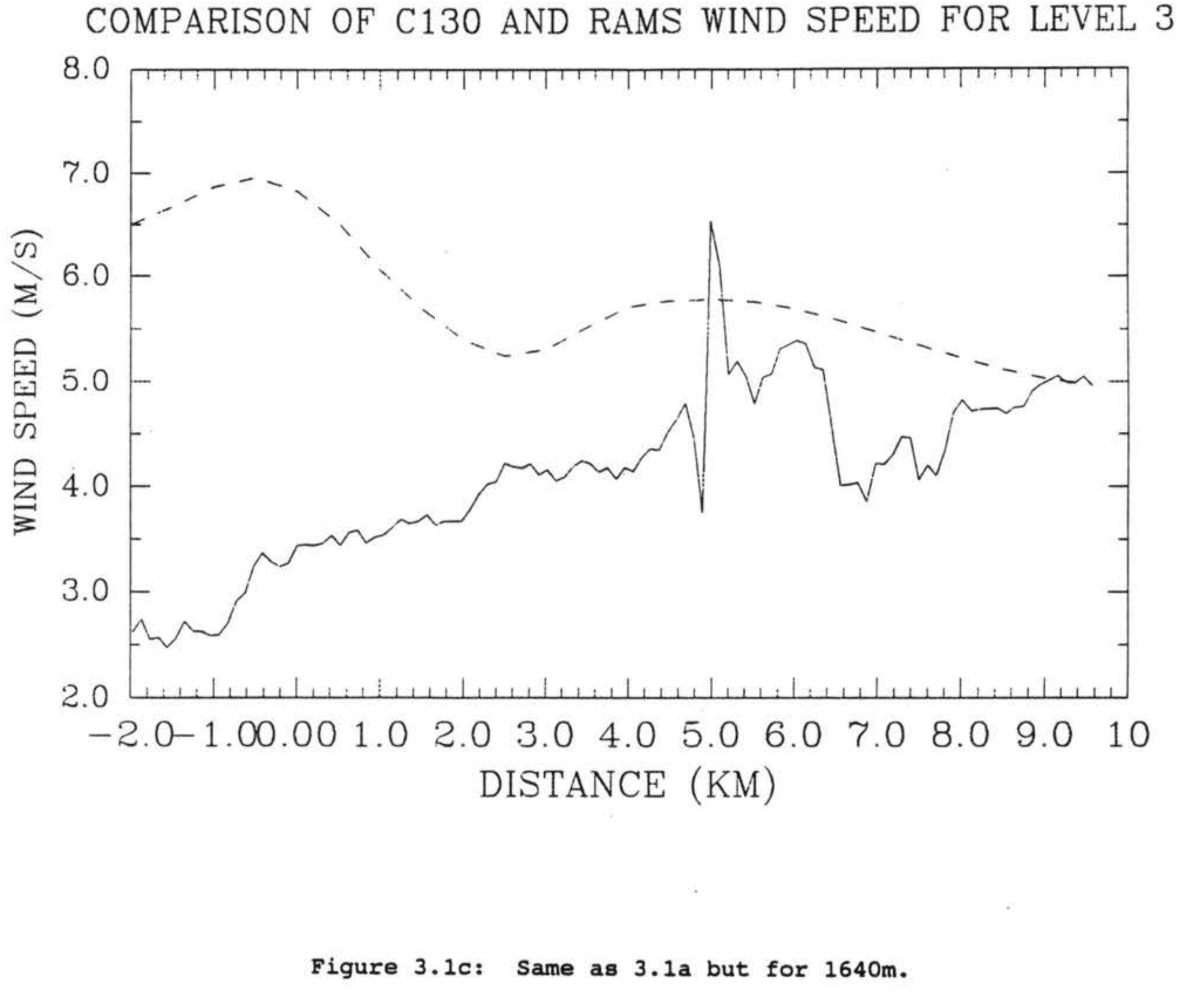

Figure 3.1c: Same as 3.1a but for 1640m.

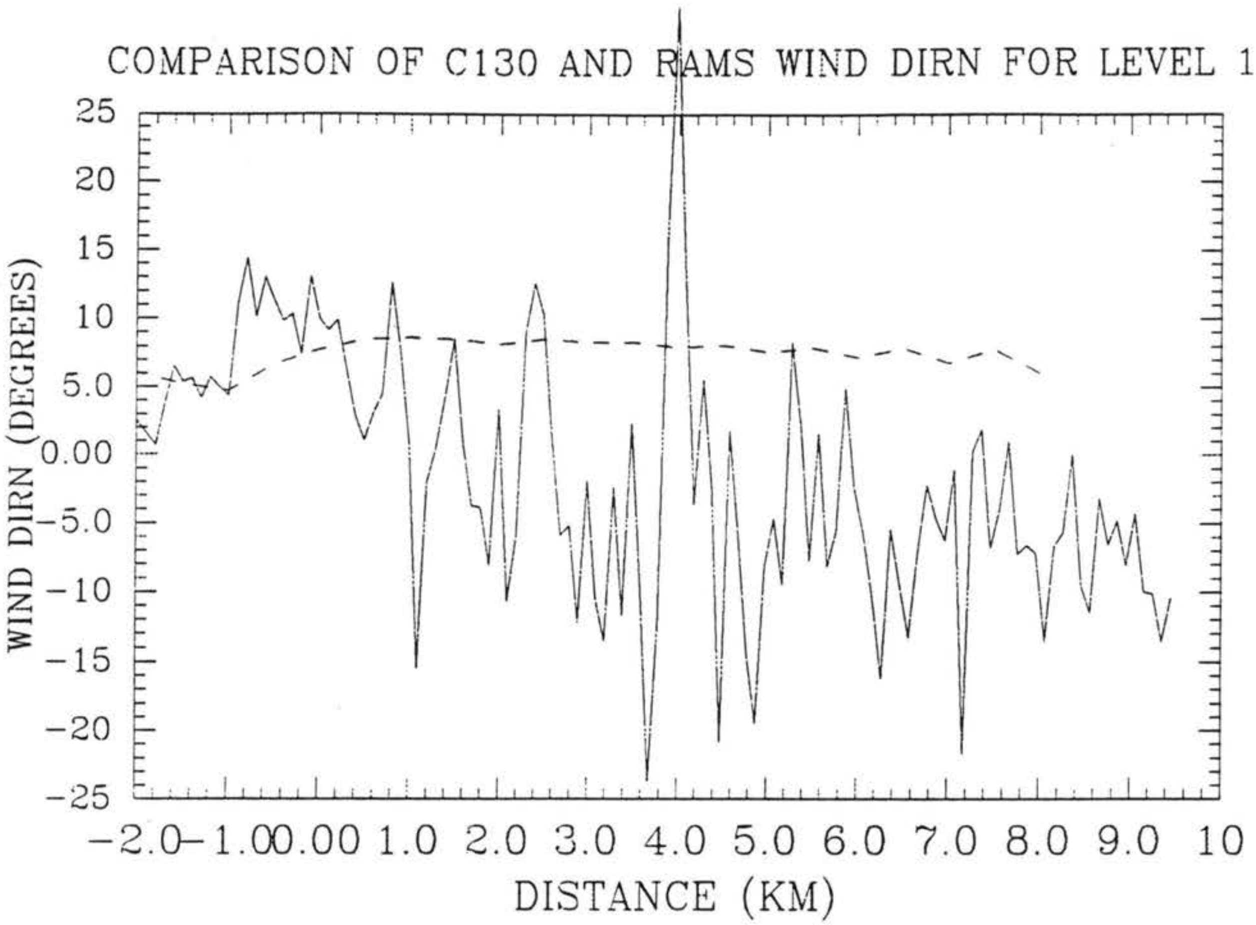

Figure 3.2a: Comparison of wind direction transects through the measurement site between RAMS (dashed line) and the C130 aircraft data (solid line) at 420m for June 10th. Negative distances are upwind of the island. The area from 0.0 to 5.5km encompasses the island from north to south. From 5.5km to 10km is the area downwind of the island. Negative directions are subtracted from 360.

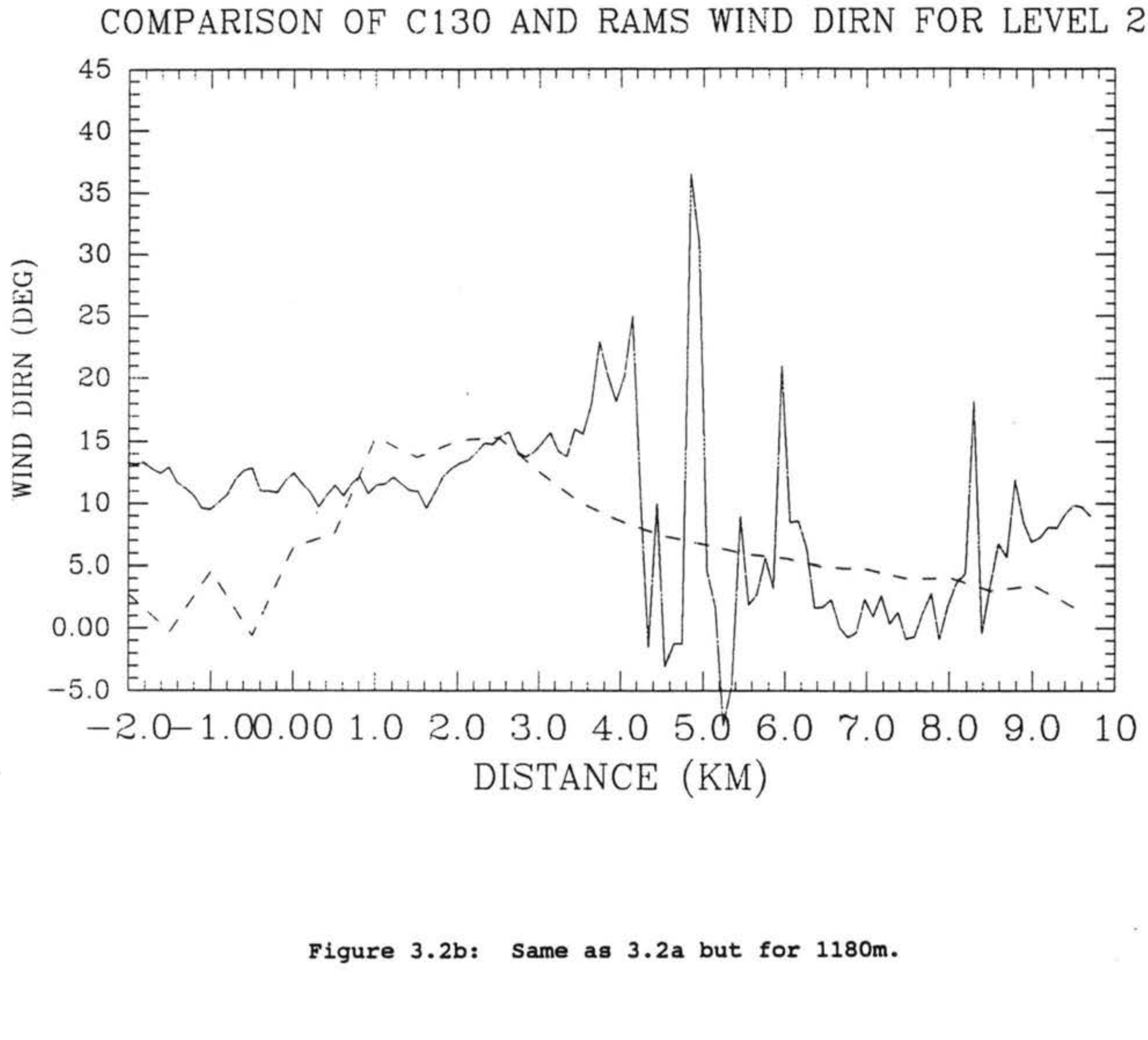

Figure 3.2b: Same as 3.2a but for 1180m.

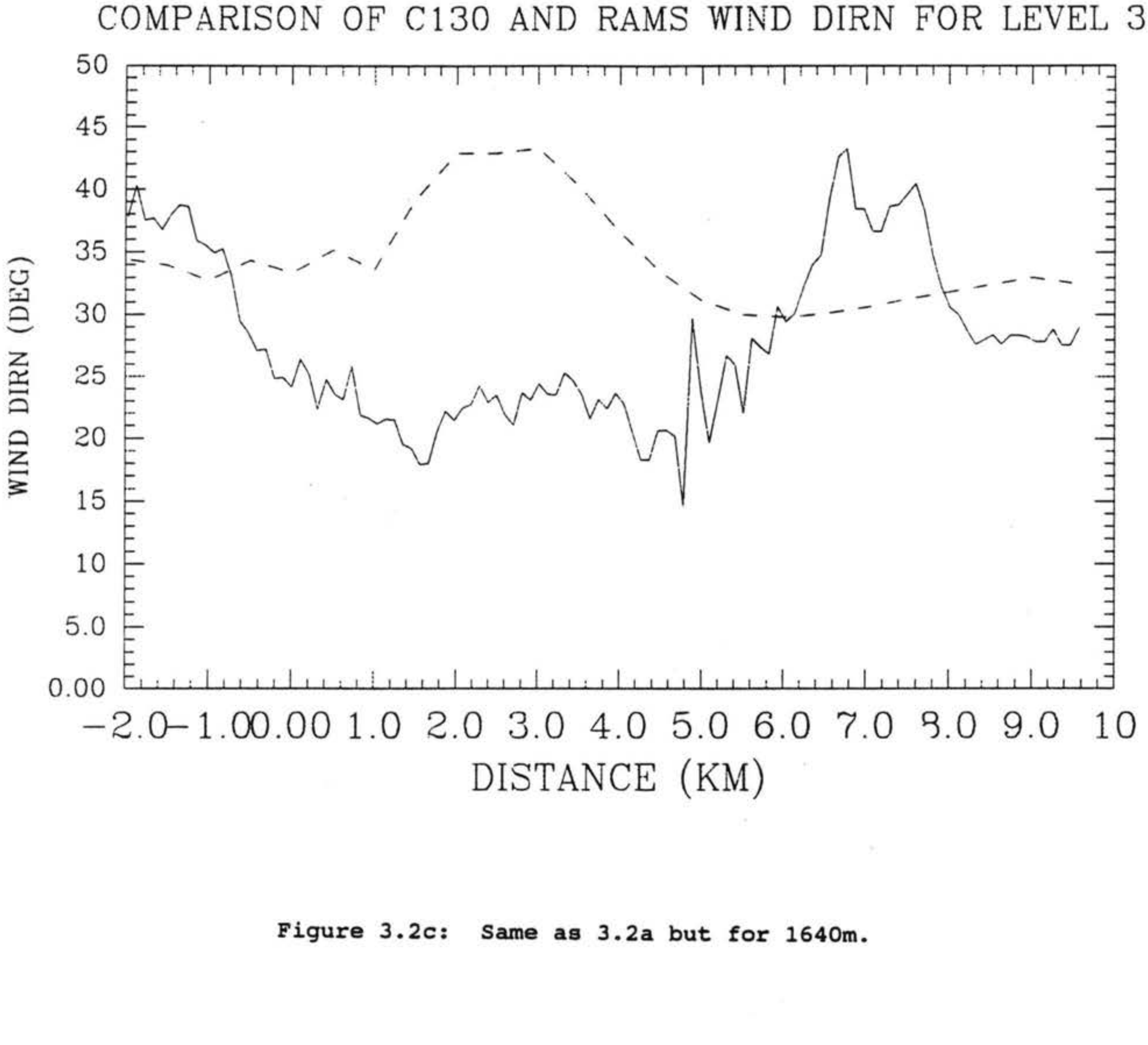

Figure 3.2c: Same as 3.2a but for 1640m.

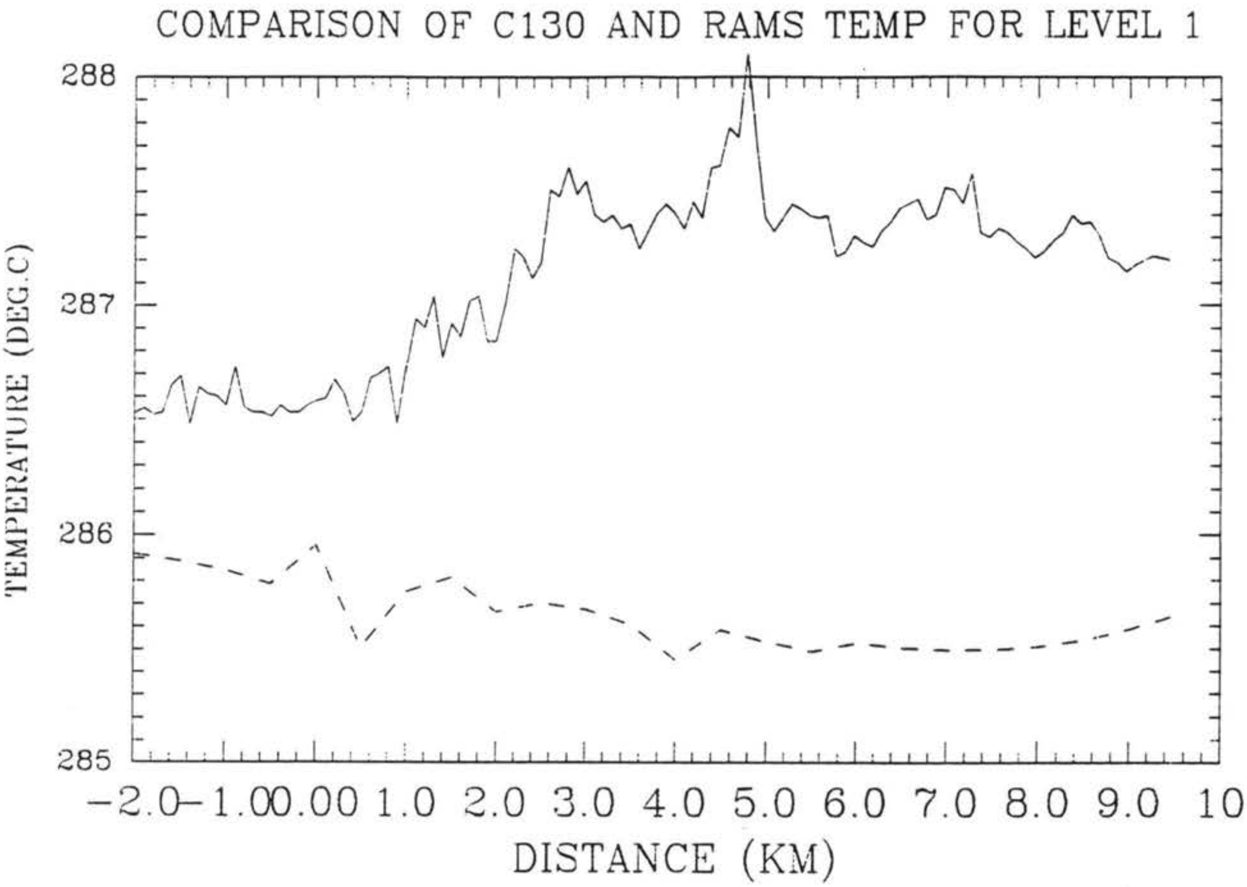

Figure 3.3a: Comparison of temperature transects through the measurement site between RAMS (dashed line) and the C130 aircraft data (solid line) at 420m for June 10th. Negative distances are upwind of the island. The area from 0.0 to 5.5km encompasses the island from north to south. From 5.5km to 10km is the area downwind of the island.

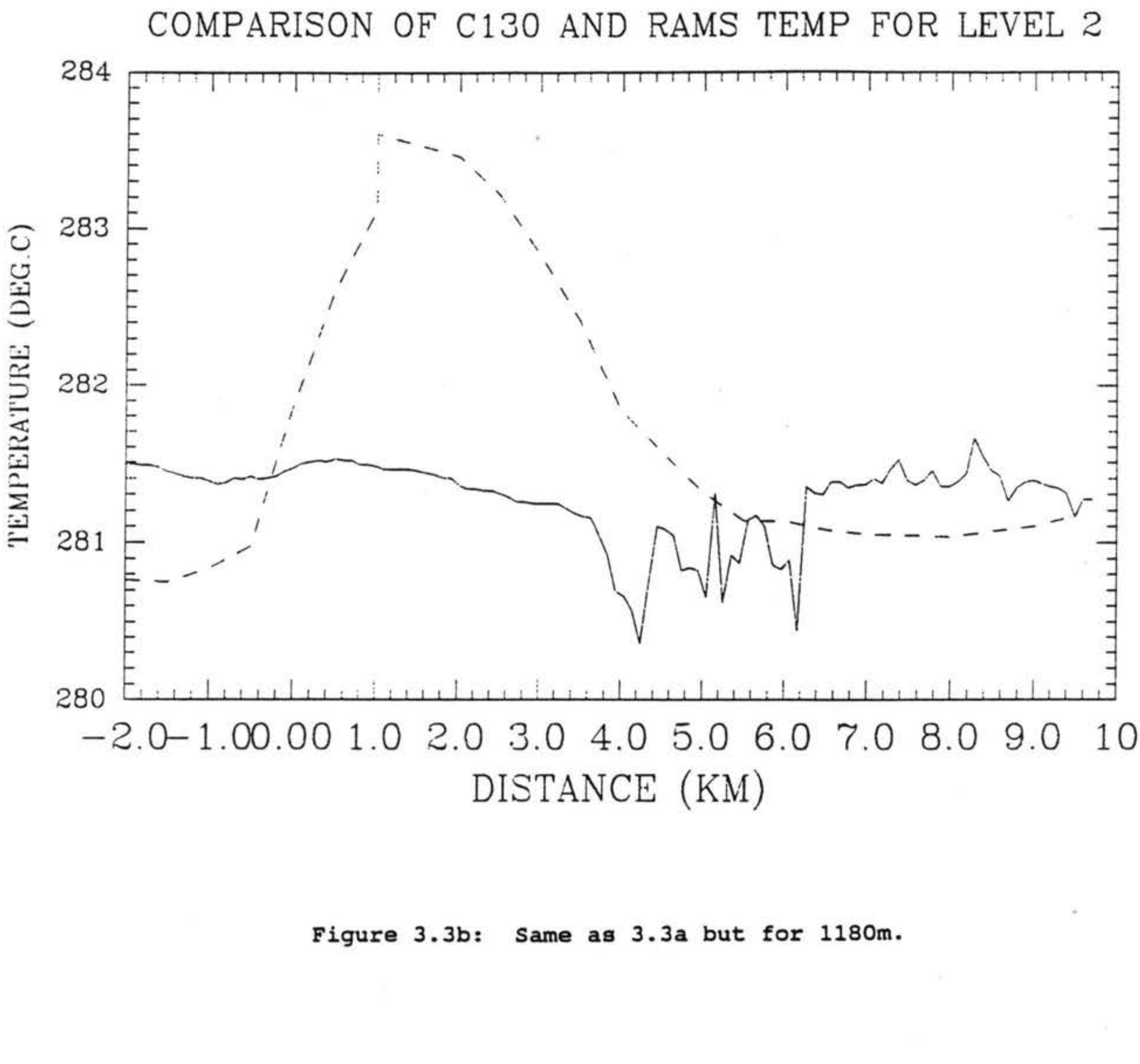

Figure 3.3b: Same as 3.3a but for 1180m.

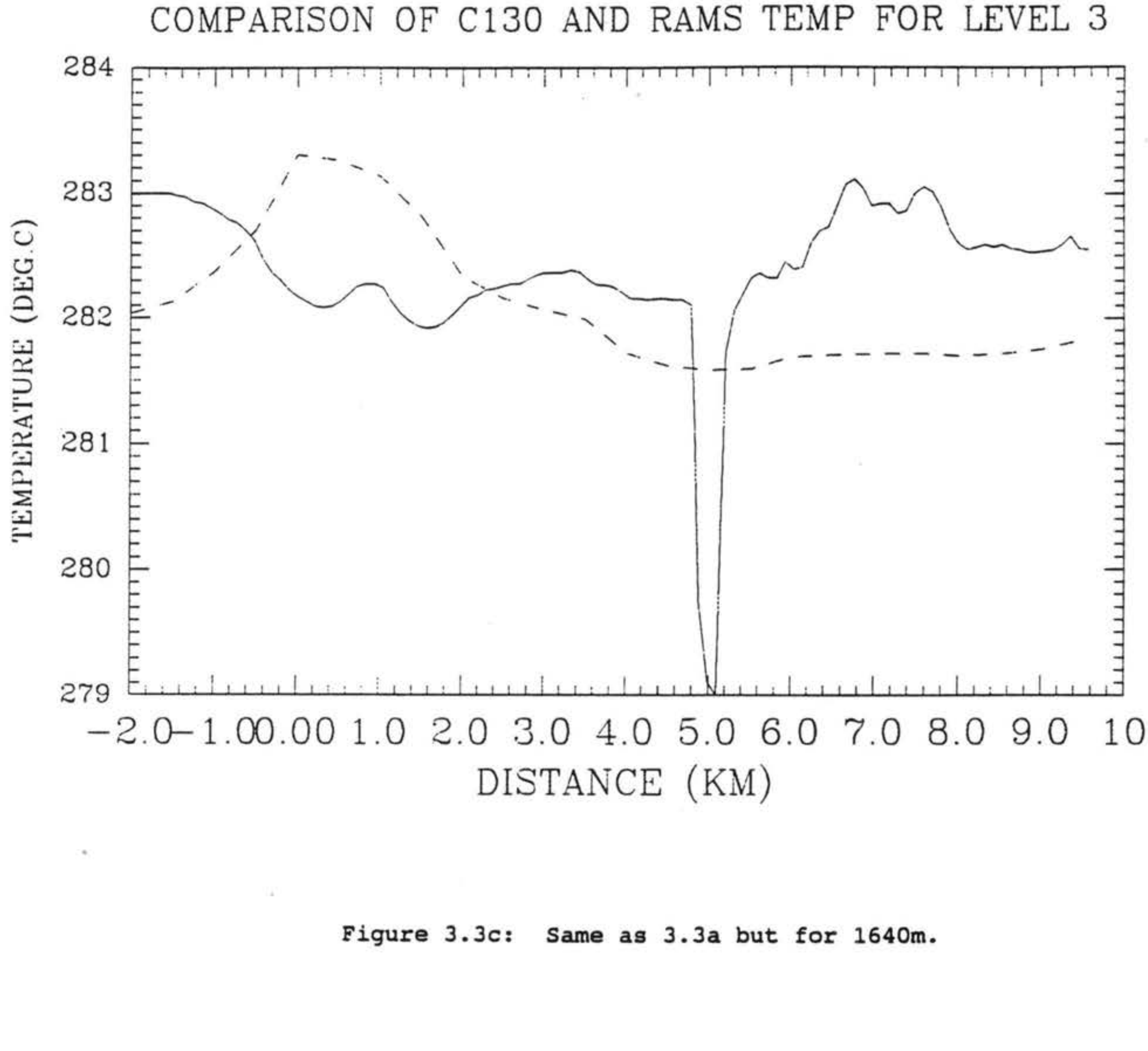

Figure 3.3c: Same as 3.3a but for 1640m.

trends" or "decreasing trends" are misleading. These negative correlations may again be noise around a fairly constant mean which agrees for both RAMS and the C130.

In general, however, the striking thing to note is that there appears to be more negative correlation between the C130 and RAMS than positive correlation. This would seem to indicate that if there were somehow a phase shift in the RAMS data, a good positive correlation would be seen. This brings up three possibilities.

1. The horizontal disturbances of the fields due to the island as predicted by RAMS are underpredicted or overpredicted in their spacial extent.
2. The horizontal disturbances of the fields due to the island as predicted by RAMS are underpredicted or overpredicted in their vertical extent. This would assume that there is a phase shift with height of the disturbance in RAMS.
3. The sources of error introduced here by approximations are large enough to throw off the results of the comparisons.

All three possibilities were examined.

3.3.2. HORIZONTALLY PHASED COMPARISONS

The comparisons of the north to south transects through the measurement site for RAMS and the C130 data were reexamined to see if the premise for number two is observed. There definitely appears to be a phase shift with height for wind speed and temperature above 500m (Figures 2.3a-c; 2.10a-c). Upon initial inspection, it appeared as if a 1km to 2km north shift or a 300m to 500m upward shift of the RAMS plots would produce significantly better positive correlation. To test this hypothesis, correlation coefficients were calculated between the C130 data and north, south, up, and down shifts in the RAMS data. To do this the aircraft data were filtered to have an equal number of points as the RAMS data; 24 north to south evenly spaced and through the site. The lines that are correlated with RAMS data shifted up or down use all

24 points for the calculation. The lines correlated with RAMS moving north or south use fewer points depending on how far the RAMS curve was shifted (ie., if RAMS was shifted 1.5km north (3 grid points), only 21 points could now be used for the calculation). The RAMS curves were shifted up to five height levels up and down and up to five grid points north and south for the correlation comparison.

In order to assess the significance of the correlation coefficients, the method of Analysis of Variance was used (Panofsky and Brier,1965). Using this test, significance values are reported in percentages. A value of 95% means that there is only a 5% chance of a correlation coefficient as high as the one calculated to have occurred completely by chance. This test assumes that the samples are random and independent and that there is a normal distribution of error about the mean. The latter of these can be shown to be true and the independence of the samples can be argued since no direct relationship exists between the measurements of the C130 aircraft and RAMS. The following are the cutoff correlation values calculated for the stated significances: 75% for 0.24; 90% for 0.34; 95% for 0.4; 97.5% for 0.45; and, 99% for 0.51. Figure 3.4 and Figures 3.8- 3.10 show all the positively calculated correlation values and their significances for all the lag studies done.

The value of the correlation coefficients for wind speed for levels one and two show the highest value at plus two lag (Figures 3.4a-b)(Plus lags here indicate that RAMS was shifted north and negative lags indicate RAMS was shifted south). Level three is negatively correlated for all cases. A value of 0.57 was evaluated for level two which is significant to the 99% level and 0.30 was calculated at level one for this lag. While the value at level one represents just a weak correlation (significant to 75%), it is the highest calculated for any horizontal phase shift between the two variables.

Correlation coefficient values for wind direction suggest a similar picture (Figures 3.4c-d). At levels two and three the correlation is highest with the RAMS curves shifted windward plus two or three points. A lag of plus three here produced the highest values; 0.77 at level two and 0.49 at level

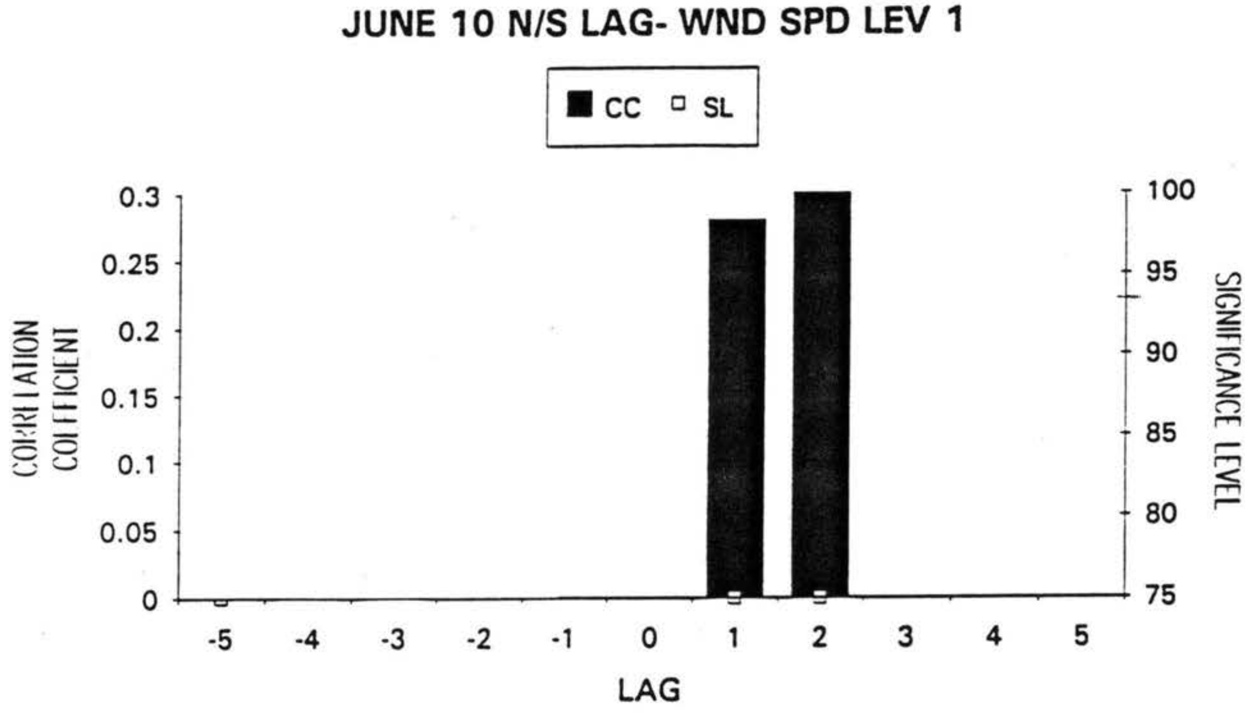

Figure 3.4a: Correlation coefficients and significance levels for wind speed for a north/south or upwind/downwind lag of the RAMS data on June 10th at 420m. Plus lags indicate that the RAMS data was shifted windward. Negative lags- downwind.

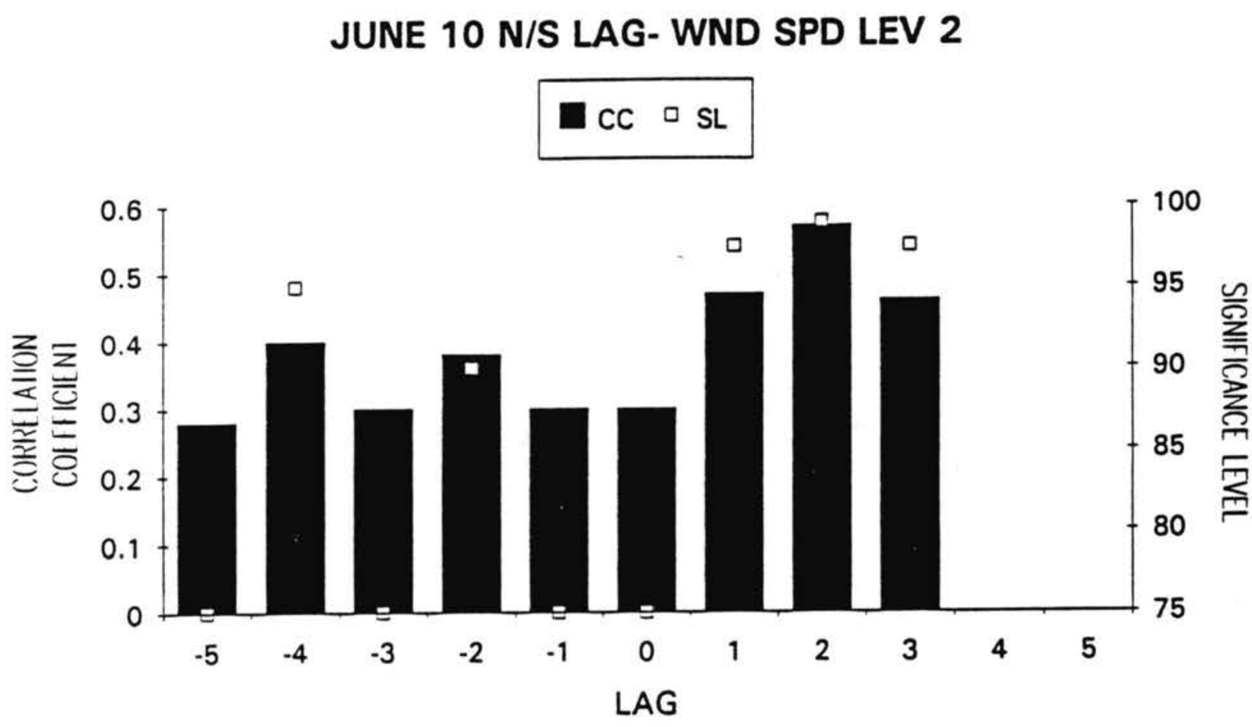

Figure 3.4b: Same as 3.4a but for 1180m.

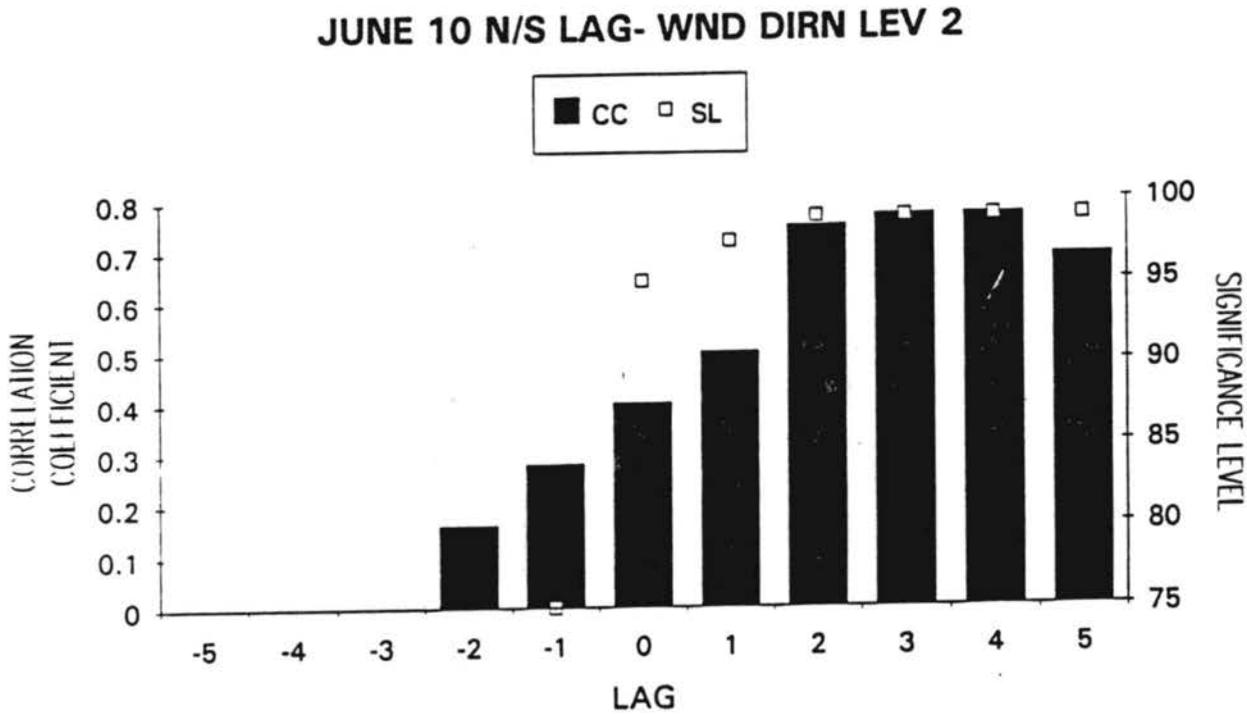

Figure 3.4c: Same as 3.4a but for wind direction at 1180m.

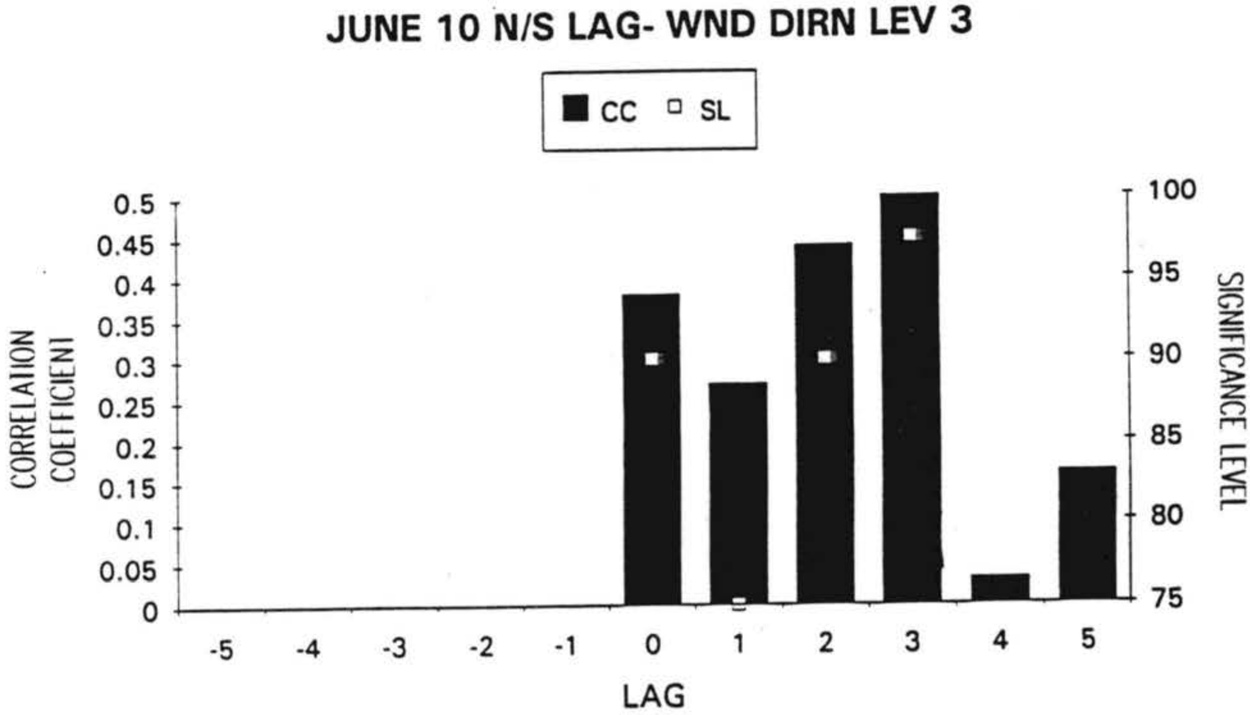

Figure 3.4d: Same as 3.4a but for wind direction at 1640m.

three with significance levels of 99% and 97.5% respectively. Here, level one presents the problem with all correlations being negative.

Temperature produced mostly negative correlation coefficients with some small positive correlation at levels two and three with RAMS shifted five points south. As previously mentioned, however, the results of the temperature analysis are not extremely meaningful due to the very small amount of temperature variability observed across the entire island.

It appears that, for the wind variables, a shift of RAMS results windward by one to two kilometers would produce overall much better agreement with the C130 aircraft data. The lack of agreement for wind speed at level three is not of much concern here as, at 1640m above the island, the island's influence may be minimal so that the correlation is insignificant with respect to any effect the island may have. The lack of correlation at level one for wind direction is somewhat bothersome, but upon inspection of the graph which produced these correlations, it is seen that actual magnitudes are not significantly different. Thus, the negative correlation can be attributed to small fluctuations around a fairly constant mean which is close for the two graphs. This information provides enough support to probe this idea further. The 22nd of June was used for this purpose. This day represented similar weather conditions and a similar initial sounding. The same procedures for data filtering were performed here as on June 10th. The results are encouraging.

The correlations are in general higher than for the tenth (Figures 3.5a-b; 3.6a-b; 3.7a-b). The highest correlation values for wind speed at both levels on the 22nd are at plus two or three lags. The actual values are 0.94 for level one and 0.96 for level two representing highly correlated data sets to the 99% significance level (Figures 3.8a-b). For wind direction, there is no significantly positive correlation for level two, but level one shows a value of 0.85 with a plus two lag (Figure 3.8c). Once again, the existence of virtually no correlation at 1490m(level 2) above the island is of little concern since the island's effects by this level are minimal. Temperature correlation on the 22nd even shows some confirmation of a higher correlation

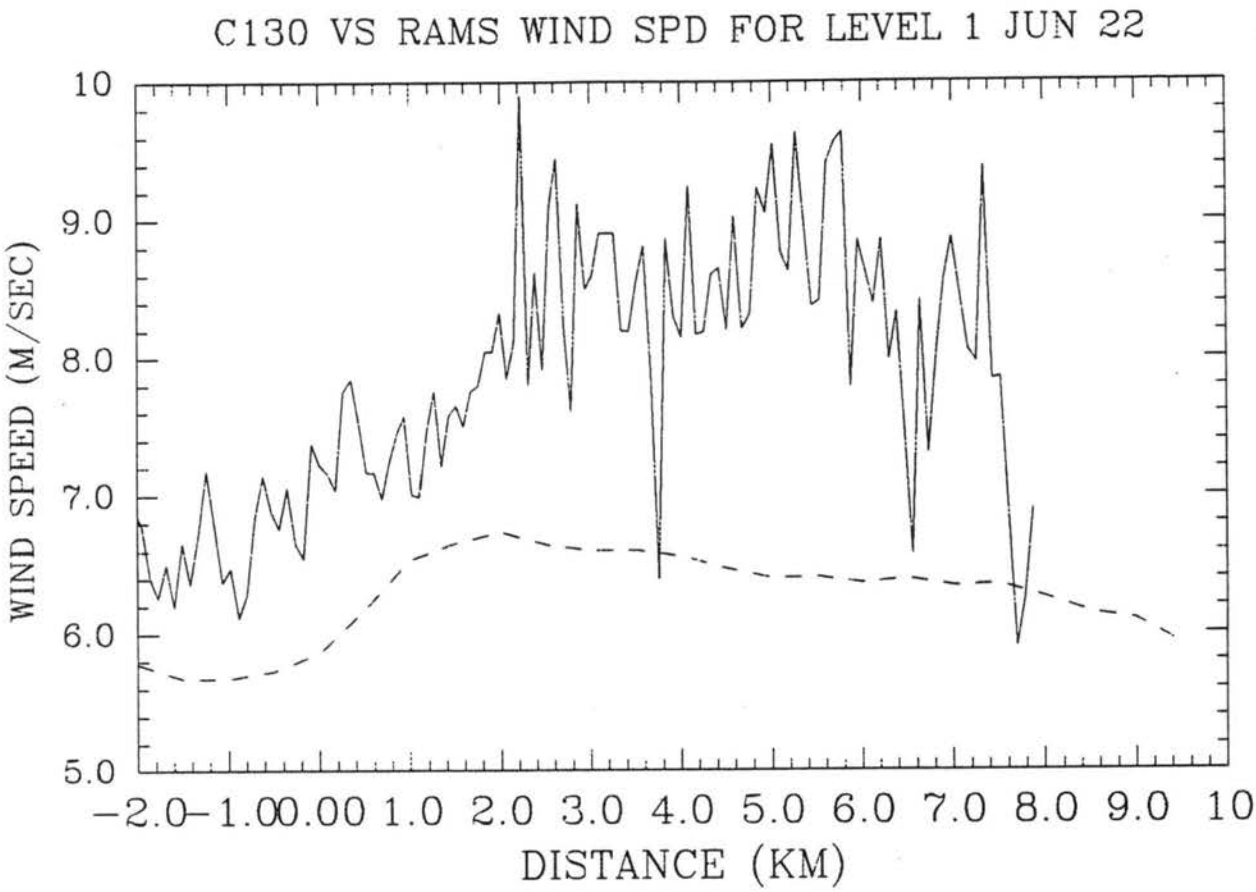

Figure 3.5a: Comparison of wind speed transects through the measurement site between RAMS (dashed line) and the C130 aircraft data (solid line) at 250m for June 22nd. Negative distances are upwind of the island. The area from 0.0 to 5.5km encompasses the island from north to south. From 5.5km to 10km is the area downwind of the island.

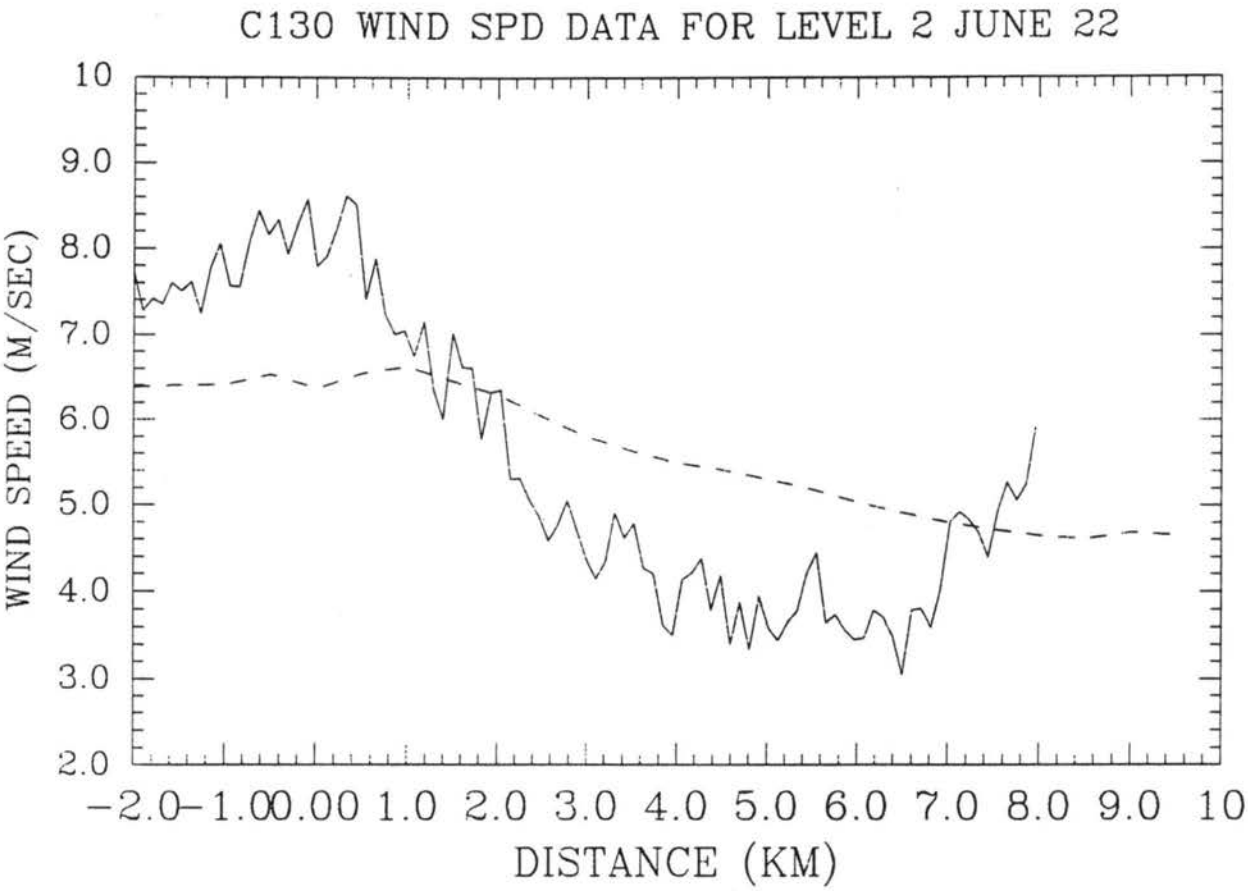

Figure 3.5b: Same as 3.5a but for 1490m.

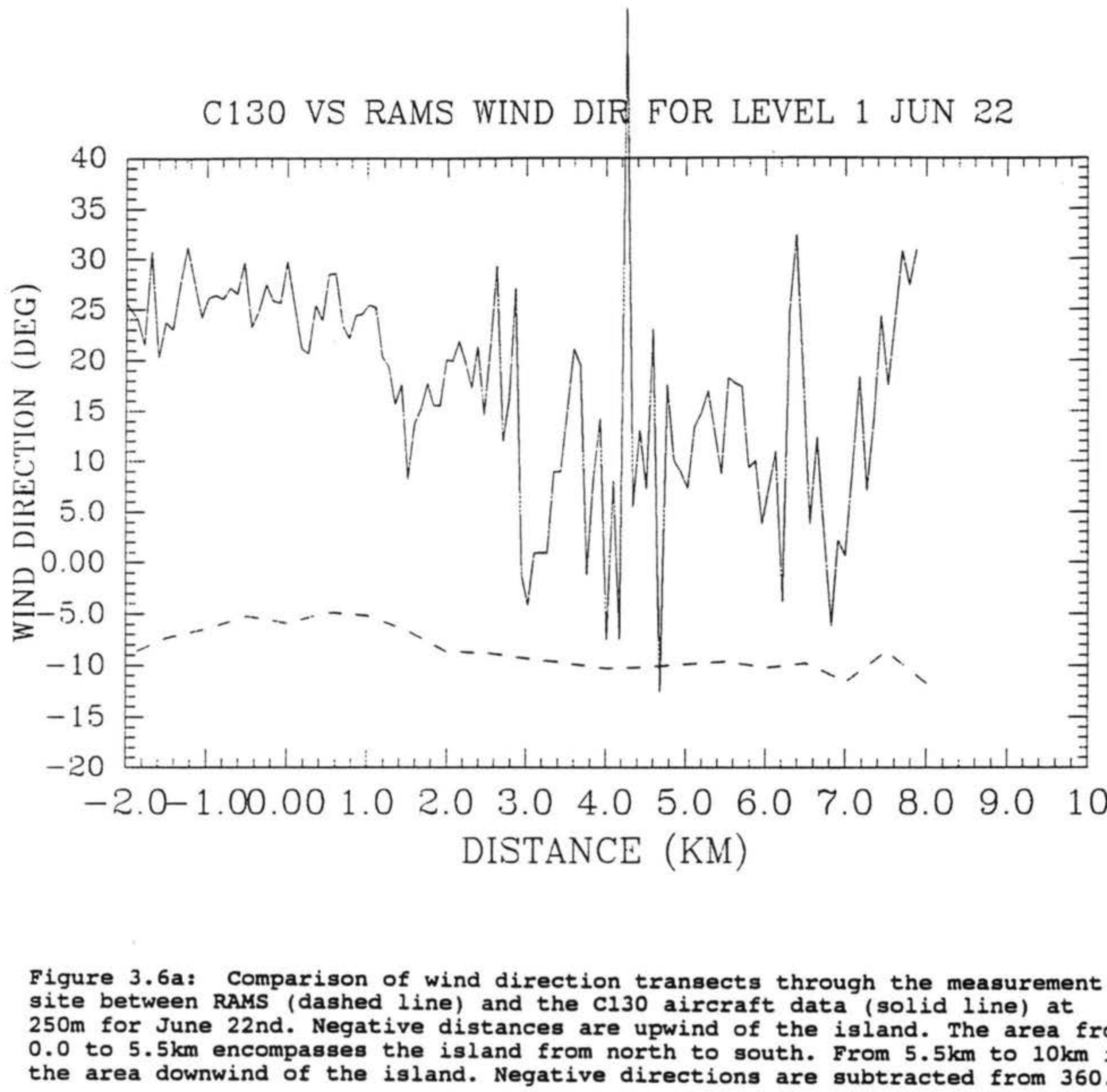

Figure 3.6a: Comparison of wind direction transects through the measurement site between RAMS (dashed line) and the C130 aircraft data (solid line) at 250m for June 22nd. Negative distances are upwind of the island. The area from 0.0 to 5.5km encompasses the island from north to south. From 5.5km to 10km is the area downwind of the island. Negative directions are subtracted from 360.

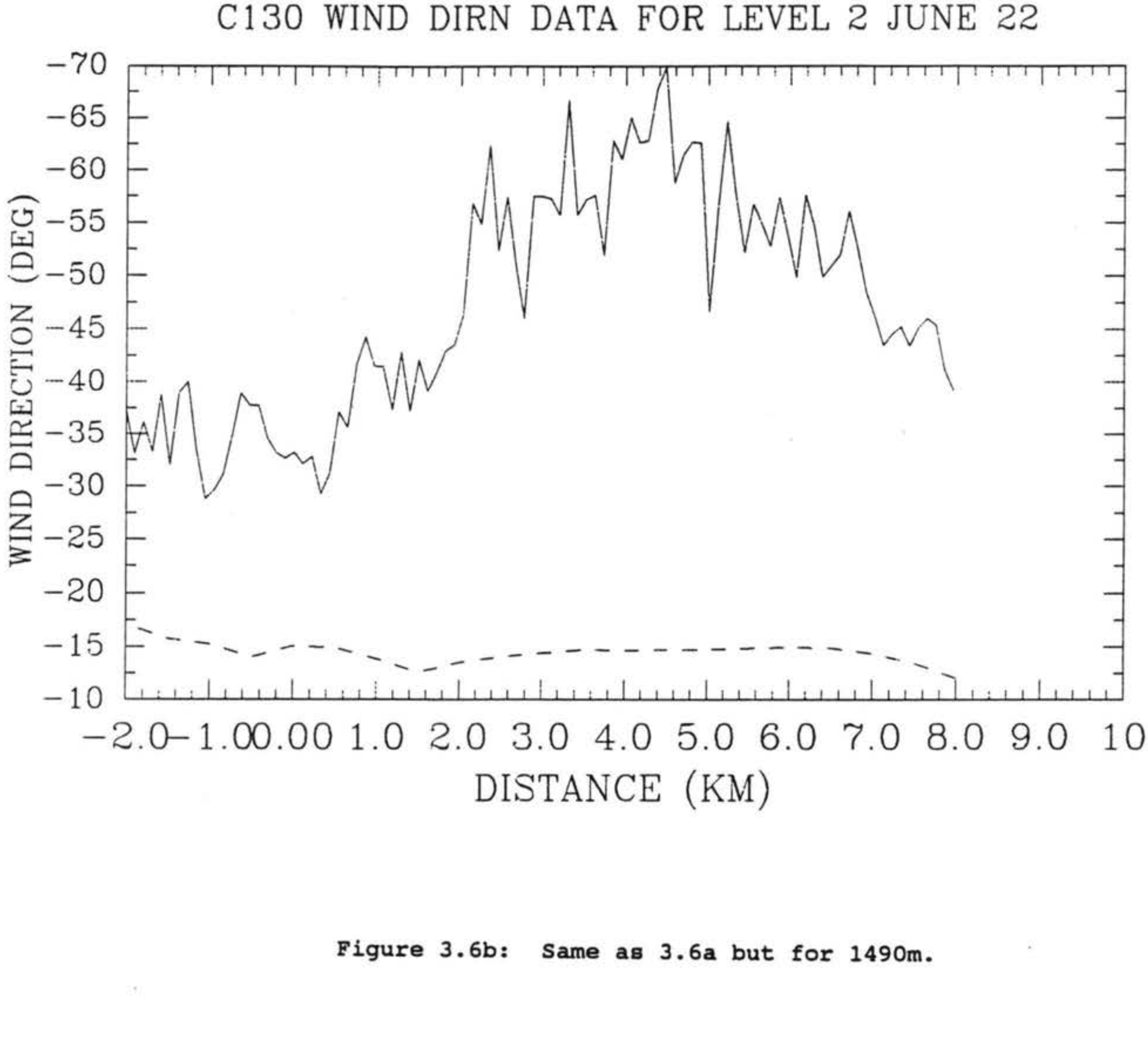

Figure 3.6b: Same as 3.6a but for 1490m.

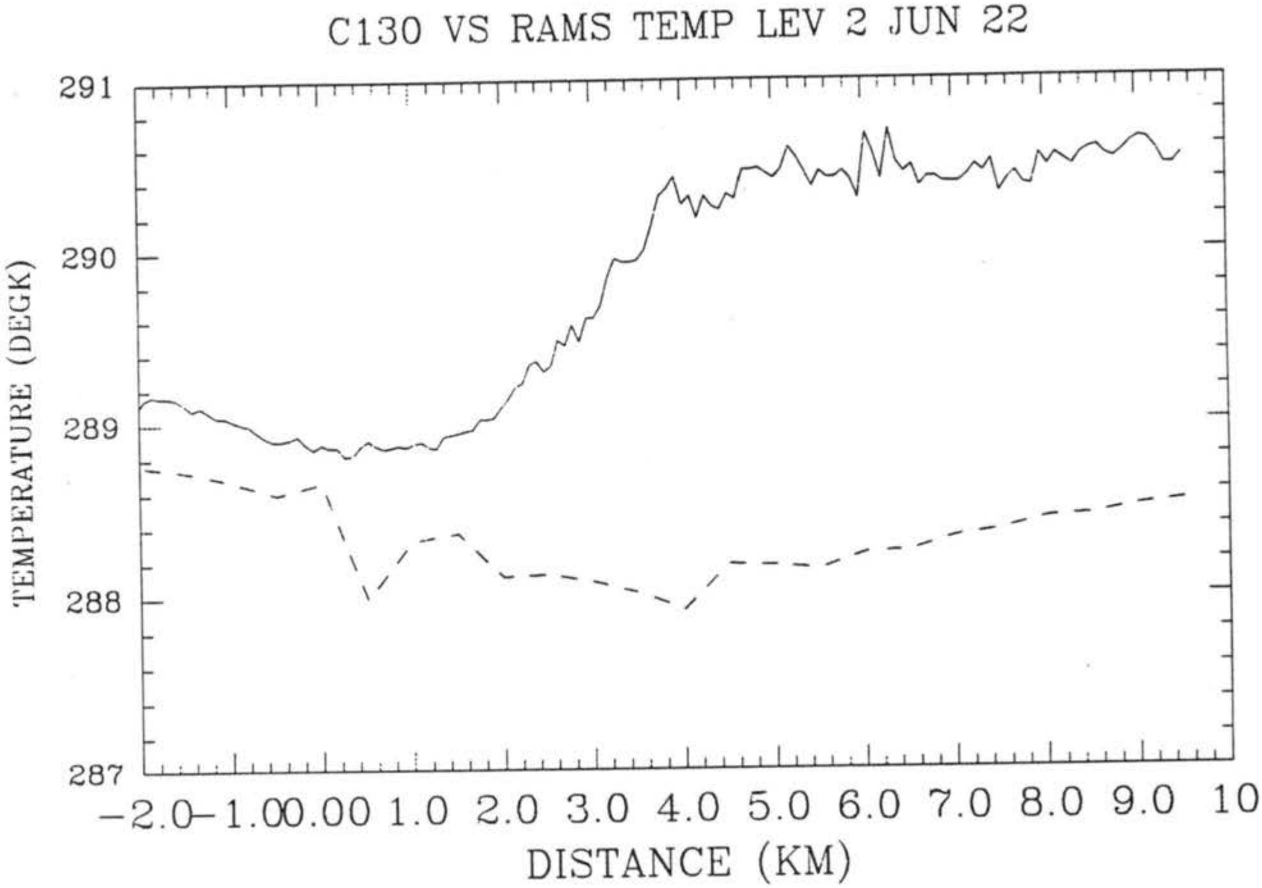

Figure 3.7a: Comparison of temperature transects through the measurement site between RAMS (dashed line) and the C130 aircraft data (solid line) at 250m for June 22nd. Negative distances are upwind of the island. The area from 0.0 to 5.5km encompasses the island from north to south. From 5.5km to 10km is the area downwind of the island.

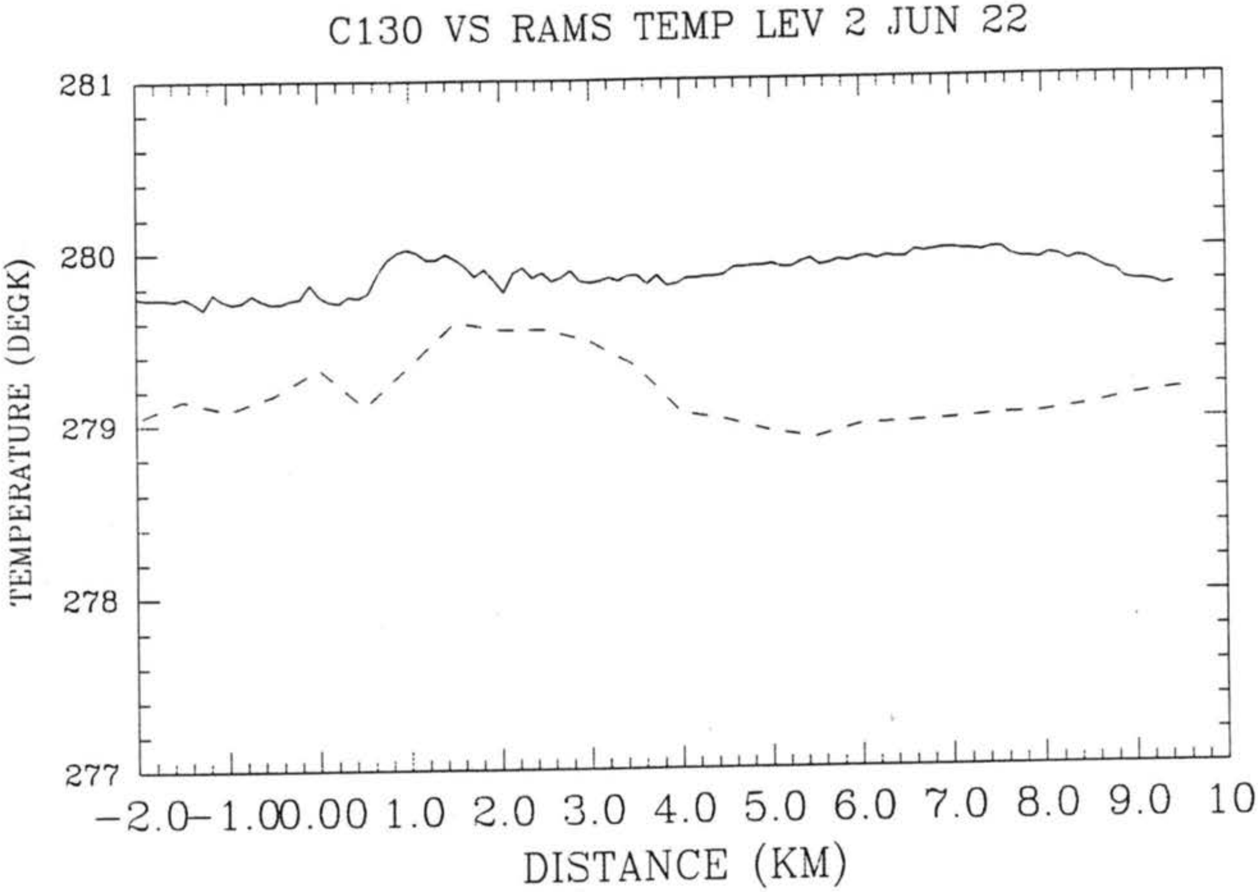

Figure 3.7b: Same as 3.7a but for 1490m.

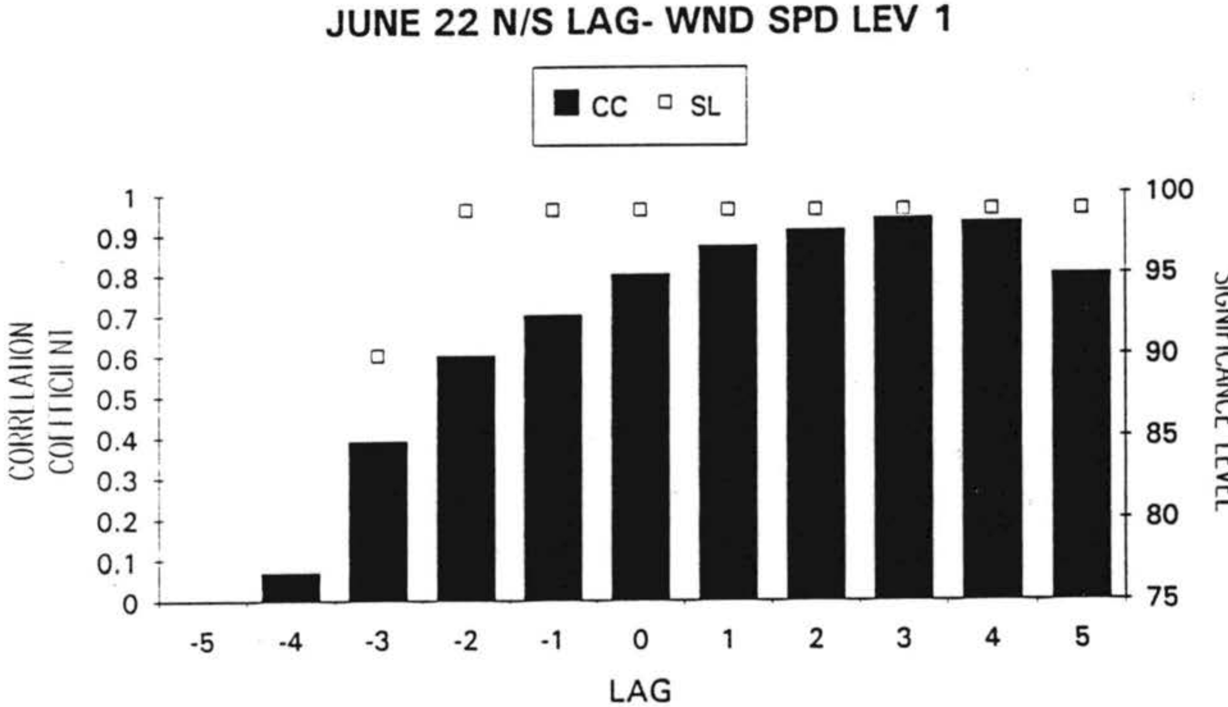

Figure 3.8a: Correlation coefficients and significance levels for wind speed for a north/south or upwind/downwind lag of the RAMS data on June 22nd at 250m. Plus lags indicate that the RAMS data was shifted windward. Negative lags- downwind.

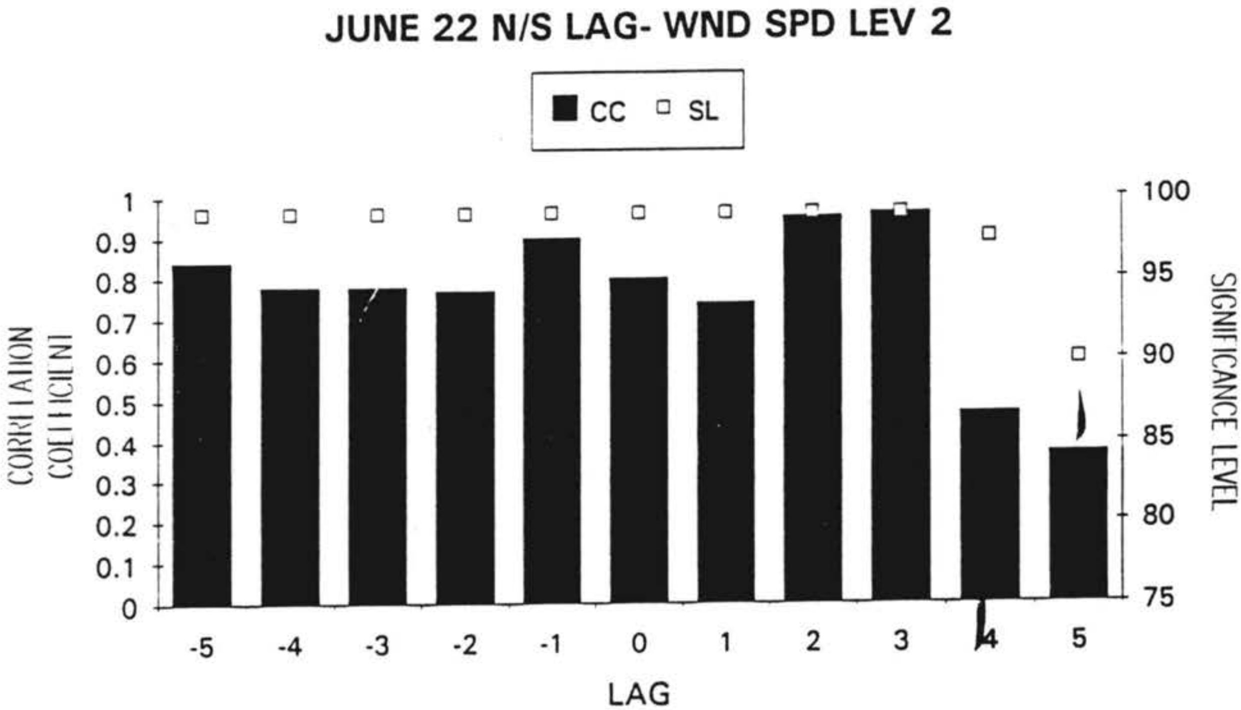

Figure 3.8b: Same as 3.8a but for 1490m.

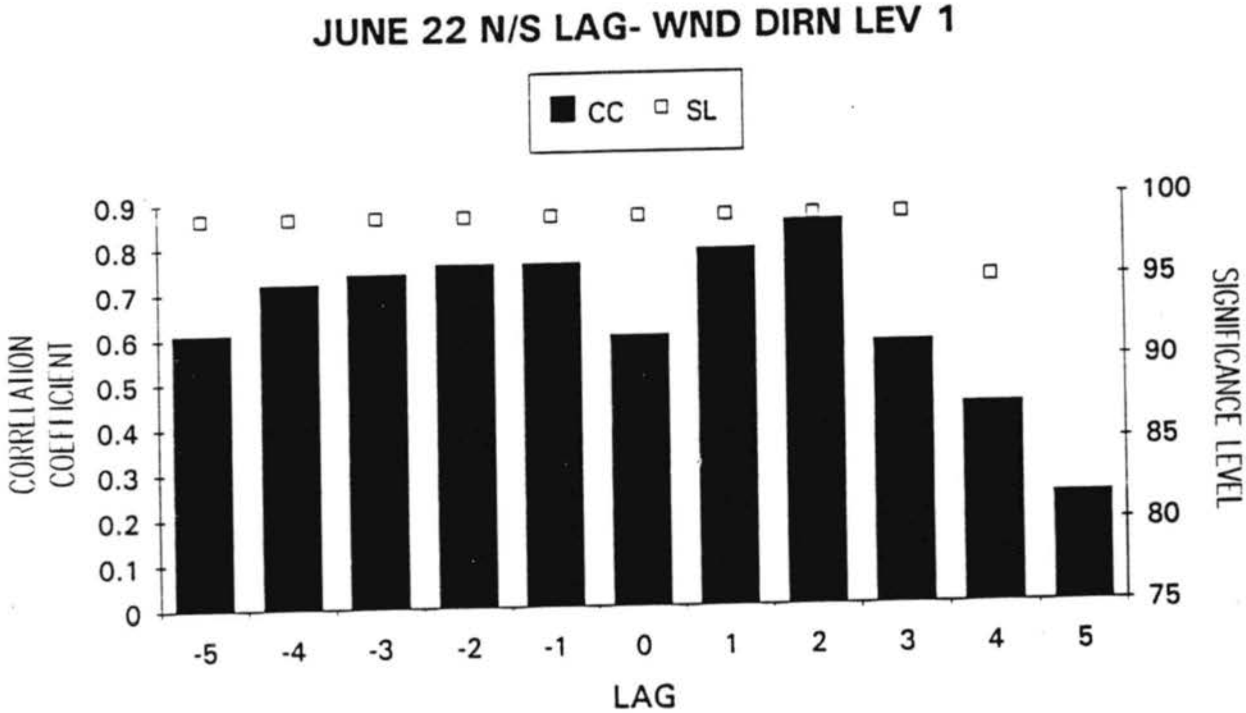

Figure 3.8c: Same as 3.8a but for wind direction at 250m.

with RAMS shifted windward although the temperature variability is still small overall.

Thus, the data from the 22nd add positive support to the suggestion of a windward horizontal phase shift in the RAMS results. Before any possible explanations are hypothesized for why RAMS would produce data with a spacial lag, the correlation coefficients for the height lag should be examined to see if RAMS also produces an offset in height relative to the observed data.

3.3.3. VERTICALLY PHASED COMPARISONS

It is important to note here that while a north-south lag in the previous section was indicative of a constant distance differential, the height lags are not that consistent. As previously explained, due to stability criteria in the model, the vertical grid spacing is stretched with height for subsequent levels. Thus, even one lag at level one represents a different distance than one lag at levels two or three. And, two lags does not represent double the distance of one lag. To help clarify what is meant by the various lags, distances will be attached to each statement. In this section, positive lag represents upward shifts of the RAMS data and negative lag represents downward shifts of the RAMS data.

On June 10th, the highest positive correlations were seen with RAMS results shifted upward for wind speed, wind direction, and temperature (Figures 3.9a-c). At level one, the greatest correlation for wind speed was calculated to be at plus 5 lag(567m) although its value is weak at only 0.29 and significant at the 75% level (Figure 3.9a). At level two, it was at plus 3 lag(545m) and the coefficient was 0.6 (99% significant)(Figure 3.9b). And at level three, the maximum correlation occurred at plus two lag(460m) and had a value of 0.48 (97.5% significant)(Figure 3.9c). The consistency for all three levels (approximately 500m height lag) here is very interesting.

The wind direction data confirm this trend as well. Once again, the highest correlation for level one was at plus five lag(567m) with a weak value of 0.26 (75% significant)(Figure 3.9d). At level two, the correlation was high at 0.76 at plus three lag(545m)(Figure 3.9e). And, at level three, the highest value appeared at plus two lag(460m) and was 0.55 (Figure 3.9f). Both of these are significant at the 99% level. The wind direction data all show good correlation with RAMS data shifted approximately 500m up just as the wind speed data did. Thus, there appears to be a definite pattern of increased correlation with the observations when an upward height adjustment of the RAMS results is performed. In addition, because it appears very consistently for all three levels, this is a much stronger relation than the north-south lag study.

Temperature correlation with height lags was also performed. The values of the correlations were weak; between 0.34 and 0.4 (75% to 90% significance) for all three levels (Figures 3.9g-i). However, the highest of these positive values all occurred with the RAMS data shifted a few height levels upward. Although weak, this is another corroborating factor.

The June 22nd case was also examined for height lag correspondence (Figures 3.10a-c). Wind speed data were in virtually perfect agreement with the 500m upward shift of RAMS. At level one(250m), RAMS shows a correlation of 0.97 with the aircraft data at a plus five lag(469m)(Figure 3.10a). At level two, at plus two lag(418m), the correlation was 0.9 (Figure 3.10b). The wind direction coefficients are not as supporting. The best agreement for wind direction at level one is at plus three lag(254m)(Figure 3.10c) and for level two, at minus two lag(-133m). The lower level data at least shows a higher correspondence with RAMS shifted upwards although only by 254m. The higher level disagreement may be a result of a temperature inversion which increased over the day in magnitude at this height. RAMS was not updated throughout the simulation and thus could have no knowledge of this change. Thus, RAMS may be showing remnants of the island's effects at higher levels where the C130 is showing the increased magnitude of the inversion which overpowered any small island effect which may still have been present at this level.

Temperature data on the 22nd showed little correlation. The highest at level one occurs at plus four lag(357m) but is only 0.26 in value significant

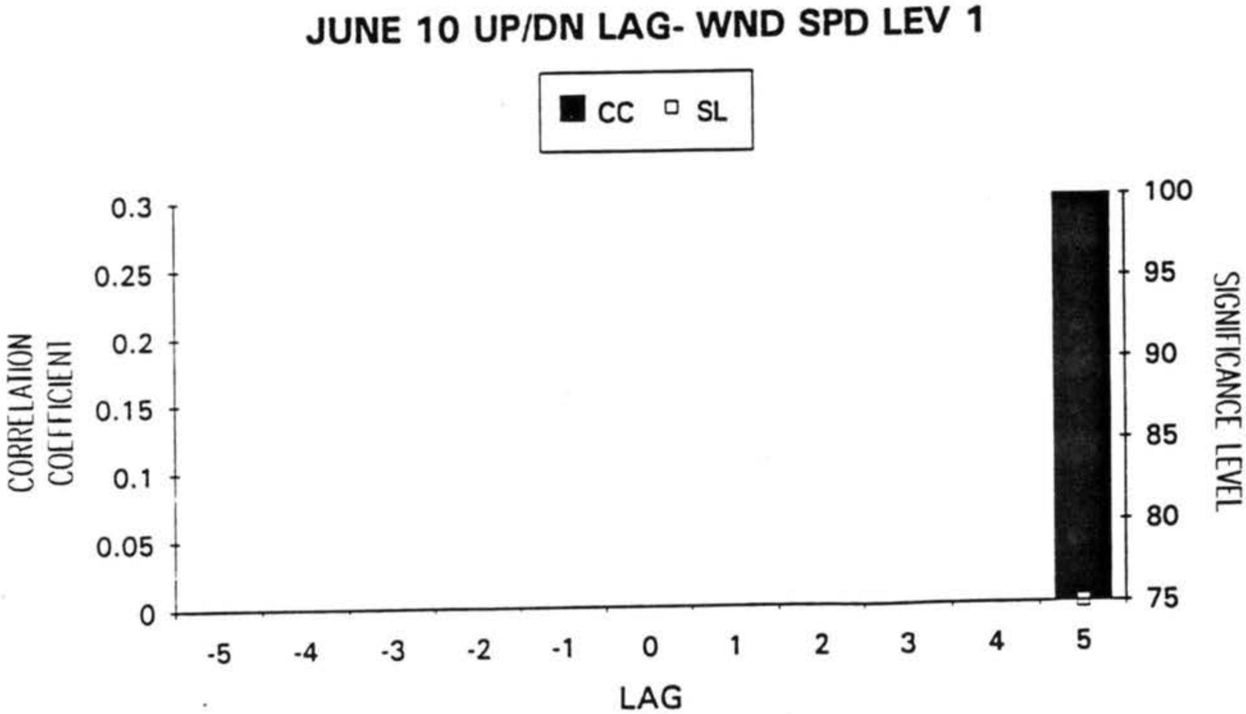

Figure 3.9a: Correlation coefficients and significance levels for wind speed for a up/down lag of the RAMS data on June 10th at 420m. Plus lags indicate that the RAMS data was shifted upward. Negative lags- downward.

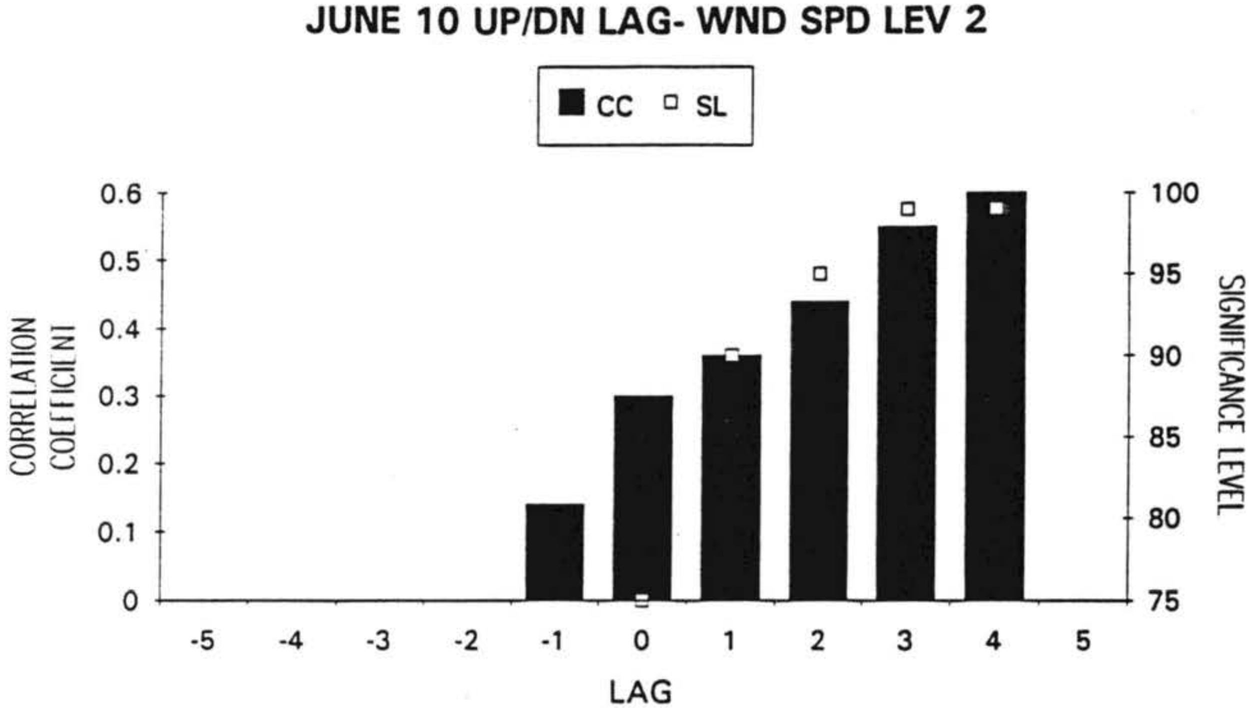

Figure 3.9b: Same as 3.9a but for 1180m.

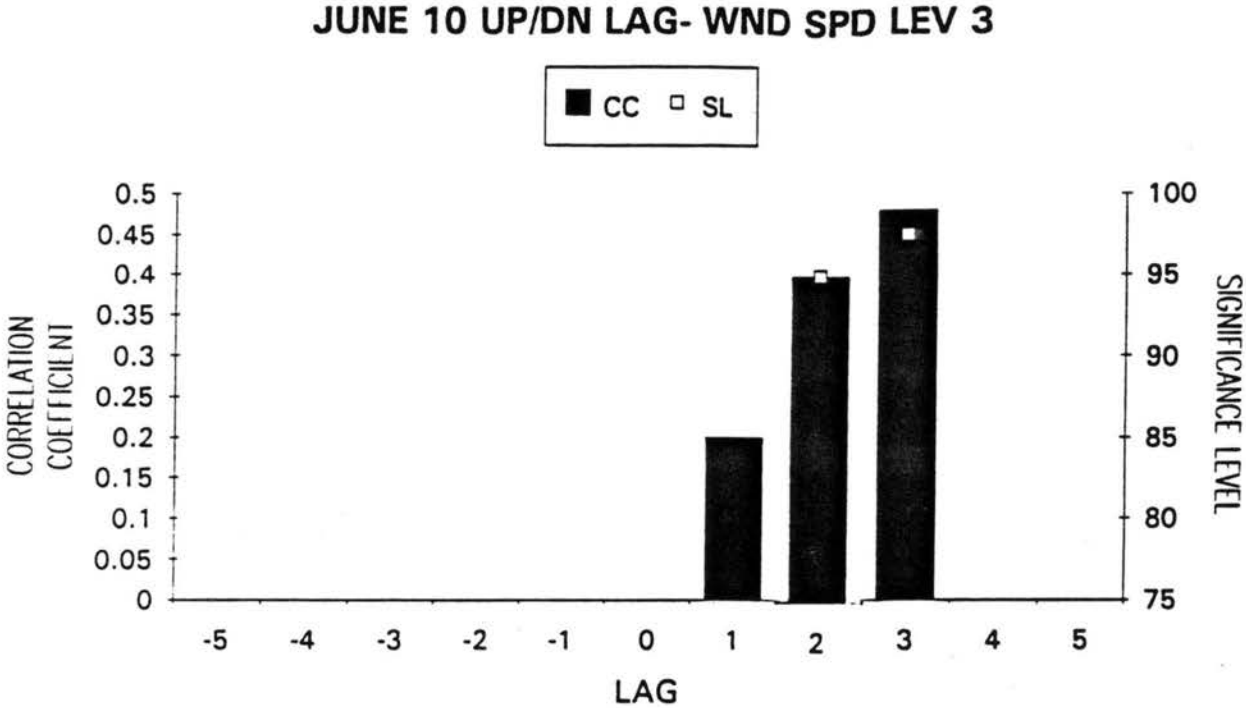

Figure 3.9c: Same as 3.9a but for 1640m.

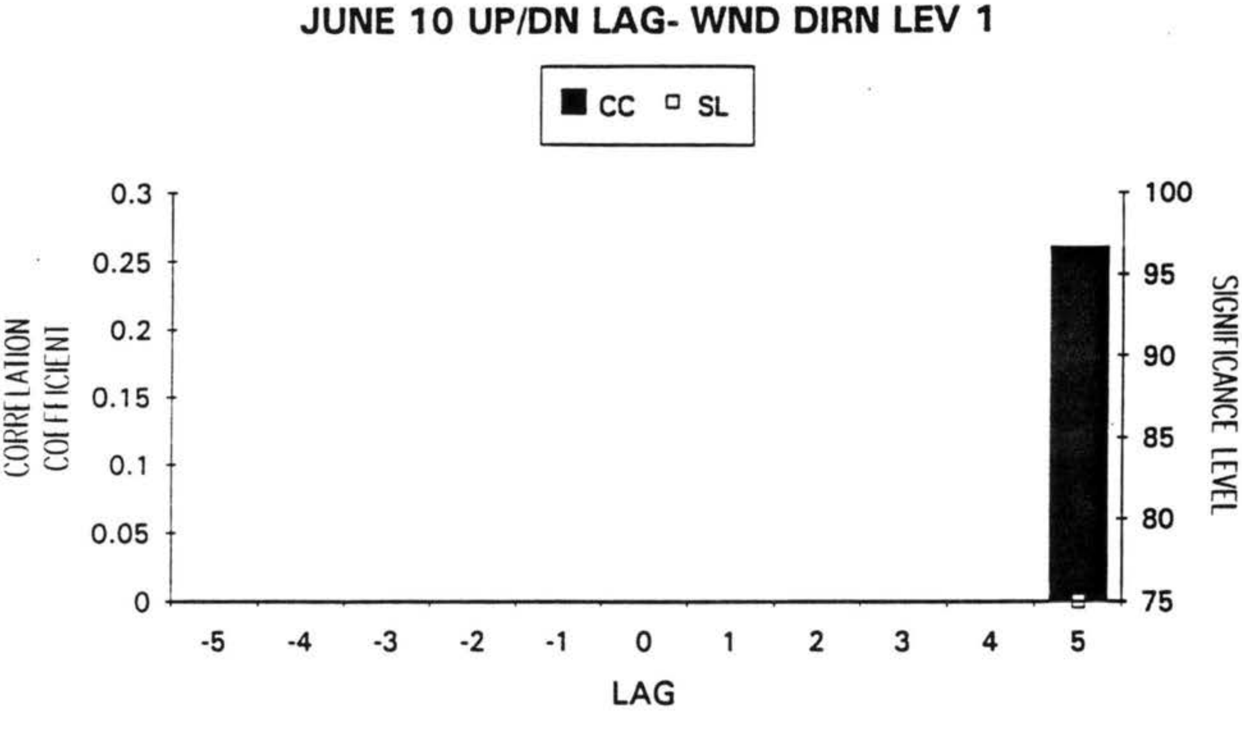

Figure 3.9d: Same as 3.9a but for wind direction at 420m.

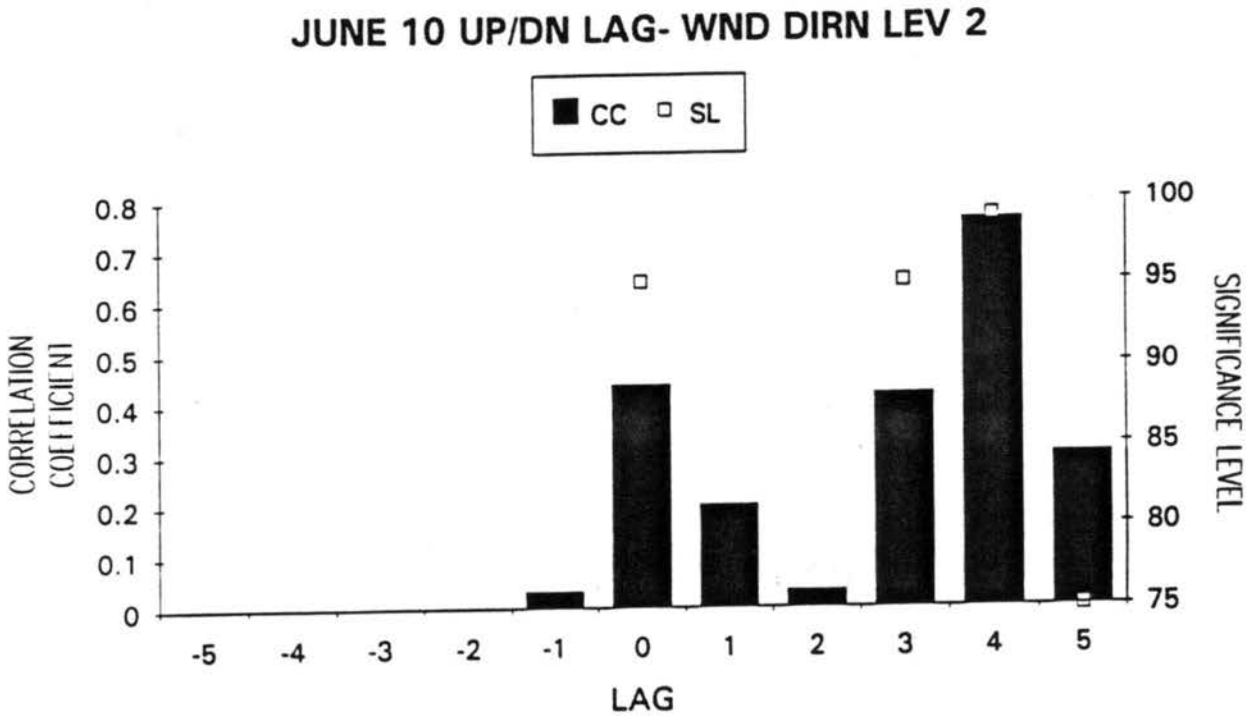

Figure 3.9e: Same as 3.9a but for wind direction at 1180m.

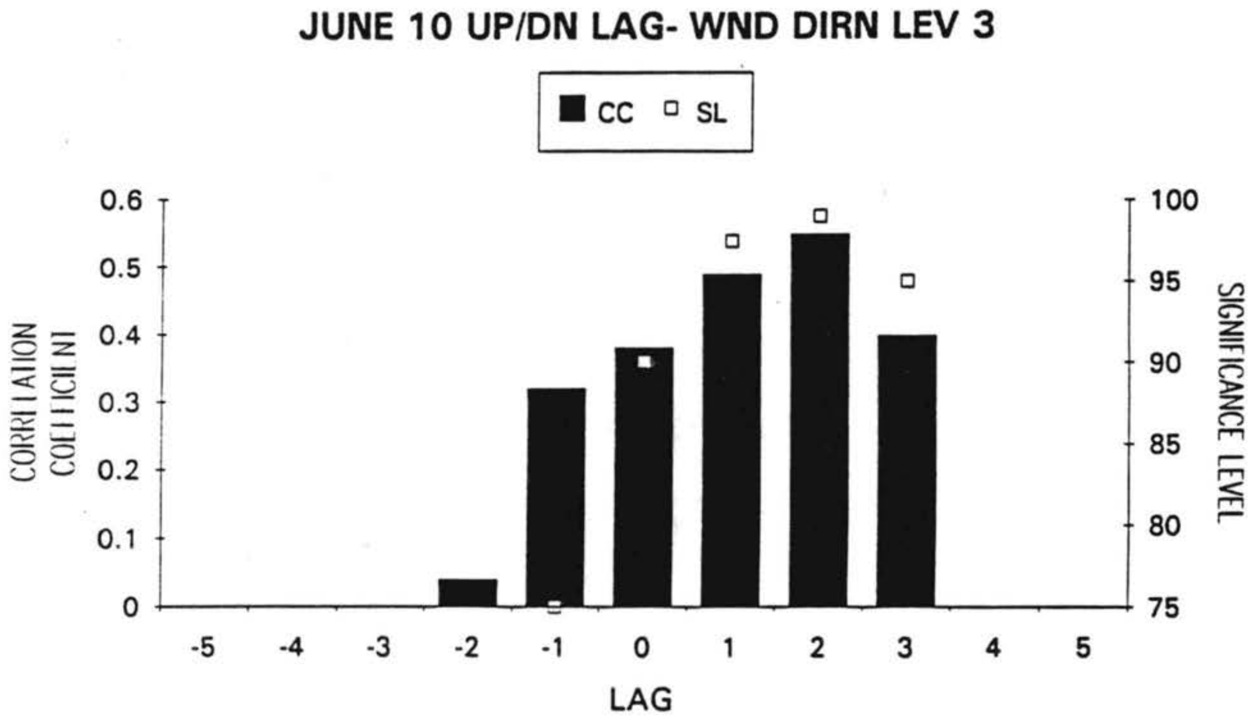

Figure 3.9f: Same as 3.9a but for wind direction at 1640m.

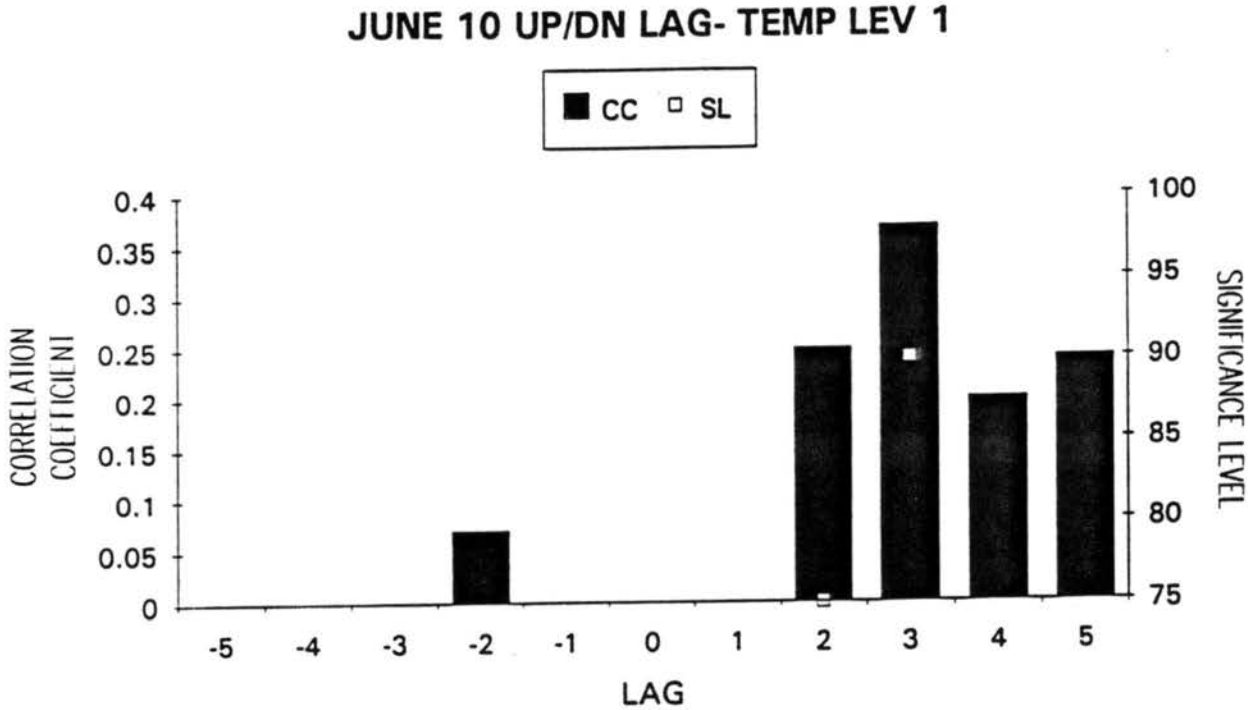

Figure 3.9g: Same as 3.9a but for temperature at 420m.

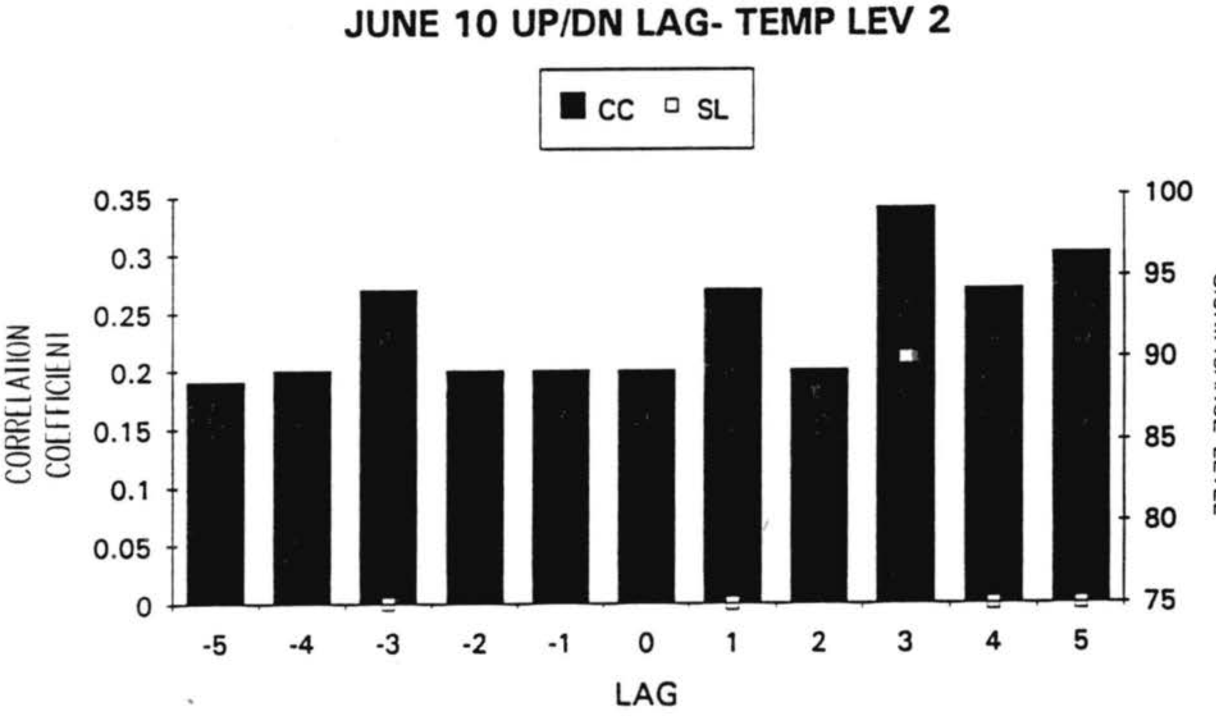

Figure 3.9h: Same as 3.9a but for temperature at 1180m.

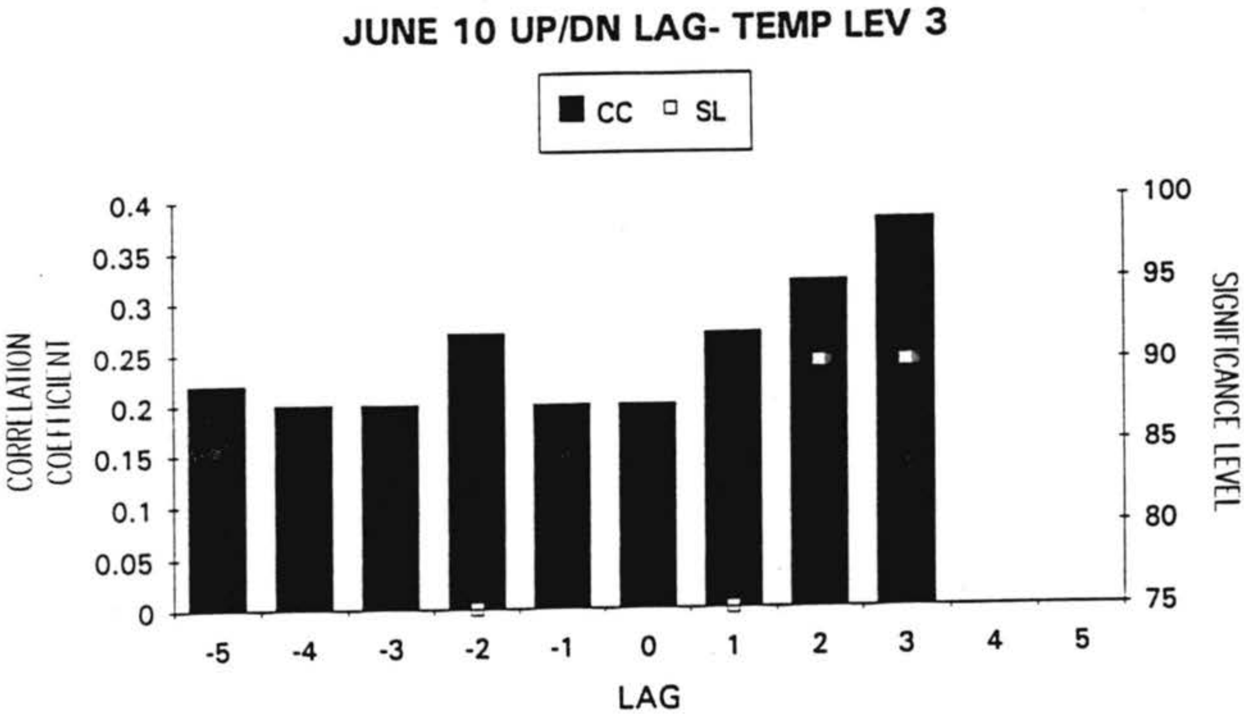

Figure 3.9i: Same as 3.9a but for temperature at 1640m.

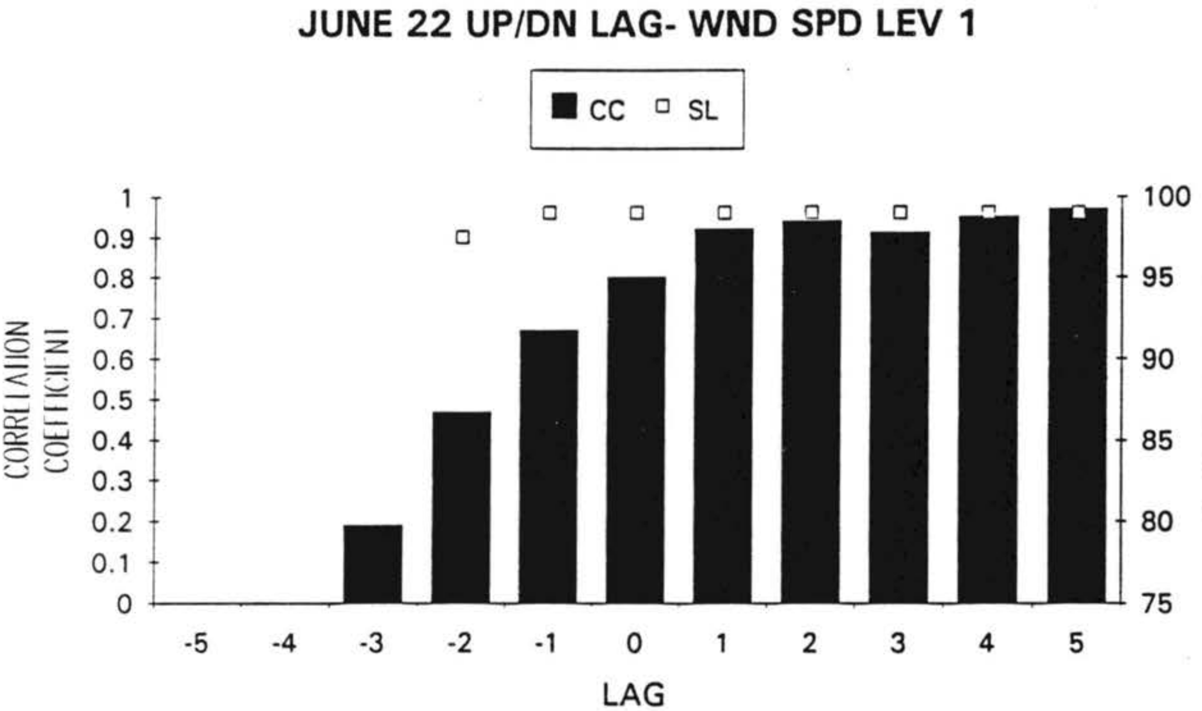

Figure 3.10a: Correlation coefficients and significance levels for wind speed for a up/down lag of the RAMS data on June 22nd at 250m. Plus lags indicate that the RAMS data was shifted upward. Negative lags- downward.

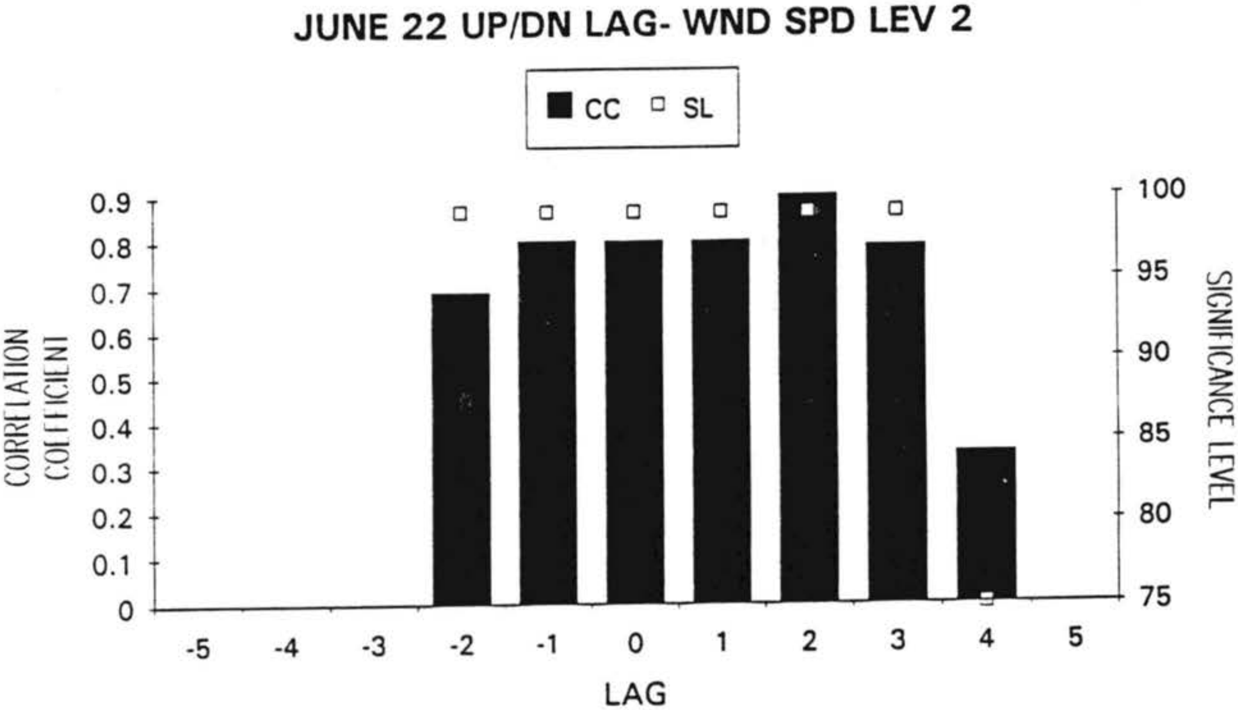

Figure 3.10b: Same as 3.10a but for 1490m.

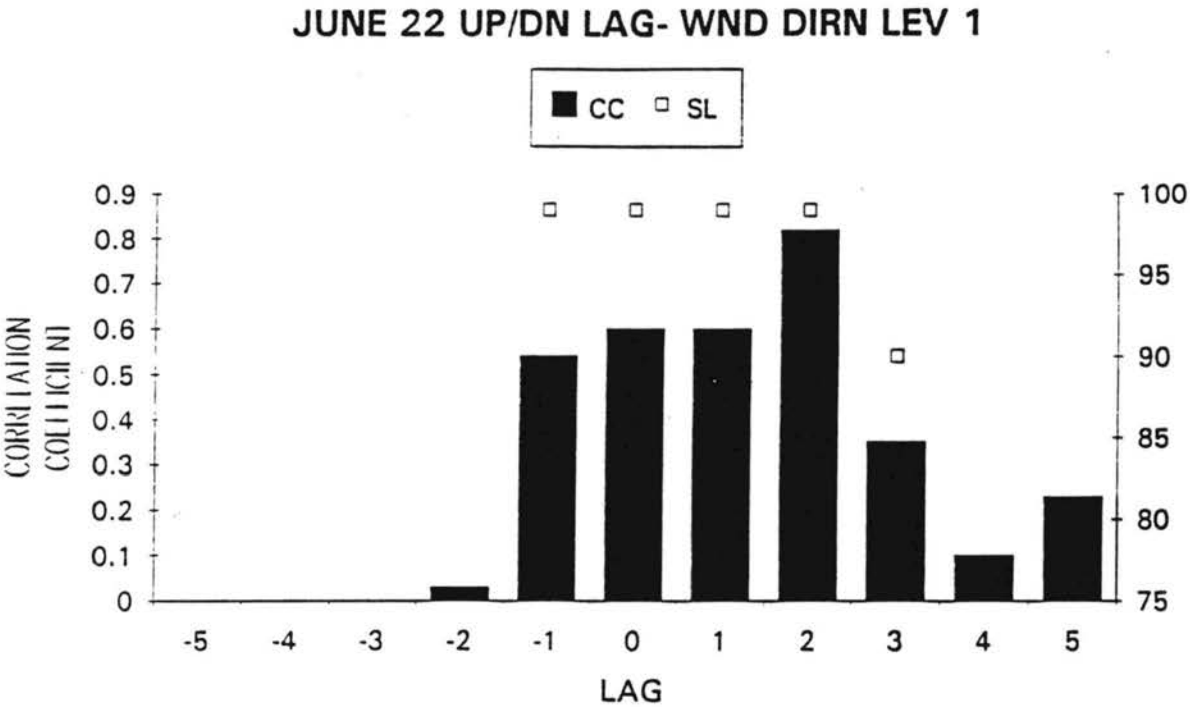

Figure 3.10c: Same as 3.10a but for wind direction at 250m.

to only 75%. Level two has a 0.42 (90% significance) coefficient at plus two lag(418m). This supports the contention of a height offset between RAMS results and observations but since the correlations are weak, not much weight can be given to these results.

3.3.4. SUMMARY OF PHASED COMPARISON STUDY

Of the three possible explanations for the lack of agreement between RAMS and the C130 aircraft, the first two- horizontal lag and vertical lag- are viable possibilities. The other mentioned contender was that the sources of error introduced during data manipulation sum up to be large enough to throw off results.

Errors were introduced by data averaging, estimations of such things as the location of the island-ocean interface and plane speed, time differences between RAMS and the actual measurement times of the instruments, and height level discrepancies. Errors could also stem from the fact that RAMS values are area-averaged over a grid box and the aircraft takes point measurements. And, finally errors are present due to the difference in resolution of RAMS (500m resolution on the finest grid) and the C130 aircraft which took measurements every second (approximately 100m resolution). While the errors alone are most likely not responsible for the lack of agreement, they are numerous and must contribute in some way. Support for the other two explanations, however, is strong. Thus, it is more likely that the summation of these sources of error contribute to decreasing the value of the correlation coefficient, but is not in itself responsible for the discrepancies observed with the direct comparison of the aircraft and RAMS.

In summary, it appears as though RAMS and the C130 aircraft data do not agree well for level one(420m) and level three(1640m) on June 10th for a straight point to point comparison of wind speed, wind direction, and temperature. Level two(1180m) shows some agreement for wind speed and direction but not for temperature. When RAMS results are shifted 400m to 500m upward in height or 1km to 2km windward (upwind) and then compared to the aircraft data for the level in question, the agreement improves significantly.

For the June 10th case, there were only a few instances where the shifting of the RAMS data did not improve the correlation. These instances were wind speed at level three, wind direction at level one, and temperature at all three levels. On the 22nd, there were no problems with wind variables at either level. Thus, on the 10th, the lack of correlation is most likely due to the lack of variability across the island initially. Both the C130 and RAMS depict this well; thus, there is agreement. The lack of a high correlation is likely the result of small noise fluctuations about this relatively constant value. The same is true for temperature.

Finally, the only place where the correlation results did not improve for an upward shift of RAMS was for wind direction at level two(1490m) on June 22nd. As previously discussed, this could be due to the increased magnitude of an inversion near this level throughout the day of which RAMS could have no knowledge.

When examining the significance values of the calculated correlation coefficients, a few things should be kept in mind. First, errors definitely exist within each data set which could have a tendency to reduce the correlation coefficient. This may be applicable to any of the supporting correlations which are a bit low in magnitude. Secondly, wind speed values across the island are partially influenced by the values next to them. Thus, the sample is not completely random. This may reduce the amount of weight given to the stated significance values. But, thirdly, the results are confirmed by two completely different days. This would add credibility to the significance results. Thus, while the significance values may in fact have some error, there exists enough corroboration to give them weight in this analysis.

It is now reasonably established that the RAMS data are somehow out of phase with the observations, either vertically, horizontally, or both. Thus far, nothing has been said as to why this may be the case. Certainly if RAMS is producing results which are out of phase consistently for three variables, there must be a logical explanation. Referring back to the sources of error introduced in this comparison, one stands out with regard to this issue; the resolution difference between RAMS and the C130 aircraft.

The north side of the island is masked by a steep cliff. Under conditions of northerly wind, the change in the wind structure induced by this cliff should have a significant effect downstream of the cliff, over the island. The cliff was 100m high. If RAMS was only able to resolve this cliff to 500m horizontally, the slope of the cliff would not be accurately represented. Intuitively, if the slope of the cliff is underrepresented, disturbances induced by the cliff should be found further downstream, but not as high as they are in actuality. This intuition would support the results found in this chapter; namely, that an upward or a windward shift in the RAMS data provides statistically higher correlation values when compared to the observational data of the C130 aircraft data. The possibility of the topographic resolution of the cliff being responsible for a phase shift in the RAMS data will be examined in the next section.

4. RESOLUTION OF CLIFF

4.1. BACKGROUND INFORMATION

On the north side of the island, providing a direct barrier to the northerly winds, was a 100m high cliff. On top of this cliff, set back approximately 500m, was the measurement site. It is the aim of this study to determine the effect of the island on the measurements taken at this site. Thus, understanding the structure of air flow around this cliff is of utmost importance. And, accurately representing the steepness of this cliff is critical.

The slope of the cliff will always be properly accounted for in the observational data. When using the model, however, resolution of steep topography can be a problem due to stability criteria. Using the nested gridding system of RAMS, the finest grid was resolved to 500m in the horizontal for the island simulation. In other words, the 100m tall cliff corresponds to only a 12 degree slope. Thus, for the island simulation, the steepness of the cliff is not adequately represented and the resulting flow patterns may be misleading.

In the last section, it was seen that there was an apparent phase shift between the RAMS data and the C130 aircraft data. It was shown that a 1-2km windward shift or a 400-500m upward shift in the RAMS wind and temperature data provided significantly better correlation with the observations of the C130 aircraft. It was then postulated that the improper resolution of the cliff in the model may be responsible for this phase shift. In the following section, this will be examined.

For this investigation, RAMS was used in four different runs. In each run, the cliff was resolved to different horizontal length scales- 1000m, 500m, 250m, and 100m. To simplify the results and to guarantee that the differences in results between the runs were solely a result of the cliff resolution, the topography of the island was eliminated. Instead, the topography input to the model on the finest grid was a simple north facing 100m cliff. The cliff began five grid boxes south on the smallest grid's domain and extended east, west, and south across the remainder of the small grid. In all four runs, the model was initialized horizontally homogeneous using the June 10th island simulation sounding with one exception; the wind directions were all set to northerly. All other model parameters in these four runs were identical to those used for the island simulation. Thus, the differences in the wind fields from the four runs must solely be due to the varying resolutions of the cliff in the model (or the resolved motions).

Each of the four simulations was run for one hour and the wind fields were examined. This examination involved three components:

1. A streamline analysis was done using horizontal and vertical cross sections to examine the spacial extent of the flow deflection from the cliff. Froude numbers were calculated to justify the model's prediction of flow separation for only the two finer resolution runs.
2. North-south cross sections of wind speed were plotted for all height levels through the center of the domain. The location relative to the cliff of the wind speed maximum as well as the height to which disturbances propagated was examined for the four runs to determine the possibility of any phase shift.
3. Amplification factors (The wind speed at a particular height divided by the wind speed at the same height upwind and away from the influence of the cliff) were calculated along north-south transects through the center of the domain. This was done in order to examine the regions of cliff-induced wind speed increases and decreases and to compare RAMS results with previous studies employing the same techniques.

4.2. STREAMLINE ANALYSIS

The streamline analyses give no measure of the magnitude of the changes in wind speed. They do, however, give a good indication of the ability of the model to resolve the deflection of flow over and around the cliff for the four different cliff runs.

Examination of north to south vertical streamline cross sections through the center of the domain and through the sides of the domain were done. In addition, east-west vertical cross sections (parallel to the edge of the cliff) were examined in the vicinity of the cliff as well as downwind of the cliff in order to assess the extent of cliff-induced flow separation. And, finally, horizontal cross sections were studied to determine the areas of horizontal wind convergence and divergence and to determine at what height the effect of the cliff is no longer felt.

The streamline cross sections for the 100m resolution case show significantly more detail than the other three runs. In the yz plots, it appears as though the wind hits the cliff in the center of the domain and is deflected (Figure 4.1). There is evidence of upward deflection throughout the height domain which, below 500m, is quite turbulent. This turbulent structure extends downwind of the cliff throughout the grid domain but is largest within 200m of the cliff. Downstream of this, it is evident in small amplitude ripples. Higher than 500m the wind vectors follow the contour of the cliff showing an upward deflection of about the cliff's magnitude and a gradual downward motion over the rest of the domain.

Throughout the region upwind of the cliff, there is evidence of backward and outward deflection. The xy and xz plots confirm this (Figures 4.2- 4.3). At low levels, in the center of the domain, the streamlines show that air actually moves back toward the north against the mean flow (Figure 4.2a). Along the sides of the domain, however, these streamlines diverge as they ascend the cliff. This is seen throughout the entire region upwind of the cliff. It important to note that this partial flow separation is occurring. The implications of flow separation will be discussed in a future section at greater length. Evidence of flow separation decreases with height but can be seen up to 500m. It is also apparent at least 400m upwind of the cliff.

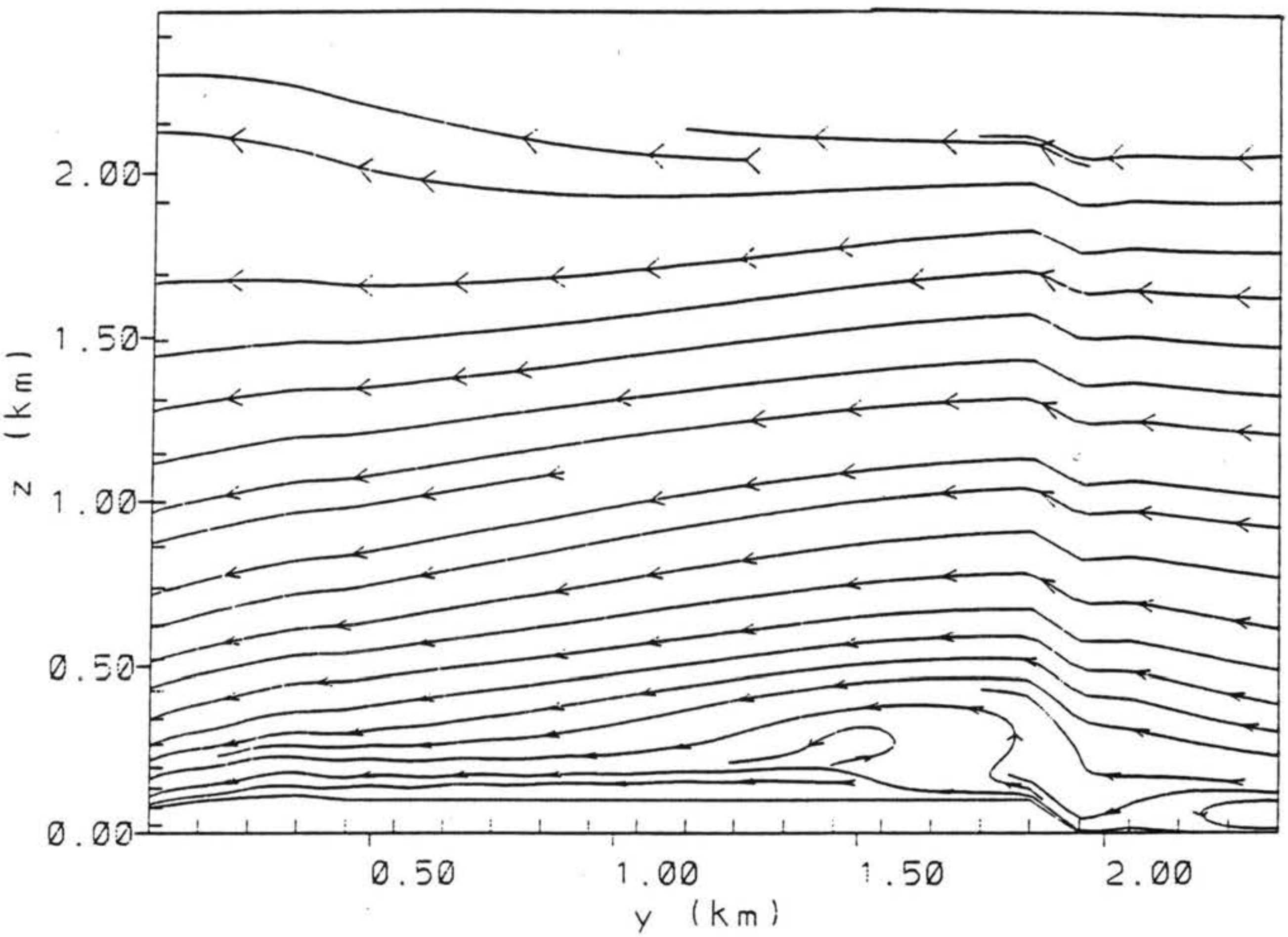

Figure 4.1: Yz cross section through the cliff's center of the streamlines for the 100m resolution cliff. The outline of the cliff is at the bottom.

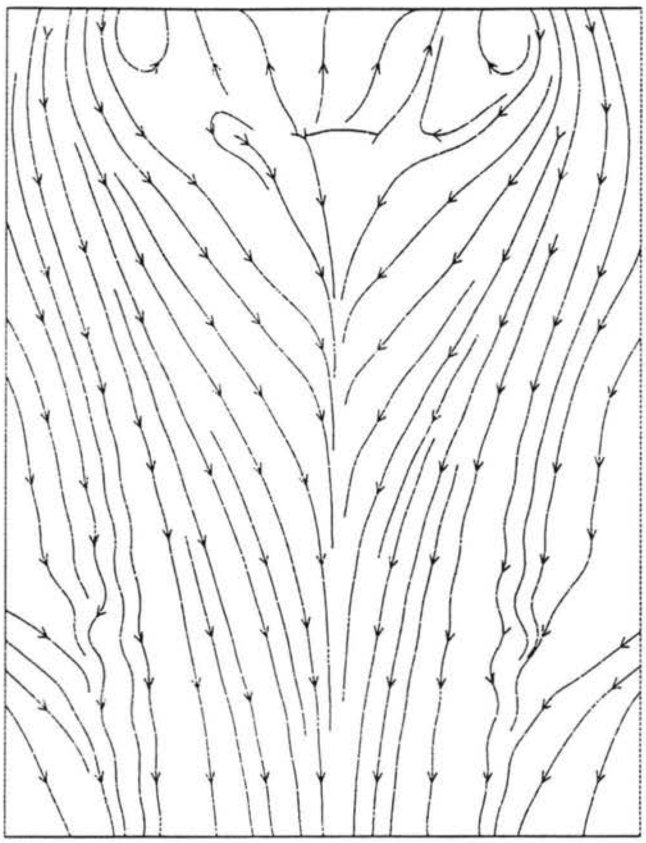

Figure 4.2a: Cross section of streamlines for the 100m resolution cliff at 24m high.

The streamlines, after ascending the cliff, merge together approximately 200m downwind of the cliff at levels below 300m (Figure 4.2b). From 300m to 600m, this region is one of streamline divergence (Figure 4.2c). And, above this, the flow is northerly and undeflected across the entire domain (Figure 4.2d). It is thus unaffected by the topography. Thus, the results from the 100m resolution simulation show wind convergence below 300m, divergence between 300m and 600m, and no change above 600m.

Another thing to note from the xz cross sections is the extent of upward motion at different points north to south across the domain (Figures 4.3a-e). From upwind of the cliff, to cliff bottom, upward motion extends at least 2km in height (Figures 4.3a-b). By clifftop, this region ends at 1km (Figure 4.3c). At 200m downwind, the region of upward motion is confined to the lowest 750m (Figure 4.3d) and by 600m downwind, this region of upward motion diminishes to within 100m of the ground (Figure 4.3e). Thus, not surprisingly, the closer to the topographic perturbation, the greater the vertical extent of the disturbance.

For the 250m resolution case, as expected, the streamlines show a less detailed structure. Initial inspection show the yz cross sections to be virtually featureless (Figure 4.4). The air follows the topography and is deflected upwards the same distance as the height of the cliff. No backward defection is seen at all in this case. Thus, an important flow characteristic has already been lost for a resolution that is still finer than that used in the island simulations.

Other features are lost or diminished as well. The horizontal cross sections show some evidence of flow separation, although the degree is significantly less than for the 100m resolution case (Figure 4.5a). In addition, by 350m high, the flow already appears undisturbed (Figure 4.5b). This is much lower than the 600m level for the 100m case. In the xz cross sections, upstream of the cliff, the wind at very low levels flows from west to east along the cliff base and no flow separation is observed (Figure 4.6a). Slightly higher, above 100m- the height of the cliff, flow separation is once again apparent although slight. This flow separation occurs east of the

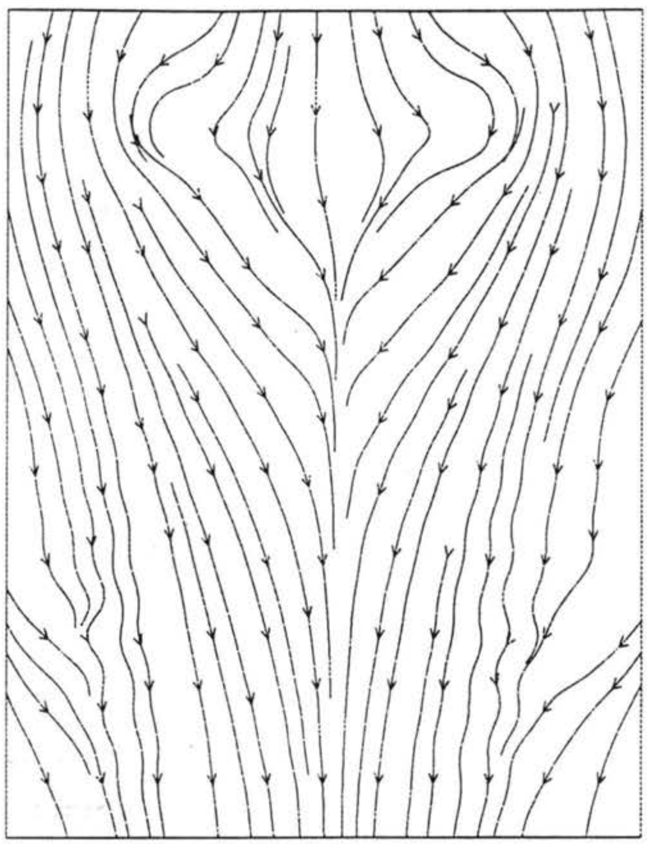

Figure 4.2b: Same as 4.2a but for 134m.

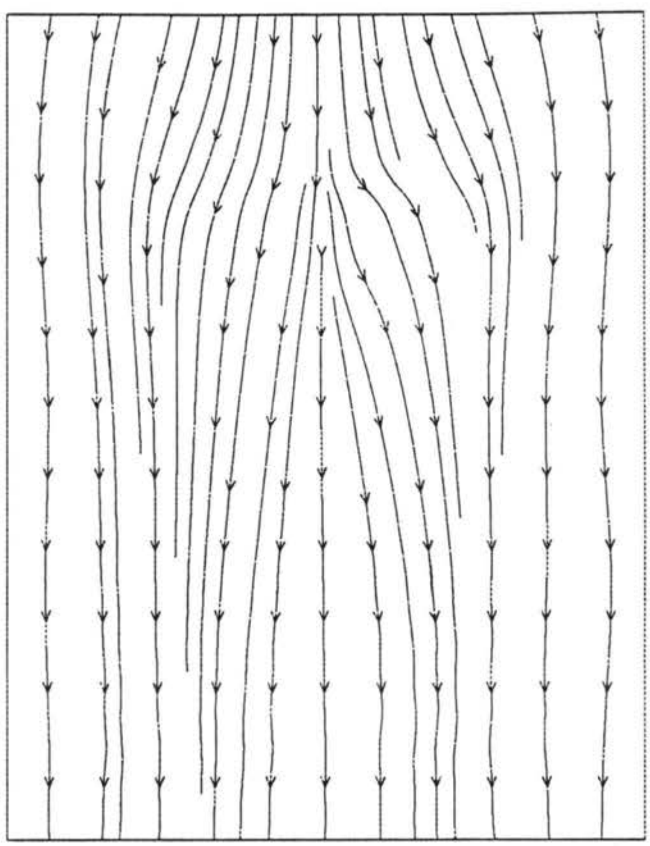

Figure 4.2c: Same as 4.2a but for 344m.

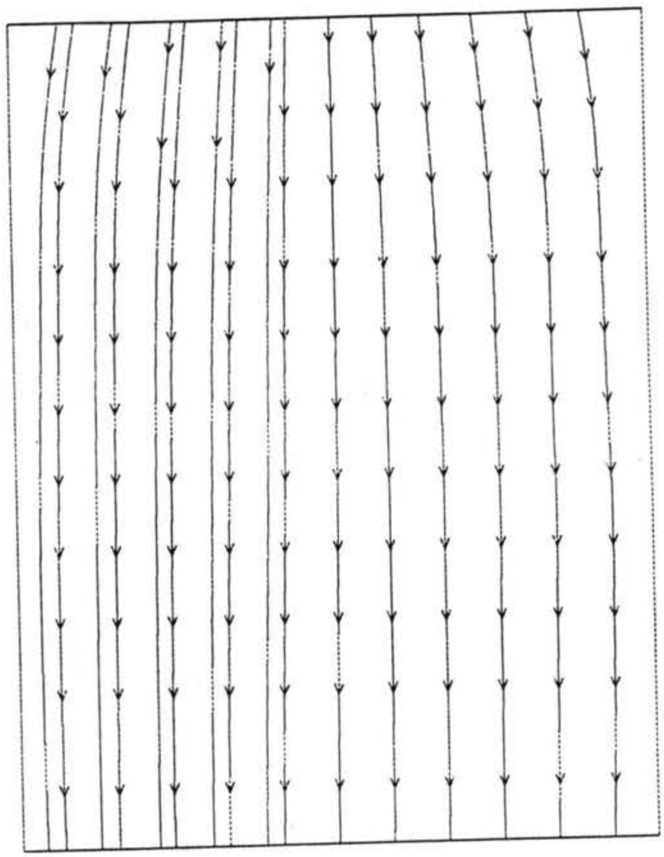

Figure 4.2d: Same as 4.2a but for 624m.

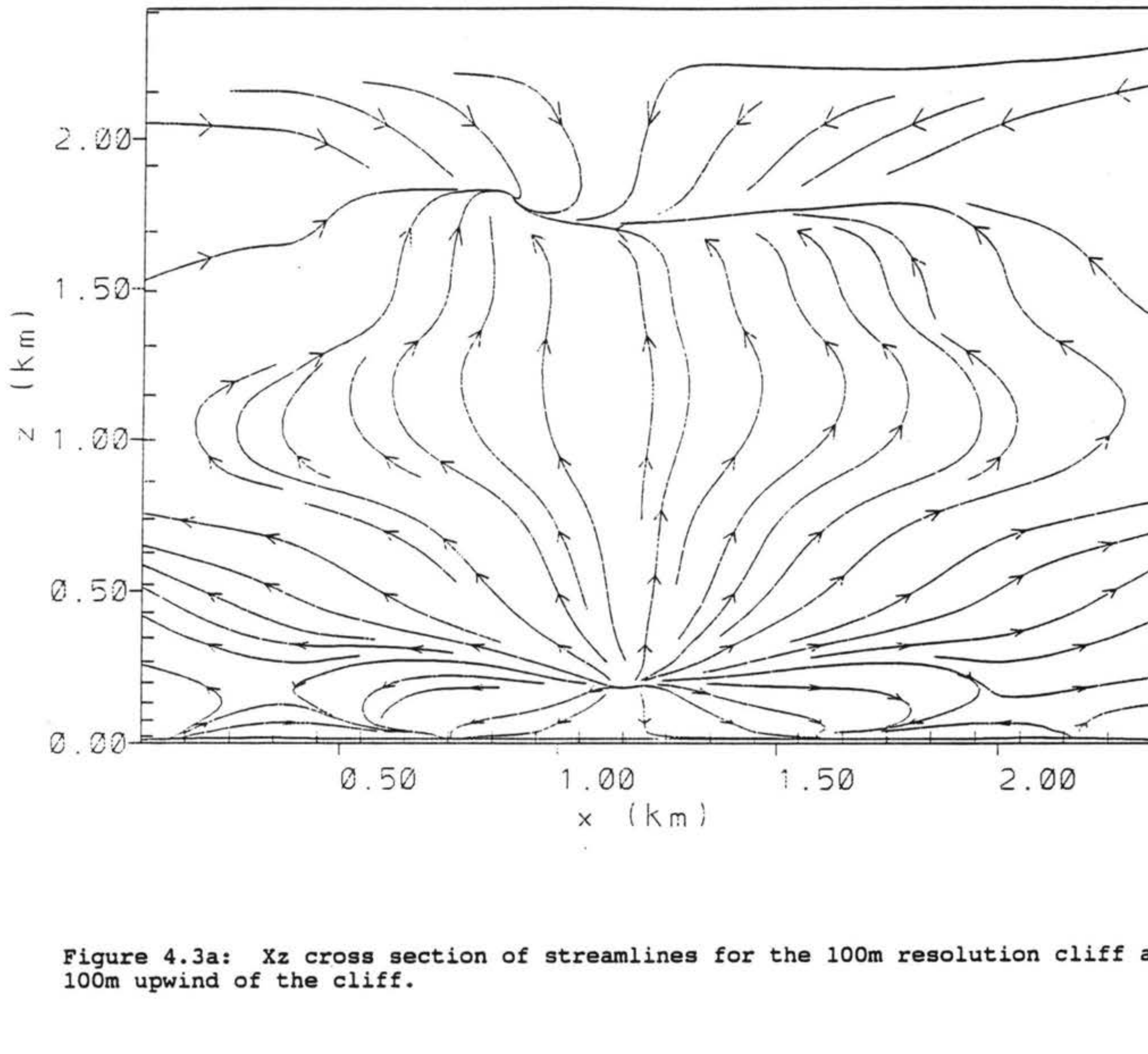

Figure 4.3a: Xz cross section of streamlines for the 100m resolution cliff at 100m upwind of the cliff.

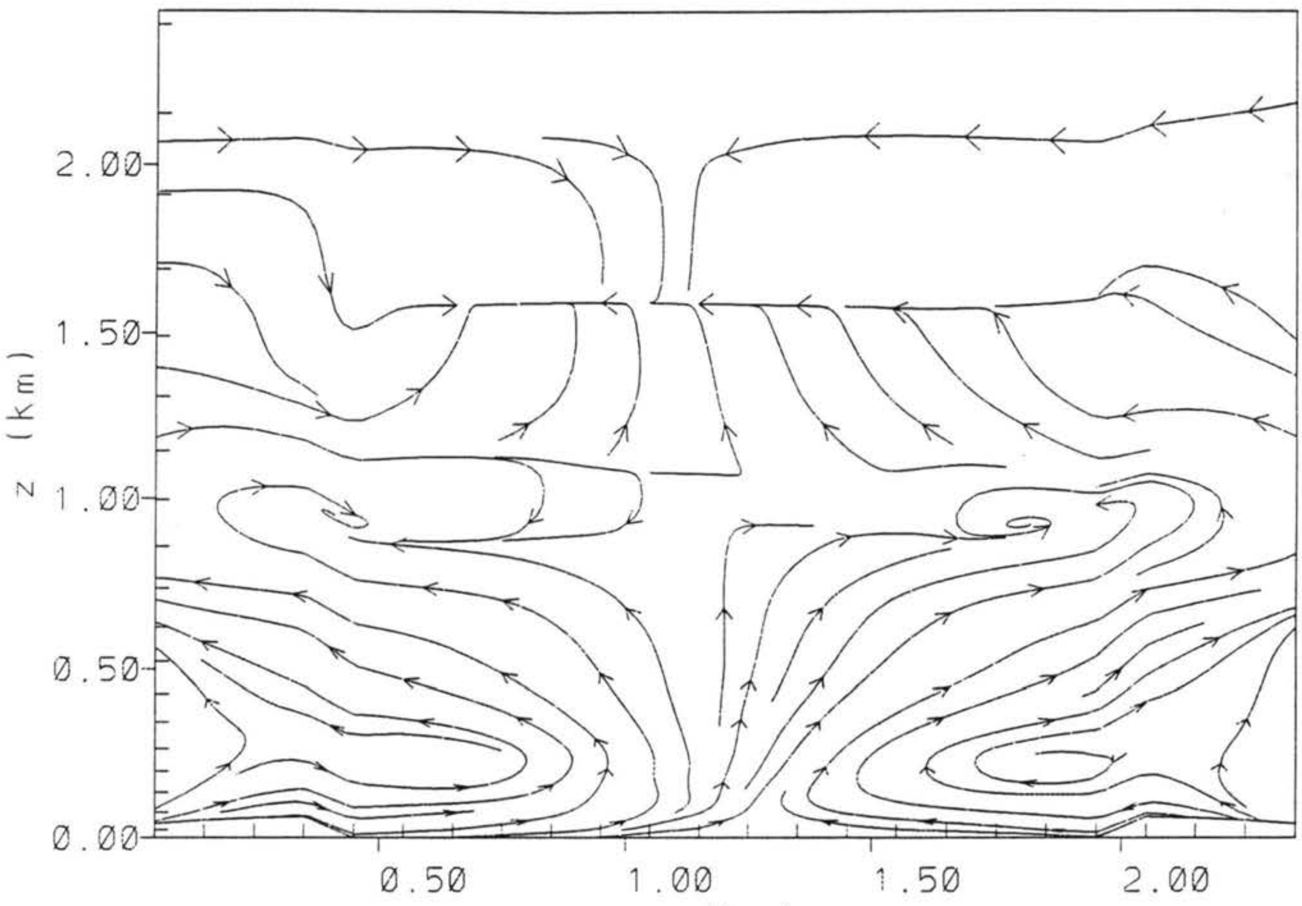

Figure 4.3b: Same as 4.3a but at cliff base.

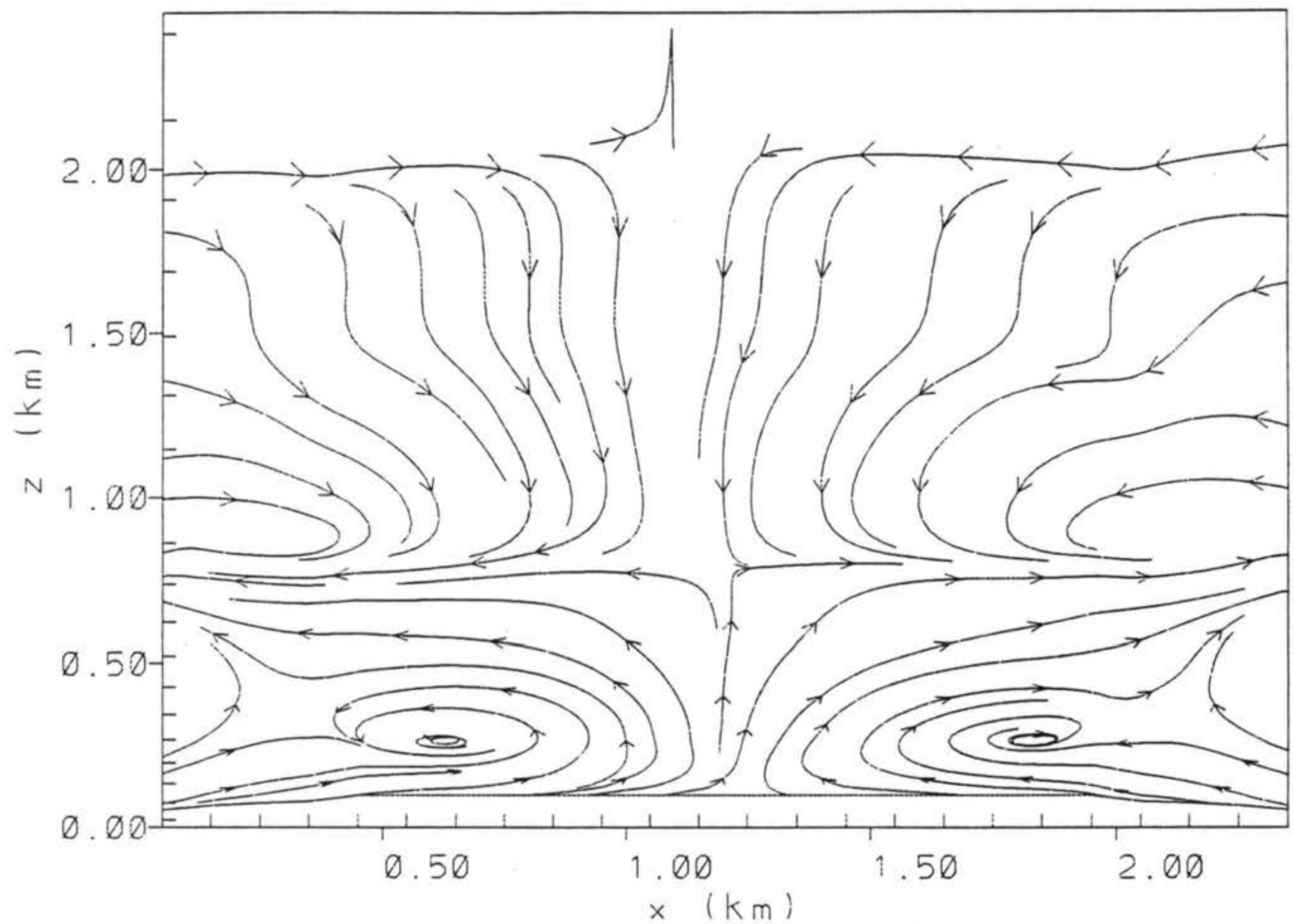

Figure 4.3c: Same as 4.3a but at cliff top.

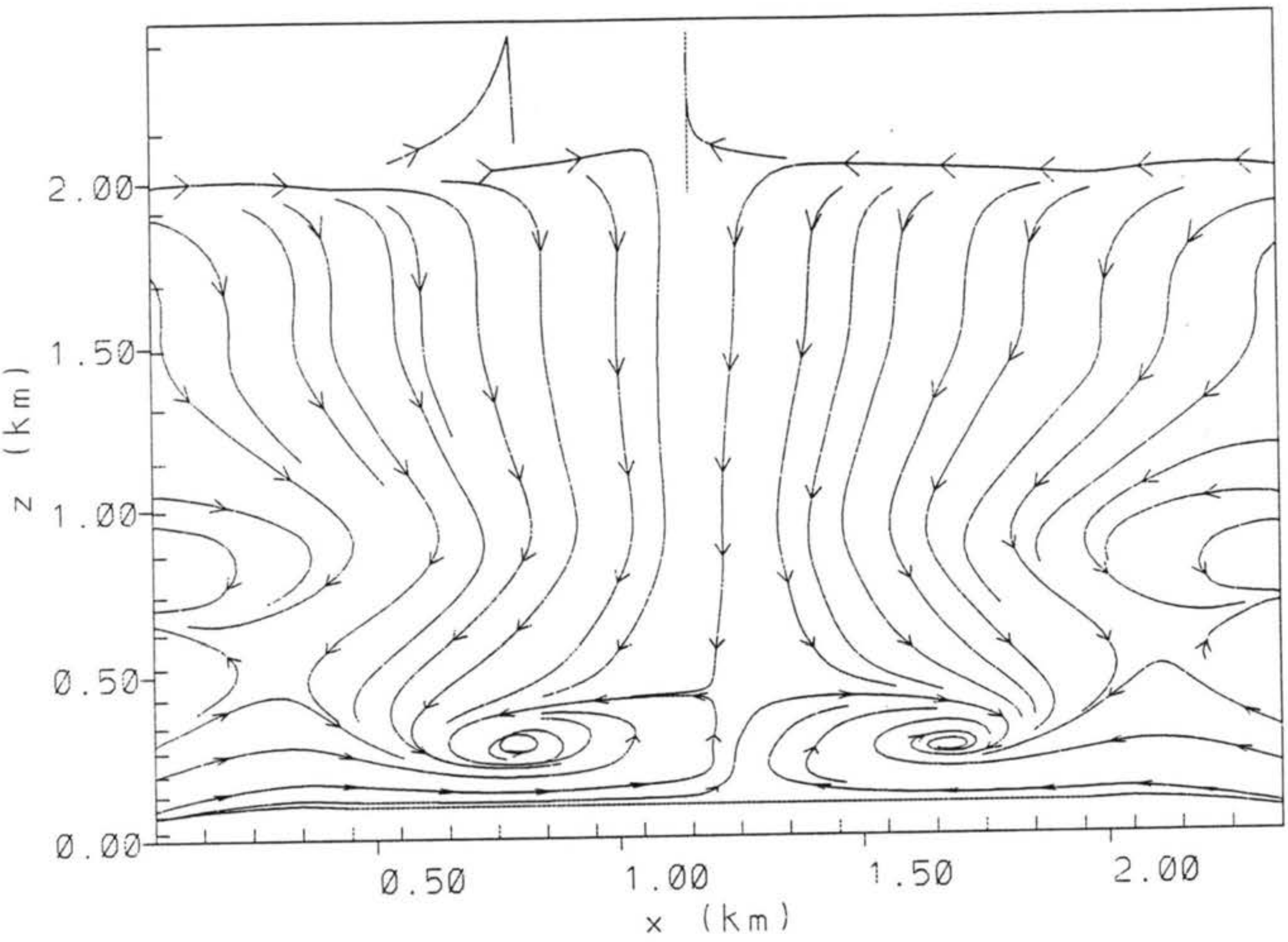

Figure 4.3d: Same as 4.3a but at 200m downwind of the cliff.

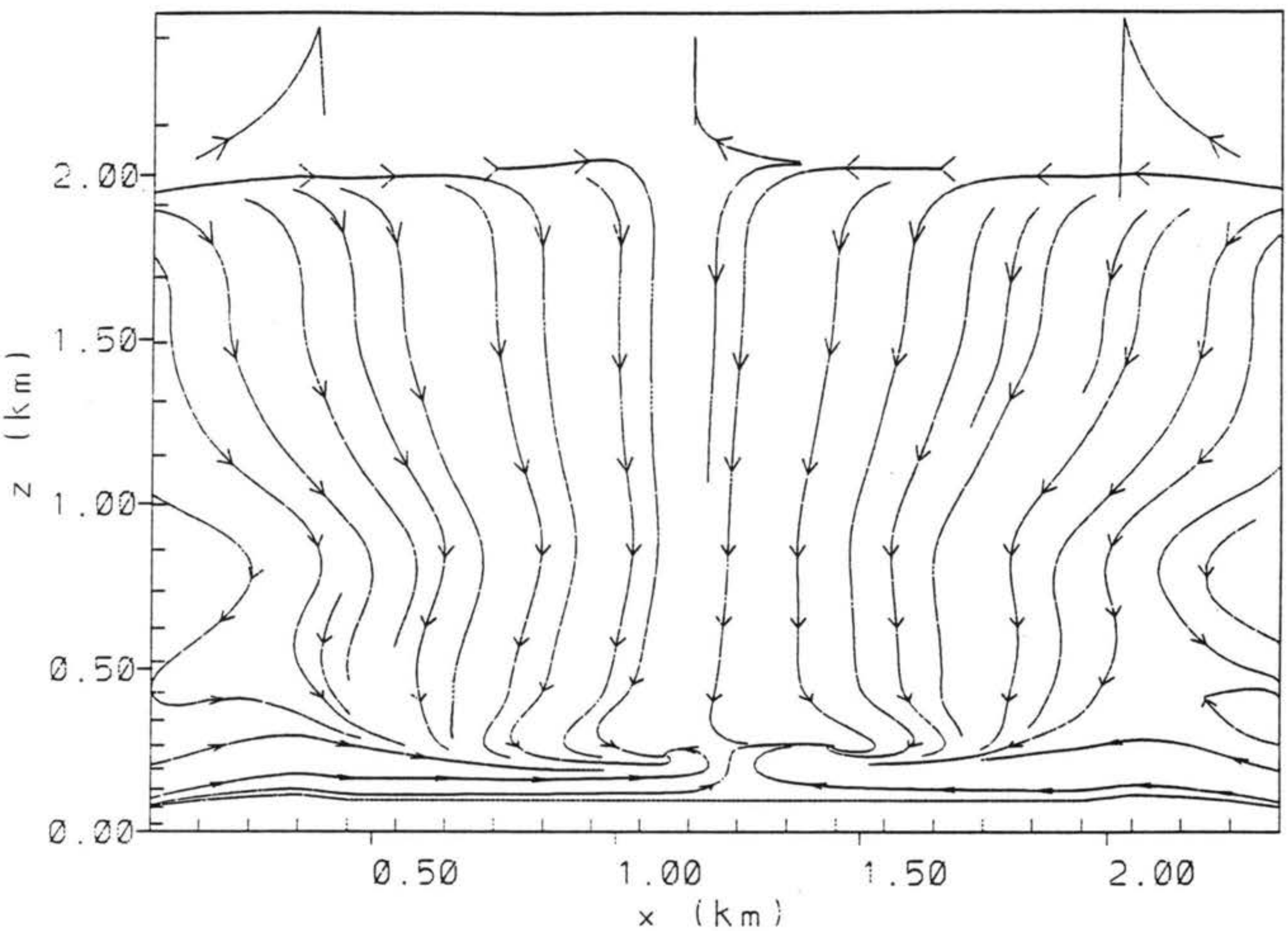

Figure 4.3e: Same as 4.3a but at 500m downwind of the cliff.

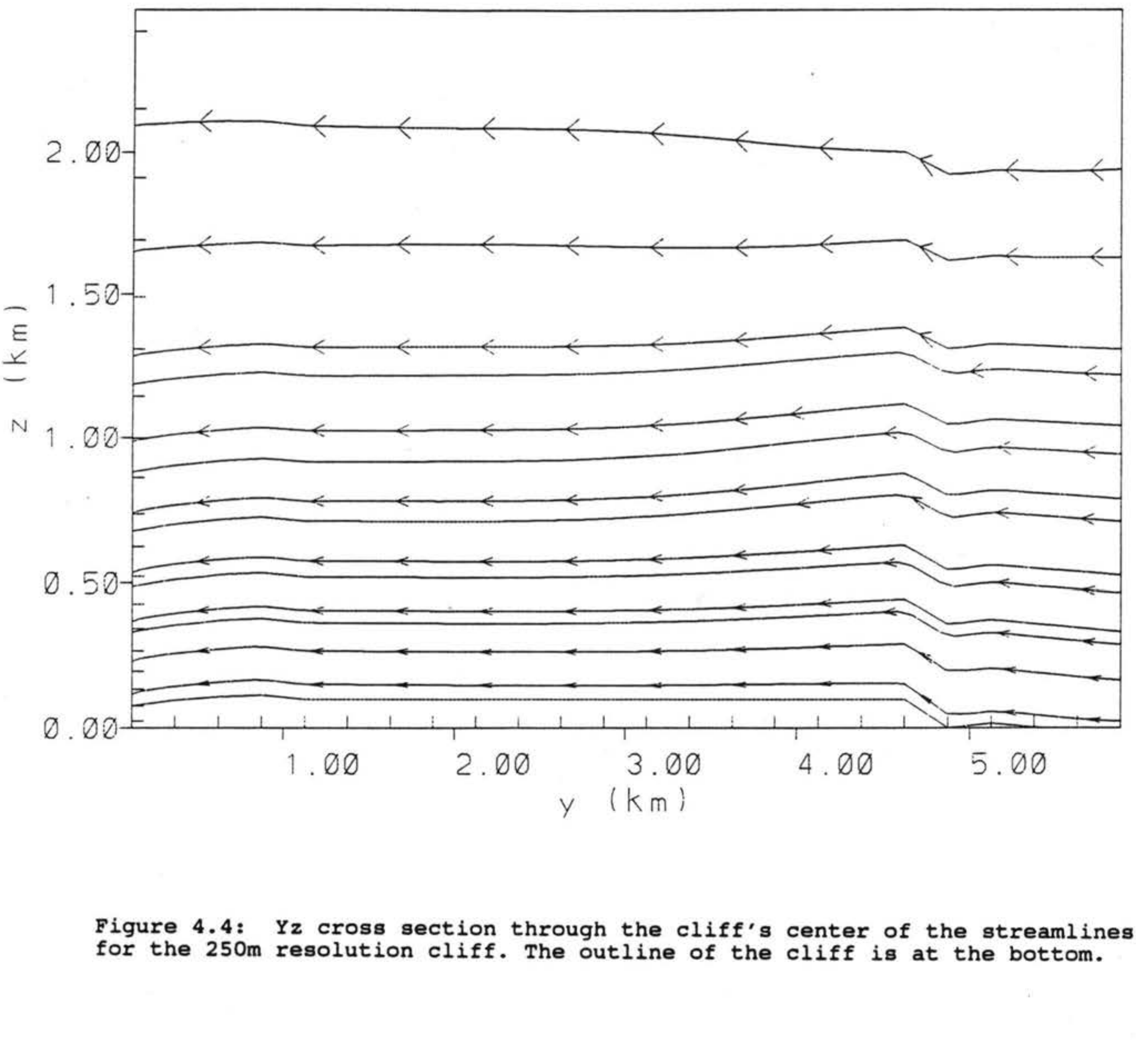

Figure 4.4: Yz cross section through the cliff's center of the streamlines for the 250m resolution cliff. The outline of the cliff is at the bottom.

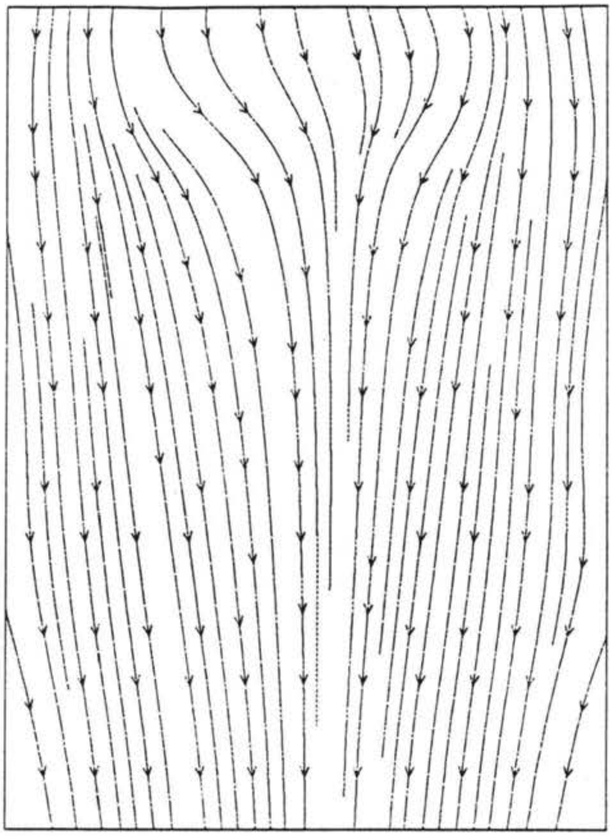

Figure 4.5a: Cross section of streamlines for the 250m resolution cliff at 24m high.

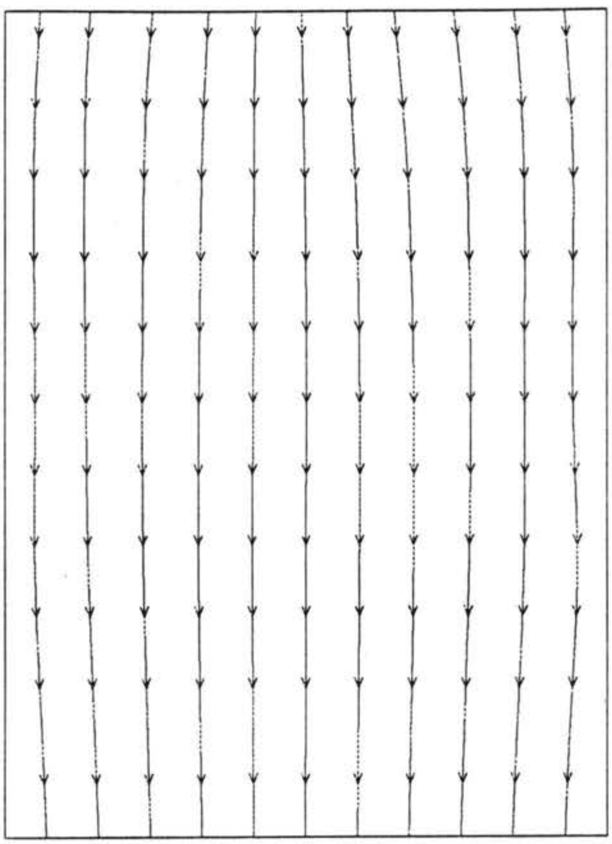

Figure 4.5b: Same as 4.5a but for 344m.

domain's center. In the finer resolution run, flow separation was observed directly in the domain's center. Thus, the change in resolution for these horizontal cross sections changes the appearance of the wind flow pattern. The area and amount of flow separation is shifted and lessened and the height through which a disturbance is felt is lowered.

The extent of the upward motion disturbance can also be seen in the xz cross sections for the 250m resolution run (Figures 4.6a-c). Upwind of the cliff, the region of upward motion extends to 900m- much lower than for the 100m case where it extended to 2km (Figure 4.6a). By the cliff this upward motion region is confined to 350m and by 250m downwind it is within 100m of the ground (Figure 4.6b-c). Thus, the cliff-induced flow disturbance is greatly reduced in the horizontal as well as the vertical when decreasing the horizontal resolution from 100m to 250m.

For the other two runs, the 500m resolution and the 1000m resolution runs, the trend continues. For the 500m case, there is evidence of some small flow separation near the ground upwind of the cliff. This only extends to 250m high, however, and is completely gone for the 1000m case. The yz plots for the 250m, 500m, and 1000m cases are identical indicating much detail in cross sections along the flow is lost in the lower resolution cases. The xz slices show very slight amounts of divergence for the 500m resolution case in the vicinity of the cliff up to 100m. The 1000m case shows no disturbances in the horizontal at any level.

Since flow separation was predicted to occur from the RAMS analyses for the 100m and 250m cases only, Froude numbers were calculated for all four of these runs to see if they support this prediction using the formula,

$$Fr = U_o(gH\Delta T/\overline{T})^{-1/2}$$

where U_o is the approaching wind speed, $g=9.8ms^{-2}$ the acceleration of gravity, H=100m the height of the cliff, delta T the potential temperature difference between the surface and the top of the cliff, and T bar the vertically

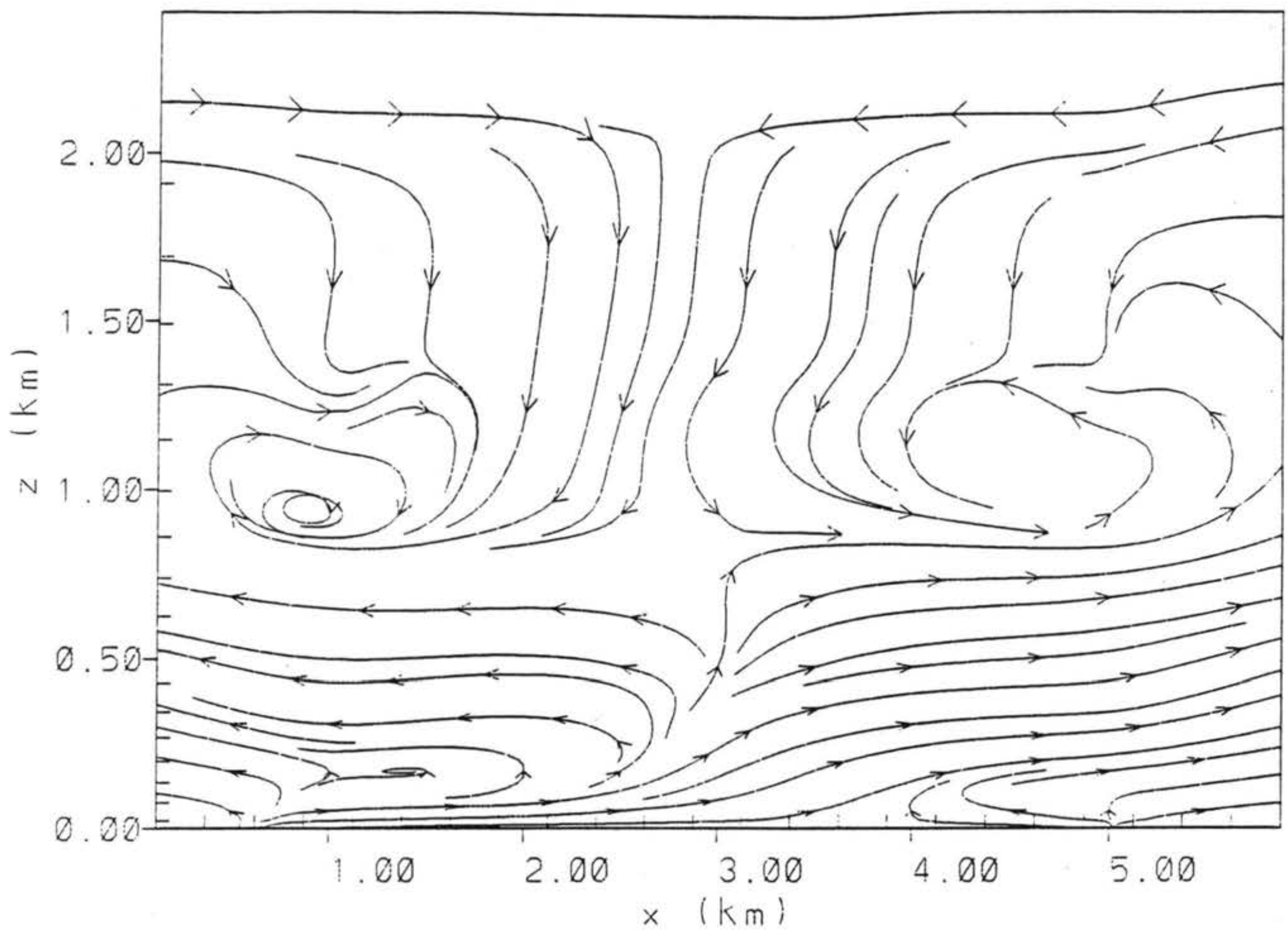

Figure 4.6a: Xz cross section of streamlines for the 250m resolution cliff at 500m upwind of the cliff.

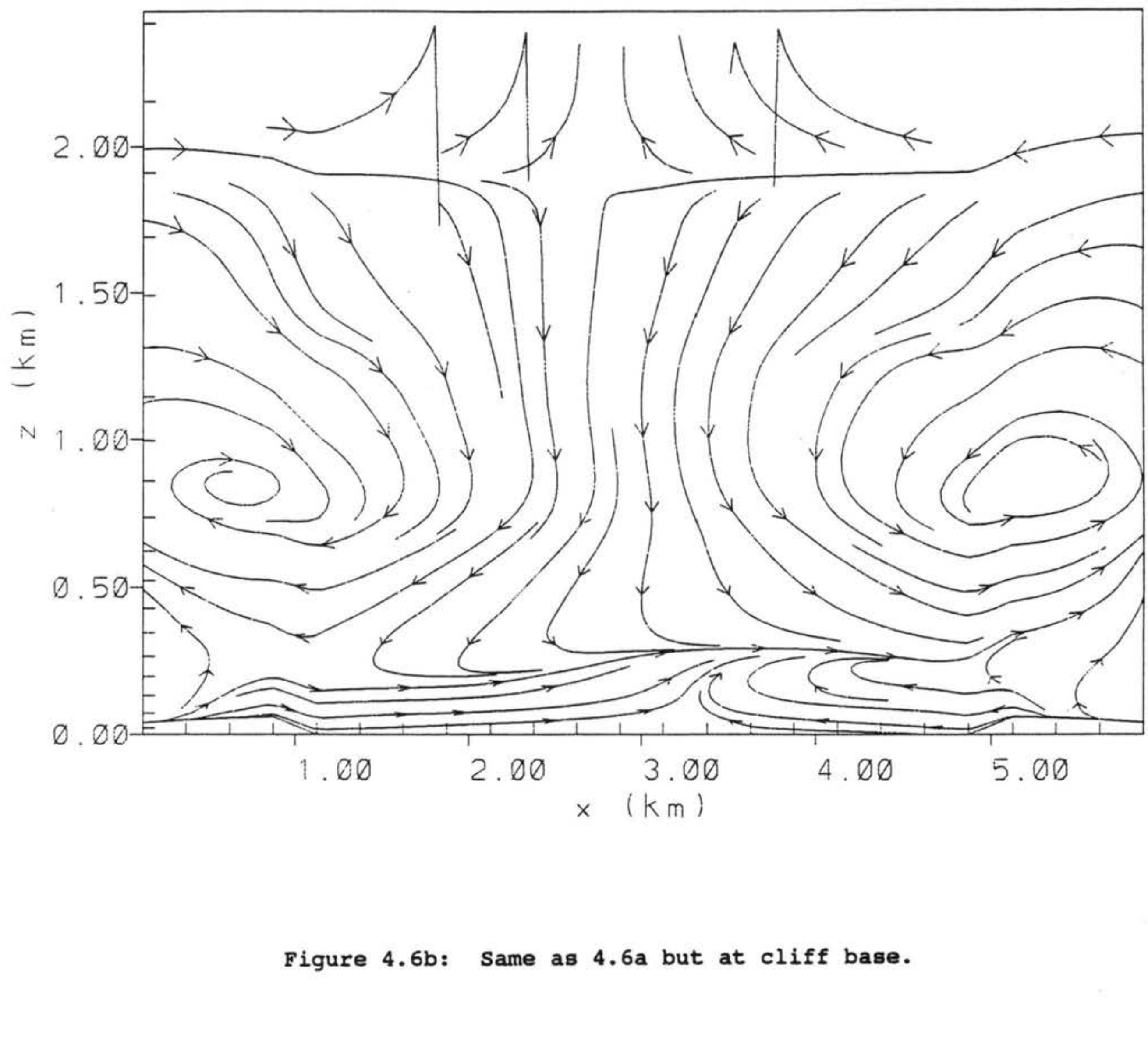

Figure 4.6b: Same as 4.6a but at cliff base.

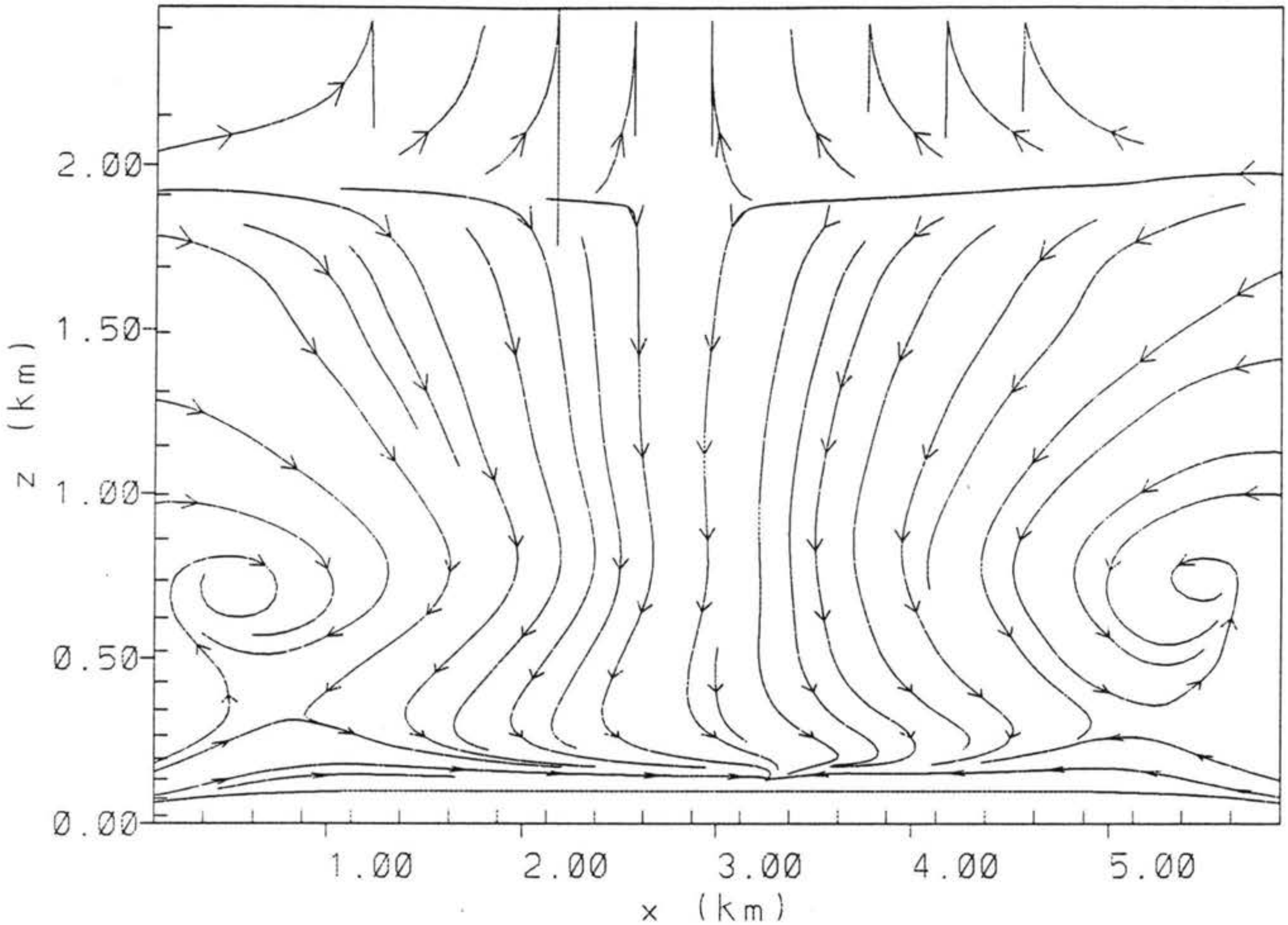

Figure 4.6c: Same as 4.6a but at 250m downwind of the cliff.

averaged potential temperature over this layer. O'connor and Bromwich (1988)found the critical Froude number to be 2.3. Values higher than 2.3 indicated flow would proceed up and over the ridge while values lower than 2.3 were indicative of flow blockage and separation up to some height on the ridge.

This value was calculated to be 0.615 for the 100m case, 1.0 for the 250m case, 2.6 for the 500m case, and 3.1 for the 1000m case. Values of delta T were set to 0.5K and the average potential temperature for the layer was set to 289K. The value of the mean wind speed was 0.8m/sec for the 100m case, 1.2m/sec for the 250m case, 3.5m/sec for the 500m case, and 4.0m/sec for the 1000m case. These results are in agreement with the findings of O'connor and Bromwich for a critical Froude number of 2.3.

Thus, the streamline analysis indicates the following effects of cliff resolution on the resulting wind flow patterns:

1. The horizontal extent of the disturbance is less downstream of the cliff as well along the cliff base for the lower resolution data.
2. The vertical extent of the disturbances is less at higher levels for lower resolution cases.
3. There appear to be other features which are not lessened but change in nature such as the point where flow separation occurs which shifts easterly in the vicinity of the cliff for lower resolution runs.

4.3. WIND SPEED TRANSECT ANALYSES

Wind speed cross sections similar to the ones analyzed through the experiment site for the island simulation were examined. These cross sections were chosen to go through the center of the domain as there is no measurement site in these simulations. Since this analysis was also done for the island simulation, a comparison between this and the island results can be made as well as an intercomparison between the variously resolved cliff-induced disturbances. It is the aim of this analysis to determine if the location corresponding to the maximum wind speed moves upwind with finer resolution. If this can be shown to be the case, then a good argument can be made for the apparent increase in the correlation between RAMS analyses and the C130 aircraft data as RAMS is shifted windward. In addition, this analysis should give an indication of the relationship between the height to which a disturbance propagates and cliff steepness. If it is found that the penetration is higher as the resolution increases, then a good argument can also be made for the better agreement between RAMS and the C130 aircraft as RAMS results are shifted upwards.

Results of the 100m resolution run show definite height groupings within which similar wind speed patterns are observed (Figures 4.7a-c). From 0m to 600m, the model predicts the wind to decrease upwind of the cliff, increase sharply until 200m downwind of the cliff, and slowly increase over the rest of the domain. From 600m to 900m, little wind speed variability exists over the whole domain. In the next section, this will be shown to be a result of gravity waves. From 900m to 1200m, the wind is relatively constant until directly above cliff base where it sharply increases until 200m downwind; It is fairly steady after that. The shape of this curve is similar to the shape of the curves in the lowest level grouping. From 1200m upwards, there is little or no variation in wind speed across the domain.

Similar groupings exist for the 250m resolution run (Figures 4.8a-c). They do, however, appear to be shifted vertically from the 100m resolution runs. From 0m to 450m, the wind speed decreases with height until cliff base. Then, at the base of the cliff, there is a sharp increase until approximately 500m downstream. Following this, there is a slow steady increase over the rest of the topography. This curve is of similar shape to curves in this height grouping for the 100m run with two key exceptions. First, this disturbance extends to only 450m in height as opposed to 600m. And, secondly, the wind speed maximum is located further downstream- 500m as opposed to 200m.

The next grouping in the 250m resolution set is from 450m to 700m. It has a fairly constant wind speed upwind of the cliff. At cliff base, it decreases until 750m downstream. Downwind of this, it remains steady or

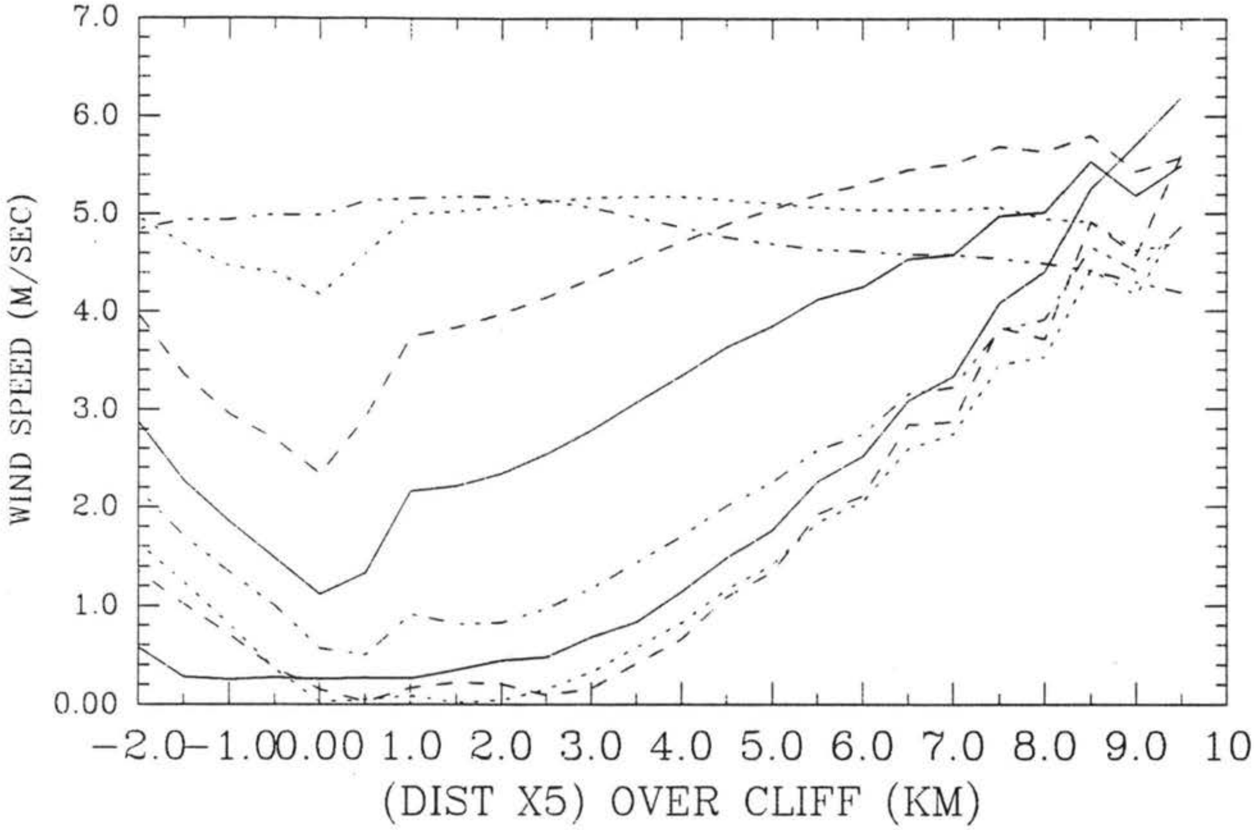

Figure 4.7a: Transects of wind speed over the 100m resolution cliff through the center of the cliff at low levels; Lower lines: solid-76m, dashed-134m, dotted-198m, double dashed-267m; Upper lines: solid-344m, dashed-429m, dotted-521m, double dashed-624m. Negative distances are upwind of the island. The area from 0.0 to 5.5km encompasses the island from north to south. From 5.5km to 10km is the area downwind of the island. Negative distances are upwind of the cliff.

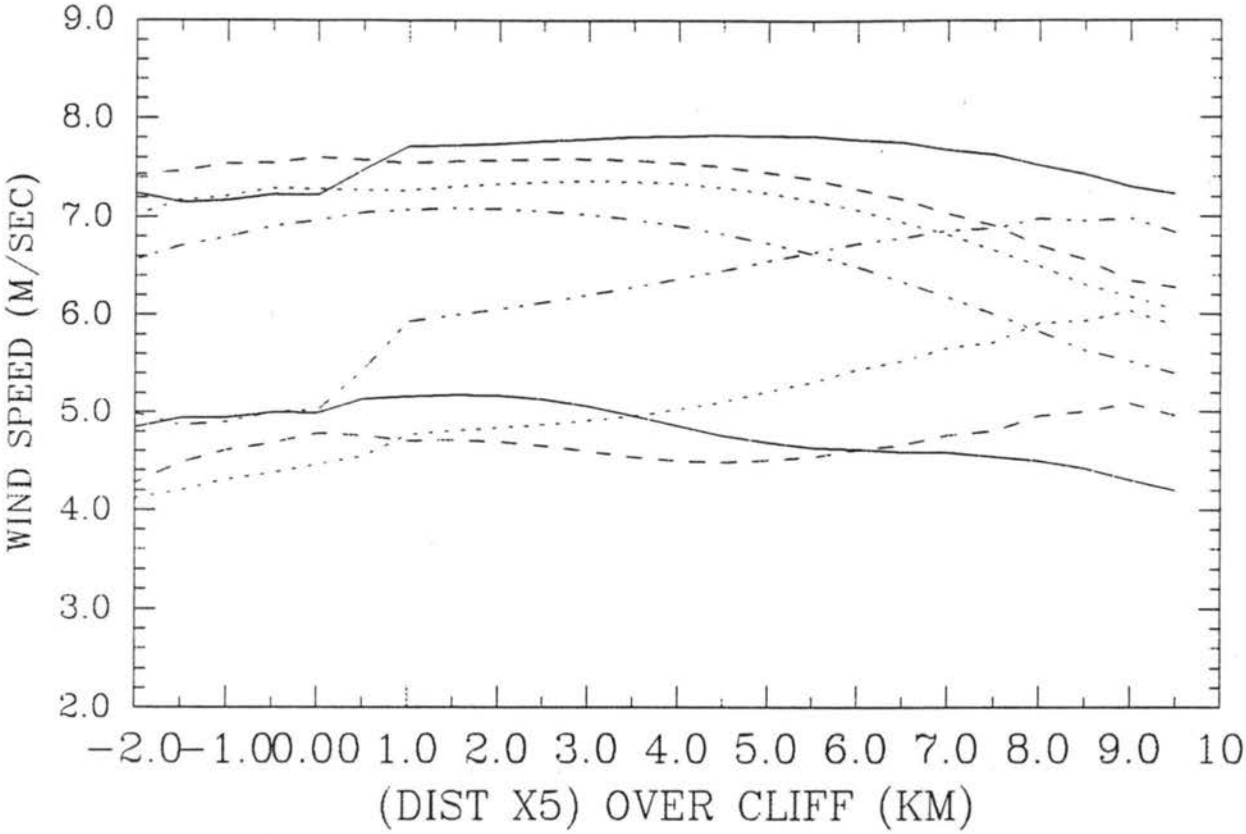

Figure 4.7b: Same as 4.7a but for middle levels; Lower lines: solid-524m, dashed-736m, dotted-860m, double dashed-996m; Upper lines: solid-1145m, dashed-1310m, dotted-1491m, double dashed-1690m.

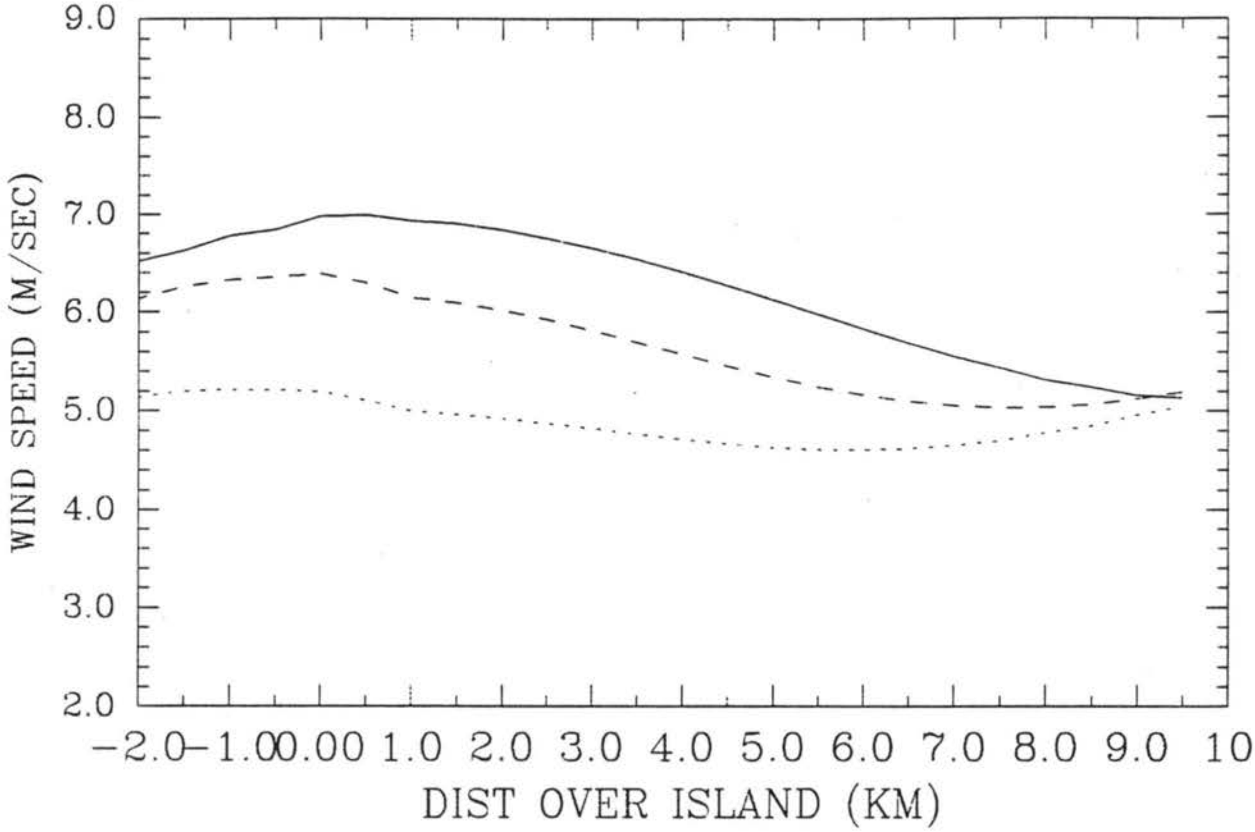

Figure 4.7c: Same as 4.7a but for upper levels; solid line-1909m, dashed line-2150m, dotted line-2415m.

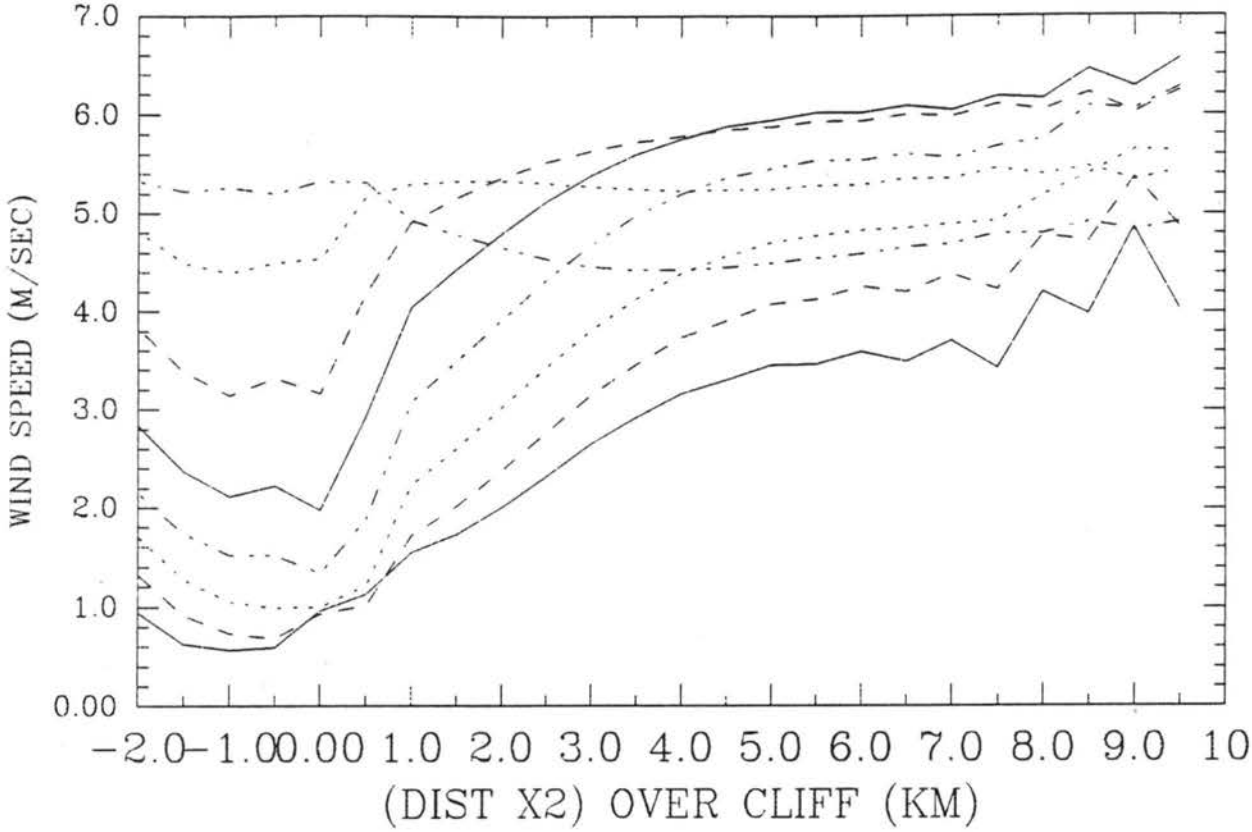

Figure 4.8a: Transects of wind speed over the 250m resolution cliff through the center of the cliff at low levels; Lower lines: solid-24m, dashed-76m, dotted-134m, double dashed-198m; Upper lines: solid-267m, dashed-344m, dotted-429m, double dashed-521m. Negative distances are upwind of the island. The area from 0.0 to 5.5km encompasses the island from north to south. From 5.5km to 10km is the area downwind of the island. Negative distances are upwind of the cliff.

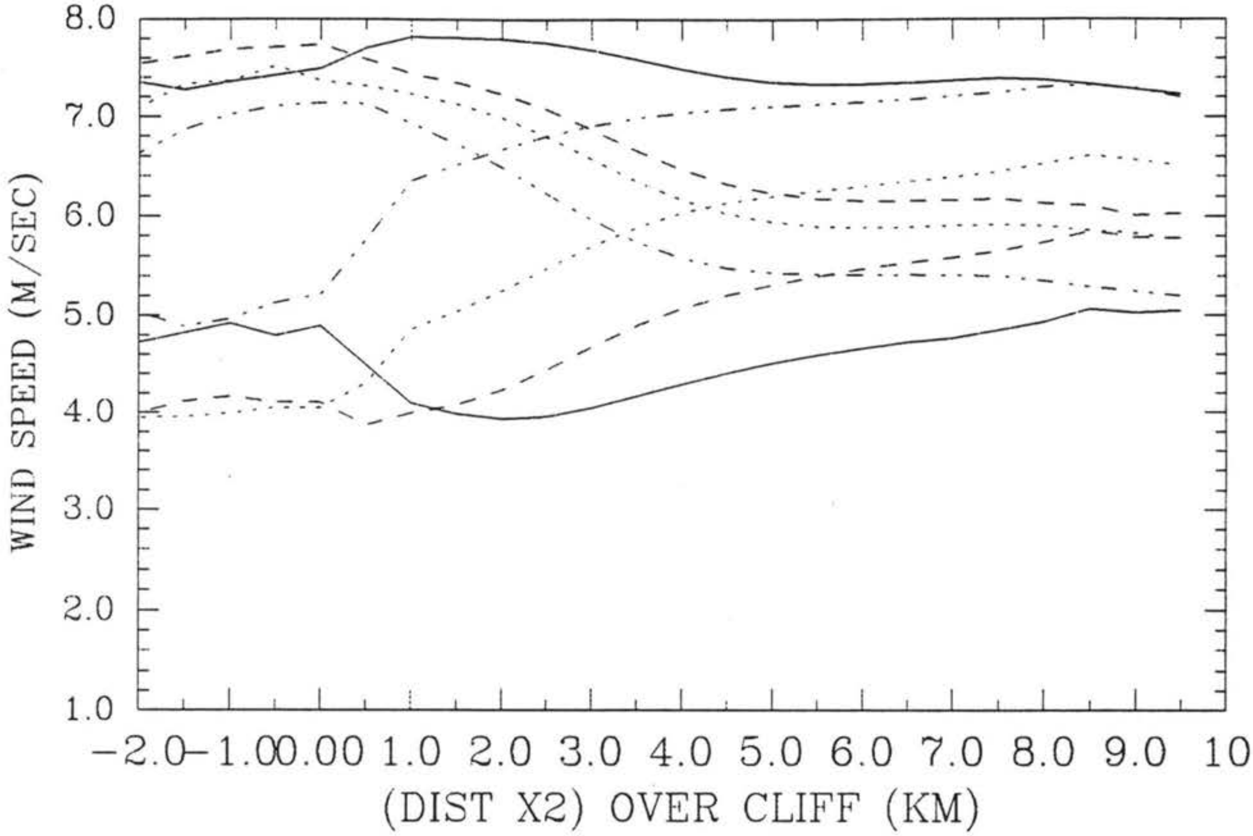

Figure 4.8b: Same as 4.8a but for middle levels; Lower lines: solid-624m, dashed-736m, dotted-860m, double dashed-996m; Upper lines: solid-1145m, dashed-1310m, dotted-1491m, double dashed-1690m.

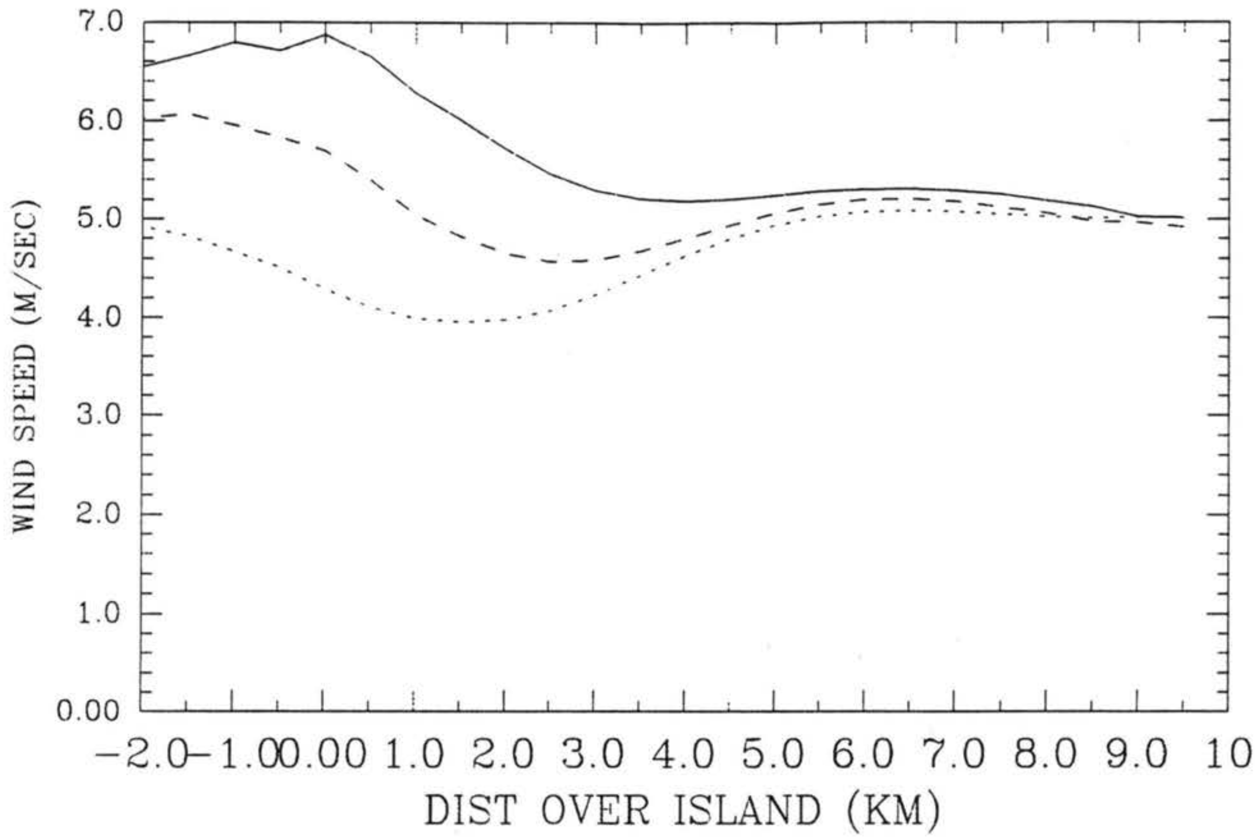

Figure 4.8c: Same as 4.8a but for upper levels; solid line-1909m, dashed line-2150m, dotted line-2415m.

exhibits a slow increase. The whole pattern here, however, does not have a great deal of variability. The analogous grouping for the 100m case went from 600m to 900m- again a higher range. From 700m to 1000m, the pattern shifts to one similar to the low level pattern similar to the 900m to 1200m range of the finer resolution study. And, by 1100m, there is little variability across the domain. This level corresponds to approximately the 1200m level for the 100m resolution simulation.

Thus, just from the intercomparison between the 250m and the 100m resolution cases, a pattern seems to be evolving in support of RAMS and the C130 having better correlation when a phase shift is performed on the RAMS' data. It appears that two things are taking place. One, RAMS is predicting the propagation of the cliff-induced disturbances to be higher for the finer resolution. And, secondly, the location of the maximum wind speed occurs further upstream for the finer resolution run. The first of these supports an upward shift in the RAMS data and the latter of these supports a windward shift in the RAMS data for studies done with a topography resolution which is too low. It is now important to see if this trend continues for even coarser resolutions.

The wind speed transects for the 500m resolution case- the same as the island simulations- and the 1000m case show encouraging support of this theory (Figures 4.9a-c; 4.10a-c). The low level grouping seen for both finer resolution runs is also seen for these two cases. In the 500m case, however, this pattern is apparent to only 400m in height and for the 1000m case to only 300m. In addition, the location of the wind speed maximum along these transects is found at 1km and 2km downwind of the cliff for the 500m and 1000m cases respectively. The other groupings for these two lower resolution simulations are similar to the groupings of the finer cases but continue to follow the clear trends outlined above- namely, disturbances propagate higher for steeper terrain and the location of features such as a wind speed maximum are located further upstream and closer to the cliff for finer resolution runs. This supports the results of the streamline analysis. This also

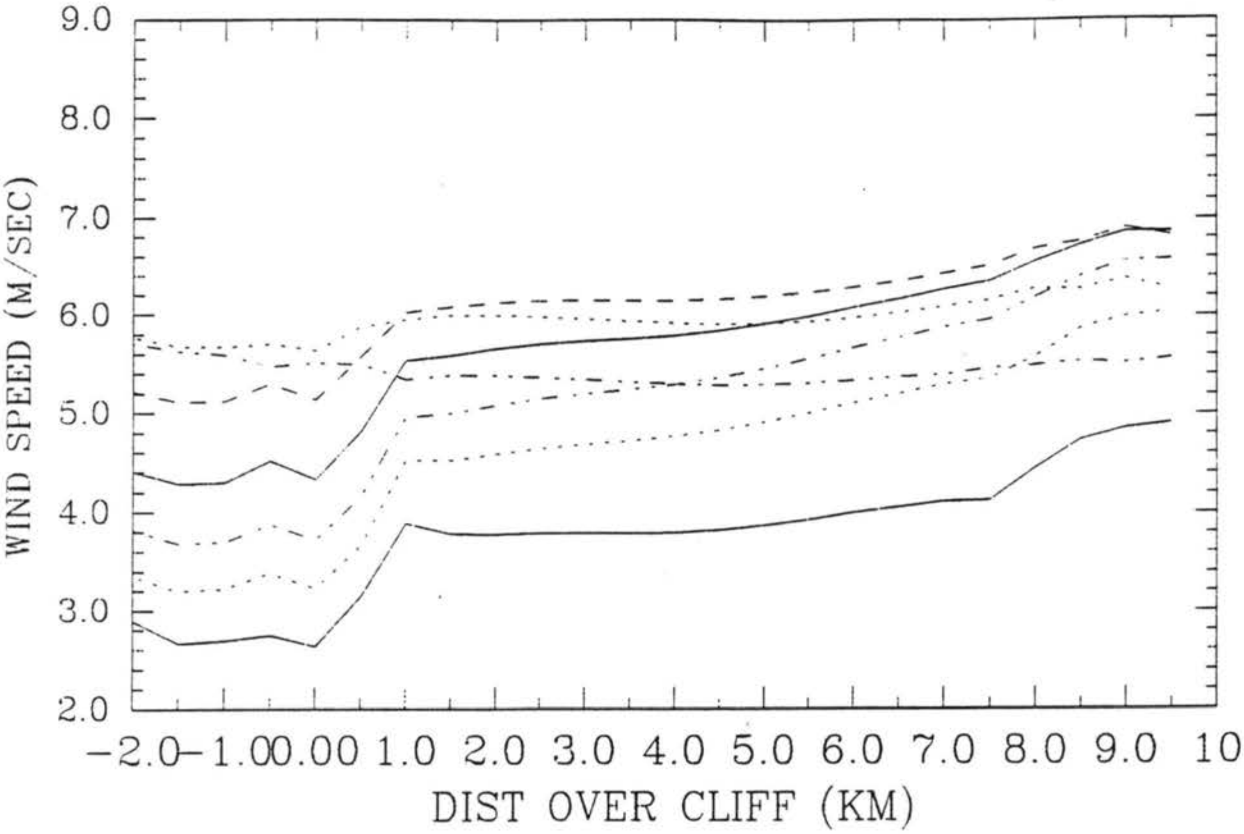

Figure 4.9a: Transects of wind speed over the 500m resolution cliff through the center of the cliff at low levels; Lower lines: solid-24m, dotted-76m, double dashed-134m; Upper lines: solid-198m, dashed-267m, dotted-344m, double dashed-429m. Negative distances are upwind of the island. The area from 0.0 to 5.5km encompasses the island from north to south. From 5.5km to 10km is the area downwind of the island. Negative distances are upwind of the cliff.

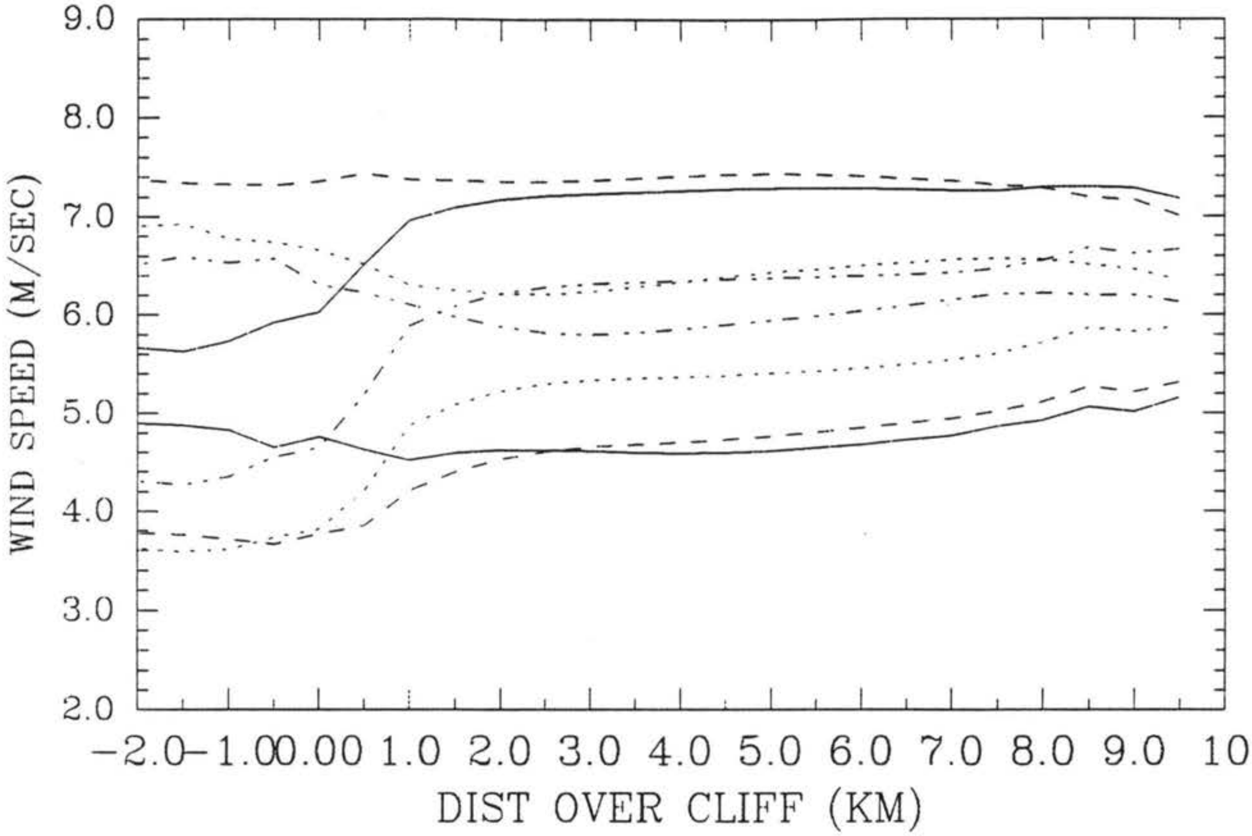

Figure 4.9b: Same as 4.9a but for middle levels; Lower lines: solid-521m, dashed-624m, dotted-736m, double dashed-860m; Upper lines: solid-996m, dashed-1145m, dotted-1310m, double dashed-1491m.

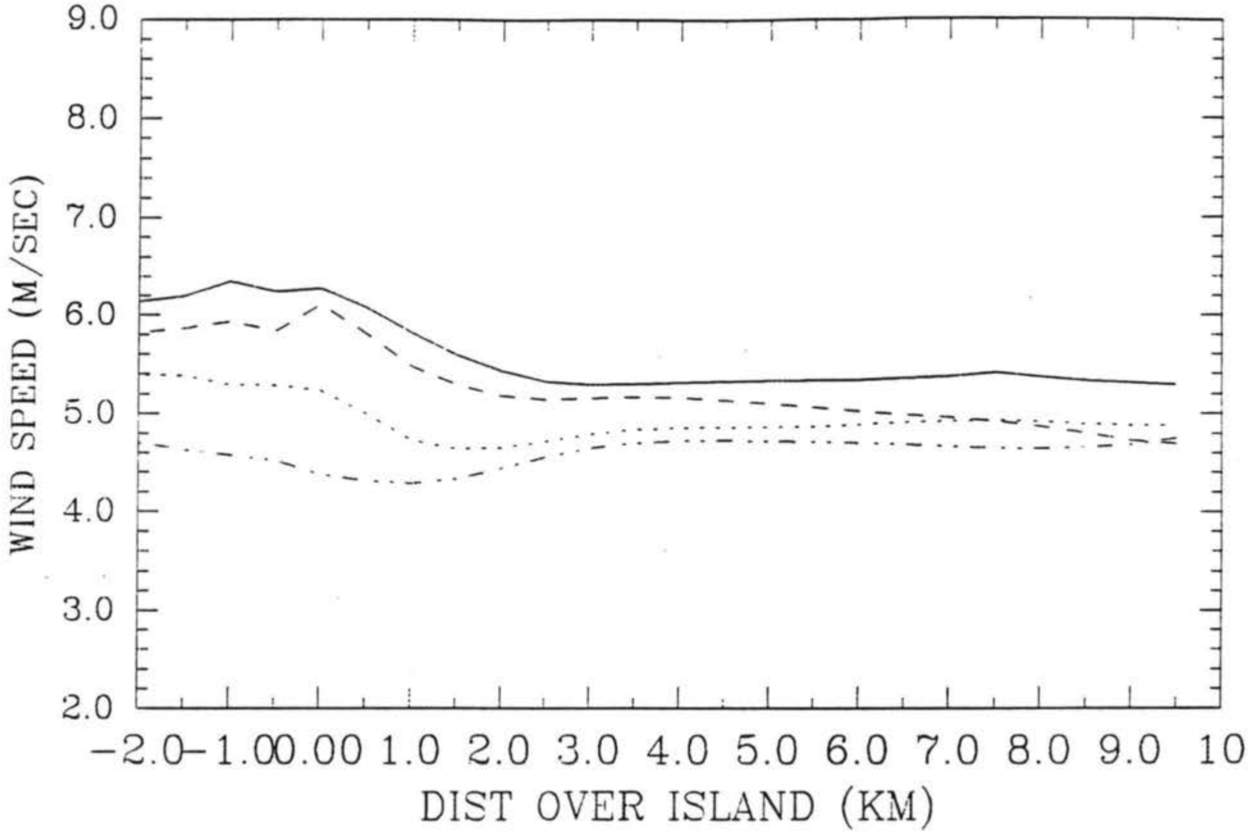

Figure 4.9c: Same as 4.9a but for upper levels; solid line-1690m, dashed line-1909m, dotted line-2150m, double dashed line-2415m.

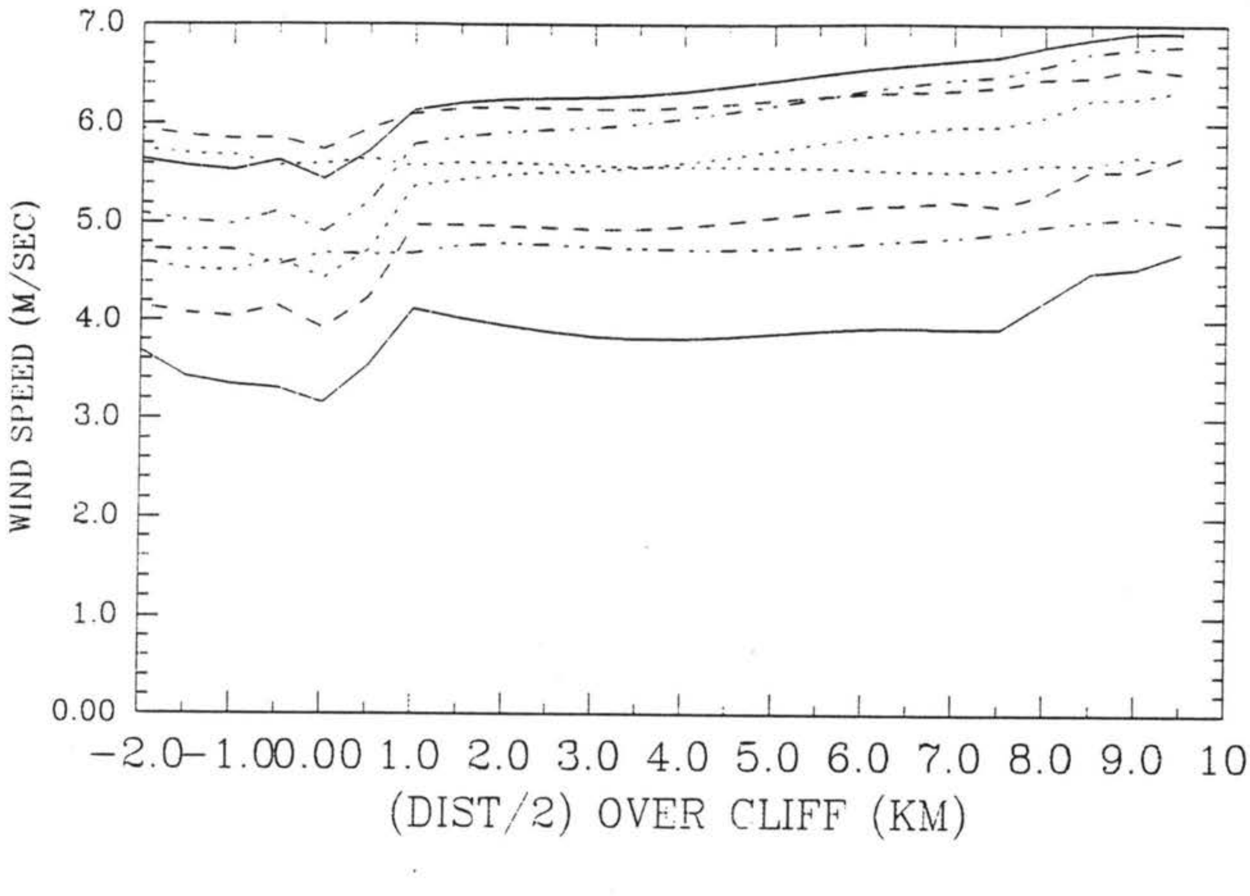

Figure 4.10a: Transects of wind speed over the 1000m resolution cliff through the center of the cliff at low levels; Lower lines: solid-24m, dashed-76m, dotted-134m, double dashed-429m; Upper lines: solid-267m, dashed-344m, dotted-521m, double dashed-198m. Negative distances are upwind of the island. The area from 0.0 to 5.5km encompasses the island from north to south. From 5.5km to 10km is the area downwind of the island. Negative distances are upwind of the cliff.

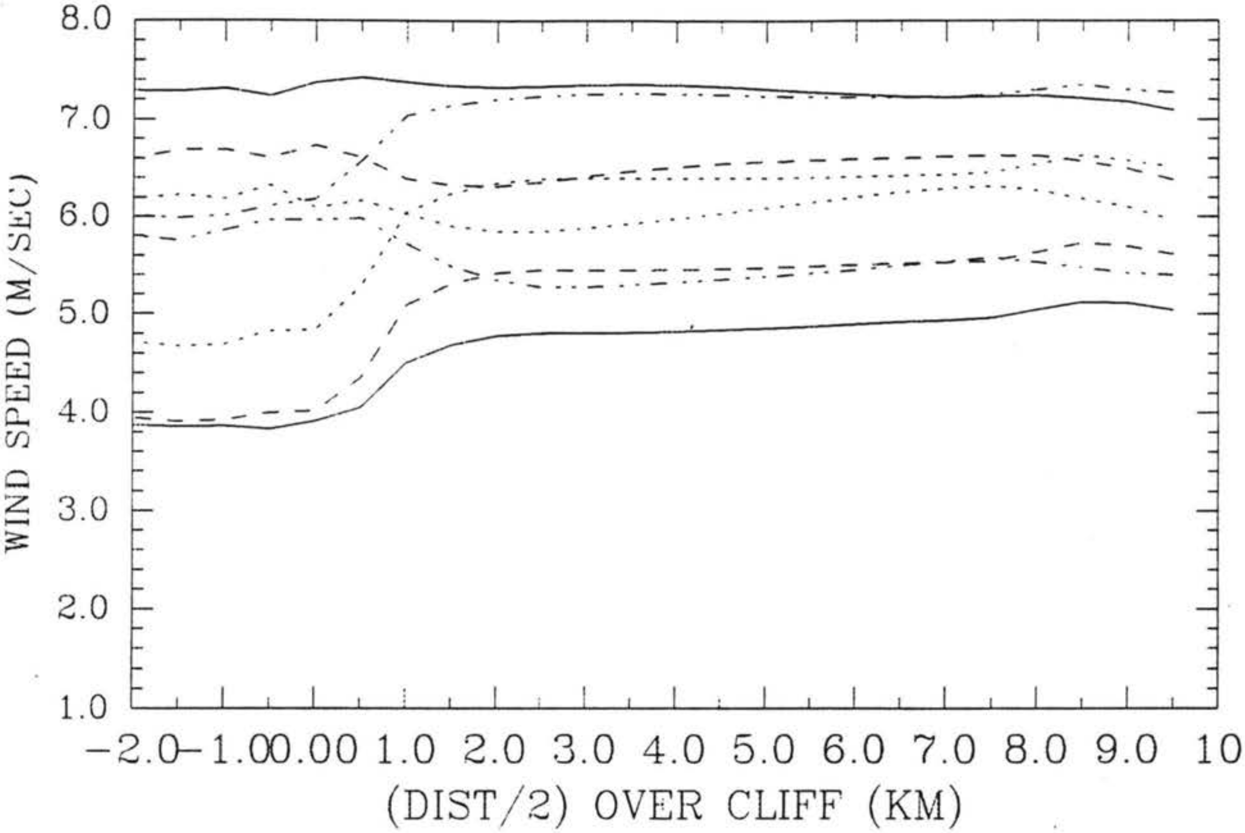

Figure 4.10b: Same as 4.10a but for middle levels; On the left side of the graph from top to bottom: Solid-624m, dashed-736m, dotted-860m, double dashed-1690m, double dashed-996m, dotted-1491m, dashed-1310m, solid-1145m.

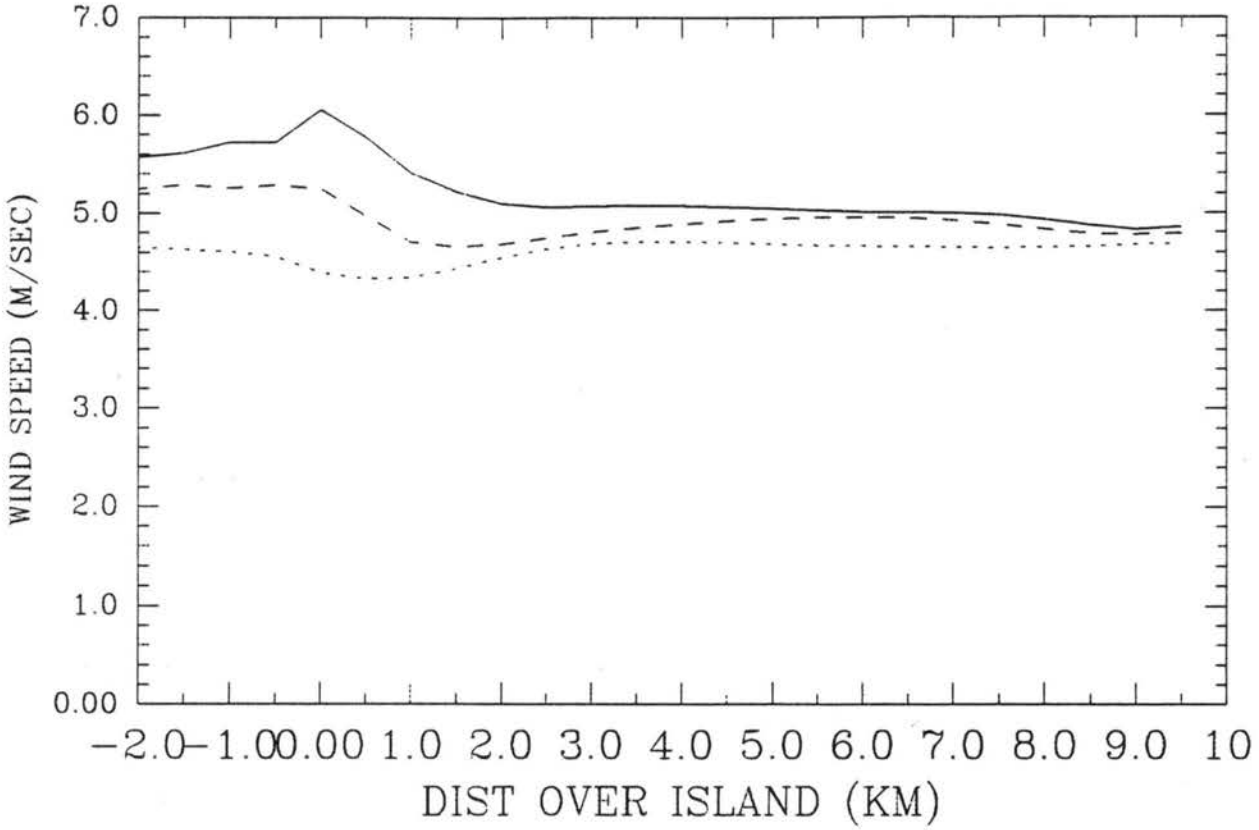

Figure 4.10c: Same as 4.10a but for upper levels; solid line-1909m, dashed line-2150m, dotted line-2415m.

strongly supports the work of Arya and Gadiyaram (1985) which found that the vertical extent of the flow is larger for steeper hills.

4.4. AMPLIFICATION FACTOR ANALYSIS

4.4.1. AMPLIFICATION FACTOR ANALYSIS OF THE CLIFF RUNS

Thus far, the streamline and the wind speed transect analyses have given a picture of wind speed and wind direction over the cliff topography for each of the four runs. This made it possible to estimate the relative effects of varying cliff steepness on the horizontal and vertical extent of the induced disturbance. These two analyses, however, give little insight into the magnitude of the change. Next, these four runs will be compared with the natural variability that would exist in these fields in the absence of a cliff.

Amplification factors were calculated for the four cliff runs with different horizontal resolution. The amplification factor(AF) is defined as the ratio of horizontal wind speed at a given height over a topographic feature divided by the horizontal wind speed at the same height upstream and away from the influence of topography. It is thus a direct measure of the effect of topography on wind speed compared with its natural variability. Areas where the amplification factor is less than one are areas where the topography acts to decrease the otherwise undisturbed wind speed and areas where the amplification factor is greater than one represent areas where topography induces an increase in the undisturbed wind flow.

This analysis is depicted as yz cross sections through the center of the domain of contours of amplification factor. The 100m resolution case is distinctly different from the other three (Figure 4.11a). Over most of the area below 700m, the AF is less than one. The minimum is centered around the base of the cliff at the surface where the AF is near zero and increases outward to approximately 700m where the value is approximately one (no change from the natural variability) for the rest of the height domain. This

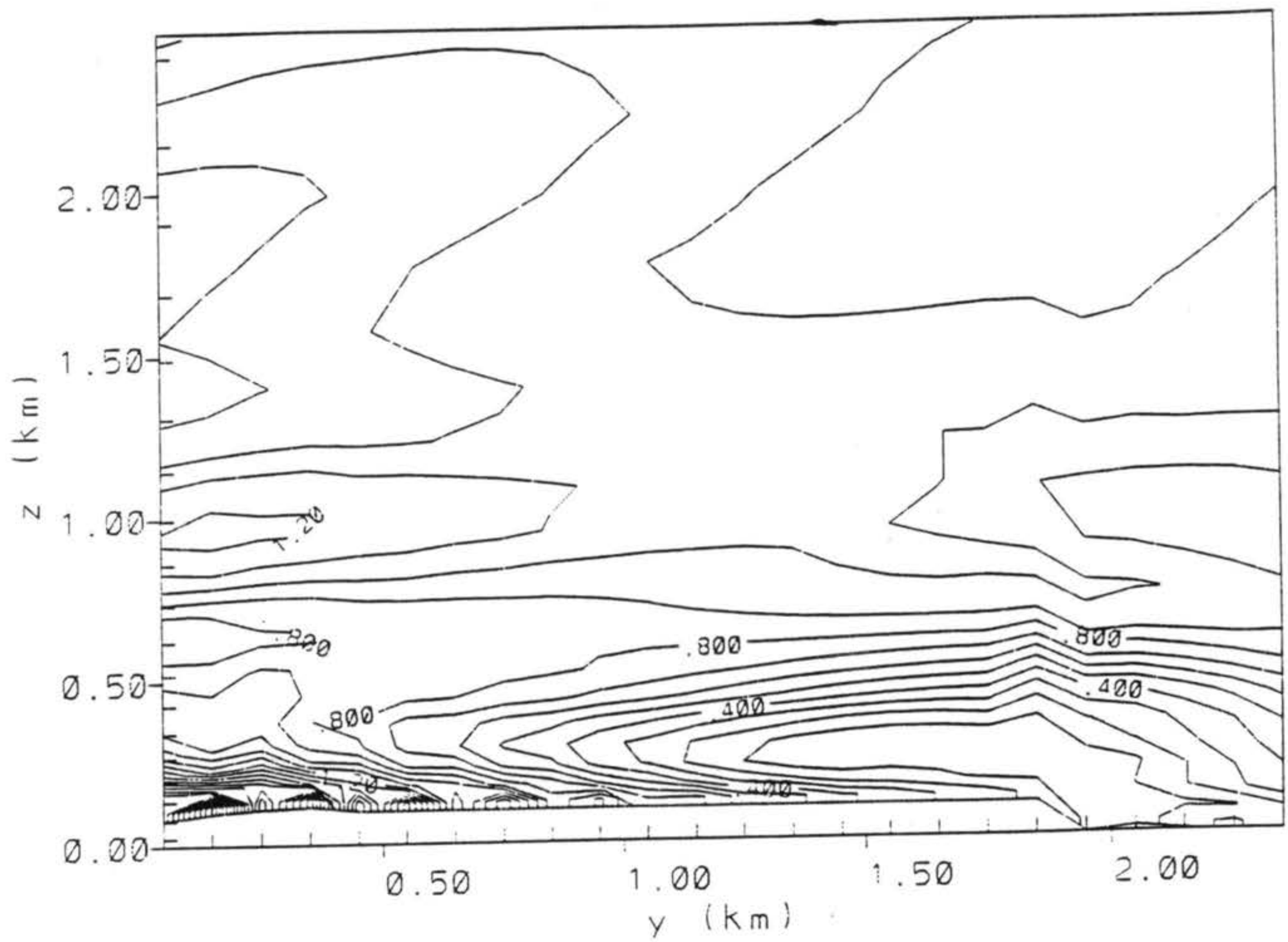

Figure 4.11a: Yz cross section of amplification factor through the center of the cliff for the 100m resolution cliff. The cliff is outlined at the bottom. Wind is from the right.

indicates the effect of the cliff topography is felt up to 700m which is close to the 600m value estimated from the streamline analysis.

The area where the amplification factor is less than 0.2 extends 200m in height and 800m downstream of the cliff. This would seem to indicate an area of flow stagnation near the ground for the area near the cliff. Arya and Gadiyaram (1985) found a similar result although their study was confined to a region closer to the ground than the present study. They showed that weak trailing vortices and a recirculating zone were present in the wake of a 26.5 degree sloping hill. This was not found for the same study of a 17 degree hill slope. The region of flow stagnation in their study, however was confined to an area within 0.3H (H-hill height) of the ground. While this is closer to the ground than the results of this study, the region above this was not examined. In addition, this feature was seen in the streamline analysis of the previous section. For the 100m resolution streamlines along this same cross section, an area of backward and upward air deflection was seen in this region. This results in a severe decrease in the horizontal wind speed in these regions as indicated by the amplification factor cross sections.

Downstream of the cliff, at distances greater than 1100m, very high amplification factors are seen near the ground. Since an increase in wind speed, near the ground and downwind of the disturbance, is found for the other cliff cases as well, this result is at least qualitatively valid. However, some of these values change very rapidly near the ground and exceed values of two. Most likely, these artificially high values are a result of the model's difficulty in resolving these features near the boundaries of the domain with 100m horizontal resolution. Thus, it can be partly considered an artifact of the model.

At 250m resolution, the picture is quite different (Figure 4.11b). There still exists an area of stagnation in the vicinity of the cliff, but this area is much smaller. The area where the amplification factor is less than 0.2 is a small area upwind of the cliff which extends to only 100m. The area around this increases outward and becomes one at a height of approximately 650m. This is less than the height of 700m found for the 100m

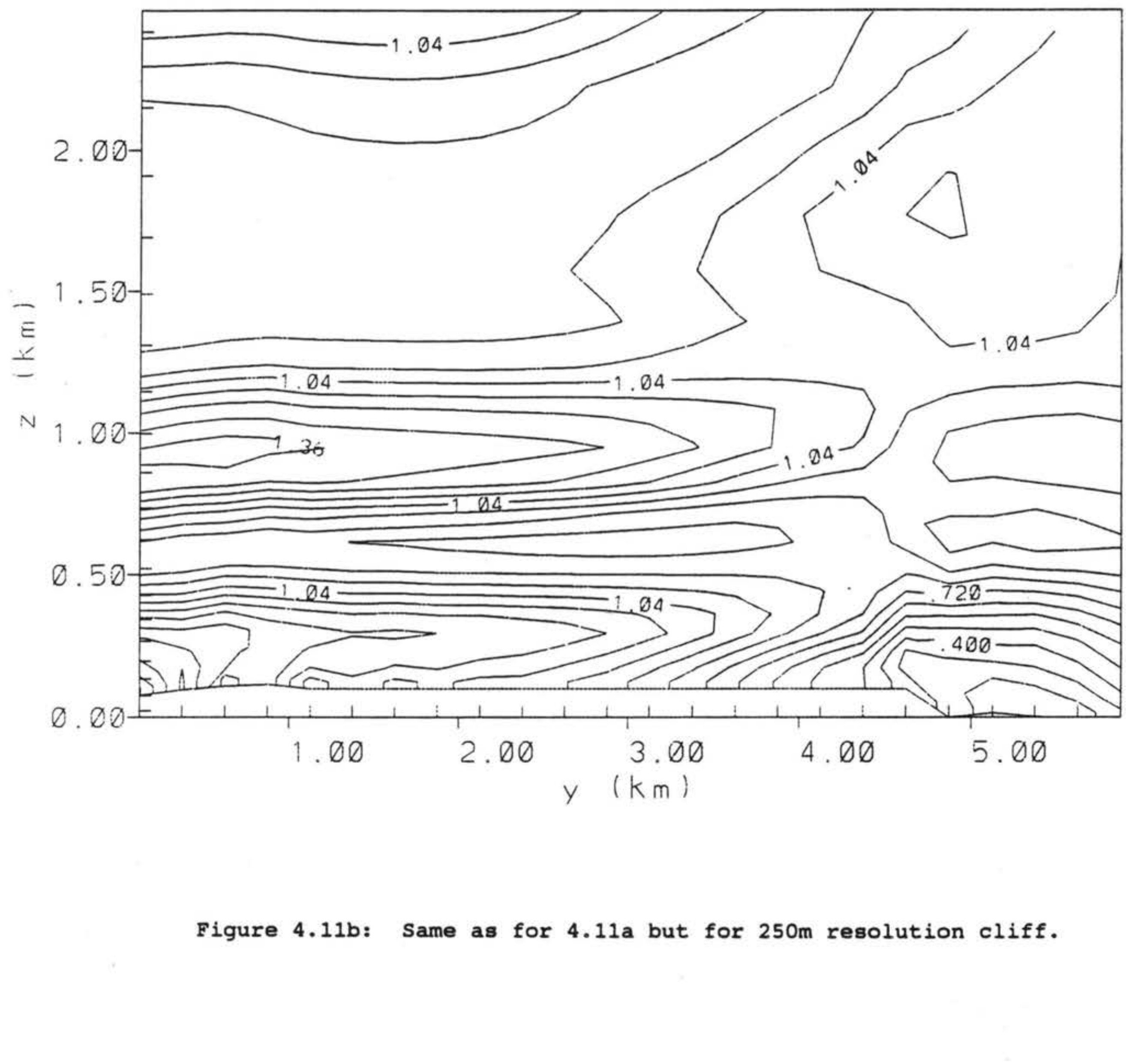

Figure 4.11b: Same as for 4.11a but for 250m resolution cliff.

case. This further supports the idea that disturbances propagate higher for steeper terrain.

Another difference between the 100m resolution and the 250m resolution cases occurs at a higher level. In the 100m case, above a height of 700m, the amplification factor is close to unity. The one exception to this is a small region at the edge of the downwind domain near the 900m level where it reaches a value of 1.2. For the 250m case, this feature is larger in magnitude and extent. From the region upwind of the cliff to 700m downwind of the cliff, the AF is close to unity above 700m. Throughout the region downwind of this, however, there is an area of increase where amplification factors reach values of 1.36 near the 900m level and decrease back to one at approximately 1200m. For the 500m and 1000m resolution runs, the size and strength of this feature is retained. It is difficult to say why this feature is smaller in the 100m case. It most likely is affected by the artificially high AF value found near the ground in this region which could upset continuity balance in the region above it. This feature in general, however, is difficult to explain. Upon examination of cross sections of the temperature and vertical velocity fields for these simulations, it appears as if this feature is related to a gravity wave phenomenon similar to the one discussed in chapter two for the island simulation. A profile through a gravity wave should depict alternating areas where the wind speed has components with and against the mean wind. This would produce alternating layers of AF increases and decreases which is what is observed for these cliff runs. Thus, this feature is most likely a direct effect of an internal gravity wave induced by air rising over the cliff.

The 250m resolution run has some other strong features as well. There is an area, approximately 1500m downstream of the cliff, near the ground, where the AF is greater than one. This continues throughout the rest of the downstream domain and extends to 500m in height. This corresponds to an area of streamline convergence in the streamline analysis of the previous section. Thus, a likely scenario is as follows: As the wind flow approaches the cliff, the flow separates as it ascends the obstacle. Further downstream, the wind converges again. In the region where the flow is divergent, the amplification of the wind decreases to less than one and in the region where the air reconvenes, the wind speed is again amplified. This scenario supports the fact that the unusually high values of the amplification factor found downstream near the ground for the 100m resolution run do hold at least qualitative significance.

In order to further examine the effects of the wind speed amplification with coarser topographic resolution, the 500m and 1000m resolution runs were analyzed (Figures 4.11c-d). The general features of these two cases greatly resembled the 250m resolution case with two exceptions. One, there is no area where the amplification factor was less than 0.2 for either of these simulations. This is not surprising as the streamlines indicate no backward deflection at the base of the cliff for these two cases. There is an area of wind speed decrease upwind of the cliff base which has a minimum value of 0.85 for the 1000m case and 0.75 for the 500m case. This concurs with the work of Arya and Gadiyaram (1985) and Pearse (1982). They found that the speed up of flow near the hill slope becomes limited as the hill slope increases.

The second major difference between the 250m resolution runs and these two runs is the extent of the area near the ground where the amplification factor is greater than one. For the 500m and 1000m runs, this area begins near the cliff's crest and extends throughout the domain downwind of the cliff up to approximately 450m. It has a maximum value near the 250m height level. This difference is also not surprising. Since there is no flow separation observed near the cliff for these two runs, the wind speeds up directly as it flows over the cliff. For the 250m resolution run, the separation of the flow upwind of the cliff and the reconvening of the flow downwind of the cliff made the increase in wind speed from the cliff appear further downstream.

Aside from these two exceptions, the 250m, 500m, and 1000m runs all show a similar scenario. The region between 600m and 1200m where the AF was greater than one in the 250m run is also present for these two cases. And, the maximum value in this region occurs at approximately 900m for all three cases. As discussed, this is a gravity wave effect.

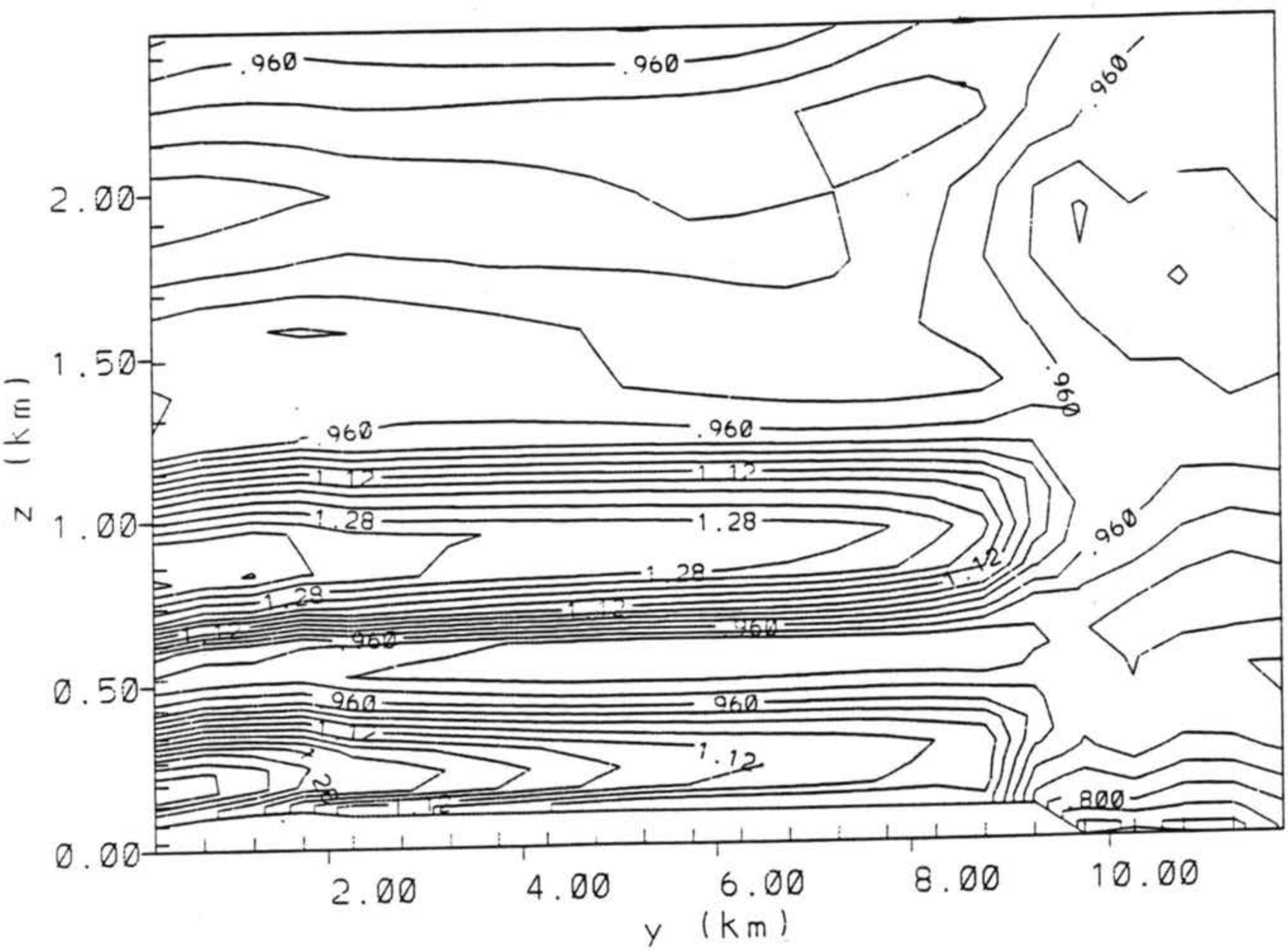

Figure 4.11c: Same as for 4.11a but for 500m resolution cliff.

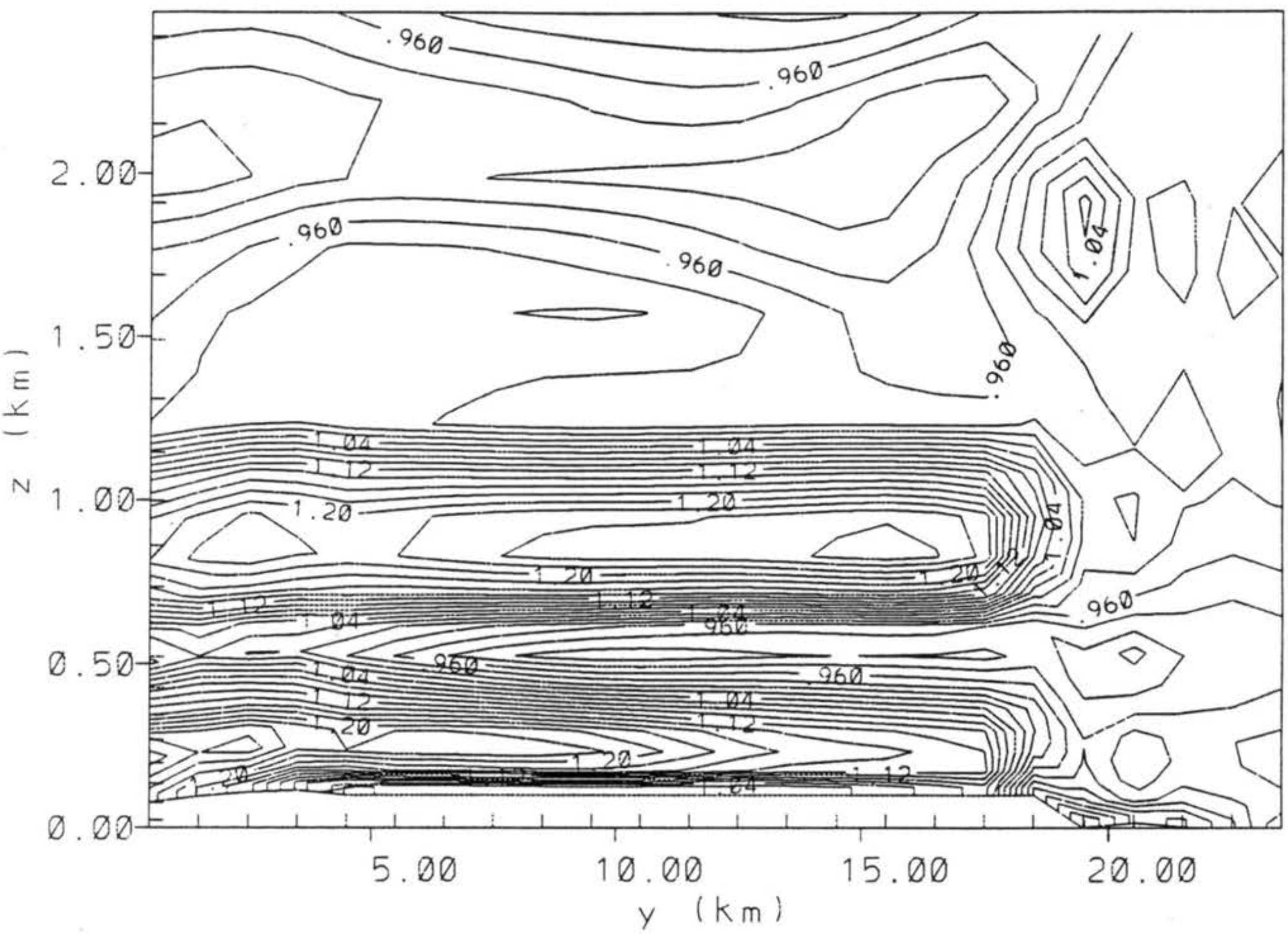

Figure 4.11d: Same as for 4.11a but for 1000m resolution cliff.

Before progressing to the analysis of the island simulation, however, it is relevant to mention the results of a study by Bowen and Lindley (1977). Their results showed that, for four different escarpment slopes ranging from 14 degrees to 90 degrees, the amplification factor is greatest at the ground beginning at the crest of the escarpment and extending downstream of the escarpment (Figure 4.12). Figures 4.11c-d show that the 1000m and the 500m resolution runs concur with this finding. Figures 4.11a-b of the 250m and the 100m runs, however, show a different picture. This is likely a result of the partial flow separation that is occurring for these two finer resolution cases that was not present in the study by Bowen and Lindley. For the island simulation, 500m resolution was used with no observed flow separation and thus, will be compared to the study by Bowen and Lindley in the next section.

4.4.2. AMPLIFICATION FACTOR ANALYSIS OF THE ISLAND SIMULATION

For this analysis, the run from June 22nd will be used. On the 22nd, the winds were closer to north than the winds on June 10th. This day thus represents a situation closer to the four runs discussed in the previous section and may be compared more directly. A yz cross section of the amplification factors over the island can be seen in Figure 4.13. The topography of the island is outlined at the bottom of the graph. The cliff appears as a gentle slope of 12 degrees on the north side of the island. It is important to keep in mind that this actually represents a cliff of nearly 90 degrees. The results shown here agree well with Bowen and Lindley (1977) for a 14 degree slope and no flow separation.

The maximum values of amplification factor are at the ground beginning from the crest of the hill and extending downwind of the hill 3.5km or 35 hill lengths. Hansen and Cermak (1975) studied the wakes of three dimensional hills and also found evidence of their effect over 30 hill lengths downstream. The amplification contours bulge downwind from the hill crest. Bowen and Lindley (1977) show a very similar scenario for the results of wind flowing

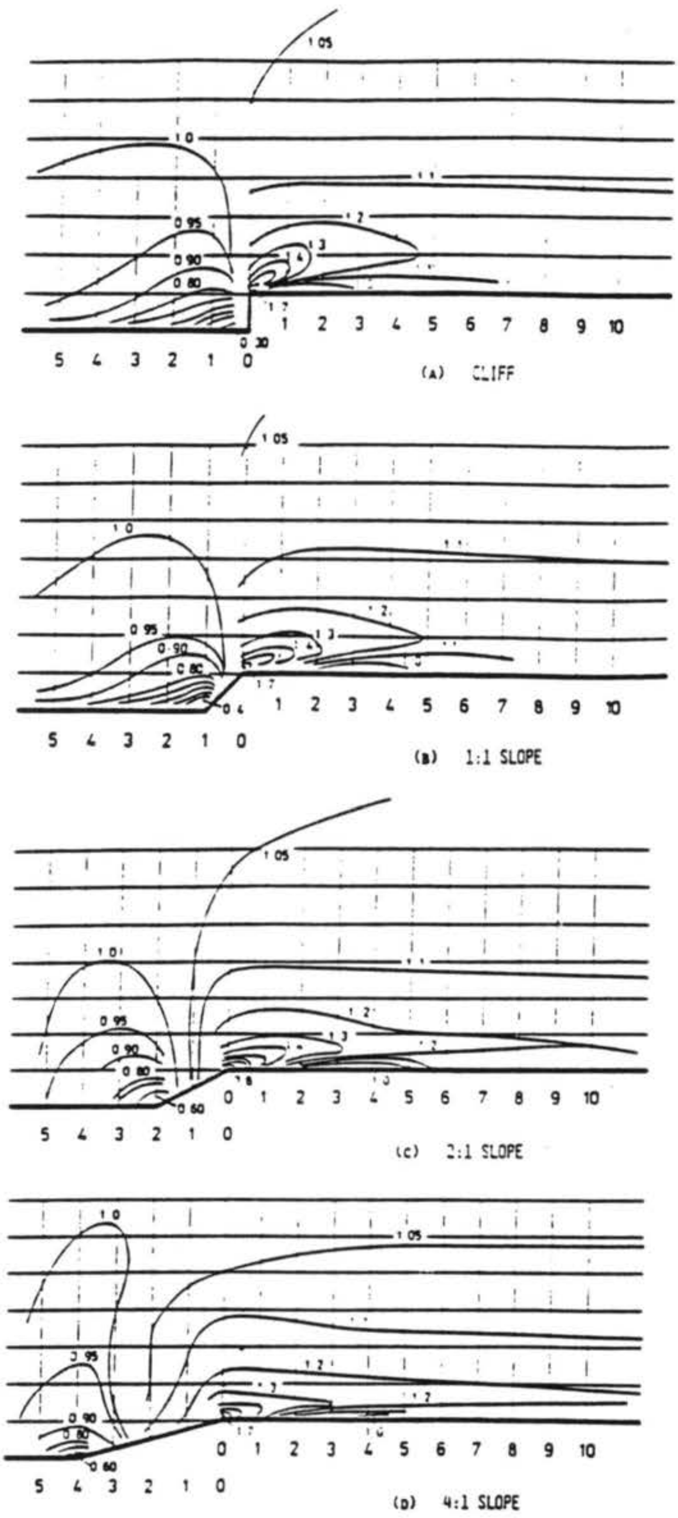

Figure 4.12: (A)-(D)Contours of amplification factor over various escarpment slopes; from Bowen and Lindley, 1974.

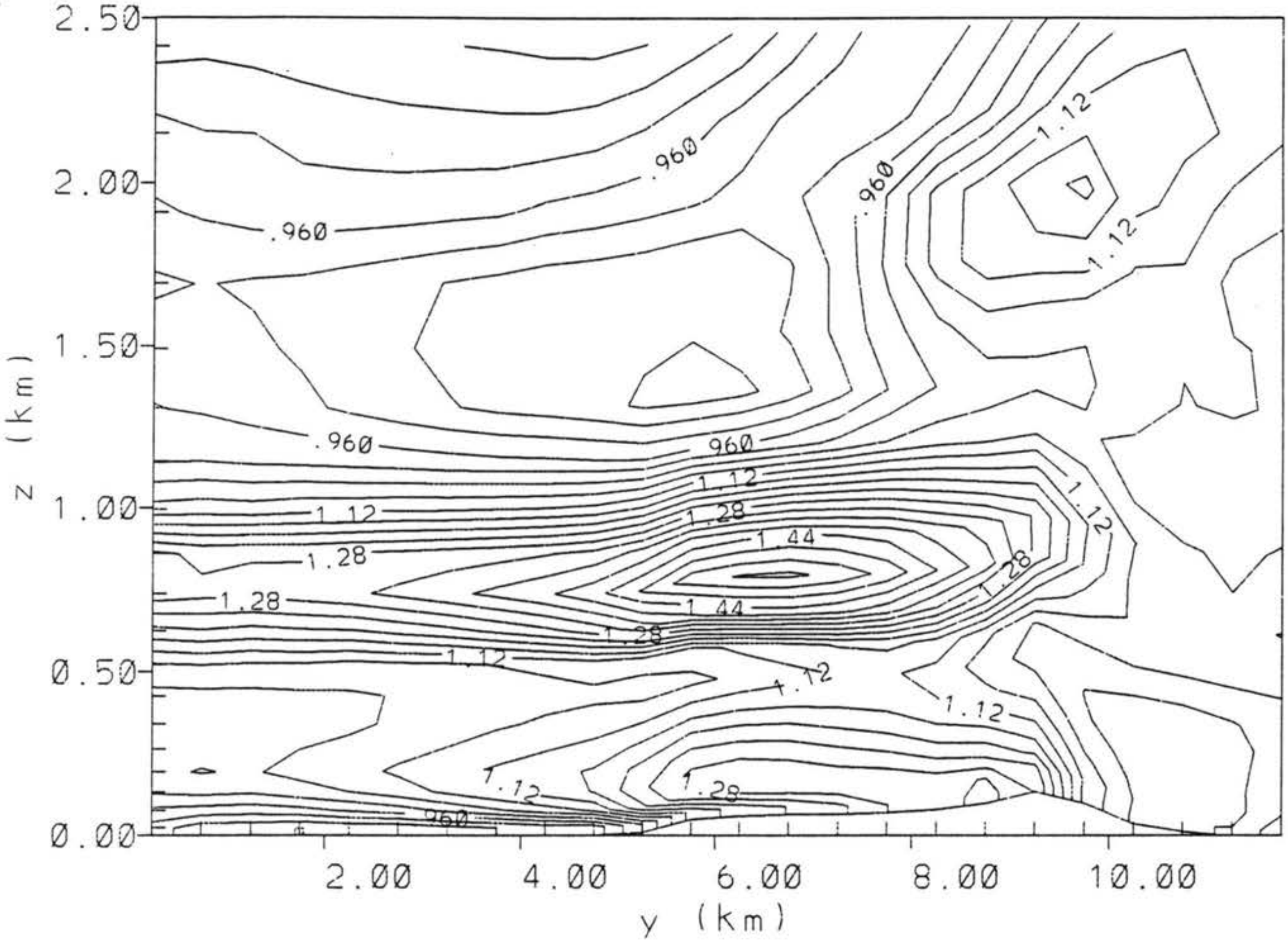

Figure 4.13: Yz cross section through the measurement site of amplification factor. The outline of the island topography can be seen at the bottom.

over a 14 degree sloped escarpment (Figure 4.12). They found the maximum value to be at the ground from hill crest until 10 hill lengths downstream where their study ended.

The overall highest value of amplification found, however varied slightly in value and location between the two studies. Bowen and Lindley found the greatest value to be 1.7 located exactly at the hill crest on the ground. From this point, the contours bulged outward downstream and decreased in value. In the present study, the overall highest value was 1.4 located 500m downwind of the hill crest at the ground with similarly shaped contours bulging downstream around it. There is one major difference between the two studies which offers the most likely explanation for this discrepancy.

In the present study the topography downwind from the cliff gently slopes back to sea level. In the study by Bowen and Lindley, the escarpment retains its altitude throughout the rest of the domain. Thus, this apparent shift downstream of the amplification maximum could be a downslope effect which induces an additional acceleration of the air after it passes the crest. The difference in the value of this maximum (1.4 in the present study as opposed to 1.7) is not of great concern. De Bray (1973), Freeston (1974), and Sacre (1973) all show this value to be 1.4 to 1.5.

The study of Bowen and Lindley extends 6H (H- hill height) in the vertical. They showed that at 6H above the terrain, downwind of the cliff, the amplification factor decreased to a value of 1.05. This would correspond to a height of 600m in the present study. By this level, the present study also indicates a decrease to a value in the vicinity of unity. Above this level, however, a reversal occurs where the amplification factor begins to increase again. This reversal is found above the cliff and continues downwind of the crest. It reaches a maximum value of 1.56 near the 900m level before decreasing back to unity near 1200m.

In the last section, this feature was also identified for the four cliff runs. As discussed in that section, and as discussed in chapter two for the island simulation of the June 10th, this feature is likely related to a combined effect of a gravity wave and a thermally-driven wind. Thus, this feature is an island-induced effect. It is then reasonable to conclude that the island's effect can be felt through a height of 1200m for this analysis. Between 600m and 900m, however the effect is somewhat masked by the wave-induced winds having a component opposite to the mean flow. In situations where the steepness of the cliff is more accurately represented and thus is more indicative of reality, this level is higher. For a 45 degree slope, this level was shown to begin at 750m.

Thus far, the discussion has focused on the region downwind of the cliff. Some points should also be made concerning the region upwind of the cliff for both the present study and that of Bowen and Lindley. Bowen and Lindley found that for the sloping escarpments less than 90 degrees the amplification factor reached was less than one upwind of the cliff near the ground, reached unity somewhere along the escarpment, and increased to values greater than unity at the crest. In the region upwind, the values increased with height to unity at levels between 3H and 5H above the ground depending on the steepness of the escarpment slope. For this island study, the same pattern was observed. A value of one was reached approximately half way up the slope of the cliff and increased toward the crest. In the region upwind of the cliff, this value was less than one near the ground and increased to unity at approximately 4H above the ground.

Thus, in all three regions- upwind of the cliff, in the vicinity of the cliff, and downstream of the cliff- the results of the island simulation performed in this study support results from previous studies.

4.5. SUMMARY OF CLIFF RESOLUTION STUDY

Three analyses were performed in this chapter (a streamline analysis, a wind speed cross section analysis, and an amplification factor analysis) to determine the possible effect of the resolution of cliff steepness on the resulting model-produced wind fields in RAMS. It was the aim to show that disturbances both propagate higher and they appear further upstream as the resolution of a cliff becomes finer. It was necessary to show this in order to give credibility to the finding that RAMS better agrees with observational data when an upward or windward phase shift is performed on the model-produced wind fields.

All three analyses supported the phase shift theory. In the streamline analysis, xy cross sections showed that flow appeared undisturbed at successively lower levels as the resolution became coarser. Vertical cross sections showed that the vertical extent of upward motion induced by the cliff also became lower for coarser runs.

The wind speed cross section analysis confirmed this as well. Vertical sections of the atmosphere that contained wind speed curves of similar shape were grouped together. All four runs showed groupings with the same shape but the vertical extent of the each group became successively lower for coarser runs.

Finally, the amplification factor analysis, which actually compared the fields in each of the four runs to the natural variability of these fields also added support to the theory. This analysis showed that areas of wind speed increase or decrease in the vicinity of the cliff were greater in their spacial extent for finer resolution runs. In addition, features of the amplification factor analysis confirmed the results of the streamline and cross section analyses concerning areas of flow stagnation, flow convergence and divergence, and the locations of wind speed maxima in each of the four runs.

The work done here also supports the work previously done by Arya and Gadiyaram (1985), Pearse (1982), and other mentioned studies on wind flow patterns around barriers of varying steepness. Further, the distribution of amplification factor in the island simulation is very close in magnitude and extent to the amplification factor distribution found by Lindley (1977) for wind flow over a 14 degree sloped escarpment.

From these analyses, the disturbing initial disagreement between RAMS and the C130 aircraft data can be explained. Due to the fact that the steepness of the cliff on the north side of the island is inadequately resolved in the model, there is a justifiable argument here for shifting RAMS wind data upwind and/or windward when performing a comparison between RAMS and observational data. And, in performing this phase shift, it was shown that the agreement is significantly better.

5. SURFACE OBSERVATIONS

Thus far, the model-produced wind fields and the C130 aircraft wind data have been examined and compared to assess the vertical and horizontal extents of the island's influence on the profiles of wind over the island. In chapter two, using north-south cross sections of wind speed, it was shown that the model-produced fields fell into height groupings within which the same general features of wind speed were found. These groupings were between the ground and 1000m, between 1000m and 1900m, and above 1900m where the pattern was similar to the lowest level grouping. The variability in the middle was shown to be a thermally-driven wind/gravity wave dual effect. The former was most likely a result of the combination of an inversion, which existed over the island near this level on the day of the simulation, and island effects. The latter was induced by air rising over the cliff on the north of the island.

The modification of the wind field by the island over the experiment site was shown to extend up to 2km in height with the region near the ground and the region near the 1200m level being most affected and the region between 700m and 1000m being least affected.

North-south cross sections of wind speed for the three height levels of the C130 aircraft were examined to confirm this result in chapter three. Here, it appeared that if a vertical and/or horizontal phase shift were performed on the RAMS data, a good correlation would exist between the two data sets. Chapter four demonstrated that improper resolution of topography was responsible for horizontally and vertically underpredicting the extent of island-induced disturbances. This justified performing a phase shift which allowed the two data sets to agree quite well.

In this section, wind profiler and rawinsonde data will be used as additional source of data for confirmation of the results of chapters two through four.

The wind profiler used was a 400MHz five beam profiler. It provided measurements of wind up to 15km with 10 minute horizontal wind profiles. The height resolution of the profiler was 250m up to 9.25km and 1000m above this.

Results from the wind profiler can be seen in Figure 5.1. The vertical resolution of the wind profiler data is coarser thaN the model. Only eight data points are represented by the vertical area between the ground and 2500m. However, some features similar to the model and aircraft data can be seen. One obvious agreement is the existence of the stratifications mentioned above. The wind profiler data show that between 1000m and 2000m a change in the wind speed takes place. Above and below this range, the wind speed is very close in magnitude. Likewise, the rawinsonde data also shows a wind speed decrease in this region (Figure 5.1).

For the model, a plot of wind speed verses height above the site is shown in Figure 5.1. Here, the change in wind speed first appears at a slightly lower height interval- approximately 700m. This would be expected if one takes into account the results of chapter four concerning the effects of lower resolution topography. Results of chapter four show that a vertical phase shift should be performed on the RAMS data in order for agreement to exist between it and observational data. When the RAMS data are shifted upwards approximately 500m in this case, good agreement exists across the board between RAMS, the C130 aircraft data, wind profiler measurements, and rawinsondes.

Although data presented in chapter four is convincing, it did not address the specific case of the wind profile above the measurement site. Thus, the four cliff runs will be examined briefly here using a vertical profile of wind speed above this point. Figures 5.2a- 5.2d show the profiles for each of the four cliff resolution cases.

These four diagrams show that, throughout the region below 2000m, the wind speed profile shifts upward in height as the topography becomes finer. This effect, however, becomes less pronounced with height. This supports the observed phase shift that appears between the results of model and those of the wind profiler and rawinsondes in Figure 5.1.

Thus, the wind profiler data and the rawinsonde data provide additional support for the agreement between RAMS and the observations. In addition, they agree with the results of chapter four which demonstrate the necessity of performing a phase shift on the RAMS data to accurately account for the inadequate resolution of topography.

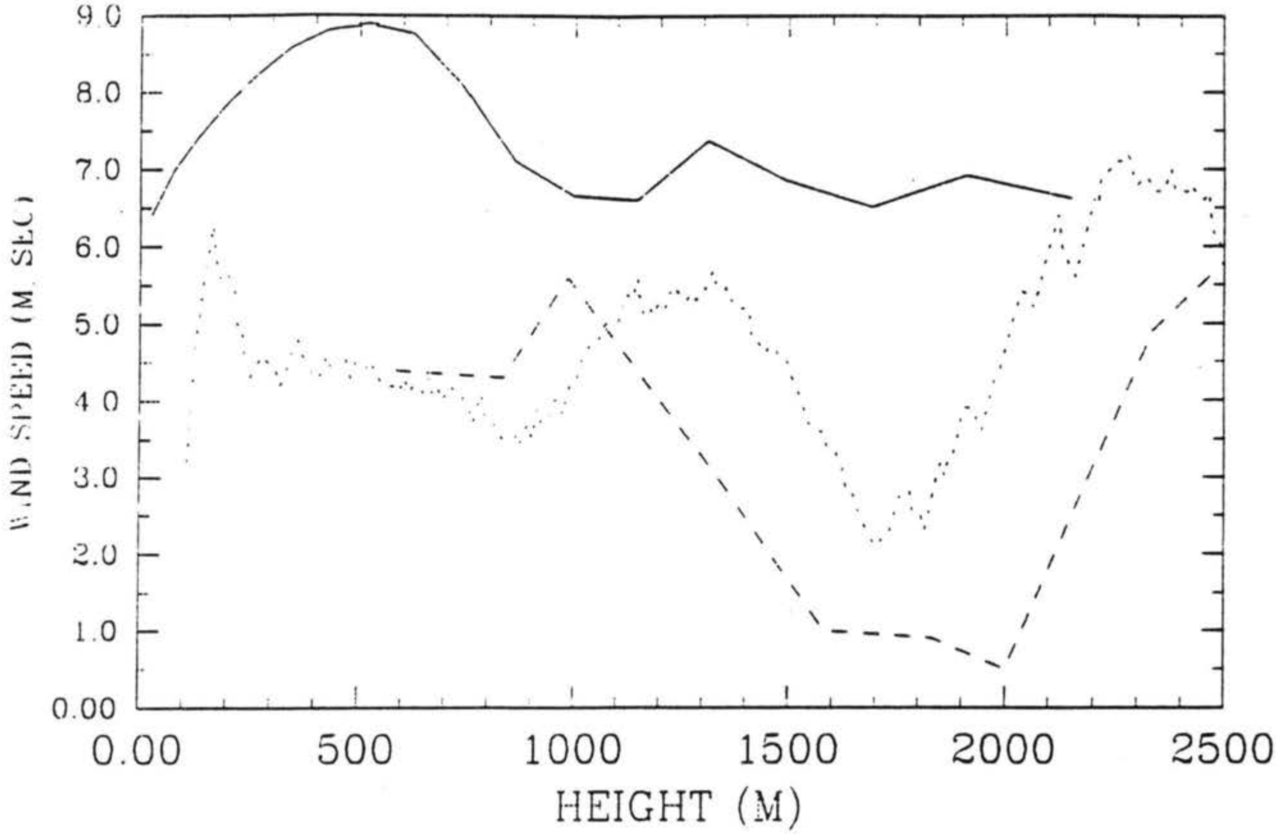

Figure 5.1: Comparison of wind speed with height for the RAMS model (solid line), the wind profiler (dashed line), and rawinsonde (dotted line).

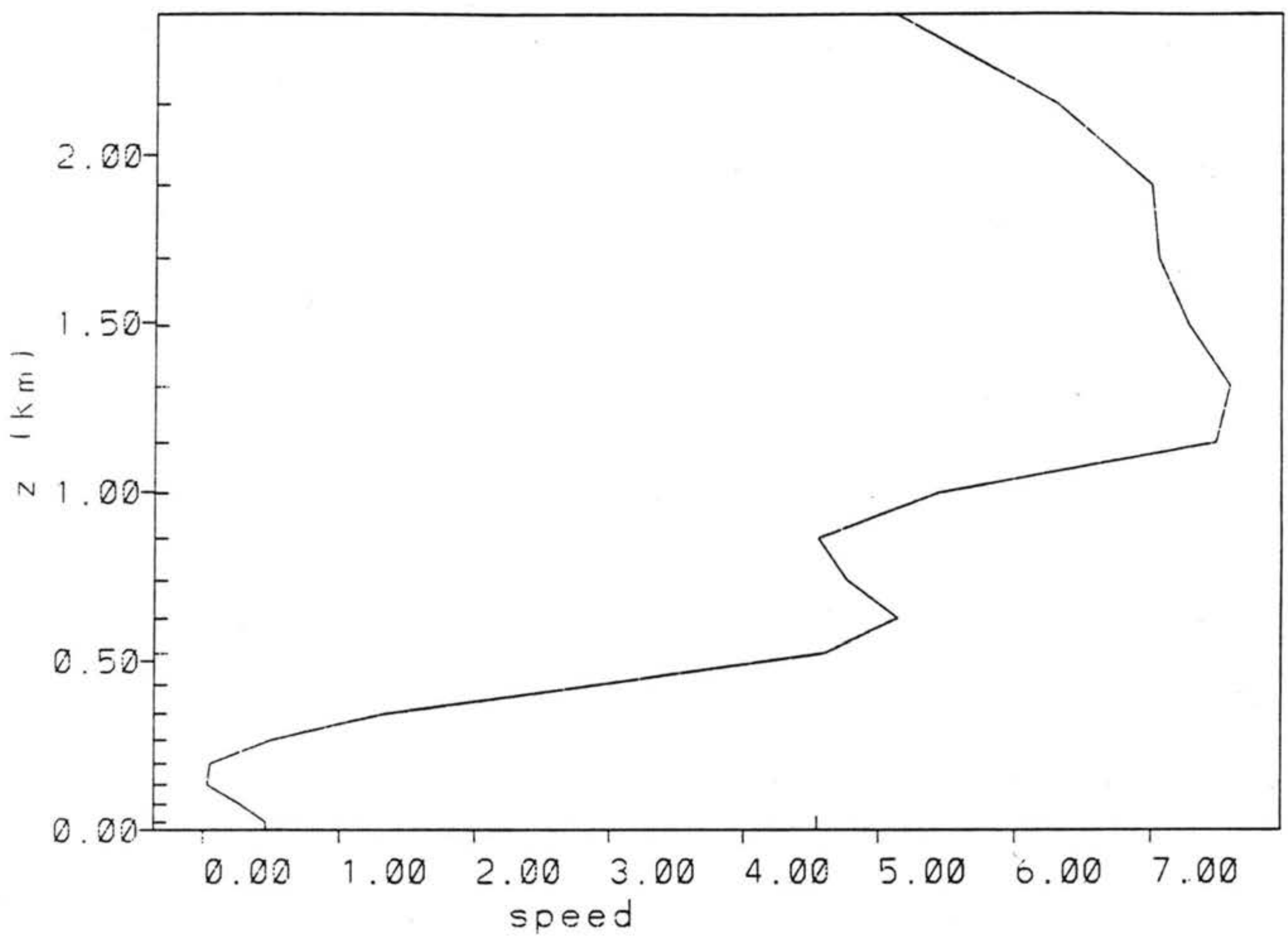

Figure 5.2a: Profiles of wind speed with height for the 100m resolution cliff. The profile was taken at cliff top in the center of the cliff east-west.

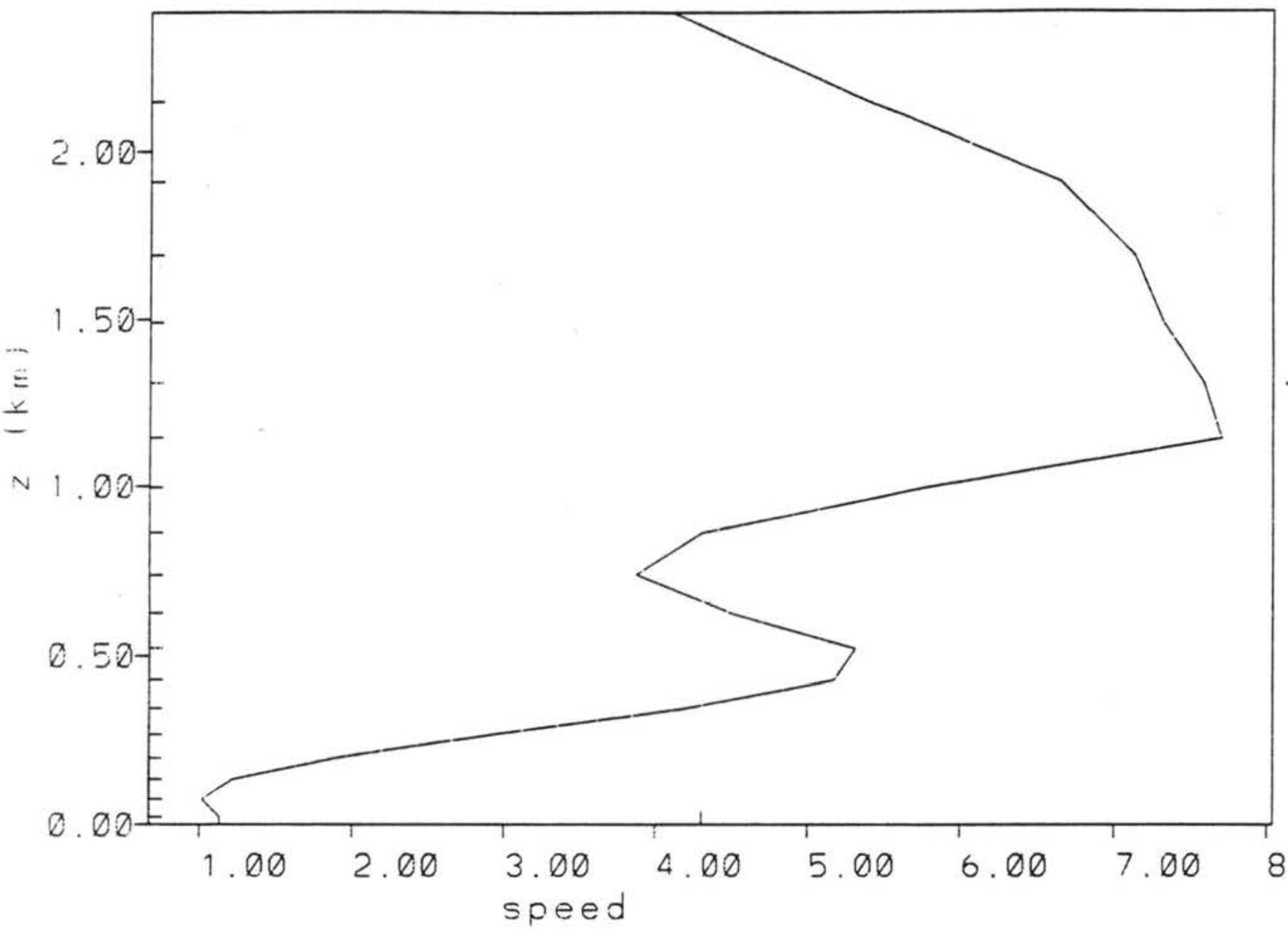

Figure 5.2b: Same as 5.2a but for the 250m resolution cliff.

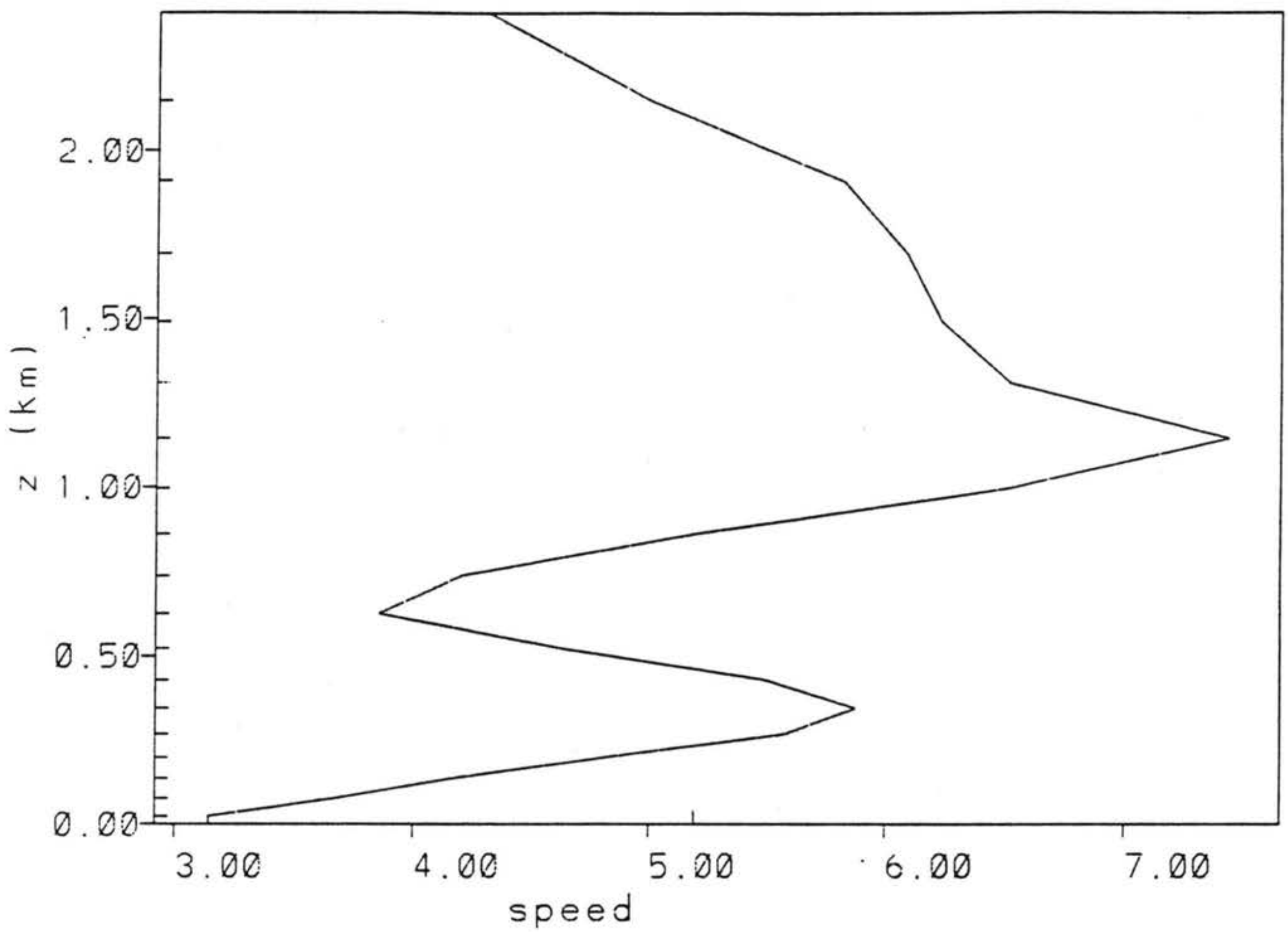

Figure 5.2c: Same as 5.2a but for the 500m resolution cliff.

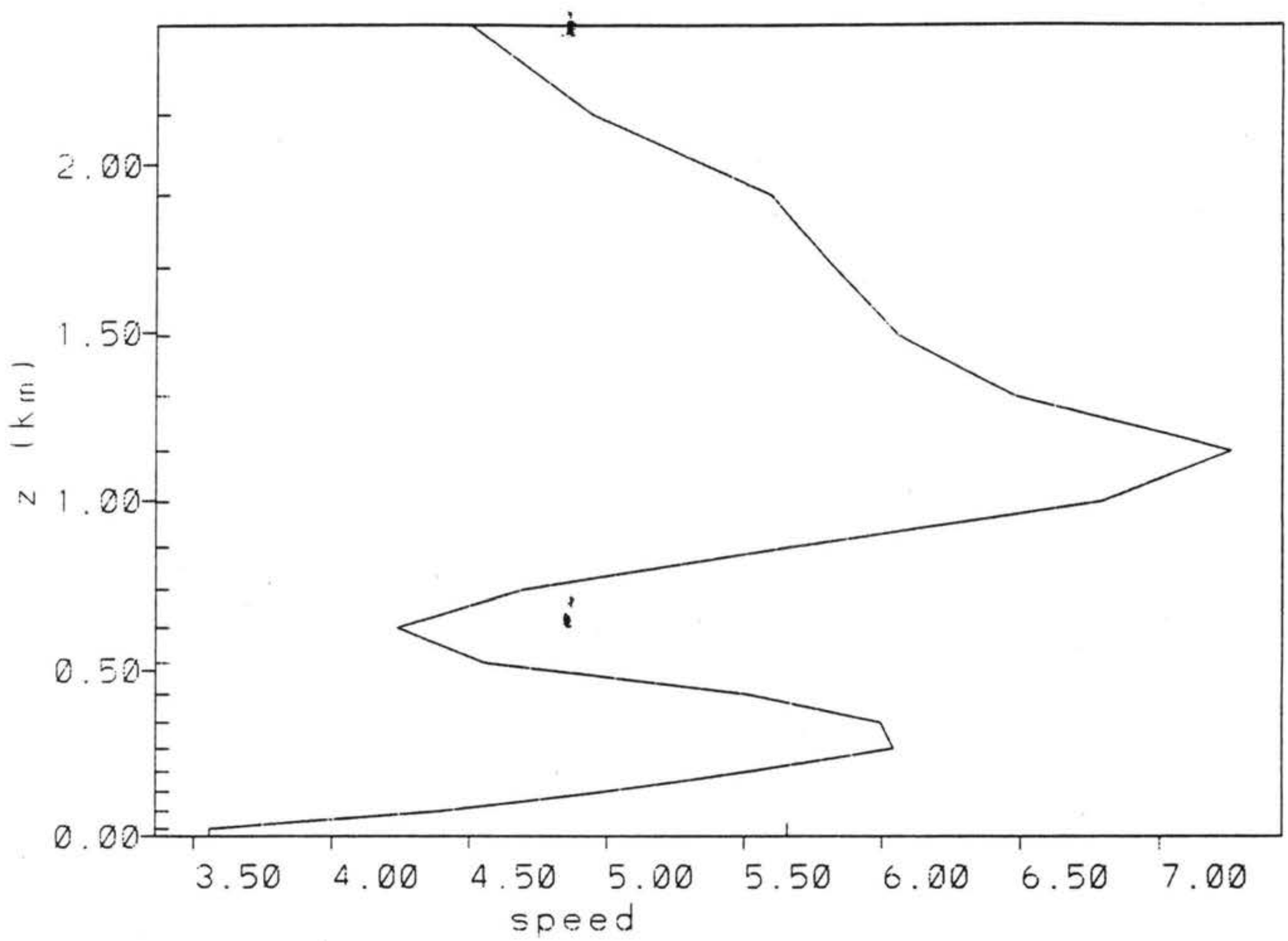

Figure 5.2d: Same as 5.2a but for the 1000m resolution cliff.

6. SUMMARY AND CONCLUSIONS

The ASTEX experiment was conducted in June, 1992 in the vicinity of the Azores and Madeira to measure and examine the properties of the marine boundary layer. Ground based measurements taken on the islands of Porto Santo, Madeira and Santa Maria, Azores experienced some contamination from pure marine conditions due to the effects of the topography of the islands. The aim of this study was to assess the vertical and horizontal extents of these island-induced effects for the island of Porto Santo; in other words, to determine the magnitude and spatial extent of the difference between the measurements taken and that of a pure marine environment.

This was achieved by analyzing model results as well as observational data from aircraft, rawinsondes, and a wind profiler from June 10, 1992 and intercomparing the four data sets. In addition, the possible effects of improper resolution of topography in the model's simulation of the island were examined.

Cross sections through the island's measurement site (located on the north side of the island- 500m from a north facing 100m cliff) of model-produced wind speed and direction were examined at different heights. This analysis showed height groupings within which similarly shaped wind profiles existed. Below 1000m and above 1900m, the wind speed and direction transects were similar in shape. In between, an area of variability existed. This was shown to be a combined effect of a thermally-driven wind which developed over the island at only these levels and a gravity wave which was induced by the wind hitting the cliff on the north side of the island. Results from the C130 aircraft data, the wind profiler, and rawinsonde all confirm the existence of this level of variability.

The magnitude and extent of island contamination in the horizontal and the vertical was assessed from the standpoint of the model results alone. Standard deviations of wind speed and direction over a small area surrounding five chosen locations were used. The five locations were upwind of the island, over the measurement site, downwind of the island, over the highest peak on the island, and over the open ocean.

The open ocean site showed little variability at any level and was thus assessed to be representative of the natural variability of the winds. This was then compared to the other points to assess the magnitude of contamination from the island. The point 2km upwind of the island and 3km downwind of the island showed more variability than the open ocean case but the magnitudes were small indicating a very weak island influence at those distances. Each of these showed small peaks in the variability at the ground and then again at approximately 1.2km. The upwind point showed an additional secondary peak at 3.5km. The points over the measurement site and over the highest peak showed a great deal of variability both near the ground and at the 1.2km level. They also had a secondary peak at 3.5km.

The increased variability at the ground was determined to be most likely a result of surface effects. The increase in variability at the 1.2km level was most likely due to the following: an inversion which was present over the island at this level on this day was distorted by island-induced changes in the wind field. This created a horizontal temperature gradient which induced a thermally-driven wind at these levels. In addition, a gravity wave phenomena was also shown to contribute to the effect. The secondary peak at the 3.5km level is most likely a residual effect of the gravity wave.

The conclusion from this part of the analysis was that the island's influence in the vertical could be felt as high as 3.5km but not continuously. Near the ground, and near the 1.2km height level, the island's effects were greatest. Between 400m and 600m and between 1.4km and 3km, the island's effects were relatively small. In the horizontal, the effect of the island decreased to a minimal effect by 2km upwind and 3km downwind. By 3km downwind, the effect could only be seen as high as 2.5km in the vertical.

A comparison was done between the C130 aircraft data and the model to assess the credibility of the model's results as well as give an additional source of information in trying to assess the extent of the island's influence. It was assessed that the horizontal disturbances of the wind fields due to island effects as predicted by RAMS were underpredicted in their spatial extent vertically and overpredicted horizontally due to inadequate horizontal resolution. A lag correlation study was performed between RAMS wind fields and the C130 aircraft wind data using horizontal transects of wind speed, direction, and temperature for the June 10th and June 22nd cases.

The results from both days showed, in general, a significantly higher correlation coefficient when the RAMS data were shifted either 500m upwards or 1-2km windward. Only in a few instances was this not true. This occurred mostly at levels above 1500m where the island's effects are minimal or from noisy data sets with little variability in the first place. In the latter cases, the average values between the data sets agreed well and thus, the low correlation was attributed to noise fluctuations about a similar mean.

In order to explain the reason that a phase shift in the RAMS data produced a higher correlation with the observations than a straight point to point comparison, topography resolution in the model was examined. If the cliff on the north side of the island was not properly resolved, the resulting wind fields would be distorted. In the island simulation, the 100m cliff was resolved to only 500m in the horizontal- giving an apparent slope of 12 degrees. Intuitively, the steeper the slope, the higher the disturbance should be found and the less downstream the disturbance should propagate. This intuition supports the conclusions of the correlation study that RAMS data should be phase shifted upward and windward for better agreement with observational data.

To test this contention, a study was performed to determine how the model will respond to wind striking barriers of different slopes. Four cases were modeled involving wind striking a cliff resolved to 1000m, 500m, 250m, and 100m in the horizontal. Three analyses were performed- a streamline analysis, a north-south wind transect analysis, and an amplification factor analysis.

The streamline and the wind speed transect analyses supported each other as well as the theory stated above. They showed that the horizontal extent of disturbances can be found further downstream and that the vertical extent of disturbances is increased when the resolution of topography is decreased. This conclusion supported the results of the work of Arya and Gadiyaram (1985).

While the streamline and transect analyses allowed an estimate to be made of the relative effects of varying cliff steepness on the extent of induced disturbances, they gave little insight into the magnitude of change. The amplification factor(AF) analysis confirmed that disturbances propagate higher for steeper terrain by showing that the vertical extent of wind speed amplification extended higher for increased resolution. In addition, it showed wind structures which agreed with the other two analyses as well as with previous studies.

For example, the location of the wind speed maximum along the transects was shown to coincide with the area of highest AF. For the 250m, 500m, and 1000m cases, this was found at the top of the cliff near the ground. For the 100m case, where flow separation was indicated in the streamline plots, the maximum AF was found slightly downwind of this coinciding to the location near the ground where the streamlines reconvened. The location of the minimum AF was always near the ground at the base of the cliff. This value decreased as the topography became steeper. These results agree well with the locations of maximum and minimum AF from the studies of Arya and Gadiyaram (1985), Pearse (1982), and Bowen and Lindley (1977).

An additional area of increased AF was found downstream approximately between 600m and 1200m. The area below this, between 400m and 600m, was shown to have AF values less than one. This structure was confirmed to be a result of an internal gravity wave induced by the wind hitting the cliff. For the island simulation, this structure is somewhat altered by the additional effect of a thermally-driven wind.

Amplification factors were then analyzed for the island simulation across the measurement site location. The results agree well with studies of Bowen and Lindley (1977) as far as the shape of the AF contours in the vicinity of the cliff is concerned. The maximum values are found at the ground centered around the cliff top and the contours bulge downwind from there. Both the present study and that of Bowen and Lindley show the amplification factor to decrease to near unity by a height of 6H (H- hill height) above the terrain.

Upwind of the cliff, the studies agree as well. Both found that for sloping escarpments less than 90 degrees the AF was less than one upwind of the cliff and reached unity somewhere along the cliff. Further, both showed that in this region upwind of the cliff the AF increased to unity between 3H and 5H above the ground.

Thus, the results of the AF study of the island support the results of previous studies and coincide well with other analyses in this study for the regions upwind, over, and downwind of the island. The results of the AF study of the four cliffs provide additional support of the suggestion that disturbances propagate higher, but not as far downstream with the increasing steepness of a barrier. Thus, there is a sound basis for applying an upward or windward phase shift to the RAMS wind data when analyzing the extent of the island's effects on the measurements. After doing this, RAMS agrees well with the observational data.

From this study, the RAMS model was shown to give a reasonable picture of the general features of the wind fields over the island of Porto Santo. Inadequate resolution of topography, however, made it necessary to adjust the spacial extent of these features to agree with observational data. From a combination of model results, aircraft data, wind profiler data and rawinsonde measurements, the extent of the island's effects on the local wind fields were determined. In the horizontal, they decreased with distance from the island out to approximately 2km upwind and downwind where the effects were minimal. In the vertical, the effects were more varied. Effects could be felt up to 3.5km but regions existed within which the effects were a maximum and a minimum. Due to surface effects and the presence of an inversion combined with the presence of a gravity wave, the effects were a maximum at the ground and near the 1.2km level respectively. A secondary max near 3.5km was shown to be a residual effect of the gravity wave.

In order to accurately deduce wind fields which are representative of a pure marine atmosphere the wind data taken at Porto Santo must be filtered at the ground and at the 1.2km and 3.5km levels. In between these levels, wind measurements taken on the island would appear to provide an accurate representation of the pure marine environment.

7. SUGGESTIONS FOR FURTHER RESEARCH

Most of the previous studies which dealt with the mean wind and turbulence structures over various barriers limited their studies to areas within four hill heights of the ground. In addition, few of these studies included the far upstream or downstream regions of flow. More work could be done in these regions for both two and three dimensional studies.

While this study did look at these other regions, this was a limited study as well. First, the same study could be run with different initial sounding information. It would be interesting to see what effect skewing the initial wind direction, varying initial wind speeds, changing the stability of the lowest layer, adding clouds, or changing the inversion characteristics would have on the resulting flow patterns far upstream or downstream, and at various height levels.

The height of the inversion is an important parameter in a marine boundary layer study such as ASTEX. It would thus be of value to determine if the height of the inversion measured over the test site on Porto Santo is representative of the height of the inversion of the typical marine boundary layer in this region without the island. An average of measured inversion height levels scattered over the island may give a more accurate value due to the island contamination of this height induced at any one point such as the measurement site.

From the changes discussed above, the extent of measurement contamination assessed from June 10th and June 22nd (clear days with northerly flow) in this study could be extended to include other conditions also commonly found over the region.

Another study which would be of interest is a sensitivity study which would determine if using an NMC geostrophic wind profile (instead of a rawinsonde profile which already has island contamination built into it) to initialize the model would produce results that agree better with the observations. Meyers and Cotton(1992) concluded that flow simulated by RAMS over the Sierra Nevadas compared more favorably to the observations when RAMS was initialized using the NMC geostrophic wind profile than a profile of winds which were more representative of the local mountain effects.

In addition to changing the initial sounding, the effect of changing the topography could be examined. How would changing features such as the height of the windward facing cliff, the location or elevation of the test site, the height of the highest peak on the island, or the shape of the island effect the flow?

In addition, it would be of great value to have a regression-type scheme developed in which the model produced results and the observations can be processed to give the undisturbed marine conditions. The focus of this study was to determine to what horizontal and vertical extent the measurements taken at Porto Santo were contaminated from representing a pure marine atmosphere. While this was determined, a quantitative method to correct this contamination is a needed step toward producing accurate pictures of the marine atmosphere from the data taken during the ASTEX field study. One possible method for approaching this could be to use amplification factor profiles to deduce the undisturbed flow.

Bibliography

Arakawa, A. and V.R. Lamb, 1981: A potential enstrophy and energy conserving scheme for the shallow water equations. *Mon. Wea. Rev.*, **109**, 18-36.

Arya, S. P. S. and P. S. Gadiyaram, 1985: An experimental study of flow dispersion in the wakes of three-dimensional hills. *Atmos. Environment*, **20**, No. 4, 729-740.

Bowen, A. J. and D. Lindley, 1977: A wind tunnel investigation of the wind speed and turbulence characteristics close to the ground over various escarpment shapes. *Bound. Lay. Met.*, **12**, 259-271.

Bradley, E. F., 1980: An experimental study of the profiles of wind speed, shearing stress, and turbulence at the crest of a large hill. *Quart. J. Roy. Meteorol. Soc.*, **106**, 101-123.

Castro I. P. and W. H. Snyder, 1982: A wind tunnel study of dispersion from sources downwind of three-dimensional hills. *Atmos. Environment*, **16**, 1869-1887.

Chen, C. and W. R. Cotton, 1983b: A one-dimensional simulation of the statocumulus-capped mixed layer. *Bound. Lay. Met.*, **25**, 289-321.

Clark, T. L., 1977: A small-scale dynamic model using a terrain-following coordinate transformation. *J. Comput. Phys.*, **24**, 186-215.

de Bray, B. G., 1973: Atmospheric shear flows over ramps and escarpments. *Industrial Aerodynamics Abstracts*, **5**, Sept.-Oct. 1973.

Flatau P. J., G. J. Tripoli, J. Verlinde, and W. R. Cotton, 1989: The CSU-RAMS cloud microphysics module: General theory and code documentation. Technical Report 451, Colorado State University, Fort Collins, Colorado 80523.

Freeston, D. H.,1974: Atmospheric shear flows over ramps and escarpments. Presented to the Fifth Australian Conference on Hydraulics and Fluid Mechanics, University of Canterbury, N.Z., Dec. 1974, 258-268.

Hansen A. C. and J. E. Cermak, 1975: Vortex-containing wakes of surface obstacles. Fluid Dynamics and Diffusion Laboratory Report CER75-76ACH-JEC16, Colorado State University, Fort Collins, CO.

Holton, James R., 1992: Introduction to Dynamic Meteorology. Academic Press Inc., Harcourt Brace Javanovich Publishers, San Diego, CA, 198-206.

Hosker, R. P., 1984: Flow and diffusion near obstacles. *Atmospheric Science and Power Production,* Chapter 7, 241-326. Technical Information Center US Department of Energy.

Hunt, J. C. R., 1975: Wind over hills. *Proceedings of the Workshop on the Planetary Boundary Layer,* 14-18 August 1978, Boulder, Colorado, (edited by Wyngaard, J. C.) 107-157. Am. Met. Soc.

Jackson, P. S. and J. C. R. Hunt, 1975: Wind flow over low hills. *Quart. J. Roy. Meteorol. Soc.,* **101**, 929-955.

Jenkins, G. J. Mason, P. J. Mason, W. H. Moore, and R. I. Sykes, 1981: Measurements of flow structure around Ailsa Craig, a steep three-dimensional isolated hill. *Quart. J. Roy. Meteorol. Soc.,* **107**, 833-851.

Lavoie, Ronald L., 1974: A numerical model of trade wind weather on Oahu. *Mon. Wea. Rev.,* **102**, 630-637.

Klemp, J. B. and R. B. Wilhelmson, 1978a: The simulation of three-dimensional convective storm dynamics. *J. Atmos. Sci.,* **35**, 1070-1096.

Mason, P. J. and R. I. Sykes, 1979: Flow over an isolated hill of moderate slope. *Quart. J. Roy. Meteorol. Soc.,* **105**, 383-395.

Meyers, Michael P. and William R. Cotton, 1992: Evaluation of the potential wintertime quantitative precipitation forecasting over mountainous terrain with an explicit cloud model. Part I: Two-dimensional sensitivty experiments. *J. Applied Meteorol.*, **31**, 26-50.

O'connor, Willaim P. and David H. Bromwich, 1988: Surface airflow around Windless Bight, Ross Island, Antarctica. *Quart. J. Roy. Meteorol. Soc.*, **114**, 917-938.

Panofsky, Hans A. and Glenn W. Brier, 1965: Some Applications of Statistics to Meteorology, first edition. Pennsylvania State University, University Park, PA, 92-96.

Pearse, J. R., 1982: Wind flow over conical hills in a simulated atmospheric boundary layer. *J. Wind Eng. Indus. Aerodyn.*, **10**, 303-313.

Ryan, W. B. Lamb, and E. Robinson, 1984: An atmospheric tracer investigation of transport and diffusion around a large isolated hill. *Atmos. Environ.*, **18**, 2003-2021.

Sacre, C., 1973: Influence d'une colline sur la vitesse du vent dans la couche limite de surface. Internal Report, Centre Scientifique de Technique du Batiment, Nantes, France.

Strimaitis, D. G. A. Venkatram, B. R. Greene, S. R. Hanna, S. Heisler, T. F. Lavery, A. Bass, and B. A. Egan, 1983: EPA complex terrain model development-Second Milestone Report-1982, EPA-600/3-83-015, Environmental Protection Agency, Research Triangle Park, N.C., U.S.A.

Taylor, P. A., 1984: Wind flow over conical hills. *J. Wind Eng. Indus. Aerodyn.*, **16**, 119-124.

Tremback, C. J., 1990: *Numerical simulation of a convective complex: model development and numerical results*. PhD thesis, Colorado State University, Dept. of Atmospheric Science, Fort Collins, Co 80523,274. Also published as Atmos. Sci. Paper No. 465.

Tremback, C. J., G. J. Tripoli, and W. R. Cotton, 1985: A regional scale atmospheric numerical model including explicit moist physics and a hydrostatic time-split scheme. In *Preprints, 7th Conference on Numerical Weather Predicion,* AMS, Montreal, 355-358.

Tripoli, G. J. and W. R. Cotton, 1982: The Colorado State University three-dimensional cloud/mesoscale model-1982. Part I: General theoretical framework and sensitivity experiments. *J. Rech. Atmos.,* **16**, 185-220.